

Cell Death Regulation and Function in Plant-Fungal Symbiosis

Inaugural-Dissertation

zur

Erlangung des Doktorgrades

der Mathematisch-Naturwissenschaftlichen Fakultät

der Universität zu Köln



UNIVERSITY
OF COLOGNE

vorgelegt von

Nick Leon Dunken

aus Eschweiler

Köln, August 14, 2025

Begutachtung:

Prof. Dr. Alga Zuccaro

Prof. Dr. Jane E. Parker

Prof. Dr. Núria Sánchez Coll

Abstract

Regulated cell death (RCD) is a hallmark of plant immunity, traditionally associated with defense against pathogens. However, its role in beneficial plant–microbe interactions remains largely uncharacterized. The root endophyte *Serendipita indica*, with its biphasic lifestyle, comprising an initial biotrophic phase followed by a cell death-associated phase, serves as an excellent model to dissect the molecular regulation of RCD in mutualistic contexts. While individual host factors implicated in the cell death-associated phase have been previously identified, the mechanisms governing RCD initiation and regulation remained poorly defined. In this thesis (Chapter 4), I characterized the synergistic activity of two fungal effector enzymes, SiNucA and SiE5NT, as the primary trigger of RCD. Their activity leads to the apoplastic production of deoxyadenosine (dAdo), a purine-derived infochemical that triggers signaling and RCD in host roots. I further identify the equilibrative nucleoside transporter ENT3 as the key mediator of both dAdo-induced and *S. indica*-mediated cell death. To dissect the molecular responses underlying this process, integrated transcriptomic, proteomic, and metabolomic profiling were employed. These analyses revealed substantial overlap with known RCD pathways and uncovered additional infochemical candidates involved in host–microbe communication. To monitor cell death dynamics *in planta*, I developed a high-throughput assay combining Pulse Amplitude Modulation (PAM) fluorometry with ion leakage measurements (Chapter 3). A genetic screen using this assay identified a previously uncharacterized TIR-NLR receptor Induced by *S. indica* (ISI) as a modulator of root cell death and a regulator of dAdo-triggered RCD, supporting the role of dAdo as an active immunometabolite. Beyond this, ISI was found to modulate distinct root cell death phenotypes and to influence *S. indica* colonization patterns, suggesting a broader role in regulating mutualistic interactions. Together, these findings support a model in which synergistic effector activity and purine-based signaling tightly regulate RCD as part of a controlled mutualistic program. This work redefines RCD as a functional component of beneficial symbioses used to shape microbial niche structure, uncovers a novel intersection between purine metabolism and immune signaling, and broadens the functional repertoire of TIR-NLR proteins beyond classical pathogen resistance (Chapter 5). These findings advance the emerging field of plant immunometabolism and provide a conceptual framework for understanding how root immunity integrates metabolic and microbial cues.

Zusammenfassung

Regulierter Zelltod (RCD) ist ein zentrales Merkmal pflanzlicher Immunität und wird traditionell mit der Abwehr von Krankheitserregern in Verbindung gebracht. Seine Rolle bei nützlichen Interaktionen zwischen Pflanzen und Mikroben ist jedoch noch weitgehend unklar.

Der Wurzelendophyt *Serendipita indica* mit seiner biphasischen Lebensweise, die eine anfängliche biotrophe Phase, gefolgt von einer Zelltod-assoziierten Phase beinhaltet, dient als hervorragendes Modell zur Untersuchung der molekularen Regulierung des RCD in mutualistischen Symbiosen. Während einzelne Wirtsfaktoren, die an der Zelltod-assoziierten Phase beteiligt sind, bereits identifiziert wurden, sind die Mechanismen, die für die Auslösung und Regulierung des RCD verantwortlich sind, noch unzureichend definiert. In dieser Dissertation (Kapitel 4) habe ich die synergistische Aktivität von zwei pilzlichen Effektorenzymen, SiNucA und SiE5NT, als primären Auslöser des RCD identifiziert. Ihre Aktivität führt zur apoplastischen Produktion von Desoxyadenosin (dAdo), einer auf Purin basierenden Infochemikalie, die in den Wirtswurzeln die Stresssignale und RCD auslöst. Darüber hinaus identifiziere ich den äquilibrativen Nukleosid-Transporter ENT3 als Schlüsselkomponente sowohl von dAdo-induzierten, als auch *S. indica*-vermittelten Zelltod.

Um die molekularen Reaktionen, die diesem Prozess zugrunde liegen zu entschlüsseln, wurden integrierte transkriptomische, proteomische und metabolomische Analysen angewandt. Diese Analysen ergaben erhebliche Überschneidungen mit bekannten RCD-Signalwegen und enthüllten zusätzliche Kandidaten für Infochemikalien, die an der Kommunikation zwischen Wirt und Mikrobe beteiligt sind. Um die Dynamik von Zelltodwegen in Pflanzen nachzuverfolgen, habe ich einen Hochdurchsatztest entwickelt, der die Fluorometrie der Pulsamplitudenmodulation (PAM) mit Konduktivitäts-Messungen kombiniert (Kapitel 3). Bei einem genetischen Screening mit dieser Methode wurde ein bisher nicht charakterisierter TIR-NLR-Rezeptor "Induced by *S. indica*" (ISI) als Modulator von Wurzelzelltod und als Regulator des durch dAdo ausgelösten RCD bestimmt, was die Rolle von dAdo als aktiver Immunmetabolit unterstützt. Darüber hinaus wurde festgestellt, dass ISI verschiedene Phänotypen des Wurzelzelltods moduliert und die Besiedlungsmuster von *S. indica* beeinflusst, was auf eine umfassendere Rolle bei der Regulierung mutualistischer Interaktionen hindeutet.

Zusammengefasst, stützen diese Ergebnisse ein Modell, in dem synergistische Effektoraktivität und purinbasierte Signalübertragung RCD als Teil eines kontrollierten, mutualistischen Programms stark regulieren. Diese Arbeit definiert RCD neu als eine funktionelle Komponente nützlicher Symbiosen, die zur Gestaltung von mikrobiellen Nischen verwendet wird, deckt einen Schnittpunkt zwischen dem Purin-Stoffwechsel und Immunsignalen und erweitert das funktionelle Repertoire der TIR-NLR-Proteine über die klassische Pathogenresistenz hinaus (Kapitel 5). Diese Erkenntnisse bringen das aufstrebende Gebiet des pflanzlichen Immunmetabolismus voran und bieten einen konzeptionellen Rahmen für das Verständnis dafür, wie die Wurzelimmunität metabolische und mikrobielle Signale integriert.

List of Abbreviations

5'NT 5' nucleotidase.

ADA adenosine deaminase.

ADP adenosine diphosphate.

ADPR adenosine diphosphate ribose.

ADPR-ATP/di-ADPR adenosine diphosphate ribose-ATP/diadenosine diphosphate ribose.

ADR1 Activated Disease Resistance 1.

AMF arbuscular mycorrhiza fungi.

AMP adenosine monophosphate.

APY ecto-apyrase.

ART ecto-ADP ribosyltransferase.

ATP adenosine triphosphate.

BAK1 BRASSINOSTEROID INSENSITIVE1-ASSOCIATED KINASE1.

BAX-I Inhibitor of Bcl-2-like protein 4.

BFN1 Bifunctional Nuclease 1.

BKK1 BAK1-like 1.

Ca²⁺ calcium ion.

cADPR cyclic adenosine diphosphate ribose.

cAMP cyclic adenosine monophosphate.

CAMTA calmodulin-binding transcription activator.

CC coiled coil.

CD cluster of differentiation.

CDK calcium-dependent protein kinase.

cGAMP cyclic GMP-AMP

cGAS cyclic GMP-AMP synthase.

cGMP cyclic guanosine monophosphate.

CldAdo 2-chloro-2'-deoxyadenosine.

Cryo-EM cryo-electron microscopy.

dAdo deoxyadenosine.

DAMP damage-associated molecular pattern.

dATP deoxyadenosine triphosphate.

dCK deoxycytidine kinase.

dGuo deoxyguanosine.

dRCD developmental regulated cell death.

ds double-stranded.

dsDNA double-stranded DNA.

E5'NT ecto-5'-nucleotidase.

E-NPP ecto-nucleotide pyrophosphatase.

eATP extracellular adenosine triphosphate.

eDNA extracellular DNA.

EDS1 Enhanced Disease Susceptibility 1.

ENT equilibrative nucleoside transporter.

ER endoplasmic reticulum.

ETD effector-triggered defense.

ETI effector-triggered immunity.

ETS effector-triggered susceptibility.

GA gibberellic acid.

GTP guanosine triphosphate.

HR hypersensitive response.

Hsp90 Heat Shock Protein 90.

IFN- β interferon beta.

ILR1 interleukin-1 receptor.

ISI Induced by *Serendipita indica*.

ISIC1 Inhibitor of Stomatal Immunity C2-domain protein 1.

JA jasmonic acid.

LOV1 Locus Orchestrating Victorin effects 1.

LRR leucine-rich repeat.

LysM lysin motif.

MAMP microbe-associated molecular pattern.

MAP mitogen-associated protein.

MAPK mitogen-associated protein kinase.

MEcPP 2-C-Methyl-d-erythritol-2,4-cyclopyrophosphate.

MLKL Mixed Lineage Kinase domain Like.

MMF1 Mediator of Microbiome Feedback 1.

NAADP⁺ oxidized nicotinic acid adenine dinucleotide phosphate.

NAD⁺ nicotinamide adenine dinucleotide.

NADP⁺ oxidized nicotinamide adenine dinucleotide phosphate.

NADPH nicotinamide adenine dinucleotide phosphate.

NAM nicotinamide.

NB nucleotide-binding.

NB-ARC nucleotide-binding adapter shared by APAF-1, certain R gene products, and CED-4.

NDK nucleoside diphosphate kinase.

NET neutrophil extracellular trap.

NLR nucleotide-binding/leucine-rich repeat receptor.

NMN nicotinamide mononucleotide.

NO nitric oxide.

NPP1 nucleotide pyrophosphatase / phosphodiesterase 1.

NR nicotinamide riboside.

NRG1 N Requirement Gene 1.

NSH3 Nucleoside Hydrolase 3.

PAD4 Phytoalexin Deficient 4.

PAM Pulse Amplitude Modulation.

PAP purple acid phosphatase.

PNP purine nucleoside phosphorylase.

PolyQ polyglutamine tract.

PR pathogenesis-related.

pRib-AMP/ADP 2'-(5''-phosphoribosyl)-5'-adenosine monophosphate and diphosphate.

PRR pattern-recognition receptor.

PTI pattern-triggered immunity.

PUP purine permease.

R resistance.

RAR1 Required for Mla12 Resistance 1.

RBA1 Response to the bacterial type III effector protein HopBA1.

RBOH Respiratory Burst Oxidase Homolog.

RCD regulated cell death.

RET root extracellular trap.

RK receptor kinase.

RLP receptor-like protein.

ROD1 resistance of rice to diseases1.

ROS reactive oxygen species.

RPP1 Recognition of *Peronospora parasitica* 1.

RPS4 Resistant to *P. syringae* 4.

RPW8 Resistance to Powdery mildew 8.

SAG101 Senescence-Associated Gene 101.

SAR systemic acquired resistance.

SGT1 Suppressor of G-Two allele of Skp1.

siRNA small interfering RNA.

STING Stimulator of Interferon Genes.

SynCom synthetic microbial community.

TIR toll-interleukin-1 receptor.

TLR toll-like receptor.

TN TIR-NB protein.

TNP TIR-NB-ARC-tetratricopeptide repeat protein.

TPP thermal proteome profiling.

VICTR VARIATION IN COMPOUND TRIGGERED ROOT GROWTH RESPONSE.

VPE vacuolar processing enzyme.

ZAR1 HopZ-Activated Resistance 1.

Contents

Abstract	II
Zusammenfassung	III
List of Abbreviations	V
1 Introduction	1
1.1 The Global Importance of Studying Plant-Microbe-Interactions	1
1.2 The Plant Immune System	1
1.3 Regulated Cell Death in Plant-Microbe-Interactions	4
1.4 <i>Serendipita indica</i> as a Model for Beneficial Root Endophytes	7
1.5 Aim of this Thesis	10
2 Overview of Publications	12
3 Monitoring Cell Death Via Ion Leakage and PAM Fluorometry	14
4 A nucleoside signal generated by a fungal endophyte regulates host cell death and promotes root colonization	24
5 Purine-Based Infochemicals and Immunometabolites: A Comparative Review of Emerging Signaling Pathways in Plants and Animals	50
6 Discussion	71
6.1 Cell death in beneficial host-microbe interactions	71
6.2 Redefining the role of TIR domain proteins in immunity	72
6.2.1 Regulation of TIR protein activity in immunity and cell death	74
6.2.2 ISI - a TIR-NLR with function in immunometabolic cell death and root colonization	75
6.3 dAdo – a purine-based infochemical inducing immunometabolic cell death	77
6.4 Open Questions and Outlook	79
Supplementary Information	117

Chapter 1

Introduction

1.1 The Global Importance of Studying Plant-Microbe-Interactions

Plant diseases caused by pathogenic microbes reduce crop yields, contribute to post-harvest losses, and decrease biodiversity, posing significant challenges to global food security and environmental sustainability (Savary et al. 2019). Although the impact of anthropogenic climate change remains complex, studies predict an increased threat of plant diseases due to the heat sensitivity of plant immunity, the expansion of pathogens into previously temperate regions, and increased abiotic stresses such as drought. These stresses further compromise crop resilience and amplify the challenges posed by climate change (Bidzinski et al. 2016; Cohen and Leach 2020; Delgado-Baquerizo et al. 2020; Singh et al. 2023). In contrast, plants benefit from a diverse community of beneficial microbes, known as the microbiota, which protect against both abiotic, and biotic stresses (López et al. 2008; Lamo and Takken 2020). A well-balanced microbiota can reduce the need for fertilizers and pesticides, promoting more sustainable agricultural practices (Adesemoye and Kloepper 2009; Beyari 2025). During the past decades, research on plant-microbe interactions has expanded significantly, driven by advances in molecular tools such as genome editing and high-throughput sequencing, which enable increasingly complex studies (Bai et al. 2015; Wang et al. 2014; Cook et al. 2025).

Despite this progress, fundamental questions remain unanswered, such as how plants differentiate between beneficial and pathogenic microbes or how abiotic factors shape biotic interactions. Addressing these challenges requires a holistic approach that integrates molecular and community-level studies. Only through comprehensive research can we develop innovative strategies to ensure agricultural sustainability and global food security in the face of increasing environmental pressures.

1.2 The Plant Immune System

By growing in soil, plants are in constant contact with one of the most diverse ecosystems in the world, teeming with microbial lifeforms such as bacteria, oomycetes, nematodes, or fungi (Curtis et al. 2002; Gans et al. 2005). These microbes exhibit various lifestyles, ranging from mutualism to parasitism, posing a significant challenge for plant health: regulating the recruitment of beneficial microbes while restricting the pathogen colonization and simultaneously balancing immunity and growth (Drew et al. 2021).

The initial barrier of innate plant immunity (Figure 1.1) relies on the ability to distinguish between self and non- or modified self. This recognition is mediated by the detection of specific molecular patterns. Conserved microbe-associated molecular patterns (MAMPs), such as chitin

and flagellin, and damage-associated molecular patterns (DAMPs), such as extracellular adenosine triphosphate (eATP) - a danger signal released from damaged or stressed plants during colonization - are perceived by pattern-recognition receptors (PRRs). These receptors can be classified into receptor kinases (RKs), consisting of a ligand-binding ectodomain, a single-pass transmembrane domain and an intracellular kinase domain, and receptor-like proteins (RLPs), which lack the kinase domain. The substrate specificity is defined by the receptor's ectodomains. For example, while leucine-rich repeat (LRR) domains mainly bind proteins and peptides, lysin motif (LysM) domains bind oligosaccharides (Felix et al. 1999; Zipfel 2014).

The recognition of MAMPs and DAMPs by PRR triggers the first wave of plant immunity, initiating a cascade of interconnected signals. Initially, receptor activation induces an influx of extracellular calcium ions (Ca^{2+}) into the cytosol, activating calcium-dependent protein kinases (CDKs) and additional ion channels, leading to an apoplastic alkalization (Yuan et al. 2017; Xu et al. 2022). Furthermore, Ca^{2+} influx activates nicotinamide adenine dinucleotide phosphate (NADPH) oxidases, also known as Respiratory Burst Oxidase Homologs (RBOHs), leading to a transient production of reactive oxygen species (ROS), highly reactive molecules that serve as both antimicrobial agents and secondary messengers amplifying immune responses (Torres et al. 2002; Ogasawara et al. 2008). Alongside further downstream signaling outputs, such as the activation of mitogen-associated protein (MAP) kinases - key regulators that transmit extracellular immune signals to the nucleus and modulate gene expression - and transcriptional upregulation of pathogenesis-related (PR) genes, the recognition of MAMPs and DAMPs culminates in pattern-triggered immunity (PTI), efficiently preventing the colonization of non-adapted microbes (Loon et al. 2006).

To overcome this first tier of immunity and successfully colonize a plant host, both pathogenic and beneficial microbes secrete an arsenal of molecules, termed effectors. Traditionally, effectors have been defined as small, secreted proteins that interfere with PTI. Effector proteins are furthermore often cysteine-rich, lack conserved domains and their genes are often organized in clusters and undergo rapid evolution (Lo Presti et al. 2015). While the traditional definition led to the identification of many effector candidates, it was largely limited to proteins with direct host targets. Today, a broader definition is preferred, describing effectors as proteins and small molecules that promote microbial colonization of a host. This includes non-proteinaceous molecules and antimicrobial effectors that influence the host indirectly (Collemare et al. 2019; Snelders et al. 2020; Snelders et al. 2022). Effectors often function in the apoplast, shielding invading microbes from hydrolases or directly interfere with recognition by PRR. Some effectors are also translocated into the host cytoplasm. While the translocation via the syringe-like type III secretion system of bacteria or clathrin-mediated endocytosis of oomycete RXLR effectors have been characterized before, the fungal translocation mechanisms remain elusive. However, recent evidence suggests that the Stp proteins of the smut fungus *Ustilago maydis* contribute to virulence by forming a pore-like complex (Macho and Zipfel 2015; Ludwig et al. 2021; Wang et al. 2023). Though effectors have predominantly been studied in biotrophic (and to a lesser degree: necrotrophic) pathogens, beneficial microbes deploy a comparable arsenal to evade host immunity and establish symbiosis (Plett et al. 2014; Wawra et al. 2016; Nizam et al. 2019; Nostadt et al. 2020; Zeng et al. 2020). Moreover, recent findings indicate that effectors can also enable host colonization

by disregulating or stabilizing the host microbiota, further broadening their functional range in plant-microbe interactions (Snelders et al. 2020; Eichfeld et al. 2024; Gomez-Perez et al. 2023). Ultimately, an adapted microbe's effector repertoire can suppress PTI and modulate the host microbiota, leading to a state known as effector-triggered susceptibility (ETS).

To counteract microbial effectors, plants possess an additional tier of innate immunity. Intracellular effectors or their modified host targets are often monitored by nucleotide-binding/leucine-rich repeat receptors (NLRs). These tripartite receptors consist of a C'-terminal LRR domain for effector recognition, a nucleotide-binding adapter shared by APAF-1, certain R gene products, and CED-4 (NB-ARC) domain function as a molecular switch, by binding adenosine triphosphate (ATP) or adenosine diphosphate (ADP) and a N-terminal signaling domain. NLR are categorized by their N-terminal signaling domains as coiled coil (CC)-, toll-interleukin-1 receptor (TIR)- or Resistance to Powdery mildew 8 (RPW8)-NLR. Functionally, they are classified as sensor, helper or singleton NLR (Lolle et al. 2020; Chia and Carella 2023). Upon recognition of an intracellular effector or a modified effector target, NLRs trigger a rapid and localized form of cell death known as hypersensitive response (HR) (Morel and Dangl 1997; Balint-Kurti 2019), which restricts pathogen spread and typically halts the colonization of avirulent pathogens, leading to effector-triggered immunity (ETI). The mechanisms of NLR-mediated HR will be discussed in the following section.

While NLR-triggered HR restricts the colonization of many biotrophic pathogens, several hemi-biotrophic and necrotrophic pathogens exploit this process by inducing cell death through necrotrophic effectors or toxins, adding another layer of complexity to plant-microbe interaction (Jones and Dangl 2006; Lorang et al. 2007; Leng et al. 2025). Despite extensive research on effector-NLR interactions, most studies focus exclusively on leaves. While HR-like cell death has not been observed in roots, TIR-NLRs have been implicated in ETI-dependent root growth inhibition and nucleoside-induced cell death induced by beneficial fungi (Kim et al. 2012; Dunken et al. 2024)(Chapter 4). In addition to the recognition by NLR, certain apoplastic effector proteins are also detected by PRRs, eliciting a slow defense response known as effector-triggered defense (ETD) (Stotz et al. 2014; Albert et al. 2020; Yang et al. 2023).

Although these immune mechanisms provide a high degree of immune regulation to plant hosts, recent findings have shown that the Zig-Zag model of plant immunity cannot only be extended by additional layers of ETI-inhibiting effectors and corresponding NLR proteins (Wei et al. 2018; Yu et al. 2020), but also that PTI and ETI cannot be considered as separate tiers of the innate immune system. ETI cannot only amplify PTI signaling via a complex feedback loop, PTI signaling is also an essential requirement for ETI execution (Yuan et al. 2021; Ngou et al. 2021).

Recent findings not only highlighted the complex interplay between PTI and ETI, but also underscored that immune responses are tightly intertwined with programmed alterations in cellular physiology, including various forms of regulated cell death. While traditionally associated with defense against pathogens, cell death responses in plants represent a highly controlled process that is intricately embedded within the immune signaling network. In particular, NLR-mediated responses often culminate in HR. To place these phenomena in a broader biological context, the following chapter will introduce the concept of regulated cell death, compare its manifestation in plants to animal systems, and explore its diverse roles in plant-microbe interactions beyond the

The diagram illustrates the signaling pathways in a plant cell, showing the transition from resistance to disease based on the outcome of NLR activation. The cell is divided into the **Apoplast** (outside) and **Cytoplasm** (inside).

Resistance Pathway:

- invading microbes** release **MAMP** (Microbe-Associated Molecular Pattern).
- PRR** (Pattern Recognition Receptor) detects MAMPs.
- Ca²⁺** influx occurs through a channel.
- NADPH-oxidase** produces **ROS** (Reactive Oxygen Species).
- MAPK** (Mitogen-Activated Protein Kinase) is activated.
- PR gene induction** occurs in the **Nucleus**.
- PTI** (PAMP-Triggered Immunity) is activated, leading to **ETI** (Effector-Triggered Immunity).
- ETI** leads to **resistance**.

Disease Pathway:

- effectors** are released by the microbes.
- NLR activation** occurs, leading to the formation of **resistosomes**.
- ETS** (Effector-Triggered Susceptibility) is activated, leading to **disease**.
- ETI** is also involved in the disease pathway.
- HR** (Hypersensitive Response) is triggered, leading to cell death (skull and crossbones symbol).
- small molecules** are produced, which can lead to **HR** or **resistance**.

Key Components and Interactions:

- Ca²⁺** influx is a central event in both pathways.
- ROS** production is linked to **NADPH-oxidase** and **MAPK** activation.
- MAPK** activation leads to **PTI** and **ETI**.
- PTI** and **ETI** have a positive feedback loop (+).
- ETI** leads to **resistance** or **HR**.
- HR** leads to **small molecules** production.
- small molecules** can lead to **resistance** or **HR**.

1.3 Regulated Cell Death in Plant-Microbe-Interactions

4

leading to a controlled cell death. In animals, RCD has been further categorized into distinct cell death programs such as apoptosis, pyroptosis, and necroptosis, each characterized by specific molecular mechanisms and cellular hallmarks.

Although research on RCD in plants has gained momentum only recently and lacks the extensive body of data available for animals, a specific kind of plant RCD has been studied for over a century (Morel and Dangl 1997; Balint-Kurti 2019). As outlined in Chapter 1.1, the recognition of microbial effectors by plant NLR triggers a rapid, localized form of cell death known as HR. HR is defined as a hypersensitive reaction to a microbe following the recognition of an microbial effector or effector target, leading to rapid plant cell death and restricting pathogen proliferation (Stakman 1915; Gaumann 1950). HR is conserved across higher plants and, as outlined in the previous section, is characterized calcium ion (Ca^{2+}) influx and ROS production (Delledonne et al. 2001). This response is strongly linked to resistance (R) genes, which primarily, but not exclusively, encode NLR proteins, and requires prior activation of a PTI response (Flor 1971; Kourelis and Hoorn 2018; Yuan et al. 2021). Comparing HR to animal RCD subtypes is challenging. While both systems exhibit shared hallmarks such as cytoplasmic shrinkage, chromatin condensation, and DNA laddering (Aist and Bushnell 1991; Bestwick et al. 1995), features like apoptotic blebbing are absent in plants, likely due to the presence of a rigid cell wall. Additionally, plants lack homologs of caspases, the key executor of animal RCD. However, cysteine proteases like vacuolar processing enzymes (VPEs), which exhibit caspase-like activity, are required for successful HR execution (Hoorn and Jones 2004; Hatsugai et al. 2004). These distinctions suggests that while HR shares similarities with animal RCD, it constitutes a distinct cell death pathway found only in plants.

The initiation, execution and termination of HR are tightly controlled, as dysregulation can lead to autoimmunity and runaway cell death, as observed in mutants lines carrying autoactive NLR alleles (Wang et al. 2015). NLR activity is tightly controlled by their protein levels, which are typically low and increase in response to immune signaling (Tan et al. 2007; Mohr et al. 2010). Furthermore, NLR proteins are multi-domain proteins (see Chapter 1.1.) whose activity is tightly regulated. Intramolecularly, their N-terminal CC- or TIR-domains are kept inactive by the C-terminal LRR domain. In addition, intermolecular interactions with other NLRs or chaperone-like proteins such as Heat Shock Protein 90 (Hsp90), Suppressor of G-Two allele of Skp1 (SGT1), or Required for Mla12 Resistance 1 (RAR1) further modulate their activity (Zhang et al. 2010; Wang et al. 2019b).

Until recently, the downstream signaling events following NLR activation remained poorly understood. Mutant screens primarily identified NLR proteins and their chaperones Hsp90, SGT1, and RAR1 as putative key players, suggesting a short downstream signaling pathway (Hubert et al. 2009). This hypothesis was supported by the recent discovery of multimeric plant structures, belonging to a group frequently named "deathosomes" (Maekawa et al. 2023). In animals, deathosomes - such as inflammasomes and apoptosomes - serve as assembly platforms for executor proteases such as caspases, which drive RCD in animals (Franchi et al. 2009; Li et al. 2017). Similarly, recent studies have shown that both plant CC-NLR proteins and RPW8 helper NLR form homo-oligomeric resistosomes upon effector recognition or activation via TIR-NLR signaling (Wang et al. 2019a; Forderer et al. 2022; Zhao et al. 2022; Selvaraj et al. 2024). Unlike animal deathosomes, plant CC-NLR- and RPW8-NLR resistosomes function as Ca^{2+} -permeable ion channels, facilitating an increased, long-lasting calcium influx (Bi et al. 2021; Jacob et al. 2021). Additionally,

TIR-NLR and TIR-only proteins form resistosomes with NADase or RNase activity, producing a variety of small signaling molecules such as 2'-(5''-phosphoribosyl)-5'-adenosine monophosphate and diphosphate (pRib-AMP/ADP) - immuno-stimulatory purine-based metabolites that propagate downstream signaling by activating RPW8-NLR resistosomes through the EDS1 signaling hub. Despite their enzymatic function, TIR-protein resistosomes ultimately contribute to an increased calcium influx (Ma et al. 2020; Martin et al. 2020; Huang et al. 2022; Jia et al. 2022; Yu et al. 2022). This topic is further explored in Chapter 5.

Another parallel between plants and animals RCD is the involvement of Mixed Lineage Kinase domain Like (MLKL) proteins. In animals, MLKL oligomerization and plasma membrane localization triggers necroptosis, a pro-inflammatory form of RCD (Sun et al. 2012; Seo et al. 2021). Plants possess MLKL homologs, plasma membrane-localized proteins that function as calcium channels and act redundantly with TIR-NLRs - but not CC-NLRs - in immune signaling (Mahdi et al. 2020; Shen et al. 2024). These findings further support the hypothesis that NLR- and MLKL-mediated signaling converge on the formation of Ca^{2+} -permeable ion channels, reinforcing the initial hypothesis of a short signaling pathway downstream of the initial HR initiation. Indeed, both calcium channel blockers and channel mutants impair HR, reinforcing the previously described role of Ca^{2+} influx as a core regulatory signal (Xu and Heath 1998; Ali et al. 2007).

Ferroptosis is the most recently characterized subtype of RCD. First identified in animals as a subtype of necrosis associated with cysteine and glutathione depletion, ROS and iron accumulation, and lipid peroxidation (Dixon et al. 2012; Friedmann Angeli et al. 2014), ferroptosis has been implicated in both viral and bacterial infections, where it facilitates both immune evasion and pathogen proliferation (Camini et al. 2017; Amaral et al. 2019). In plants, ferroptosis-like RCD was first observed in *Arabidopsis thaliana* roots following a heat shock. This form of RCD correlated with reductant depletion, iron accumulation, and lipid peroxidation and was inhibited by antioxidants such as ferrostatin and iron chelators like ciclopirox, which are known inhibitors of ferroptosis in animal cells (Distéfano et al. 2017). Recently, ferroptosis has been linked to necrosis in the *Nicotiana benthamiana*-tobacco mosaic virus pathosystem and HR triggered during the infection of rice plants by *Magnaporthe oryzae* (Macharia et al. 2020; Dangol et al. 2019). Overall, ferroptosis is a conserved RCD pathway found in animals and plants and interestingly, in leaves as well as in roots, distinguishing it from HR, which has so far only been observed in leaves. Over the past decades, research on RCD in plants, particularly in plant-microbe interactions, has expanded significantly. Although plant RCD research still lags behind its animal counterpart, recent discoveries have provided critical insights into its unique mechanisms. While some conserved features, such as deathosomes, lipid peroxidation, and membrane pore formation are shared between plant and animal systems, growing evidence suggests that plant RCD operates through distinct pathways. To fully understand plant RCD, it must be studied independently rather than solely through comparisons to animal models. Finally, the discovery of cell death in beneficial plant-microbe interactions has challenged the paradigm of cell death as a hallmark of pathogen infection (D'Haeze et al. 2003; Mucha et al. 2014; Ragnelli et al. 2014) (Chapter 4).

1.4 *Serendipita indica* as a Model for Beneficial Root Endophytes

Healthy plants actively recruit beneficial microbes from the bulk soil to establish a stable root microbiota. While most studies on root microbiota assembly have focused on bacteria, fungi also play a crucial role, either independently or in synergy with other microbes (Mahdi et al. 2021). Historically, research on beneficial plant-fungal interaction has primarily centered on arbuscular mycorrhiza fungi (AMF). AMF have been instrumental in plant evolution, from the terrestrialization of early plants to an impact on modern agriculture. However, their inability to grow axenically and incompatibility with the model plant *Arabidopsis thaliana*, present challenges for studying the molecular mechanism underlying plant-fungal interactions.

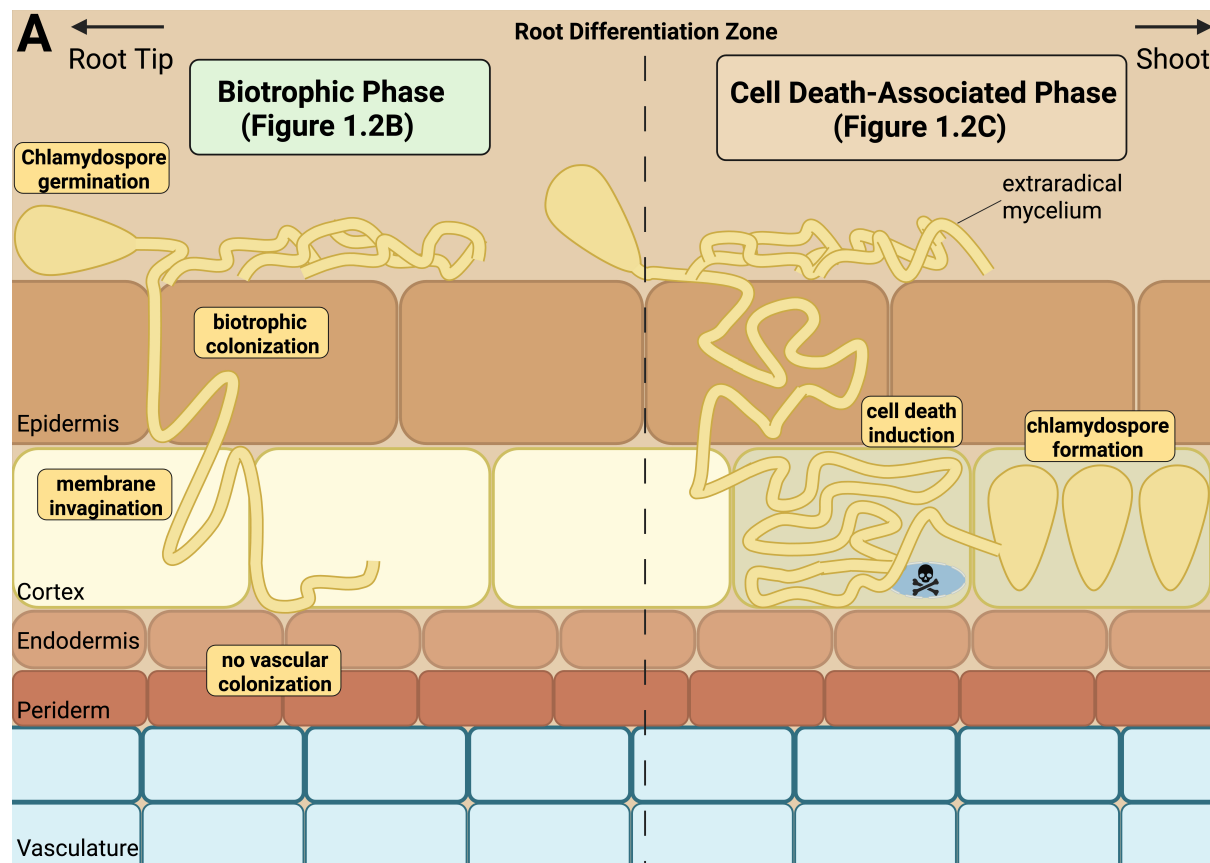
In comparison, members of the fungal order Sebaciniales (Agaricomycetes, Basidiomycota) are distributed globally and, despite being less abundant, are frequently associated with healthy plant roots. Sebaciniales colonize a broad range of host plants, employing different colonization strategies that range from mycorrhizal symbiosis to endophytism (Blechert et al. 1999; Weiss et al. 2011; Weiss et al. 2016; Mahdi et al. 2021). One particularly well-studied member of this order is *Serendipita indica*, an endophytic fungus first isolated from the roots of a shrub in the Indian Thar desert. *S. indica* has since become an important model organism for studying beneficial plant-fungal interactions (Verma et al. 1998). It colonizes a wide variety of host plants, including the model species *Arabidopsis thaliana*, as well as commercially important monocot and dicot crops like barley and tomato (Peškan-Berghöfer et al. 2004; Waller et al. 2005; Fakhro et al. 2010). Its ability to grow axenically and its genetic tractability make *S. indica* a powerful model system for studying fungal endophytes (Varma et al. 1999; Zuccaro et al. 2009).

Following chlamydospore germination, *S. indica* colonizes the epidermis and cortex of the host plant's root, both inter- and intracellularly (Figure 1.2A). Colonization of the root vascular tissue or aerial parts of the plant has not been reported. Notably, this colonization process is independent of canonical symbiosis genes required for AMF and rhizobial interactions (Banhara et al. 2015). During colonization, *S. indica* provides a range of beneficial effects to the host plant such as improved nutrient uptake, leading to enhanced biomass and yield (Shahollari et al. 2005; Waller et al. 2005; Achatz et al. 2010; Ray and Valsalakumar 2010). Additionally, *S. indica* can improve plant resistance to abiotic stresses, including drought and salinity (Zarea et al. 2012; Sherameti et al. 2008), as well as biotic stresses such as root and foliar pathogens (Stein et al. 2008; Sun et al. 2014; Li et al. 2023b; Eichfeld et al. 2024).

The lifecycle of *S. indica* follows a biphasic colonization strategy, beginning with an initial biotrophic phase (Figure 1.2B) (Franken et al. 2000; Zuccaro et al. 2011; Jacobs et al. 2011; Lahrmann et al. 2013). During this phase, invading fungal hyphae are engulfed in the host-plasma membrane, and a suite of small secreted proteins is secreted into the host apoplast. Many of these proteins function as effectors that help *S. indica* evade host immunity, scavenge ROS, and reprogram host phytohormone pathways (Akum et al. 2015; Wawra et al. 2016; Wawra et al. 2019; Nizam et al. 2019; Nostadt et al. 2020). Following the biotrophic phase, *S. indica* transitions to a cell death-associated phase, during which heavily colonized host cells undergo regulated cell death (Figure 1.2C). This phase is accompanied by transcriptional and nutritional reprogramming in *S. indica*, with nitrogen depletion likely serving as a key signal (Lahrmann et al. 2013). In addition, the dysregulation of phytohormones, such as gibberellic acid (GA), has been implicated in this

phase, potentially lowering the threshold for cell death induction (Jacobs et al. 2011). Recent findings suggest that this phase involves the production of a small purine-based metabolite that induces host cell death, marking a key mechanistic shift in the interaction (Chapter 4). Hallmarks of the *S. indica*-induced cell death include endoplasmic reticulum (ER) stress and the activation of VPEs, previously described as caspase-like proteases required for HR (Deshmukh et al. 2006; Qiang et al. 2012). Interestingly, VPEs exhibit caspase-like activity, which is essential for cell death execution in animal cells and are also required for HR execution (see Chapter 1.2) (Hatsugai et al. 2004; Qiang et al. 2012). However, the *S. indica*-induced cell death is distinct from necrosis, and beneficial effects persist even after its execution (Schäfer et al. 2009). Further evidence suggests that the controlled induction of host cell death is crucial for stable long-term colonization. Both *vpe* knockout mutants and plants overexpressing the conserved cell death inhibitor Inhibitor of Bcl-2-like protein 4 (BAX-I)-1 exhibit reduced fungal colonization, indicating that RCD is required for successful symbiosis (Mitsuhara et al. 1999; Hückelhoven 2004; Deshmukh et al. 2006; Qiang et al. 2012). Additionally, the formation of chlamydospores is frequently observed in dead host cells, suggesting that cell death might be a prerequisite for completing *S. indica*'s asexual lifecycle.

While the significance of regulated host cell death in *S. indica*-plant interactions has been recognized, the precise mechanisms of initiation, execution, regulation, and restriction remain unclear. This doctoral thesis aims to address these knowledge gaps by investigating the molecular and physiological processes underlying *S. indica*-induced cell death.



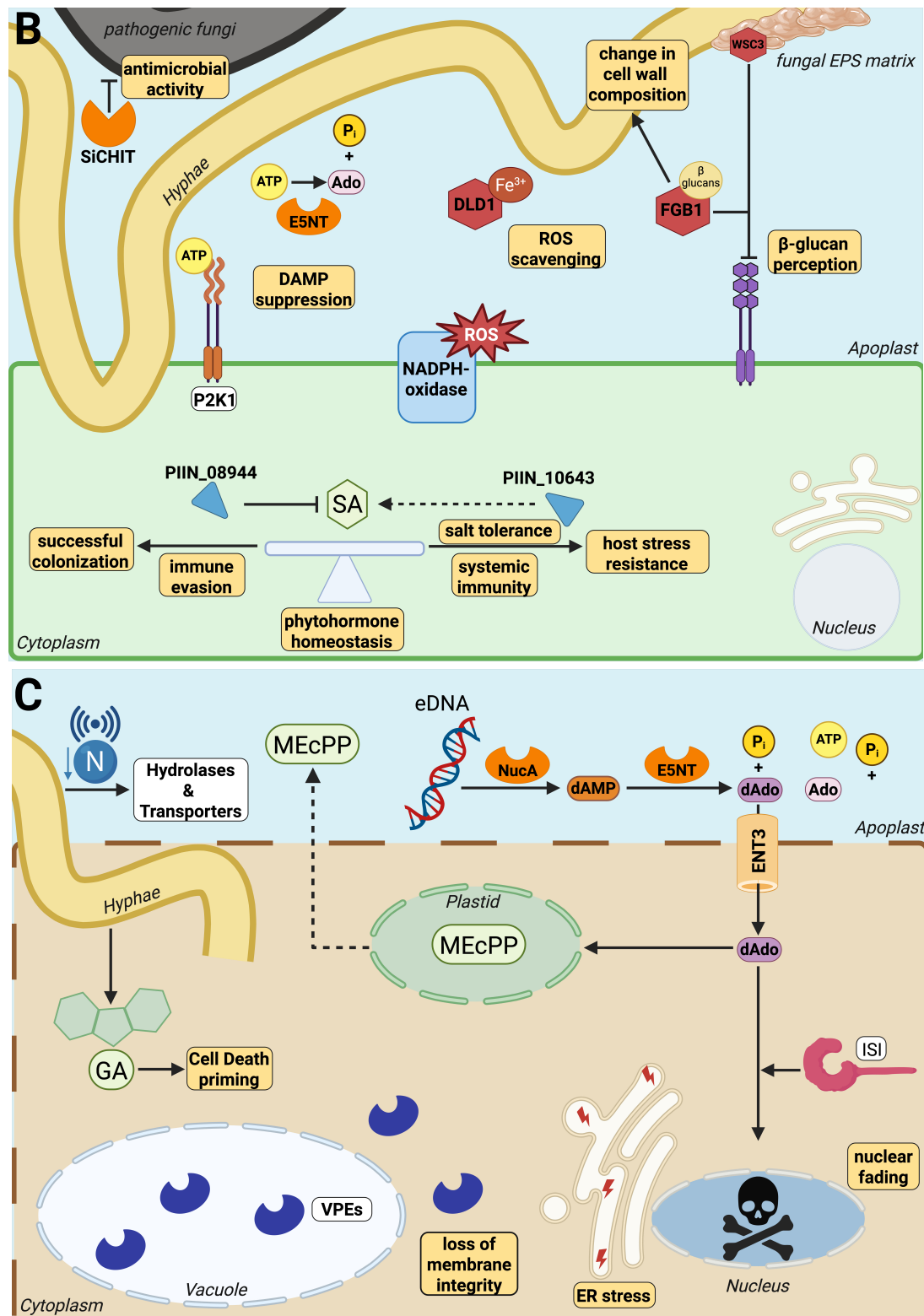


Figure 1.2: *Serendipita indica* as a Model for Beneficial Root Endophytes — A) Figure 1.2A illustrates the biphasic root colonization strategy of the beneficial endophytic fungus *Serendipita indica*. The left half of the figure depicts the biotrophic phase, which initiates with chlamydospore germination near the root surface. During this phase, fungal hyphae penetrate the epidermal layer—primarily in the root differentiation zone—invaginating the host cell membrane. Colonization is both intra- and intercellular within the epidermal and cortical layers, while the endodermis and vascular tissue remain uncolonized.

(continued) On the right half, the cell death-associated phase is characterized by localized host cell death in heavily colonized cells of the epidermis and cortex. This is accompanied by the formation of new chlamydospores within dead cortical cells. B) Biotrophic colonization phase: The early stage of root colonization is marked by the secretion of fungal effector molecules that facilitate immune evasion by sequestering MAMPs (SiE5NT, orange cleft, WSC3, & FGB1 red hexagons) and reducing ROS accumulation (DLD1, red hexagon). Although *S. indica* hyphae (yellow) invaginate the plant plasma membrane, cellular integrity is maintained during this phase. Intracellular effectors (blue triangles) can modulate the host's phytohormone signaling and antimicrobial effector (SiCHIT, orange cleft) can inhibit the growth of competing pathogenic fungi (black hyphae). C) Cell death-associated phase: Upon a nutrient-dependent switch to the cell death-associated phase, the fungal transcriptome shifts, resulting in the upregulation of hydrolases and nutrient transporter genes. A key mechanism of cell death induction is the synergistic production of dAdo by the two fungal effector enzymes SiNuCA & SiE5NT (orange clefts) in the apoplast. Hallmarks of this phase include ER stress, loss of tonoplast and plasma membrane integrity, and nuclear degradation. This phase is also characterized by the release of stress signals like MecPP into the apoplast, the involvement of the TIR-NLR ISI and VPE activity (blue clefts). Notably, cell death remains restricted to heavily colonized cells, and the beneficial effects associated with *S. indica* colonization are preserved.

1.5 Aim of this Thesis

RCD in plant–microbe interactions has been studied since the early 20th century. While the role of RCD as a defense mechanism against invading biotrophic pathogens is well established, the concept of necrotrophic pathogens hijacking host RCD has only recently gained attention. In contrast, cell death processes during beneficial plant–microbe interactions remain largely understudied. For example, while the ability of the root-colonizing endophyte *S. indica* to induce host cell death is known since its discovery two decades ago, most mechanisms of this process remained unresolved; in the root, RCD appears to facilitate colonization and the formation of intraradical chlamydospores (Deshmukh et al. 2006), with nutrient depletion likely serving as a cue for the transition from a biotrophic to a cell death-associated colonization phase (Lahrmann et al. 2013). While some host factors involved in this process, such as GA signaling and VPEs, have been identified (Jacobs et al. 2011; Qiang et al. 2012), the molecular mechanisms driving RCD initiation and execution during symbiosis remain unclear.

This thesis aims to characterize the initiation, execution, and regulation of host RCD induced by *S. indica*, with the goal of identifying key regulatory components on both the fungal and plant sides. Understanding these processes will shed light on the broader phenomenon of microbe-induced RCD, not only in pathogenic but also in mutualistic interactions. To this end, a complementary approach was employed. On the fungal side, we identified key effectors responsible for the production of RCD-inducing metabolites. On the plant side, we characterized factors that mediate RCD execution and regulation.

To enable robust high throughput phenotypic screening of cell death induced both by chemical compounds and pathogens, we developed a novel assay combining Pulse Amplitude Modulation (PAM) fluorometry and ion leakage measurements (Dunken et al. 2022) (Chapter 3).

We further investigated the mechanism of fungal RCD induction and enzymatically characterized

the two critical effector enzymes, SiNucA and SiE5NT. These enzymes synergistically produce the immunometabolite deoxyadenosine (dAdo), which we identified as a key infochemical inducing plant cell death. Through a combination of forward genetic screening, transcriptomic, and metabolomic approaches, we elucidated key host responses and contributing factors, leading to the identification of plant regulators such as the equilibrative nucleoside transporter (ENT)3 and the previously uncharacterized TIR-NLR Induced by *Serendipita indica* (ISI) (Dunken et al. 2024) (Chapter 4).

Finally, we contextualized our findings within the expanding field of plant immunity and cell death regulation. This culminated in a comprehensive review (Chapter 5) exploring purine-based signaling as a conserved and central hub of immune responses across biological kingdoms.

In summary, this thesis enhances our mechanistic understanding of cell death during *S. indica* colonization and provides broader insights into the role of RCD in beneficial plant-microbe interactions. Furthermore, it expands current perspectives on root immunity and introduces novel concepts contributing to the emerging field of immunometabolism - the study of how metabolic pathways and immune signaling intersect to regulate responses to biotic and abiotic stresses.

Chapter 2

Overview of Publications

Publications included in this thesis:

Nick Dunken, Lisa Mahdi, Rainer E. Häusler, and Alga Zuccaro (2022). Monitoring Cell Death Via Ion Leakage and PAM Fluorometry. *Methods in Molecular Biology*. https://doi.org/10.1007/978-1-0716-2079-3_14

Nick Dunken, Heidi Widmer, Gerd U. Balcke, Henryk Straube, Gregor Langen, Nyasha M. Charura, Pia Saake, Concetta De Quattro, Jonas Schön, Hanna Rövenich, Stephan Wawra, Mamoon Khan, Armin Djamei, Matias D. Zurbriggen, Alain Tissier, Claus-Peter Witte, and Alga Zuccaro (2024).

A nucleoside signal generated by a fungal endophyte regulates host cell death and promotes root colonization. *Cell Host & Microbe*. <https://doi.org/10.1016/j.chom.2024.10.020>

Ongoing submissions included in this thesis:

Nick Dunken, Tim Thomsen, and Alga Zuccaro (2025) Purine-based Infochemicals and Immunometabolites: A Comparative Review of Emerging Signaling Pathways in Plants and Animals. Under review in *FEMS MICROBIOLOGY REVIEWS* upon invitation.

Further publications arising from this thesis (not included):

Ernesto Llamas, Salvador Torres-Montilla, Hyun Ju Lee, María Victoria Barja, Elena Schlimgen, Nick Dunken, Prerana Wagle, Wolfgang Werr, Alga Zuccaro, Manuel Rodríguez-Concepción, David Vilchez (2021). The intrinsic chaperone network of Arabidopsis stem cells confers protection against proteotoxic stress. *Aging Cell*. <https://doi.org/10.1111/ace.13446>

Ernesto Llamas, Seda Koyuncu, Hyun Ju Lee, Markus Wehrmann, Ricardo Gutierrez-Garcia, Nick Dunken, Nyasha Charura, Salvador Torres-Montilla, Elena Schlimgen, Amrei M Mandel, Erik Boelen Theile, Jan Grossbach, Prerana Wagle, Jan-Wilm Lackmann, Bernhard Schermer, Thomas Benzing, Andreas Beyer, Pablo Pulido, Manuel Rodriguez-Concepcion, Alga Zuccaro, David Vilchez (2023). In planta expression of human polyQ expanded huntingtin fragment reveals mechanisms to prevent disease-related protein aggregation. *Nature aging*. <https://doi.org/10.1038/s43587-023-00502-1>

Patricia Zecua-Ramirez, Ernesto Llamas, Nyasha Charura, Nick Dunken, Concetta De Quattro, Alexander Mandel, Gregor Langen, Yasin Dagdas, Alga Zuccaro (2023). Autophagy restricts fungal accommodation in the roots of *Arabidopsis thaliana*. *bioRxiv*, currently under review in *Current Biology*. <https://doi.org/10.1101/2023.07.21.550010>

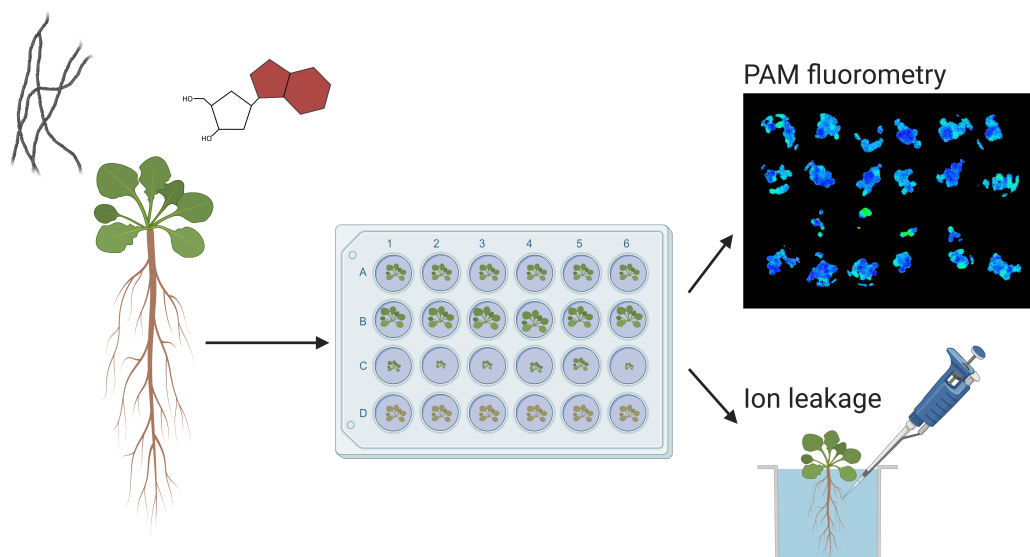
Chapter 3

Monitoring Cell Death Via Ion Leakage and PAM Fluorometry

Nick Dunken^{*}, Lisa Mahdi^{*}, Rainer E. Häusler, and Alga Zuccaro

Chapter in Methods in Molecular Biology, "Plant Proteases and Plant Cell Death" (2022) , Springer Nature, New York, NY

^{*} These authors contributed equally to this work.



Author Contributions:

Nick Dunken, Lisa Mahdi, and Alga Zuccaro developed the protocol and wrote the manuscript. Rainer E. Häusler corrected the manuscript.



Chapter 14

Monitoring Cell Death Via Ion Leakage and PAM Fluorometry

Nick Dunken, Lisa Mahdi, Rainer E. Häusler, and Alga Zuccaro

Abstract

Cell death in plants plays a major role during development as well as in response to certain biotic and abiotic stresses. For example, plant cell death can be triggered in a tightly regulated way during the hypersensitive response (HR) in defense against pathogens or be elicited by pathogenic toxin deployment. Monitoring cell death and its impact on plant health can aid in the quantification of plant disease symptoms and help to identify the underlying molecular pathways. Here, we describe our current protocol for monitoring plant cell death via ion leakage and Pulse-Amplitude-Modulation (PAM) fluorometry. We further provide a detailed protocol for the sample preparation, the measurement, and the data evaluation and discuss the complementary nature of ion leakage and PAM fluorometry as well as the potential of PAM fluorometry for high-throughput screenings.

Key words Plant cell death, ION leakage, Pulse-Amplitude-Modulation (PAM) fluorometry, Pathogen treatment, Chemical treatment, Large-scale screening

1 Introduction

Plant cell death is essential for plant development [1] as well as in response to biotic and abiotic stresses [2, 3]. Forms of regulated cell death (RCD) such as apoptosis-like cell death, necroptosis, and the hypersensitive response (HR) are induced in response to different stimuli and exhibit distinct cell death characteristics. As a drastic and irreversible transition, RCD is tightly regulated by the plant [4]. However, RCD can also be induced or suppressed by plant-associated microorganisms and pathogens can trigger host cell death independently of the plant cell death machinery via the secretion of toxins and cell-wall degrading enzymes.

Monitoring cell death allows to quantify disease as well as stress symptoms of the plant and helps to unravel the underlying molecular mechanisms.

Plant cell death results in a loss of cell membrane integrity that ultimately leads to the leakage of cellular electrolytes into the surrounding medium. Measuring the corresponding increase in

electric conductivity in the surrounding liquid is a commonly used, direct proxy to quantify plant cell death in response to abiotic and biotic stresses [5]. However, ion leakage measurements are time-consuming as each sample has to be measured individually. Thus, they are less suitable for large-scale screenings.

The photosynthetic activity reflects the health status of a plant [6, 7]. The maximum potential quantum yield of photosystem II electron transport is defined as the variable fluorescence (F_V) divided by the maximum fluorescence (F_M) (F_V/F_M), where $F_V = F_M - F_0$ (F_0 : ground fluorescence). Healthy and non-stressed plants obtain a F_V/F_M value of approximately 0.8 [8, 9] whereas biotic and abiotic stresses lead to a decrease in the F_V/F_M ratio up to a total loss of photosynthetic activity upon cell death. Thus, while PAM fluorometry is an indirect proxy for cell death, it provides additional information about the overall health status of the plant. Due to its simple implementation and time-effectiveness, PAM measurements are especially useful for large-scale screenings. Furthermore, PAM measurements do not require a liquid-based system and can also be used for plants on solid medium or soil. Both ion leakage and PAM fluorometry are noninvasive and thus suitable to measure cell death progression over time on the same samples.

Here, we show the function and specificities of cell death monitoring via a combination of ion leakage and PAM fluorometry, exemplified by a chemically induced, developmental cell death as well as a biotic stress induced cell death.

Representing a chemical induced cell death, we treated *Arabidopsis thaliana* seedlings with methyl jasmonate (MeJA), a bioactive derivate of jasmonic acid (JA) that induces leaf senescence [10]. Treatment with MeJA leads to increased electric conductivity as well as to a constant, uniform decrease in the F_V/F_M ratio (Fig. 1).

Representative of a biotic interaction inducing cell death, we took advantage of a previously described tripartite system consisting of the detrimental fungal pathogen *Bipolaris sorokiniana* and the beneficial fungal root endophyte *Serendipita vermifera* in barley [11]. While *B. sorokiniana* colonization results in host cell death, co-colonization with *S. vermifera* counteracts these detrimental effects [11]. We here applied this tripartite system in *Arabidopsis thaliana* (Fig. 1). We inoculated *Arabidopsis* roots with *S. vermifera*, *B. sorokiniana*, or a combination of both fungi (Fig. 3). As observed in barley, *B. sorokiniana* was able to colonize *Arabidopsis* roots. Upon colonization, *B. sorokiniana* caused typical disease symptoms on *Arabidopsis* roots and shoots including root browning. Consistently, *B. sorokiniana* colonization results in a constant increase in electric conductivity. This increase is diminished in plants when the roots are additionally inoculated with *S. vermifera*, reflecting the protective function of *S. vermifera*.

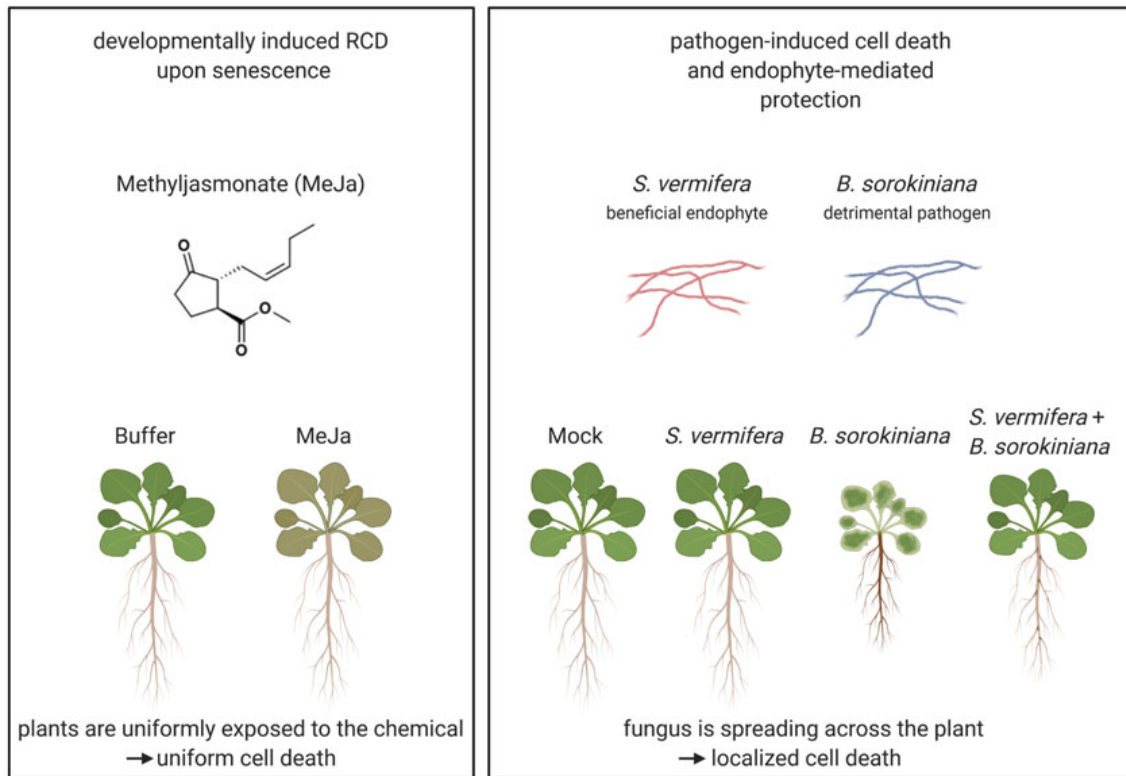


Fig. 1 Experimental setup depicting a chemically induced developmental cell death via methyl jasmonate (MeJA) (left) and a pathogen-induced cell death via *B. sorokiniana* colonization in a tripartite system with the beneficial endophyte *S. vermifera* (right)

PAM analysis revealed consistent results. Interestingly, *B. sorokiniana* colonized plants do not display a uniformly decreased F_V/F_M ratio (Fig. 2b). Instead, there is a local reduction of photosynthetic activity and cell death that slowly spreads across the whole shoot. This in turn leads to a constant reduction in the photosynthetic active leaf area over time reflecting the proceeding cell death.

2 Materials

2.1 Equipment

1. 24-Well culture plates.
2. Square plates.
3. Forceps.
4. Conductivity meter.
5. Imaging PAM fluorometer (e.g., Imaging-PAM M-Series Chlorophyll Fluorescence System (Walz)) able to measure culture plates (e.g., 24-well plates).

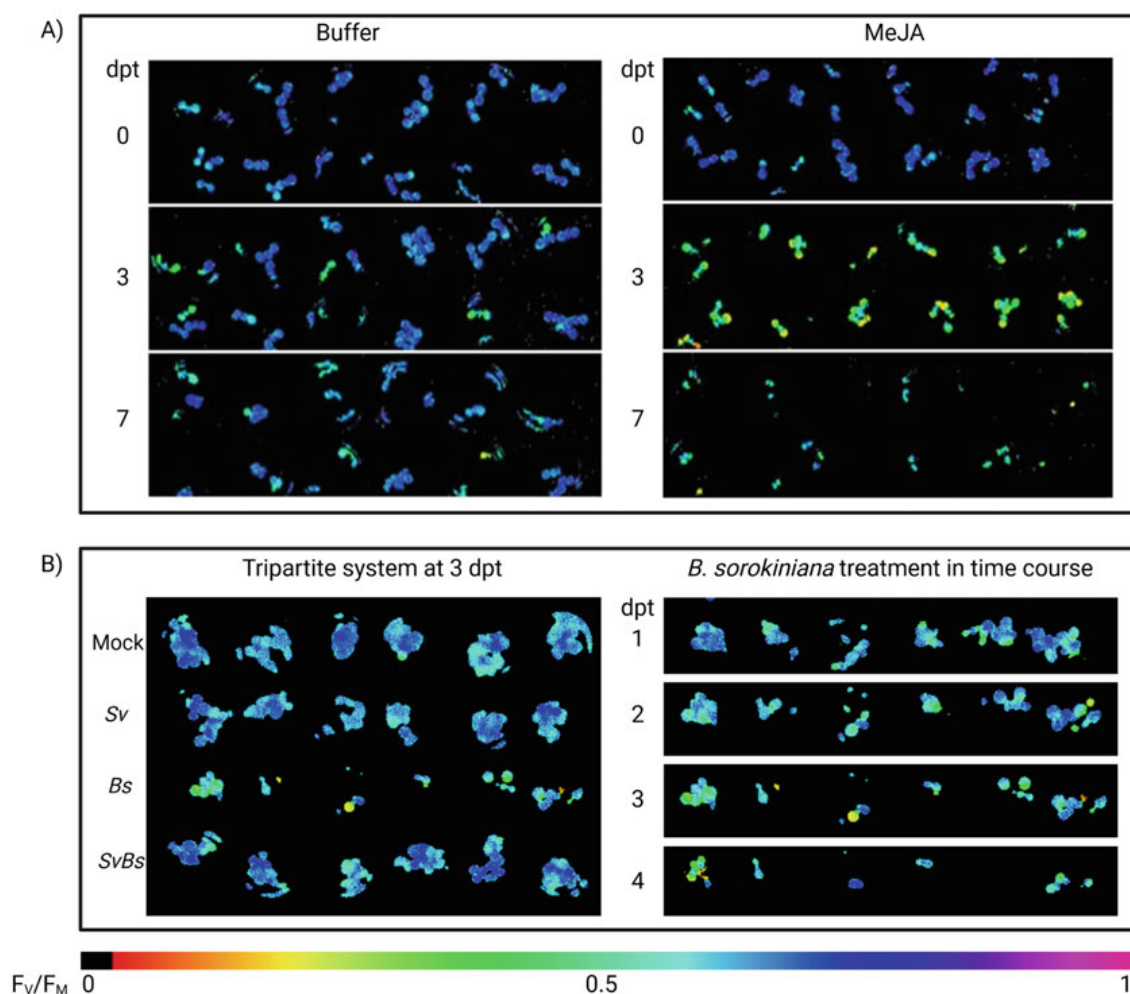


Fig. 2 PAM fluorometry pictures of (a) 7-day-old *Arabidopsis thaliana* seedlings treated with 50 mM MES buffer (pH 5.6) or 500 mM MeJA, respectively, at 0, 3, and 7 days post transfer (dpt). (b) 14-day-old *Arabidopsis thaliana* seedlings inoculated with sterile water (Mock), the beneficial fungal endophyte *S. vermifera* (Sv), the fungal pathogen *B. sorokiniana* (Bs) or a combination of both fungi (SvBs). At 7 days post inoculation (dpi) the plant roots were washed and the seedlings were transferred to deionized water. Pictures were taken every 24 h for 4 days. Blue color represents high photosynthetic activity while lighter colors represent a lower photosynthetic activity

6. Personal computer with a software suitable for PAM evaluation (e.g., ImagingWin, Walz, Germany) installed.
7. Growth cabinet or growth chamber for plant growth under controlled conditions.

2.2 Reagents and Consumables

1. *Arabidopsis thaliana* seeds.
2. Murashige-Skoog (MS) medium including vitamins.
3. Sucrose.
4. 70% Ethanol.

time course monitoring of *B. sorokiniana*-induced cell death in *Arabidopsis thaliana*

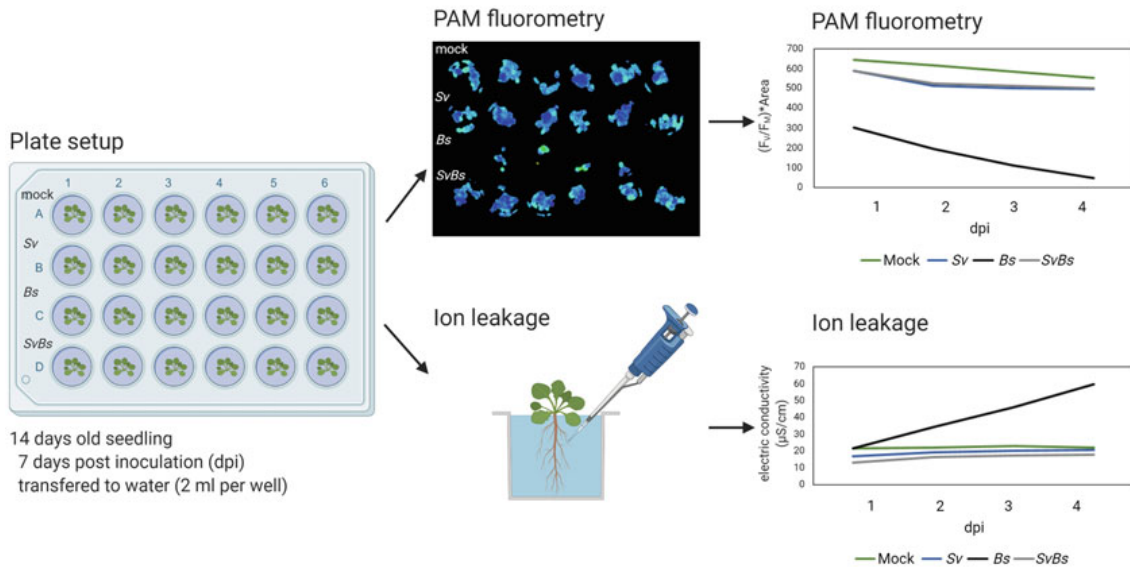


Fig. 3 Evaluation of *B. sorokiniana*-induced cell death via PAM fluorometry and ion leakage analysis. Both readouts are noninvasive and thus suitable to measure cell death progression over time on the same samples. While ion leakage represents a direct proxy, its measurement is more time-consuming. PAM fluorometry visualizes plant cell death indirectly via F_v/F_m -ratios but can represent a more efficient screening strategy and can be enhanced by additional analysis of the photosynthetic active area

5. 100% Ethanol.
6. Plant Agar.
7. Deionized water or sterile 2.5 mM 2-(N-morpholino) ethane-sulfonic acid (MES) adjusted to pH 5.6 (*see Note 1*).
8. Chemical or organism to be tested, here: 10 mM MeJA solved in 2.5 mM MES (pH 5.6) or fungal inoculum in water.

3 Method

3.1 Seedling Sterilization, Germination, and Treatment

1. Sterilize *Arabidopsis thaliana* seeds by washing them two times with 70% EtOH for 5 min followed by one washing step with 100% EtOH for 5 min.
2. Let the seeds dry under sterile conditions.
3. Sow sterilized seeds on $\frac{1}{2}$ MS, 4% plant agar, and 1% sucrose square plates.
4. Stratify the seeds for 2 days at 4 °C in darkness.
5. Then transfer plates to a growth chamber at a day/night cycle of 8/16 h at 22/18 °C, 60% humidity and a light intensity of $125 \mu\text{mol m}^{-2} \text{s}^{-1}$.

6. Let seedlings germinate for 7 days in these conditions prior to the treatment.
7. *For chemical treatment:* Fill each of the 24 wells of a sterile culture plate with 1.9 mL of 2.5 mM MES buffer (pH 5.6).
8. Transfer 3–5 7-day-old seedlings to each well and let them regenerate in the growth chamber at the abovementioned conditions (*see Note 2*).
9. After regeneration, take first measurements of ion leakage and PAM fluorometry as a time point 0.
10. Treat the 8-day-old seedlings with 100 μ L of 20 \times chemical solution (e.g., 10 mM MeJA; end concentration: 500 μ M) per well.
11. *For tripartite treatment:* transfer 20 seedlings per plate to $\frac{1}{2}$ MS plates, 4% plant agar without added sucrose.
12. Inoculate the plants with the respective fungi or fungal combination, here with 1 mL of a 1 g/L *S. vermifera* mycelium solution per plate, 1 mL of a 5000 spores/L *B. sorokiniana* spore solution per plate, or a combination of both fungi.
13. Distribute the fungal solution on the roots and the plate area below the roots. For this, distribute the solution on the roots and let it run down the plate. Recollect it with a pipette and repeat until a homogenous inoculation is achieved.
14. Incubate the plates in the growth chamber (conditions see above) for 7 days.
15. At 7 days post inoculation, when the seedlings are 14 days old, fill each well with 2 mL deionized water, wash the colonized roots to remove the extraradical hyphae, and transfer 3–5 seedlings to each well.
16. For washing, hold the seedlings carefully with forceps, dip the roots into autoclaved water, and slip the wet root over tissue paper. Extraradical hyphae will stick to the tissue paper.

3.2 Time Course PAM and Ion Leakage Measurement

1. Measure ion leakage for each well according to the manufacturer instructions. Be careful not to touch the seedlings while measuring (*see Note 3*).
2. Before measuring PAM, transfer the plates to darkness for 15 min to enable measurement of the maximum fluorescence (F_M) as well as the ground fluorescence (F_0) in the dark-adapted leaves (*see Note 4*). For dark adaption, the plates can be kept in a closed drawer or covered with aluminum foil. Afterward, measure the fluorescence by taking pictures with the fluorometer plate by plate in darkness according to the manufacturer's instructions.
3. Continue the measurements every 24 h for 4–8 days.

3.3 Evaluation of PAM with and Without Area

1. The evaluation differs depending on the Imaging PAM fluorometer and the respective evaluation-software. Here, we explain the evaluation with ImagingWin (Walz) in more detail.
2. Open the first PAM file (.pim or .xpim) in ImagingWin. Photosynthetically active leaf tissues are visualized in blurry colors (Fig. 2).
3. Click on Options and uncheck “Mean over Area of interest (AOI).”
4. Reset the AOI and calculate the F_V/F_M value of each well by adding AOI circles around each well.
5. Extract the F_V/F_M values (denoted as Y(II) by the program) using the “Report” tab. The resulting F_V/F_M values represent the mean PSII activity of living leaves of the 3–5 seedlings in each well.
6. Export a JPEG file of the F_V/F_M channel and measure the photosynthetic active leaf area via a suitable software (e.g., ImageJ [12]) to include the dimension of the living leaf area into the evaluation (see Notes 5 and 6).
7. Multiply the F_V/F_M value for each well with the photosynthetic active leaf area.

4 Notes

1. For chemical treatments, the buffer is of high importance for the experiment. Many chemicals have a strong effect on the pH of the solution. The buffer ensures that the plant health is not affected by an extremely acidic or basic pH.
2. When transferring and washing the seedlings, be careful not to injure the plants, as this induces stress and tampers the results. An additional recovery day between picking and treatment is thus recommended (see Subheading 3.1).
3. 24 h of regeneration before starting measuring are recommended to avoid artifacts in ion leakage measurements due to wounding during the seedling transfer.
4. Be sure not to expose the dark adapted plants to light before measuring. Also, do not measure the plates twice without repeating the adaption process.
5. During evaluation, be aware that dead cells are no longer photosynthetic active and are thus excluded from the program calculation. Including the area in your calculation will allow you to take the dead leaf area into account. For a cell death response such as observed upon *B. sorokiniana* treatment (Figs. 1, 2b and 3) the area is essential for quantification. For a cell death that spreads and proceeds uniformly on the plant

such as in case of MeJA (Figs. 1 and 2a), the area calculation is not necessarily needed. However, it still increases the measurement sensitivity.

6. As it is hard to perform absolute size measurements of the photosynthetic active leaf area due to the lack of a size standard, relative sizes can be compared. For this, the plates have to be continuously measured in the same setup (same height, zoom, etc.)

Acknowledgments

The authors thank Prof. Pitter Huesgen and Dr. Gregor Langen for editing the draft. We acknowledge the support by the Cluster of Excellence on Plant Sciences (CEPLAS), the Max-Planck-Gesellschaft through the International Max Planck Research School (IMPRS) on “Understanding Complex Plant Traits using Computational and Evolutionary Approaches” and the University of Cologne. The research was funded by the Deutsche Forschungsgemeinschaft (DFG, German Research Foundation) under Germany’s Excellence Strategy—EXC 2048/1–25 Project ID: 390686111 as well as the projects ZU 263/11-1 (SPP DECRyPT) and–SFB-1403–414786233 (SFB cell death and immunity).

References

1. Van Hautegeem T, Waters AJ, Goodrich J, Nowack MK (2015) Only in dying, life: programmed cell death during plant development. *Trends Plant Sci* 20(2):102–113. <https://doi.org/10.1016/j.tplants.2014.10.003>
2. Greenberg JT, Yao N (2004) The role and regulation of programmed cell death in plant-pathogen interactions. *Cell Microbiol* 6(3): 201–211. <https://doi.org/10.1111/j.1462-5822.2004.00361.x>
3. Petrov V, Hille J, Mueller-Roeber B, Gechev TS (2015) ROS-mediated abiotic stress-induced programmed cell death in plants. *Front Plant Sci* 6:69. <https://doi.org/10.3389/fpls.2015.00069>
4. Antoine Danon VD, Mailhac N, Gallois P (2000) Plant programmed cell death: a common way to die. *Plant Physiol Biochem* 38(9): 647–655. [https://doi.org/10.1016/S0981-9428\(00\)01178-5](https://doi.org/10.1016/S0981-9428(00)01178-5)
5. Demidchik V, Straltsova D, Medvedev SS, Pozhvanov GA, Sokolik A, Yurin V (2014) Stress-induced electrolyte leakage: the role of K⁺-permeable channels and involvement in programmed cell death and metabolic adjustment. *J Exp Bot* 65(5):1259–1270. <https://doi.org/10.1093/jxb/cru004>
6. Murchie EH, Lawson T (2013) Chlorophyll fluorescence analysis: a guide to good practice and understanding some new applications. *J Exp Bot* 64(13):3983–3998. <https://doi.org/10.1093/jxb/crt208>
7. Barbagallo RP, Oxborough K, Pallett KE, Baker NR (2003) Rapid, noninvasive screening for perturbations of metabolism and plant growth using chlorophyll fluorescence imaging. *Plant Physiol* 132(2):485–493. <https://doi.org/10.1104/pp.102.018093>
8. Hogewoning SW, Wientjes E, Douwstra P, Trouwborst G, van Ieperen W, Croce R, Harbinson J (2012) Photosynthetic quantum yield dynamics: from photosystems to leaves. *Plant Cell* 24(5):1921–1935. <https://doi.org/10.1105/tpc.112.097972>
9. Bjorkman O, Demmig B (1987) Photon yield of O₂ evolution and chlorophyll fluorescence characteristics at 77 K among vascular plants of diverse origins. *Planta* 170(4):489–504. <https://doi.org/10.1007/BF00402983>

10. Weaver LM, Gan S, Quirino B, Amasino RM (1998) A comparison of the expression patterns of several senescence-associated genes in response to stress and hormone treatment. *Plant Mol Biol* 37(3):455–469. <https://doi.org/10.1023/a:1005934428906>
11. Sarkar D, Rovenich H, Jeena G, Nizam S, Tissier A, Balcke GU, Mahdi LK, Bonkowski M, Langen G, Zuccaro A (2019) The inconspicuous gatekeeper: endophytic *Serendipita vermifera* acts as extended plant protection barrier in the rhizosphere. *New Phytol* 224(2):886–901. <https://doi.org/10.1111/nph.15904>
12. Schindelin J, Arganda-Carreras I, Frise E, Kaynig V, Longair M, Pietzsch T, Preibisch S, Rueden C, Saalfeld S, Schmid B, Tinevez JY, White DJ, Hartenstein V, Eliceiri K, Tomancak P, Cardona A (2012) Fiji: an open-source platform for biological-image analysis. *Nat Methods* 9(7):676–682. <https://doi.org/10.1038/nmeth.2019>

Chapter 4

A nucleoside signal generated by a fungal endophyte regulates host cell death and promotes root colonization

Nick Dunken, H. Widmer, GU. Balcke, H. Straube, G. Langen, NM Charura, P. Saake, C. De Quattro, J. Schön, H. Rövenich, S. Wawra, M. Khan, A. Djamei, MD Zurbriggen, A. Tissier, CP Witte, and Alga Zuccaro

Published in Cell Host & Microbe (2024)

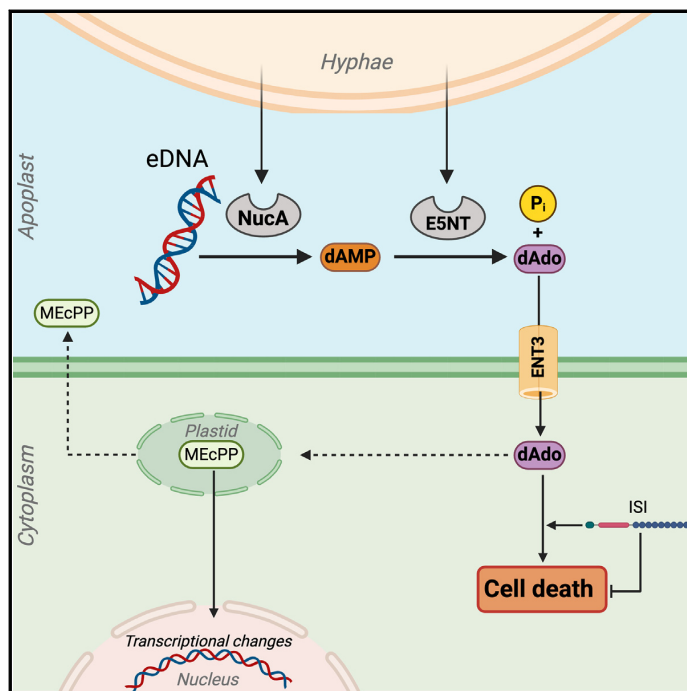
Author Contributions:

A.Z. and N.D. designed the experiment. N.D. did characterize the role of *ENT3* and *AtISI* experimentally. H.W. did analyze the role of *SiNucA*. G.U.B. and A.T. did produce metabolomics data. H.S. and C.P.W. did perform enzymatic assays and measured nucleotide concentrations. G.L. and C.D.Q. did perform all bioinformatic analyses. N.M.C. and S.W. did perform microscopy. P.S. did perform calcium influx and ROS burst assays. J.S. and M.D.Z. did perform protoplast assays. H.R. did support the conceptualization of the experiment and perform initial cell death assays. M.K. and A.D. did perform experiments with *Marchantia polymorpha*. The manuscript was written by A.Z. and N.D. with continuous input from all authors.

Cell Host & Microbe

A nucleoside signal generated by a fungal endophyte regulates host cell death and promotes root colonization

Graphical abstract



Authors

Nick Dunken, Heidi Widmer, Gerd U. Balcke, ..., Alain Tissier, Claus-Peter Witte, Alga Zuccaro

Correspondence

azuccaro@uni-koeln.de

In brief

Dunken and colleagues find that the beneficial root endophytic fungus *Serendipita indica* secretes two effector enzymes into the host apoplast to produce deoxyadenosine (dAdo). dAdo triggers host cell death and other immune responses in an ENT3-dependent manner. This process is influenced by the TIR-NLR protein *AtISI* and promotes root colonization.

Highlights

- Two apoplastic enzymes from a beneficial root endophytic fungus synergistically produce dAdo
- dAdo is a potent inducer of plant cell death
- ENT3 transporter is essential for dAdo uptake and modulates fungal-elicited cell death
- Mutations in the *AtISI* locus reduce dAdo-induced cell death and affect fungal colonization



Dunken et al., 2024, Cell Host & Microbe 32, 2161–2177
December 11, 2024 © 2024 The Author(s). Published by Elsevier Inc.
<https://doi.org/10.1016/j.chom.2024.10.020>



Article

A nucleoside signal generated by a fungal endophyte regulates host cell death and promotes root colonization

Nick Dunken,¹ Heidi Widmer,^{1,5} Gerd U. Balcke,² Henryk Straube,^{3,4} Gregor Langen,¹ Nyasha M. Charura,¹ Pia Saake,^{1,5} Concetta De Quattro,^{1,5} Jonas Schön,^{5,6} Hanna Rövenich,^{1,5} Stephan Wawra,^{1,5} Mamoon Khan,⁷ Armin Djamei,⁷ Matias D. Zurbriggen,^{5,6} Alain Tissier,^{2,8} Claus-Peter Witte,³ and Alga Zuccaro^{1,5,9,*}

¹Institute for Plant Sciences, University of Cologne, Cologne, Germany

²Department of Cell and Metabolic Biology, Leibniz Institute of Plant Biochemistry, Halle, Germany

³Molecular Nutrition and Biochemistry of Plants, Leibniz University Hannover, Herrenhäuser Str. 2, 30419 Hannover Germany

⁴Section for Plant Biochemistry and Copenhagen Plant Science Centre, Department of Plant and Environmental Sciences, University of Copenhagen, Frederiksberg, Denmark

⁵Cluster of Excellence on Plant Sciences (CEPLAS), Cologne, Germany

⁶Institute of Synthetic Biology, Heinrich-Heine-Universität Düsseldorf, Düsseldorf, Germany

⁷Department of Plant Pathology, Institute of Crop Science and Resource Conservation (INRES), University of Bonn, Bonn, Germany

⁸Institute of Pharmacy, Martin-Luther University Halle-Wittenberg, Halle, Germany

⁹Lead contact

*Correspondence: azuccaro@uni-koeln.de

<https://doi.org/10.1016/j.chom.2024.10.020>

SUMMARY

The intracellular colonization of plant roots by the beneficial fungal endophyte *Serendipita indica* follows a biphasic strategy, including a host cell death phase that enables successful colonization of *Arabidopsis thaliana* roots. How host cell death is initiated and controlled is largely unknown. Here, we show that two fungal enzymes, the ecto-5'-nucleotidase *SiE5NT* and the nuclease *SiNucA*, act synergistically in the apoplast at the onset of cell death to produce deoxyadenosine (dAdo). The uptake of extracellular dAdo but not the structurally related adenosine activates cell death via the equilibrative nucleoside transporter ENT3. We identified a previously uncharacterized Toll-like interleukin 1 receptor (TIR)-nucleotide-binding leucine-rich repeat receptor (NLR) protein, ISI (induced by *S. indica*), as an intracellular factor that affects host cell death, fungal colonization, and growth promotion. Our data show that the combined activity of two fungal apoplastic enzymes promotes the production of a metabolite that engages TIR-NLR-modulated pathways to induce plant cell death, providing a link to immunometabolism in plants.

INTRODUCTION

Regulated cell death (RCD) occurs in plants as part of normal growth and development and in response to abiotic and biotic stimuli. In plant-microbe interactions, host cell death programs can mediate either resistance or successful infection. Depending on the type of microbial lifestyle, host cell death can benefit the plant by stopping the growth of biotrophs or the microbe by promoting the growth of necrotrophs. Thus, control of plant host cell death is critical to the outcome of an interaction. Host cell death also plays a role in certain beneficial interactions, challenging the paradigm that cell death in plant-microbe interactions implies pathogenesis or host-microbe incompatibility. Both symbiosis with beneficial microbes and infection by pathogens require sophisticated control of host defenses and nutrient fluxes. Certain features of the interaction of beneficial microbes, such as affecting host immunity, metabolism, and host cell death, are reminiscent of pathogen infections. In

Rhizobium-legume symbioses, root nodules are formed to provide a niche for bacterial nitrogen fixation. The formation of infection pockets is associated with host cell death and the production of hydrogen peroxide.¹ Host cell death is also observed in ectomycorrhizal symbioses^{2,3} and is a requisite for the establishment of symbiotic interactions with the widely distributed beneficial fungi of the order Sebaciales.^{4–6} Molecular environmental studies have shown that some of the most abundant taxa of this order have little, if any, host specificity and interact with a wide variety of plant species. Sebaciales isolates, including *S. indica* and *S. vermifera*, exhibit beneficial effects such as growth promotion, increased seed production, and protection from pathogens and thus play an important role in natural and managed ecosystems.^{7–9} The requirement of restricted host cell death for the establishment of certain beneficial microorganisms leads to the hypothesis that the activation of cell death mechanisms in roots has a more important ecological function than previously thought.



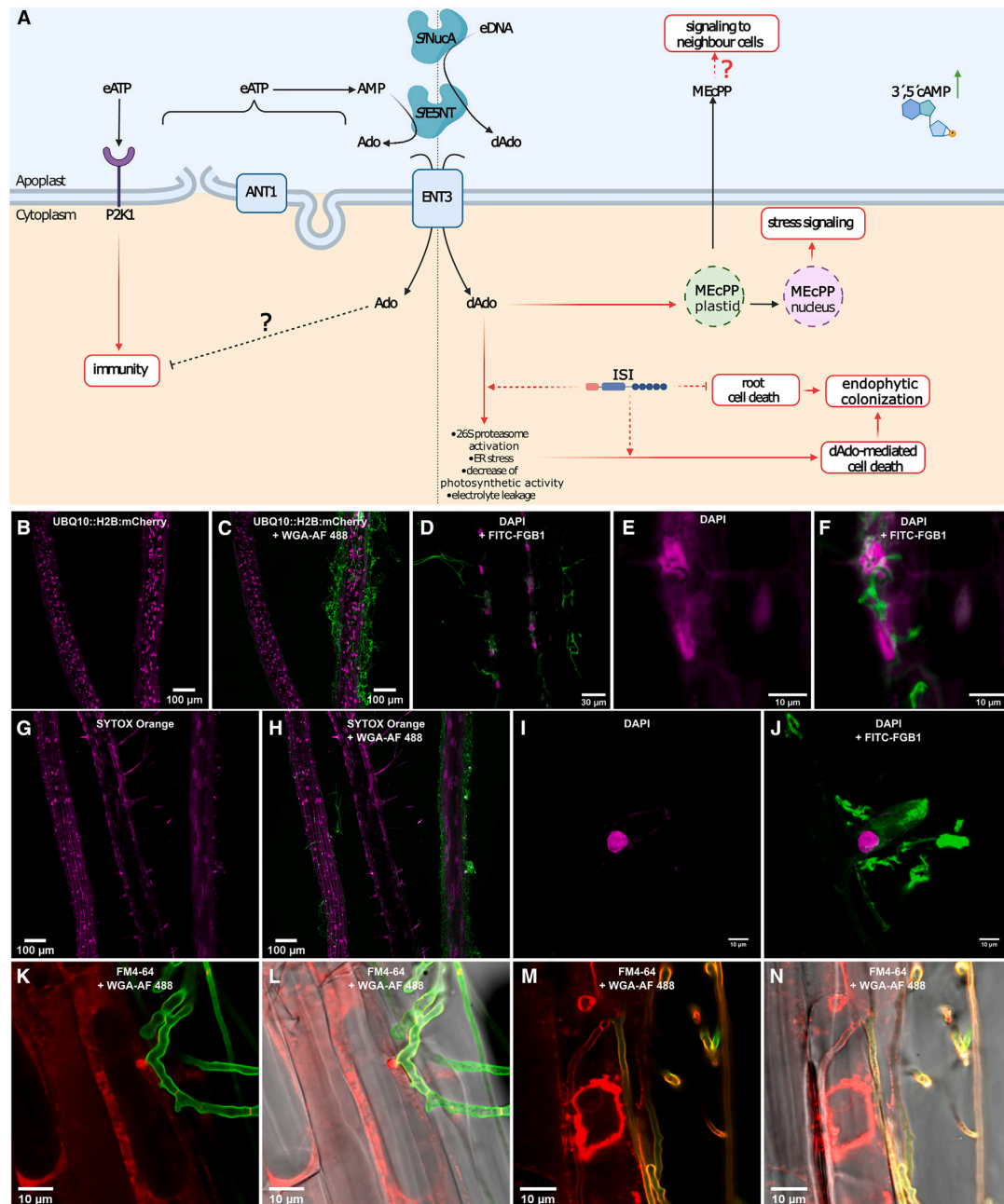


Figure 1. Host cell death during *S. indica* colonization of roots

(A) Current model for dAdo-triggered cell death during colonization of *A. thaliana* roots by *S. indica*. The beneficial endophyte *S. indica* secretes two enzymes into the apoplast, the nuclease SiNucA and the ecto-nucleotidase SiE5NT. SiE5NT is initially involved in manipulating eATP signaling (left), as described in Nizam et al.¹³ SiNucA accumulates at the onset of cell death. The combined activity of SiNucA and SiE5NT releases deoxynucleosides from DNA, with a strong preference for dAdo, a potent cell death inducer in animal systems. dAdo is transported to the cytoplasm via AtENT3, where it triggers a cell death process and contributes to successful fungal colonization. dAdo induces the production of the retrograde stress signal MEcPP from plastids, activating stress signaling and possibly intercellular communication. Cell death triggered by dAdo is modulated by an uncharacterized TIR-type NLR protein (ISI, induced by *S. indica*), providing a link to immunometabolism.

(legend continued on next page)

In the hosts *Hordeum vulgare* (hereafter barley) and *A. thaliana* (hereafter Arabidopsis), Sebacinale fungi initially colonize living cells that die during the progression of colonization.^{4–6,10–12} This symbiotic cell death is thought to contribute to niche differentiation during microbial competition for space and nutrients in the root and appears to be restricted to colonized cells in the epidermis and outer cortex. The host pathways that control the induction and execution of plant cell death and the fungal elicitors/ effectors that initiate this process in roots are still largely unknown.^{5,6,13,14} Pathogenic and beneficial fungi have a large repertoire of secreted effectors that can affect host cell physiology and suppress plant defenses, promoting fungal colonization. In fungi, effectors have been described mainly in biotrophic and hemibiotrophic foliar pathogens.¹⁵ By contrast, only a few effectors of root symbiotic fungi have been functionally characterized.^{13,16–20} Therefore, the modes of action of effectors of mutualistic fungi remain poorly understood.

Using genomics, transcriptomics, and proteomics, we identified proteins secreted by *S. indica* into the root apoplast.¹³ One secreted protein consistently found at various stages of symbiosis is the ecto-5'-nucleotidase *SiE5NT* (PIIN_01005).¹³ Expression of *SiE5NT* is induced during colonization of barley and Arabidopsis roots but not in axenic fungal culture.¹³ Animal ecto-5'-nucleotidases play a key role in the conversion of AMP to adenosine, counteracting the immunogenic effects of extracellular ATP (eATP) released from host cells.²¹ eATP is an important signal in plants that controls development and response to biotic and abiotic stresses. In Arabidopsis, eATP mediates various cellular processes through its binding to the purinergic membrane-associated receptor proteins DORN1/P2K1 and P2K2.²² In the apoplast, eATP accumulation increases cytoplasmic calcium and triggers a defense response against invading microbes. The perception of extracellular nucleotides, such as eATP, plays an important role in plant-fungal interactions—we previously demonstrated this by showing that the knockout (KO) mutant *dorn1* of Arabidopsis is better colonized by *S. indica*. Partially purified preparations of *SiE5NT* are able to hydrolyze adenylates to adenosine, which alters the eATP content in the apoplast and the plant response to fungal colonization.¹³ Secretion of *SiE5NT* in Arabidopsis leads to enhanced colonization by *S. indica*, confirming its role as an apoplastic effector protein. Considering the important role *SiE5NT* plays in fungal accommodation at early symbiotic stages, we proposed that modulation of extracellular nucleotide levels and their perception play a key role in compatibility during early plant-fungal interactions in roots.¹³ Secreted *SiE5NT* homologs are also present in fungal patho-

gens such as *Colletotrichum incanum* and *Fusarium oxysporum* and other Arabidopsis endophytes such as *Colletotrichum tofieldiae*, suggesting that purine-based extracellular biomolecules also play a role in other plant-fungal interactions.

During the colonization of barley and Arabidopsis by *S. indica*, a small fungal endonuclease, which we named *SiNucA* (PIIN_02121), is secreted with *SiE5NT* at the onset of cell death.^{13,23} In plants, the mechanisms linking immune recognition of DNA danger signals in the extracellular environment to innate signaling pathways in the cytosol are poorly understood, as is the role of (deoxy)nucleotide metabolism in root colonization and cell death. Here, we show that the synergistic activity of *SiNucA* and *SiE5NT* leads to the production of deoxyadenosine (dAdo) from extracellular DNA (eDNA). dAdo production by fungal extracellular enzymes is similar to the processes involved in dAdo-mediated immune cell death of *Staphylococcus aureus* in animals, which appears to ensure bacterial survival in host tissues.^{24,25} Staphylococcal nuclease and adenosine synthase A (AdsA, a homolog of *SiE5NT*) are both required to release dAdo from neutrophil extracellular traps (NETs), which has a potent cytotoxic effect on macrophages and other immune cells.²⁴

We demonstrate that dAdo but not the structurally similar Ado activates a previously unidentified cell death mechanism in plants. Expression of either extracellular *SiNucA* or *SiE5NT* in planta results in enhanced colonization by *S. indica* and host cell death.¹³ We found that a mutation in the equilibrative nucleoside transporter 3 (ENT3) of Arabidopsis leads to a strong and specific resistance phenotype to dAdo-induced cell death. Accordingly, the *ent3* KO line shows less fungal-induced cell death in the root and accumulates less of the extracellular signaling metabolite methylerythritol cyclodiphosphate (MEcPP) in response to fungal colonization or dAdo treatment.

Finally, through a mutant screen of Arabidopsis transfer DNA (T-DNA) insertion lines, we identified a previously uncharacterized locus including several Toll-like interleukin 1 receptor (TIR)-nucleotide-binding leucine-rich repeat receptor (NLR) proteins. Mutation in one of these proteins appears to modulate cell death triggered by dAdo, as well as fungal colonization and growth promotion. While most characterized TIR-NLRs (TNLs) function as sensors of pathogen-secreted effectors, our findings suggest that this TNL may be involved in the regulation of cell death induced by a metabolite produced during symbiosis. We hypothesize that the hydrolysis of extracellular metabolites by the fungal enzymes *SiNucA* and *SiE5NT* provides a link between purine metabolism, immunity, and cell death pathways in roots (Figure 1A).

(B and C) Arabidopsis roots expressing the fluorescent nuclear marker UBQ10::H2B:mCherry (magenta) stained with the fungal cell wall marker wheat germ agglutinin Alexa Fluor 488 conjugate WGA-AF 488 (green) at 10 dpi.

(D) Plant nuclei stained with DAPI (magenta) and fungal cell wall and matrix stained with the β -glucan binding lectin FGB1-fluorescein isothiocyanate (FITC) 488 (green) at 6 dpi. As colonization by *S. indica* progresses, host nuclei often become elongated and fade.

(E and F) Close-up of *S. indica* hyphae embedded in a host nucleus from (D).

(G and H) Staining of nucleic acids of roots colonized with *S. indica* with the dead cell indicator (membrane integrity marker) SYTOX Orange (magenta) and fungal hyphae with WGA-AF 488 (green) at 10 dpi.

(I and J) *S. indica* hyphae fluorescently labeled with the β -glucan-binding lectin FGB1-FITC 488 (green) embedded in a DAPI-stained host nucleus (magenta) at 6 dpi.

(K–N) Progressive vacuolar collapse of colonized root cells. Fungal hyphae are stained with WGA-AF 488 (green), while membranes are stained with FM4-64 (red).

(J and K) Initial biotrophic colonization. (M and N) Vacuolar collapse in a dying host cell. CLSM was repeated at least five times with 3 to 4 plants colonized by *S. indica*. Fading of nuclei at the onset of cell death during fungal colonization was regularly observed.

RESULTS

Fading of host nuclei and vacuolar collapse are hallmarks of symbiotic cell death during *S. indica* root colonization

S. indica induces restricted cell death in colonized root cells of Arabidopsis and barley, resulting in characteristic cytological features at later stages of colonization. In these two hosts, the timing and extent of cell death differ.^{5,6} In Arabidopsis, the cell death phenotype is less pronounced than in barley, but cytological analyses showed fading of host nuclei, vacuolar collapse, and swelling of the endoplasmic reticulum (ER) in colonized cells,⁵ indicating ER stress and host cell death during root colonization (Figures 1B–1N). To characterize the timing of fungal-induced cell death, the presence and shape of plant nuclei during colonization by *S. indica* were monitored by confocal laser scanning microscopy using either an Arabidopsis line expressing the nuclear marker H2B:mCherry (Figures 1B and 1C) or the nucleic acid dye DAPI (Figures 1D–1F) and the cell death dye SYTOX Orange (Figures 1G and 1H). In the Arabidopsis H2B:mCherry line, plant nuclei in the epidermal layer were often elongated (Figures 1B and 1C), faded, and eventually disappeared by 8 to 10 dpi in heavily colonized areas of the root. Nuclei stained with SYTOX Orange were visible at 7 to 8 days post inoculation (dpi), indicating that at this time the plasma and nuclear membranes of Arabidopsis were permeable to the dye, which is a hallmark of cell death (Figures 1G and 1H). In dying cells, *S. indica* hyphae embedded in plant nuclei were frequently observed, indicating that during activation of cell death, the fungus might digest and feed on host nuclear DNA (Figures 1E, 1F, 1I, and 1J). These results show that Arabidopsis root cell death begins around 7 dpi, and by 10 dpi, most host nuclei have faded or disappeared in cells colonized by *S. indica*.

SiNucA and SiE5NT act synergistically in the production of deoxynucleosides

Although the interaction between *S. indica* and roots has been extensively studied, comparatively little is known about the contribution of apoplastic effectors to fungal accommodation or the mechanism of cell death in this system.^{13,18,20,26} We previously analyzed soluble apoplastic proteins in barley at different stages of *S. indica* colonization. We found that SiE5NT was consistently one of the predominant fungal proteins.¹³ We demonstrated that SiE5NT functions as a membrane-bound nucleotidase that is released into the apoplast during host colonization. Partially purified preparations of SiE5NT are capable of releasing phosphate and adenosine from ATP, ADP, and AMP.¹³ In addition, the small secreted protein SiNucA with predicted endonuclease activity (Figure S1) was found in the apoplastic fluid of colonized barley roots at the onset of cell death (5 dpi).¹³ SiNucA is also secreted during root colonization in Arabidopsis.²³ SiNucA expression is transiently induced during cell death in barley and Arabidopsis, as shown by transcriptomic data⁶ and quantitative PCR analyses (Figure 2A). This prompted us to further investigate the involvement of SiNucA in fungal colonization and host cell death. The secretion of SiNucA and its enzymatic activity were investigated by overexpressing a SiNucA:HA:His construct in *S. indica* (Figures 2B and S1). Supernatants from fungal overexpression (OE) strains and affinity-purified

SiNucA were able to degrade double-stranded DNA and single-stranded RNA from fungal and plant material, indicating nonspecific nuclease activity (Figure 2C). Addition of magnesium and calcium increased SiNucA activity in *in vitro* assays, whereas EDTA inhibited it (Figure S1F).

To investigate the effects of SiNucA on colonization, we tested independent homozygous T3 lines heterologously expressing a native version of SiNucA in Arabidopsis under control of the 35S promoter. Expression of SiNucA in Arabidopsis resulted in higher fungal colonization at 7 dpi, which correlated with the SiNucA expression level (Figures 2D and 2E), demonstrating its importance in fungal accommodation. Overcolonization resulted in a reduction in plant biomass that was not observed in the mock-treated SiNucA expression lines (Figure S2A). Localization studies by confocal microscopy of Arabidopsis roots expressing either full-length SiNucA or a version lacking the N-terminal signal peptide (SP) fused to mCherry confirmed secretion of the full-length SiNucA fusion protein into the apoplast and functionality of the SP. After plasmolysis, the mCherry fluorescence signal was visible on the cell walls and apparently on the membrane of the shrinking cells for the full-length SiNucA fusion protein but not for the cytoplasmic version without SP (Figures S2B and S2C). Remarkably, *S. indica* colonization was associated with the observation that the full-length mCherry-tagged SiNucA localized to host nuclei specifically in colonized cells. By contrast, in adjacent non-colonized cells, the mCherry signal was localized at the cell periphery, even following plasmolysis (Figures 2F and S2B–S2D). The detection of SiNucA in the apoplast¹³ and within the nuclei of colonized host cells (Figure 2F) suggests that it may be directed toward the nucleus during colonization, where it could potentially interact with both eDNA and nuclear DNA.

The co-occurrence of SiNucA and SiE5NT in the apoplast at 5 dpi led us to speculate that these two enzymes might cooperate in promoting fungal colonization of roots. Using affinity-purified SiE5NT from leaves of *Nicotiana benthamiana*, we found activity with dAMP and AMP substrates (Figures 3A and 3B), whereas no activity was detected for other deoxynucleotides (deoxycytidine monophosphate, deoxyguanosine monophosphate, deoxythymidine monophosphate) or nucleotides (guanosine monophosphate, uridine monophosphate, 3',5'-cAMP) tested. Moreover, dATP and the general phosphatase substrate *para*-nitrophenyl pyrophosphate (pNPP) were not SiE5NT substrates. Interestingly, only dAMP was hydrolyzed at a constant rate, whereas the AMP hydrolysis rate gradually decreased under the selected reaction conditions (Figures S3A and S3B). The K_M for AMP (15.9 μ M) was \sim 20-fold lower than for dAMP (361.6 μ M), but the k_{cat} for dAMP (11.9 s^{-1}) exceeded that of AMP (1.1 s^{-1}) by a factor of \sim 10 (Figures 3A and 3B). These data suggest that SiE5NT hydrolyzes AMP slightly better at low substrate concentrations (below 20 μ M) but is far more efficient for dAMP at higher substrate concentrations that might prevail in a nucleus undergoing degradation and in the case of eDNA degradation. To test potential synergistic activity of SiNucA and SiE5NT, we incubated DNA with SiE5NT and SiNucA alone and in combination. As expected, SiNucA degraded DNA (Figure 3C), but neither deoxynucleotides nor deoxynucleosides were detected as reaction products by LC-MS analysis, suggesting that SiNucA degrades DNA to oligonucleotides. SiE5NT also did not release deoxynucleotides from DNA but produced small amounts of

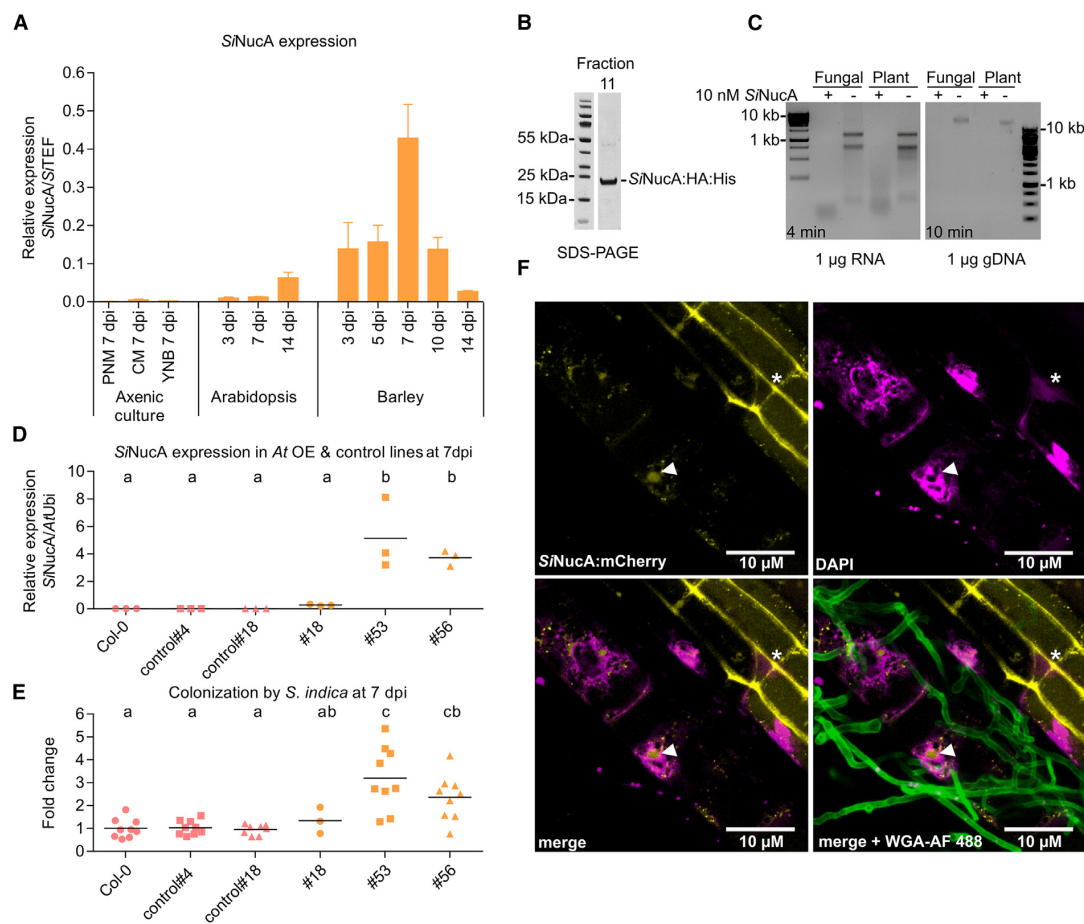


Figure 2. *SiNucA* is a small secreted nuclease involved in fungal accommodation

(A) *SiNucA* expression in Arabidopsis and barley roots colonized by *S. indica* and axenic cultures measured by the $2^{-\Delta CT}$ method. Error bars: SD, $n = 3$ (biological replicates).

(B) *SiNucA*:HA:His protein enrichment from culture filtrate precipitated with 80% ammonium sulfate and separated by size exclusion chromatography. The resulting fraction was separated by SDS-PAGE, and *SiNucA*:HA:His was stained with Coomassie brilliant blue.

(C) The purified *SiNucA*:HA:His protein was incubated with fungal (*S. indica*) or plant (Arabidopsis) RNA or DNA in 5 mM Tris buffer (pH = 8) containing 1 mM $MgCl_2$ and 1 mM $CaCl_2$ for 4 (RNA) or 10 (DNA) min and visualized after gel electrophoresis.

(D) Arabidopsis lines expressing *SiNucA* driven by the 35S promoter (lines 18, 53, and 56) compared with control lines (4 and 18; segregating from T2 generation and Col-0 WT). Roots of plants grown on $\frac{1}{2}$ MS medium were inoculated with *S. indica* and analyzed after 7 dpi. The dots represent independent biological replicates, and the lines represent the mean. Different letters indicate significantly different groups as determined by one-way ANOVA with post-hoc Tukey HSD test ($p < 0.05$).

(E) Root colonization by *S. indica* in transgenic 35S::*SiNucA*-Arabidopsis lines at 7 dpi was assessed by RT-qPCR by comparing expression of the fungal housekeeping gene *STEF* and the plant gene *AtUbi* and the $2^{-\Delta\Delta CT}$ method, normalized to colonization in the WT Col-0. The dots represent independent biological replicates, while the lines represent the mean. Different letters indicate significantly different groups as determined by one-way ANOVA with post-hoc Tukey HSD test ($p < 0.05$).

(F) CLSM live cell images of an Arabidopsis root expressing *SiNucA*:mCherry (yellow) and inoculated with *S. indica*. Fungal cell walls are stained with WGA-AF 488 (green) and nuclei with DAPI (magenta). *SiNucA*:mCherry fluorescence signal accumulates in the apoplast/cell periphery in non-colonized root cells (asterisk) and relocalizes in host nuclei in colonized cells (arrow).

deoxynucleosides (Figure 3D). However, in combination, *SiNucA* and *SiE5NT* released deoxynucleosides from DNA with a strong preference for dAdo. This demonstrates the ability of *SiE5NT* to use oligonucleotides released by *SiNucA* as a substrate and act synergistically with *SiNucA* to preferentially release dAdo from DNA (Figure S3C).

dAdo induces host cell death

The production of dAdo by the synergistic activity of the two secreted fungal enzymes resembles the processes involved in dAdo-mediated immune cell death of *S. aureus* in animal cells, which ensures the exclusion of macrophages from the center of abscesses where the bacteria survive.^{24,25} This motivated

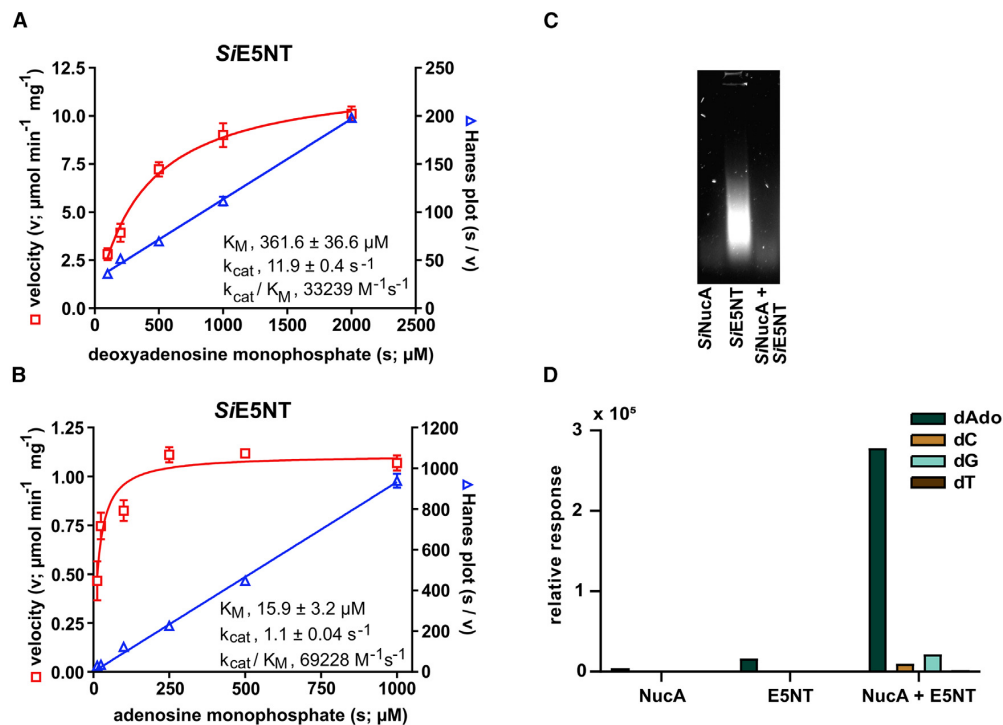


Figure 3. SiNucA and SiE5NT act synergistically in the production of deoxy nucleosides from DNA

(A) Enzymatic activity and kinetic constants of SiE5NT. Left axis, initial catalytic velocity (v) for phosphate production at different dAMP concentrations fitted with the Michaelis-Menten equation. Right axis, ratio of dAMP concentrations and velocities (s/ v) plotted against dAMP concentrations (s) fitted by linear regression (Hanes plot). Error bars: SD, $n = 3$.

(B) As in (A), but using AMP as substrate ($n = 3$).

(C) Degradation of DNA by SiNucA and/or SiE5NT. 2% agarose gel loaded with the products of a 1-h incubation of 10 μg salmon sperm DNA at 25°C with different enzyme combinations. (D) Relative quantification of deoxyadenosine (dAdo), deoxycytidine (dC), deoxyguanosine (dG), and deoxythymidine (dT) released during incubation in (C) by HPLC-MS/MS. Deoxynucleotides could not be detected in any of the reactions.

us to test the effect of dAdo in plants. Incubation of the Arabidopsis H2B-mCherry line with extracellular dAdo but not with Ado resulted in the fading and disappearance of nuclei in roots within 48 h (Figure 4A). This root cell death phenotype could be quantified using Evans blue azo dye (Figures 4B and 4C). In addition, extracellular dAdo-triggered hallmarks of cell death, such as increased electrolyte leakage, induction of cell death marker gene expression, as well as activation of the 26S proteasome, and decreased photosynthetic activity (F_v/F_m) (Figures 4D–4H and S4A). The effects were concentration-dependent, and removal of dAdo from the culture supernatant 24 h post treatment (hpt) resulted in recovery of Arabidopsis seedlings, indicating that activation of this cell death program is still reversible at this stage (Figures S4B and S4C).

A cell death phenotype was also observed in young leaves of *N. benthamiana* during expression by *Agrobacterium tumefaciens* infiltration of a SiE5NT construct, including the SP for secretion (Figure S5) and in seedlings incubated with dAdo (Figure S6A). Cell death was not visible in older leaves or in leaves of *N. benthamiana* expressing SiNucA or the suppressor of gene silencing p19. The observed phenotype suggests that the

presence of SiE5NT is sufficient to trigger cell death in this plant host upon wounding by agroinfiltration, which could release DNA and DNases into the apoplast or elicit a response to the presence of the bacterium or its proteins. To test whether cell death triggered by dAdo is conserved in basal plant lineages, we additionally tested its effect on the liverwort *Marchantia polymorpha*. Incubation with dAdo also induced cell death in this plant species (Figure S6B). These findings suggest that dAdo-mediated cell death operates through a conserved mechanism across diverse plant lineages. However, the precise extent and regulatory pathways involved in different species require further investigation.

dAdo induces the MEP pathway and accumulation of the stress-signaling metabolite MEcPP

To investigate the mechanism by which dAdo triggers cell death in plants and to determine whether it activates stress-signaling pathways, we analyzed the transcriptional response of Arabidopsis at 0, 3, and 12 hpt using RNA-seq. Most marker genes for RCD²⁸ were upregulated at 12 h (Figure 4I; Tables S1, S2, and S3). In addition, the plastidial 2-C-methyl-D-erythritol-4-phosphate (MEP) pathway was induced at 12

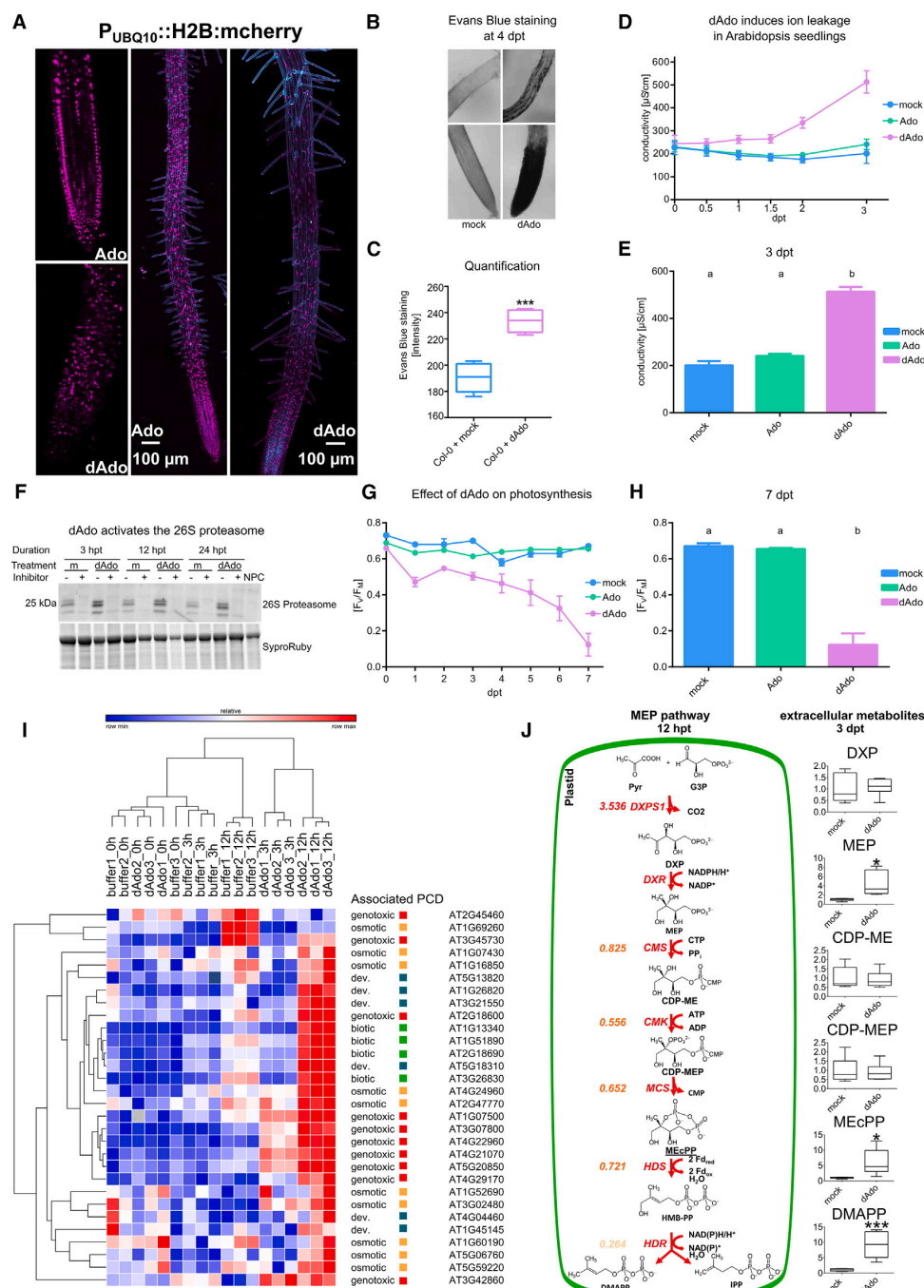


Figure 4. dAdo induces cell death in planta

(A) CLSM images of 7-day-old Arabidopsis roots expressing the nuclear marker UBQ10::H2B:mCherry. Incubation with dAdo but not Ado (500 μ M) results in disorganization of Arabidopsis cells in the root tip and disappearance or fading of nuclear material.
(B) Bright-field microscopy of the root tip and differentiation zone of Arabidopsis seedlings treated with mock/dAdo (500 μ M) and stained with Evans blue cell death dye.

(legend continued on next page)

hpt (Figure 4J; Table S4). Accordingly, MEcPP, a precursor of plastidial isoprenoids and a stress-specific retrograde signaling metabolite produced by the MEP pathway, accumulated extracellularly 3 days post treatment (dpt) as measured by liquid chromatography-tandem mass spectrometry (LC-MS/MS) (Figure 4J). Abiotic stress and wounding increase levels of cytoplasmic MEcPP, which coordinates stress response pathways in plants.²⁹ The detection of this isoprenoid intermediate in the extracellular environment after dAdo treatment suggests that this metabolite may serve as a stress signal in bystander cells. Incubation of Arabidopsis with extracellular MEcPP did not result in cell death, demonstrating that accumulation of this metabolite is not sufficient to trigger cell death and therefore is not the cause of the observed dAdo-mediated cell death (Figure S6C).

dAdo-triggered signaling and cell death are not mediated by canonical pattern-triggered immune responses

To determine whether cell death triggered by dAdo is mediated by signals generated by an immune receptor at the cell surface, we tested the ability of it to trigger a rapid response by monitoring calcium influx and ROS production. Both responses are part of pattern-triggered immunity (PTI), a process activated by recognition of microbe-associated molecular patterns (MAMPs) or damage-associated molecular patterns (DAMPs) by pattern-recognition receptors (PRRs) at the plasma membrane.^{30–32}

Incubation of Arabidopsis seedlings with dAdo did not elicit calcium influx, whereas treatment with ATP or ADP, which have been previously described as DAMPs^{33,34} but also with dATP or dADP, triggered a rapid calcium influx that was dependent on the eATP receptor P2K1/DORN1 (Figures S7A–S7C). Treatment with dAdo or with any of the other purine derivatives did not induce a ROS burst (Figures S7F and S7G). On the other hand, incubation with dAdo and to a lesser extent with ATP or dAMP but not Ado resulted in accumulation of the stress marker metabolite MEcPP and induction of the DAMP/MAMP- and fungus-responsive gene AT1G58420 at 3 dpt (Figures S7D and S7E;

Table S5).^{13,33,35} Overall, these data suggest that dAdo does not act as a typical extracellular DAMP or MAMP but induces a signaling pathway independent of calcium influx and ROS production.

The Arabidopsis transporter ENT3 is required for dAdo-mediated signaling and cell death

The fact that we did not observe a canonical PTI response to dAdo led us to speculate that uptake of this metabolite is necessary to promote plant signaling and trigger cell death. In the animal system, treatment with extracellular dAdo leads to the accumulation of intracellular dATP, which appears to impair DNA synthesis and induces apoptosis via activation of caspase 3.²⁵ Rapidly dividing cells are particularly susceptible to cell death triggered by dAdo, and it has been shown that the toxic effect of dAdo in the animal system depends on dAdo uptake by the human ENT1 (hENT1).²⁵ Similarly, we observed high sensitivity of dividing cells in root tips using Evans blue staining and young *N. benthamiana* plants (Figures 4A, 4B, and S6A). On the contrary, *S. indica* was not sensitive to dAdo and showed normal growth even at high concentrations (Figure S8). In Arabidopsis, eight potential ENT family members are annotated in the genome. Two of them are expressed in roots, namely ENT3, which is localized at the plasma membrane, and ENT1, which is localized at the tonoplast. The Arabidopsis KO line *ent3* showed a stronger resistance phenotype to dAdo-induced cell death compared with both the WT and *ent1* KO lines but is unaffected in the response to MeJA-induced cell death (positive control) (Figures 5A–5C and S9A–S9E). ENT3 has been shown to transport adenosine and uridine with high affinity, and their uptake is competitively inhibited by co-treatment with various purine and pyrimidine nucleosides and 2'-deoxynucleosides, including dAdo.³⁶ This suggests that ENT3 has a broad substrate specificity and is a strong candidate for uptake of extracellular dAdo. In a competition assay, addition of extracellular Ado decreased the cell death phenotype induced by dAdo, suggesting that these two extracellular metabolites compete for the same transporter at the cell membrane (Figure 5D). Interestingly,

(C) Quantification of root cell death in Col-0 root tips 4 days after dAdo treatment. Cell death was assessed by Evans blue staining. Boxplots show data from 5 biological replicates. Asterisks represent a significant difference from the mock-treated samples analyzed by Student's t test ($p < 0.005$ ***). The experiment was independently repeated 3 times with similar results.

(D) Electrolyte leakage of Col-0 seedlings (9 days old) in MES buffer after mock, Ado, or dAdo treatment. Error bars show the standard error of the mean (SEM) from 6 biological replicates. The experiment was independently repeated at least 3 times with similar results.

(E) Electrolyte leakage at 3 dpt of seedlings from (D). Error bars show the SEM of 6 biological replicates. Different letters indicate significantly different groups as determined by one-way ANOVA with post-hoc Tukey HSD test ($p < 0.05$). The experiment was independently repeated at least 3 times with similar results.

(F) Activity of the 26S proteasome of Arabidopsis. Total protein extracts from 14-day-old seedlings treated with 500 μ M dAdo or 2.5 mM MES buffer (M) were incubated with 1 μ M of probe MVB072.²⁷ Prior to labeling, samples were incubated with 50 μ M of the proteasome inhibitor epoxomicin (+) or DMSO (–). Samples were then labeled for 2 h and separated by SDS-PAGE. 26S proteasome activity was visualized by fluorescence scanning. SYPRO™ Ruby staining was performed to compare sample amounts. A non-probe control (NPC) consisting of a mixture of all samples incubated with DMSO was used as an additional control. The experiment was repeated twice with similar results.

(G) Photosynthetic activity (F_v/F_m) of 7-day-old Col-0 seedlings incubated with 500 μ M Ado or dAdo. Error bars represent the SEM obtained from twelve biological replicates. The experiment was repeated three times with similar results.

(H) Photosynthetic activity (F_v/F_m) of 7-day-old Col-0 seedlings incubated with 500 μ M Ado or dAdo at 7 dpt from (G). Error bars represent the SEM obtained from twelve technical replicates. Different letters indicate significantly different groups as determined by one-way ANOVA with post-hoc Tukey HSD test ($p < 0.05$).

(I) Heatmap of core regulated cell death (RCD) marker-genes expression (selected from Olvera-Carrillo et al.²⁸) of 7-day-old Arabidopsis seedlings after dAdo treatment at 0, 3, and 12 h. RNA-seq data are presented as \log_2 (tpm) (Table S6). Heatmaps and hierarchical clustering (one-minus Pearson correlation) were generated using Morpheus, <https://software.broadinstitute.org/morpheus>.

(J) Graphical representation of the methyl erythritol 4-phosphate (MEP) pathway. The colored numbers on the left represent the \log_2 fold-change after 12 h of dAdo treatment ($p_{adj} < 0.05$) as measured by RNA-seq. The boxplots on the right show the corresponding extracellular metabolites at 3 dpt. Asterisks represent significant differences from the mock-treated sample analyzed by Student's t test (* $p < 0.05$; *** $p < 0.001$).

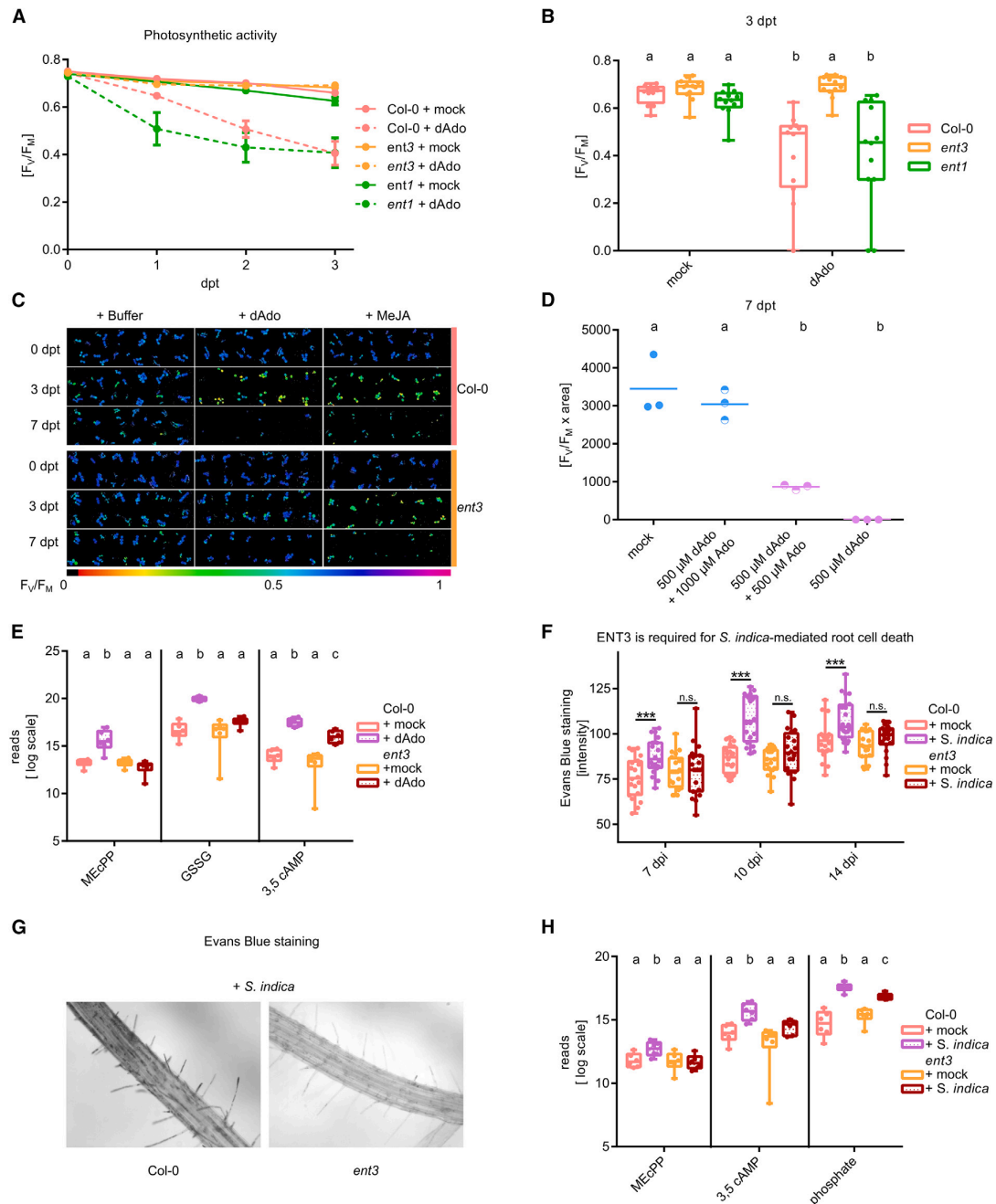


Figure 5. The equilibrative nucleoside transporter ENT3 of Arabidopsis is required for dAdo-mediated signal transduction and cell death
(A) Photosynthetic activity (F_v/F_m) of 9-day-old mock- and dAdo-treated (500 μ M) Col-0, *ent3*, and *ent1* seedlings. Measurements were taken 3 days after treatment (dpt) every 24 h. Data show the mean, and error bars show the SEM obtained from 12 technical replicates with 3 seedlings each. The experiment was repeated more than three times independently with similar results.
(B) F_v/F_m of seedlings from (A) at 3 dpt. Boxplots show data from 12 technical replicates with 3 seedlings each. Different letters indicate significant differences as determined by one-way ANOVA with post-hoc Tukey HSD test ($p < 0.05$).

(legend continued on next page)

ENT3 is expressed at higher levels in the epidermis compared with the rest of the root,³⁷ suggesting that dAdo-induced cell death may be cell-type specific to some extent. This is consistent with the phenotype of root cell death observed after dAdo treatment with Evans blue staining (Figures 4B and 4C). Taken together, these data indicate that a functional ENT3 plays an important role in dAdo-triggered cell death in Arabidopsis, most likely by importing dAdo into the cytoplasm, where it activates signaling leading to cell death. Accordingly, the *ent3* KO line accumulates lower levels of extracellular signaling metabolites such as MEcPP, GSSG, and 3',5'-cAMP in response to dAdo at 3 dpi compared with the WT line (Figure 5E; Table S6).

Mutation of ENT3 impairs *S. indica*-mediated cell death

Next, we investigated whether ENT3 plays a role in fungal accommodation and cell death mediated by *S. indica* in roots. The *ent3* line showed significantly less cell death upon colonization by *S. indica* compared with the WT line at 7, 10, and 14 dpi (Figures 5F and 5G). In addition, we observed a transient effect on fungal colonization at 8 dpi, where the *ent3* KO line was less colonized by *S. indica* compared with the WT control (Figure S9F).

Colonization with *S. indica* also resulted in transient accumulation of the extracellular signaling metabolites 3',5'-cAMP at 3 dpi (early biotrophic phase) and MEcPP at 6 dpi (onset of cell death). In addition, a higher level of free phosphate was observed at 10 dpi (Figure 5H; Table S6). Consistent with the decreased cell death phenotype in the *ent3* KO line, the amount of these metabolites was lower in colonized *ent3* seedlings, suggesting that ENT3 is important for fungal-mediated signal transduction and cell death in Arabidopsis. The activity of the fungal-derived enzymes SiNucA and SiE5NT, along with the host transporter ENT3, modifies extracellular metabolite levels, establishing for the first time a direct link between purine metabolism, immunity, and cell death in roots. How the metabolic state of the host affects *S. indica*-induced cell death remains to be thoroughly elucidated.

Screening of Arabidopsis T-DNA insertion mutants reveals a TIR-NLR gene involved in dAdo-mediated cell death

To identify downstream genetic determinants associated with dAdo-mediated cell death in plants, we performed a mutant screen of 6,868 SALK-Arabidopsis T-DNA insertion lines (Fig-

ure S10A). Sensitivity to dAdo was tested using Arabidopsis Col-0 WT as control and the SALK mutant lines grown for 14 days on solid media (½ MS) in 24-well plates with and without 500 μM dAdo. The dAdo-insensitive lines (survivors) from the screening were then analyzed by pulse amplitude modulation (PAM) fluorometry in three independent biological replicates. Thirteen lines with varying degrees of dAdo resistance were identified (Table S7). One of the resistant SALK lines had an insertion at the AT5G45240 locus (SALK_034517C), which encodes a predicted TIR-domain NLR (TIR-NLR). Mutation in this locus resulted in reproducible and significantly high resistance to dAdo-induced cell death, as evidenced by reduced electrolyte leakage, higher photosynthetic activity, and increased germination rate compared with Col-0 WT after incubation with dAdo (Figure 6). No differences were observed in response to the cell death inducer MeJA (Figure S10B). An independent KO line, *CRISPRisi*, generated using a CRISPR-CAS9-based approach (Figure S11A)^{38,39} and carrying two indel mutations in the TIR domain (Figure S11B), also exhibited a dAdo-resistant phenotype (Figures S11C and S11D), further supporting a connection between this locus and dAdo-mediated cell death. Complementation using a cell-based transient expression system with the full-length TIR domain restored sensitivity to dAdo, suggesting that the TIR domain may play a role in mediating dAdo-induced cell death in Arabidopsis (Figure 6E). The TIR-NLR gene AT5G45240 is located in close proximity to *RPS4* and *RRS1* and is part of a larger locus containing multiple TNL genes, most of which are functionally uncharacterized. Four of the five TNL genes at this locus showed transiently increased expression during cell death associated with colonization by *S. indica*, with the AT5G45240 gene displaying the strongest relative induction (Figures S12A and S12B). We therefore named this gene *ISI*, induced by *S. indica*. Induction could be detected, especially during the onset of the cell death-associated phase (Figure 7A). While the *isi* line showed less cell death after dAdo treatment (Figure S12C), there was increased cell death in the older parts of the mock-treated roots and during colonization with *S. indica* compared with the WT line (Figure 7B), which correlated with significantly greater fungal colonization (Figure 7C). In addition, colonized *isi* KO seedlings did not show *S. indica*-mediated promotion of root growth, as observed in WT and *ent3* seedlings (Figures 7D and S12D). These results could be explained by the activation of an alternative cell death

(C) Visualization of F_v/F_m measured by PAM fluorometry. The F_v/F_m value is visualized by the color scale shown below. Shown are 12 wells with 9-day-old seedlings probed at 0, 3, and 7 dpi with either mock treatment (2.5 mM MES buffer pH 5.6), 500 μM dAdo, or 500 μM MeJA. The experiment was repeated more than three times independently with similar results.

(D) Photosynthetic activity ($F_v/F_m \times$ photosynthetically active area) of 9-day-old Col-0 seedlings incubated with different concentrations of Ado and dAdo at 7 dpi. Dots represent 3 biologically independent replicates consisting of 12 wells with 3 seedlings each. Different letters indicate significant differences as determined by one-way ANOVA with post-hoc Tukey HSD test ($p < 0.05$).

(E) Metabolic analysis of supernatants from 7-day-old Col-0 and *ent3* seedlings treated with dAdo at 3 dpi. Boxplots show data from 6 biologically independent replicates. Data are plotted on a \log_2 scale. Different letters indicate significant differences in measurements of a metabolite as determined by two-way ANOVA with post-hoc Tukey HSD test ($p < 0.05$).

(F) Quantification of root cell death in 7-day-old Col-0 and *ent3* roots colonized with *S. indica* at 7, 10, and 14 dpi. Cell death was assessed by Evans blue staining. Boxplots show data from 20 biological replicates. Asterisks represent significant differences analyzed by Student's *t* test (* $p < 0.05$, ** $p < 0.01$, *** $p < 0.005$). The experiment was repeated independently three times with similar results.

(G) Evans blue staining of *S. indica*-colonized Col-0 and *ent3* roots at 10 dpi.

(H) Metabolic analysis of the supernatant of 7-day-old Col-0 and *ent3* seedlings inoculated with *S. indica* at different time points after treatment (3',5'-cAMP: 3 dpi; MEcPP: 6 dpi; phosphate: 10 dpi). Boxplots show data from 6 biologically independent replicates. Data are plotted on a \log_2 scale. Different letters indicate significant differences in measurements of a metabolite using a two-way ANOVA with post-hoc Tukey HSD test ($p < 0.05$).

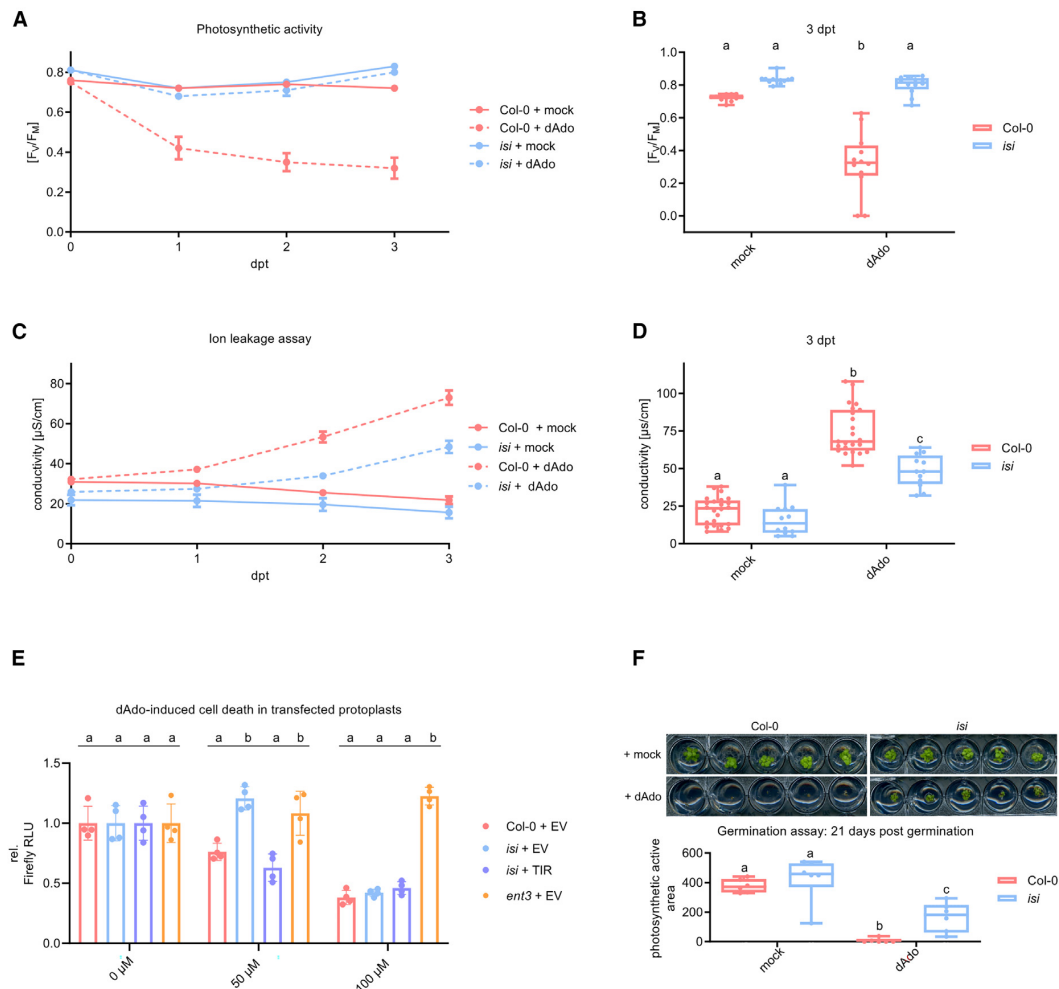


Figure 6. The AtTIR-NLR AT5G45240 is involved in dAdo-mediated cell death

(A) F_v/F_m of 9-day-old mock- and dAdo-treated (500 μ M) Col-0 and *isi* (AT5G45240 KO mutant) seedlings. Measurements were performed over 3 days. Data show the mean, and error bars show the SEM obtained from 12 technical replicates with 3 seedlings each. The experiment was repeated three times independently with similar results.

(B) Boxplots of the measurements of F_v/F_m from (A) at 3 dpt. Different letters indicate significant differences as determined by two-way ANOVA and post-hoc Tukey HSD test ($p < 0.05$).

(C) Conductivity of water containing 9-day-old Col-0 or *isi* seedlings 0–3 days after mock or dAdo treatment (500 μ M). Data points represent the mean, while error bars show the SEM from 12 biological replicates.

(D) Boxplots of conductivity measurements from (C) at 3 dpt. Different letters indicate significant differences as determined by two-way ANOVA with post-hoc Tukey HSD test ($p < 0.05$).

(E) Relative luciferase activity of *A. thaliana* protoplasts transfected with luciferase and either a construct expressing the TIR domain of ISI or an empty vector. Values were normalized to mock treatment (0 μ M dAdo). Different letters indicate significantly different groups per treatment, as determined by one-way ANOVA with post-hoc Tukey HSD test ($p < 0.05$).

(F) Germination of Col-0 WT and *isi* seedlings on 1/10 PNM medium containing 500 μ M dAdo or MES. The upper half shows photographs of the seedlings after 21 days. The lower half shows the quantification of F_v/F_m measured by PAM fluorometry. Boxplots show F_v/F_m measurements per well, containing six seedlings. Different letters indicate significant differences as determined by two-way ANOVA with post-hoc Tukey HSD test ($p < 0.05$). The experiment was repeated three times independently with similar results.

pathway in the absence of a functional ISI TIR-NLR, leading to overcolonization by *S. indica* and loss of growth promotion (Figure 7E). Overall, our data suggest that the ISI TIR-NLR protein is

involved in modulating different cell death programs in roots and mediating *S. indica* growth promotion. We further analyzed the expression of both TIR- and CC-NLRs in the roots of Arabidopsis

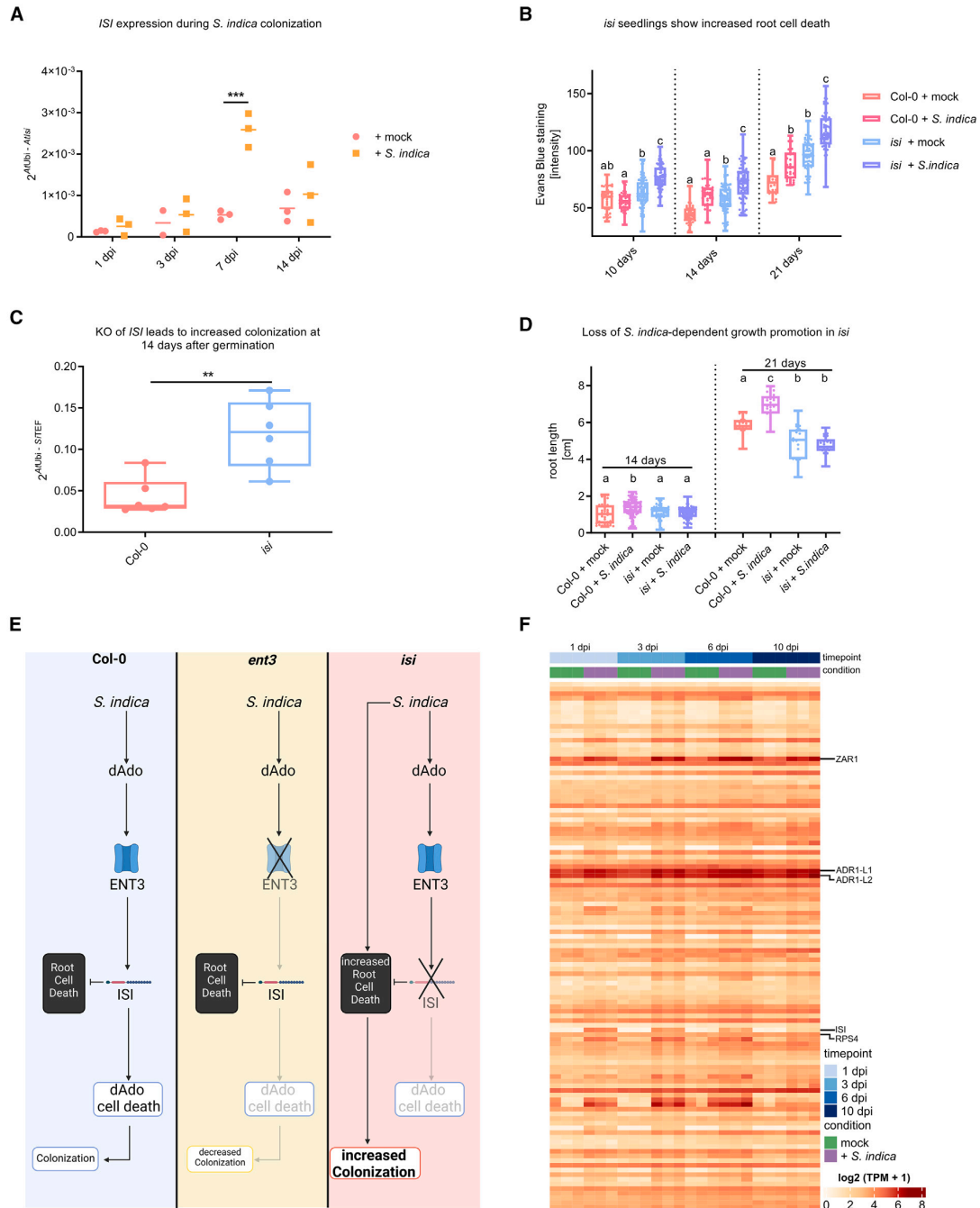


Figure 7. The *AtTIR-NLR* AT5G45240 is involved in fungal-mediated growth promotion

(A) AT5G45240 (*AtISI*) expression in Arabidopsis roots inoculated with *S. indica* or mock treated. Expression was measured via RT-qPCR and calculated with the $2^{-\Delta CT}$ method. Data points depict biological replicates, and asterisks represent significant differences analyzed by Student's t test ($***p < 0.005$).

(B) Quantification of root cell death in Col-0 WT and *isi* roots colonized by *S. indica* at 10, 14, and 21 days after germination. Cell death was assessed by Evans blue staining. Boxplots show data from 28–80 biological replicates. Different letters indicate significant differences between samples from one time point as assessed by two-way ANOVA with post-hoc Tukey HSD test ($p < 0.05$).

(legend continued on next page)

during *S. indica* colonization using time-resolved transcriptomics. We detected an induction of expression for *ISI* and also for previously functionally characterized NLRs such as *ZAR1* during beneficial colonization (Figures 7F and S13). Overall, the role of a TIR-NLR in dAdo-induced cell death suggests that this cell death is influenced by the plant immune response and is not a pure consequence of cytoplasmic toxicity, as assumed for animal cells.

DISCUSSION

Symbiotic cell death: An evolutionarily conserved mechanism?

Root colonization by *S. indica* is associated with restricted host cell death. The mechanisms behind the induction and regulation of this symbiotic cell death are poorly understood. Previous work has shown that *S. indica* secretes *SiE5NT*, a ubiquitous apoplastic fungal enzyme that catalyzes the conversion of adenosine nucleotides released from immune-activated or damaged host tissues to adenosine.¹³ The mechanism of the secreted ecto-5'-nucleotidase for host colonization appears to be similar to that evolved by *S. aureus* to evade the host immune response by secreting *Adsa*, which converts AMP to Ado, a suppressor of immunity in animal cells.⁴¹ In addition to the release of eATP by damaged animal cells, activated neutrophils release NETs, extracellular matrices composed of nuclear and mitochondrial DNA and equipped with granular proteins, cell-specific proteases, and antimicrobial peptides.⁴² NETs rapidly immobilize and kill bacterial pathogens.⁴³ *S. aureus* escapes NETs by secreting proteases and the nuclease Nuc, which degrade antimicrobial peptides and DNA. Nuclease-mediated degradation of neutrophil NETs results in the formation of dAMP, which is converted to dAdo by *S. aureus* *Adsa*. Macrophages and other immune cells are highly sensitive to dAdo. This cellular intoxication is mediated by uptake via ENTs.^{24,25} The escape mechanism of *S. aureus* relies on the interaction of two extracellular microbial enzymes and allows staphylococci to block infiltration of abscess lesions by phagocytes and subsequent elimination. Similar to neutrophils, plant roots secrete root extracellular traps (RETs) composed of eDNA and a variety of antimicrobial compounds and polysaccharides. RETs and NETs share similar compositional and functional properties, but unlike NETs, RET production is not triggered only upon microbial infection; instead, RETs are continuously released during root development and form a large, mucus-rich network in the rhizosphere.^{43–46} By cytological analyses, we observed that *S. indica* is able to grow within RETs and along the root tip (Figure S14). The ability of *S. indica* to digest DNA via secretion of the nuclease NucA¹³ suggests the possibility of RET digestion by

S. indica during colonization. Moreover, localization of NucA in the nuclei of plant cells during *S. indica* colonization shows that this enzyme is able to digest host nuclear and eDNA. The combined enzymatic activity of *SiE5NT* and *SiNucA*, present simultaneously in the apoplast, results in the conversion of oligonucleotides with terminal dAdo obtained by nuclease digestion of DNA to free dAdo. Most importantly, we demonstrated that uptake of dAdo via ENT3 is required for host cell death in roots. Mutation of ENT3 results in reduced cell death during colonization by *S. indica*, demonstrating the importance of extracellular nucleoside uptake in regulating fungal-induced cell death. The identification of a previously unknown immune-metabolic axis by which cells respond to extracellular purine nucleosides and trigger cell death in plants suggests some conservation or functional convergence between the immune avoidance and escape mechanisms developed by *S. aureus* and other bacterial pathogens in animals and the cell death triggered by dAdo during plant-fungal endophyte interactions in roots.

A TIR-NLR regulates host cell death in roots

To fight off infections by microbial pathogens, plants have evolved immune receptors that are essential for a successful defense response. PRRs localized in the plasma membrane are capable of sensing conserved MAMPs/DAMPs and eliciting a relatively mild PTI immune response. Successful plant-associated microbes can provide a range of effectors to attenuate PTI to enable successful host colonization. In turn, plants have evolved polymorphic intracellular resistance proteins (R-proteins) to recognize the presence and/or activity of effectors, resulting in a robust defense response called effector-triggered immunity (ETI) that potentiates PTI.^{31,32} Most R-proteins belong to the nucleotide-binding (NB) leucine-rich repeat (LRR) family (NLR), which are classified on the basis of their N-terminal domains as TIR-type NLRs (TNLs) or coiled-coil type NLRs (CNLs).⁴⁷ TNLs generally function as sensors for microbial effectors, whereas several CNLs are referred to as helper NLRs and are downstream of many sensor NLRs in Arabidopsis.^{47,48} TNL sensing and signaling mechanisms have primarily been studied in leaf cells, leaving much to be discovered about their function in roots, including which specific TNLs are involved.⁴⁹ The role of the TNL *ISI* in resistance to dAdo-mediated cell death in Arabidopsis suggests that this TIR-NLR or a potential interaction partner might guard a protein targeted by dAdo in the roots. Alternatively, dAdo might serve as a ligand or be converted into a substrate for TNLs linked to either NAD⁺ or 2',3'-cAMP, a noncanonical cyclic nucleotide monophosphate (cNMP).^{50–52} Plant TIR domains of NLRs are enzymes capable of degrading NAD⁺. While the NADase function of the TIR domain is necessary, it is not sufficient on its own to trigger

(C) Abundance of *S. indica* in Arabidopsis seedlings 14 days after germination. Fungal (*SiTEF*) to plant (*AtUbi*) ratios were calculated using cDNA as template and method 2^{−ΔCT}. Boxplots represent 6 independent biological replicates. Asterisks indicate a significant difference from Col-0 WT samples (Student's t test, ***p* < 0.01).

(D) Root length of Arabidopsis seedlings 14 and 21 days after germination in the presence of *S. indica* or mock treatment. Boxplots show data from 23–86 biological replicates. Different letters indicate significant differences in samples from one time point using two-way ANOVA with post-hoc Tukey HSD test (*p* < 0.05). The experiment was repeated 2 times independently with similar results.

(E) Current model illustrating cell death pathways occurring during colonization of *S. indica* in Arabidopsis Col-0 (blue), *ent3* mutant (yellow), and *isi* mutant (red). (F) The heatmap shows the expression values of *A. thaliana* NLR genes with NB-ARC and LRR (NL) domains in *A. thaliana* root samples as log₂ transformed TPM values. Samples were taken at 1-, 3-, 6-, and 10-day post inoculation with *S. indica* or mock treatment. A more detailed version of the heatmap including an in-depth description can be found in Figure S13. More details about the experimental conditions underlying the dataset can also be found in Eichfeld et al.⁴⁰

plant immune responses in Arabidopsis. Recently, it was shown that plant TIR proteins can also function as 2',3'-cAMP/cGMP synthetases by hydrolyzing RNA/DNA. Mutations that specifically disrupt synthetase activity prevent TIR-mediated cell death in *N. benthamiana*, demonstrating an important role for these cNMPs in TIR signaling.⁵⁰ The accumulation of extracellular 3',5'-cAMP upon *S. indica* colonization and treatment with dAdo establishes a link to cNMPs. Further research is necessary to elucidate the metabolism of dAdo in plant cells and to understand how intracellular dAdo activates TNLs in Arabidopsis. Given that TIR-domain cell-surface receptors (TLRs) and various TIR-adaptor proteins are involved in mammalian immunity, our findings suggest the potential to explore the role of TIR domains in dAdo-triggered cell death in plants and beyond. However, more biochemical evidence is needed to definitively clarify the mechanisms by which dAdo affects TNL signaling in plants.

In animal systems, it has been shown that following import of dAdo into macrophages, dAdo-mediated toxicity involves conversion of dAdo to dAMP by deoxycytidine kinase (DCK) and adenosine kinase (ADK) activity and signaling via subsequent conversion to the corresponding di- and tri-phosphates by nucleotide kinases and activation of caspase-3-induced apoptosis.²⁵ The absence of caspases in plants and the potential involvement of a TIR-NLR protein in dAdo-mediated cell death in Arabidopsis strongly suggest that this part of the signaling pathway is not conserved between plants and animals and relies on different regulatory and execution mechanisms that require further investigation. The role of the EDS1 family of immunity regulators, which are genetically required for pathogen resistance and execution of cell death by various TIR-NLRs,⁵³ in ISI-mediated cell death also remains to be explored. The potential involvement of other ISI-like proteins as interaction partners warrants further investigation, particularly given that the dAdo-resistance phenotype associated with ISI is only partial.

In summary, we have uncovered a cellular signaling pathway that responds to extracellularly produced metabolites during fungal colonization and links nucleoside transport by an ENT to cellular activation of the MEP pathway and cell death potentially influenced by the activation of ISI, a fungal-induced TIR-NLR. The observation that dAdo triggers cell death across multiple plant species, including a basal lineage, suggests that this pathway is likely conserved and represents an ancient cell death mechanism co-opted to facilitate plant-endophyte symbiosis. This paves the way for a better understanding of immunometabolism in plant-microbe interactions.

RESOURCE AVAILABILITY

Lead contact

Further information and requests for resources and reagents should be directed to and will be fulfilled by the lead contact, Prof. Alga Zuccaro (azuccaro@uni-koeln.de).

Materials availability

This study did not generate new unique reagents. Plasmids and transgenic plant seeds generated in this study are available from the lead contact with a completed Materials Transfer Agreement.

Data and code availability

- RNA-seq data generated in this study have been deposited in the Gene Expression Omnibus (GEO) database under the accession numbers GEO:GSE209761 and GEO:GSM6394981. The data are available as of the date of publication. Microscopy data reported in this paper will be shared by the lead contact upon request.
- This paper does not report original code.
- Any additional information required to reanalyze the data reported in this paper is available from the lead contact upon request.

ACKNOWLEDGMENTS

We would like to thank Prof. Jijie Chai and Jane Parker for discussions and reading the manuscript prior to submission. We further want to thank Johana Misas Stadtel for her support during ABPP assays. N.D. was supported by the International Max Planck Research School (IMPRS) at the University of Cologne. A.Z. and M.D.Z. gratefully acknowledge support from the Cluster of Excellence on Plant Sciences (CEPLAS) funded by the German Research Foundation (DFG) under the Excellence Strategy—EXC 2048/1—project ID: 390686111. A.Z. and N.D. additionally acknowledge support from SFB 1403 project ID: 1403-414786233. We further would like to thank the US Department of Energy Joint Genome Institute (<https://ror.org/04xm1d337>) and Yu Zhang, Sravanthi Tejomurthula, Daniel Peterson, Vivian Ng, and Igor Grigoriev for producing sequencing data within the work proposal 10.46936/10.25585/60001292. C.-P.W. gratefully acknowledges support from DFG grant WI3411/8-1. M.D.Z. and J.S. acknowledge support from NEXTplant (IRTG 2466). Some of the graphical representations were generated using the online tool BioRender.

AUTHOR CONTRIBUTIONS

A.Z. and N.D. designed the experiment. N.D. did characterize the role of *ENT3* and *AtISI* experimentally. H.W. did analyze the role of *SiNucA*. G.U.B. and A.T. did produce metabolomics data. H.S. and C.-P.W. did perform enzymatic assays and measured nucleotide concentrations. G.L. and C.D.Q. did perform all bioinformatic analyses. N.M.C. and S.W. did perform microscopy. P.S. did perform calcium influx and ROS burst assays. J.S. and M.D.Z. did perform protoplast assays. H.R. did support the conceptualization of the experiment and perform initial cell death assays. M.K. and A.D. did perform experiments with *Marchantia polymorpha*. The manuscript was written by A.Z. and N.D. with continuous input from all authors.

DECLARATION OF INTERESTS

The authors declare no competing interests.

STAR★METHODS

Detailed methods are provided in the online version of this paper and include the following:

- KEY RESOURCES TABLE
- EXPERIMENTAL MODEL AND STUDY PARTICIPANT DETAILS
 - Plant Material and Growth Conditions
 - Fungal strains and cultivation techniques
- METHOD DETAILS
 - Fungal inoculation
 - Confocal microscopy
 - DNA and RNA extraction
 - Quantitative RT-PCR analysis
 - *Serendipita indica* transformation
 - Nuclease activity test
 - *SiNucA*-HA-His purification
 - Measurement of enzyme kinetics of *SiENT*
 - Measurement of release of deoxynucleosides
 - PAM fluorometric measurements
 - Cell death staining with Evans blue

- Activity-based protein profiling
- RNAseq
- Collection of extracellular fluid
- Metabolite analysis
- Ca²⁺ influx quantification
- Heterologous protein production in *Nicotiana benthamiana* and protein purification
- Ion leakage measurements
- Seed germination test
- Root length measurements
- Oxidative burst assay
- Protoplast isolation and transformation
- **QUANTIFICATION AND STATISTICAL ANALYSIS**

SUPPLEMENTAL INFORMATION

Supplemental information can be found online at <https://doi.org/10.1016/j.chom.2024.10.020>.

Received: March 17, 2022

Revised: August 9, 2024

Accepted: October 31, 2024

Published: November 26, 2024

REFERENCES

1. D'Haese, W., De Rycke, R., Mathis, R., Goormachtig, S., Pagnotta, S., Verplancke, C., Capoen, W., and Holsters, M. (2003). Reactive oxygen species and ethylene play a positive role in lateral root base nodulation of a semiaquatic legume. *Proc. Natl. Acad. Sci. USA* **100**, 11789–11794. <https://doi.org/10.1073/pnas.1333899100>.
2. Ragnelli, A.M., Aimola, P., Maione, M., Zarivi, O., Leonardi, M., and Pacioni, G. (2014). The cell death phenomenon during Tuber ectomycorrhiza morphogenesis. *Plant Biosyst. An Int. J. Dealing Aspects Plant Biol.* **148**, 473–482. <https://doi.org/10.1080/11263504.2013.788575>.
3. Mucha, J., Guzicka, M., Ratajczak, E., and Zadworny, M. (2014). Strategies utilized by trophically diverse fungal species for *Pinus sylvestris* root colonization. *Tree Physiol.* **34**, 73–86. <https://doi.org/10.1093/treephys/tps111>.
4. Deshmukh, S., Hüchelhoven, R., Schäfer, P., Imani, J., Sharma, M., Weiss, M., Waller, F., and Kogel, K.H. (2006). The root endophytic fungus *Piriformospora indica* requires host cell death for proliferation during mutualistic symbiosis with barley. *Proc. Natl. Acad. Sci. USA* **103**, 18450–18457. <https://doi.org/10.1073/pnas.0605697103>.
5. Qiang, X., Zechmann, B., Reitz, M.U., Kogel, K.H., and Schäfer, P. (2012). The mutualistic fungus *Piriformospora indica* colonizes *Arabidopsis* roots by inducing an endoplasmic reticulum stress-triggered caspase-dependent cell death. *Plant Cell* **24**, 794–809. <https://doi.org/10.1105/tpc.111.093260>.
6. Lahrmann, U., Ding, Y., Banhara, A., Rath, M., Hajirezaei, M.R., Döhlemann, S., von Wirén, N., Parniske, M., and Zuccaro, A. (2013). Host-related metabolic cues affect colonization strategies of a root endophyte. *Proc. Natl. Acad. Sci. USA* **110**, 13965–13970. <https://doi.org/10.1073/pnas.1301653110>.
7. Oberwinkler, F., Riess, K., Bauer, R., Selosse, M.-A., Weiß, M., Garnica, S., and Zuccaro, A. (2013). Enigmatic Sebaciniales. *Mycol. Progress* **12**, 1–27. <https://doi.org/10.1007/s11557-012-0880-4>.
8. Tedersoo, L., Bahram, M., Ryberg, M., Otsing, E., Kõljalg, U., and Abarenkov, K. (2014). Global biogeography of the ectomycorrhizal/sebacina lineage (Fungi, Sebaciniales) as revealed from comparative phylogenetics analyses. *Mol. Ecol.* **23**, 4168–4183. <https://doi.org/10.1111/mec.12849>.
9. Weiß, M., Waller, F., Zuccaro, A., and Selosse, M.A. (2016). Sebaciniales – one thousand and one interactions with land plants. *New Phytol.* **211**, 20–40. <https://doi.org/10.1111/nph.13977>.
10. Zuccaro, A., Lahrmann, U., Güldener, U., Langen, G., Pfiffi, S., Biedenkopf, D., Wong, P., Samans, B., Grimm, C., Basiewicz, M., et al. (2011). Endophytic Life Strategies Decoded by Genome and Transcriptome Analyses of the Mutualistic Root Symbiont *Piriformospora indica*. *PLoS Pathog.* **7**, e1002290. <https://doi.org/10.1371/journal.ppat.1002290>.
11. Lahrmann, U., and Zuccaro, A. (2012). Opprimo ergo sum–Evasion and Suppression in the Root Endophytic Fungus *Piriformospora indica*. *Mol. Plant Microbe Interact.* **25**, 727–737. <https://doi.org/10.1094/MPMI-11-11-0291>.
12. Lahrmann, U., Strehmel, N., Langen, G., Frerigmann, H., Leson, L., Ding, Y., Scheel, D., Herklotz, S., Hilbert, M., and Zuccaro, A. (2015). Mutualistic root endophytism is not associated with the reduction of saprotrophic traits and requires a noncompromised plant innate immunity. *New Phytol.* **207**, 841–857. <https://doi.org/10.1111/nph.13411>.
13. Nizam, S., Qiang, X., Wawra, S., Nostadt, R., Getzke, F., Schwanke, F., Dreyer, I., Langen, G., and Zuccaro, A. (2019). *Serendipita indica* E5'NT modulates extracellular nucleotide levels in the plant apoplast and affects fungal colonization. *EMBO Rep.* **20**, e47430. <https://doi.org/10.15252/embr.201847430>.
14. Schneider, H.M., and Lynch, J.P. (2018). Functional implications of root cortical senescence for soil resource capture. *Plant Soil* **423**, 13–26. <https://doi.org/10.1007/s11104-017-3533-1>.
15. Presti, L., Lanver, D., Schweizer, G., Tanaka, S., Liang, L., Tollot, M., Zuccaro, A., Reissmann, S., Kahmann, R., and Merchant, S. (2015). Fungal effectors and plant susceptibility. *Annu. Rev. Plant Biol.* **66**, 513–545. <https://doi.org/10.1146/annurev-arplant-043014-114623>.
16. Klopffholz, S., Kuhn, H., and Requena, N. (2011). A Secreted Fungal Effector of *Glomus intraradices* Promotes Symbiotic Biotrophy. *Curr. Biol.* **21**, 1204–1209. <https://doi.org/10.1016/j.cub.2011.06.044>.
17. Plett, J.M., Daguerre, Y., Wittulsky, S., Vayssières, A., Deveau, A., Melton, S.J., Kohler, A., Morrell-Falvey, J.L., Brun, A., Veneault-Fourrey, C., and Martin, F. (2014). Effector MiSSP7 of the mutualistic fungus *Laccaria bicolor* stabilizes the *Populus* JAZ6 protein and represses jasmonic acid (JA) responsive genes. *Proc. Natl. Acad. Sci. USA* **111**, 8299–8304. <https://doi.org/10.1073/pnas.1322671111>.
18. Wawra, S., Fesl, P., Widmer, H., Timm, M., Seibel, J., Leson, L., Kesseler, L., Nostadt, R., Hilbert, M., Langen, G., and Zuccaro, A. (2016). The fungal-specific beta-glucan-binding lectin FGB1 alters cell-wall composition and suppresses glucan-triggered immunity in plants. *Nat. Commun.* **7**, 13188. <https://doi.org/10.1038/ncomms13188>.
19. Voß, S., Betz, R., Heidt, S., Corradi, N., and Requena, N. (2018). RiCRN1, a Crinkler Effector From the Arbuscular Mycorrhizal Fungus *Rhizophagus irregularis*, Functions in Arbuscule Development. *Front. Microbiol.* **9**, 2068. <https://doi.org/10.3389/fmicb.2018.02068>.
20. Nostadt, R., Hilbert, M., Nizam, S., Rovenich, H., Wawra, S., Martin, J., Küpper, H., Mijovilovich, A., Ursinus, A., Langen, G., et al. (2020). A secreted fungal histidine- and alanine-rich protein regulates metal ion homeostasis and oxidative stress. *New Phytol.* **227**, 1174–1188. <https://doi.org/10.1111/nph.16606>.
21. Antoniolli, L., Pacher, P., Vizi, E.S., and Haskó, G. (2013). CD39 and CD73 in immunity and inflammation. *Trends Mol. Med.* **19**, 355–367. <https://doi.org/10.1016/j.molmed.2013.03.005>.
22. Pham, A.Q., Cho, S.-H., Nguyen, C.T., and Stacey, G. (2020). *Arabidopsis* Lectin Receptor Kinase P2K2 Is a Second Plant Receptor for Extracellular ATP and Contributes to Innate Immunity1 [OPEN]. *Plant Physiol.* **183**, 1364–1375. <https://doi.org/10.1104/pp.19.01265>.
23. Thürich, J., Meichner, D., Furch, A.C.U., Pfalz, J., Krüger, T., Kniemeyer, O., Brakhage, A., and Oelmüller, R. (2018). *Arabidopsis thaliana* responds to colonisation of *Piriformospora indica* by secretion of symbiosis-specific proteins. *PLoS ONE* **13**, e0209658. <https://doi.org/10.1371/journal.pone.0209658>.
24. Thammavongsa, V., Missiakas, D.M., and Schneewind, O. (2013). *Staphylococcus aureus* degrades neutrophil extracellular traps to promote immune cell death. *Science* **342**, 863–866. <https://doi.org/10.1126/science.1242255>.

25. Winstel, V., Missiakas, D., and Schneewind, O. (2018). Staphylococcus aureus targets the purine salvage pathway to kill phagocytes. *Proc. Natl. Acad. Sci. USA* 115, 6846–6851. <https://doi.org/10.1073/pnas.1805622115>.
26. Rafiqi, M., Jelonek, L., Akum, N.F., Zhang, F., and Kogel, K.H. (2013). Effector candidates in the secretome of *Piriformospora indica*, a ubiquitous plant-associated fungus. *Front. Plant Sci.* 4, 228. <https://doi.org/10.3389/fpls.2013.00228>.
27. Kolodziejek, I., Misas-Villamil, J.C., Kaschani, F., Clerc, J., Gu, C., Krahn, D., Niessen, S., Verdoes, M., Willems, L.I., Overkleeft, H.S., et al. (2011). Proteasome Activity Imaging and Profiling Characterizes Bacterial Effector Syringolin A. *Plant Physiol.* 155, 477–489. <https://doi.org/10.1104/pp.110.163733>.
28. Olvera-Carrillo, Y., Van Bel, M., Van Hautegeem, T., Fendrych, M., Huysmans, M., Simaskova, M., van Durme, M., Buscaill, P., Rivas, S., Coll, N.S., et al. (2015). A Conserved Core of Programmed Cell Death Indicator Genes Discriminates Developmentally and Environmentally Induced Programmed Cell Death in Plants. *Plant Physiol.* 169, 2684–2699. <https://doi.org/10.1104/pp.15.00769>.
29. Xiao, Y., Savchenko, T., Baidoo, E.E.K., Chehab, W.E., Hayden, D.M., Tolstikov, V., Corwin, J.A., Kliebenstein, D.J., Keasling, J.D., and Dehesh, K. (2012). Retrograde signaling by the plastidial metabolite MEcPP regulates expression of nuclear stress-response genes. *Cell* 149, 1525–1535. <https://doi.org/10.1016/j.cell.2012.04.038>.
30. Zipfel, C., and Oldroyd, G.E.D. (2017). Plant signalling in symbiosis and immunity. *Nature* 543, 328–336. <https://doi.org/10.1038/nature22009>.
31. Ngou, B.P.M., Ahn, H.K., Ding, P., and Jones, J.D.G. (2021). Mutual potentiation of plant immunity by cell-surface and intracellular receptors. *Nature* 592, 110–115. <https://doi.org/10.1038/s41586-021-03315-7>.
32. Yuan, M., Jiang, Z., Bi, G., Nomura, K., Liu, M., Wang, Y., Cai, B., Zhou, J.M., He, S.Y., and Xin, X.F. (2021). Pattern-recognition receptors are required for NLR-mediated plant immunity. *Nature* 592, 105–109. <https://doi.org/10.1038/s41586-021-03316-6>.
33. Choi, J., Tanaka, K., Cao, Y., Qi, Y., Qiu, J., Liang, Y., Lee, S.Y., and Stacey, G. (2014). Identification of a plant receptor for extracellular ATP. *Science* 343, 290–294. <https://doi.org/10.1126/science.1246168>.
34. Tanaka, K., Choi, J., Cao, Y., and Stacey, G. (2014). Extracellular ATP acts as a damage-associated molecular pattern (DAMP) signal in plants. *Front. Plant Sci.* 5, 446. <https://doi.org/10.3389/fpls.2014.00446>.
35. Kilian, J., Whitehead, D., Horak, J., Wanke, D., Weinl, S., Batistic, O., D'Angelo, C., Bornberg-Bauer, E., Kudla, J., and Harter, K. (2007). The AtGenExpress global stress expression data set: protocols, evaluation and model data analysis of UV-B light, drought and cold stress responses. *Plant J.* 50, 347–363. <https://doi.org/10.1111/j.1365-3113.2007.03052.x>.
36. Li, G., Liu, K., Baldwin, S.A., and Wang, D. (2003). Equilibrative nucleoside transporters of *Arabidopsis thaliana*. cDNA cloning, expression pattern, and analysis of transport activities. *J. Biol. Chem.* 278, 35732–35742. <https://doi.org/10.1074/jbc.M304768200>.
37. Rich-Griffin, C., Stechemesser, A., Finch, J., Lucas, E., Ott, S., and Schäfer, P. (2023). Single-Cell Transcriptomics: A High-Resolution Avenue for Plant Functional Genomics. *Trends Plant Sci.* 25, 186–197. <https://doi.org/10.1016/j.tplants.2019.10.008>.
38. Ordon, J., Kiel, N., Becker, D., Kretschmer, C., Schulze-Lefert, P., and Stüttmann, J. (2023). Targeted gene deletion with SpCas9 and multiple guide RNAs in *Arabidopsis thaliana*: four are better than two. *Plant Methods* 19, 30. <https://doi.org/10.1186/s13007-023-01010-4>.
39. Stüttmann, J., Barthel, K., Martin, P., Ordon, J., Erickson, J.L., Herr, R., Ferik, F., Kretschmer, C., Berner, T., Keilwagen, J., et al. (2021). Highly efficient multiplex editing: one-shot generation of 8x *Nicotiana benthamiana* and 12x *Arabidopsis* mutants. *Plant J.* 106, 8–22. <https://doi.org/10.1111/tpj.15197>.
40. Eichfeld, R., Mahdi, L.K., De Quattro, C., Armbruster, L., Endeshaw, A.B., Miyauchi, S., Hellmann, M.J., Cord-Landwehr, S., Peterson, D., Singan, V., et al. (2024). Transcriptomics reveal a mechanism of niche defense: two beneficial root endophytes deploy an antimicrobial GH18-CBM5 chitinase to protect their hosts. *New Phytol.* 244, 980–996. <https://doi.org/10.1111/nph.20080>.
41. Thammavongsa, V., Kern, J.W., Missiakas, D.M., and Schneewind, O. (2009). Staphylococcus aureus synthesizes adenosine to escape host immune responses. *J. Exp. Med.* 206, 2417–2427. <https://doi.org/10.1084/jem.20090097>.
42. Brinkmann, V., Reichard, U., Goosmann, C., Fauler, B., Uhlemann, Y., Weiss, D.S., Weinrauch, Y., and Zychlinsky, A. (2004). Neutrophil extracellular traps kill bacteria. *Science* 303, 1532–1535. <https://doi.org/10.1126/science.1092385>.
43. Driouch, A., Smith, C., Ropitiaux, M., Chambard, M., Boulogne, I., Bernard, S., Follet-Gueye, M.L., Vicré, M., and Moore, J. (2019). Root extracellular traps versus neutrophil extracellular traps in host defence, a case of functional convergence? *Biol. Rev. Camb. Philos. Soc.* 94, 1685–1700. <https://doi.org/10.1111/brev.12522>.
44. Chambard, M., Plasson, C., Derambure, C., Coutant, S., Tournier, I., Lefranc, B., Leprince, J.M., Kiefer-Meyer, M.C., Driouch, A., Follet-Gueye, M.L., and Boulogne, I. (2021). New Insights into Plant Extracellular DNA. A Study in Soybean Root Extracellular Trap. *Cells* 10, ARTN69. <https://doi.org/10.3390/cells10010069>.
45. Tran, T.M., MacIntyre, A., Hawes, M., and Allen, C. (2016). Escaping Underground Nets: Extracellular DNases Degrade Plant Extracellular Traps and Contribute to Virulence of the Plant Pathogenic Bacterium *Ralstonia solanacearum*. *PLoS Pathog.* 12, e1005686. <https://doi.org/10.1371/journal.ppat.1005686>.
46. Hawes, M., Allen, C., Turgeon, B.G., Curlango-Rivera, G., Minh Tran, T.M., Huskey, D.A., and Xiong, Z.G. (2016). Root Border Cells and Their Role in Plant Defense. *Annu. Rev. Phytopathol.* 54, 143–161. <https://doi.org/10.1146/annurev-phyto-080615-100140>.
47. Wu, Z., Li, M., Dong, O.X., Xia, S., Liang, W., Bao, Y., Wasteneys, G., and Li, X. (2019). Differential regulation of TNL-mediated immune signaling by redundant helper CNLs. *New Phytol.* 222, 938–953. <https://doi.org/10.1111/nph.15665>.
48. Saur, I.M.L., Panstruga, R., and Schulze-Lefert, P. (2021). NOD-like receptor-mediated plant immunity: from structure to cell death. *Nat. Rev. Immunol.* 21, 305–318. <https://doi.org/10.1038/s41577-020-00473-z>.
49. Kim, T.H., Kunz, H.H., Bhattacharjee, S., Hauser, F., Park, J., Engineer, C., Liu, A., Ha, T., Parker, J.E., Gassmann, W., and Schroeder, J.I. (2012). Natural variation in small molecule-induced TIR-NB-LRR signaling induces root growth arrest via EDS1- and PAD4-complexed R protein VICTR in *Arabidopsis*. *Plant Cell* 24, 5177–5192. <https://doi.org/10.1105/tpc.112.107235>.
50. Yu, D., Song, W., Tan, E.Y.J., Liu, L., Cao, Y., Jirschtzka, J., Li, E., Logemann, E., Xu, C., Huang, S., et al. (2022). TIR domains of plant immune receptors are 2',3'-cAMP/cGMP synthetases mediating cell death. *Cell* 185, 2370–2386.e18. <https://doi.org/10.1016/j.cell.2022.04.032>.
51. Wan, L., Essuman, K., Anderson, R.G., Sasaki, Y., Monteiro, F., Chung, E.H., Osborne Nishimura, E., DiAntonio, A., Milbrandt, J., Dangl, J.L., and Nishimura, M.T. (2019). TIR domains of plant immune receptors are NAD(+) cleaving enzymes that promote cell death. *Science* 365, 799–803. <https://doi.org/10.1126/science.aax1771>.
52. Horsefield, S., Burdett, H., Zhang, X., Manik, M.K., Shi, Y., Chen, J., Qi, T., Gilley, J., Lai, J.S., Rank, M.X., et al. (2019). NAD(+) cleavage activity by animal and plant TIR domains in cell death pathways. *Science* 365, 793–799. <https://doi.org/10.1126/science.aax1911>.
53. Lapin, D., Bhandari, D.D., and Parker, J.E. (2020). Origins and Immunity Networking Functions of EDS1 Family Proteins. *Annu. Rev. Phytopathol.* 58, 253–276. <https://doi.org/10.1146/annurev-phyto-010820-012840>.
54. Wawra, S., Fesel, P., Widmer, H., Neumann, U., Lahrmann, U., Becker, S., Hehmann, J.H., Langen, G., and Zuccaro, A. (2019). FGB1 and WSC3 are in planta-induced beta-glucan-binding fungal lectins with different functions. *New Phytol.* 222, 1493–1506. <https://doi.org/10.1111/nph.15711>.
55. Marqués-Bueno, M.D.M., Morao, A.K., Cayrel, A., Platre, M.P., Barberon, M., Caillieux, E., Colot, V., Jaillais, Y., Roudier, F., and Vert, G. (2016). A versatile Multisite Gateway-compatible promoter and transgenic line

- p>collection for cell type-specific functional genomics in Arabidopsis.
- Plant J.*
- 85, 320–333.
- <https://doi.org/10.1111/tpj.13099>
- .
56. Schindelin, J., Arganda-Carreras, I., Frise, E., Kaynig, V., Longair, M., Pietzsch, T., Preibisch, S., Rueden, C., Saalfeld, S., Schmid, B., et al. (2012). Fiji: an open-source platform for biological-image analysis. *Nat. Methods* 9, 676–682. <https://doi.org/10.1038/nmeth.2019>.
 57. Bolger, A.M., Lohse, M., and Usadel, B. (2014). Trimmomatic: a flexible trimmer for Illumina sequence data. *Bioinformatics* 30, 2114–2120. <https://doi.org/10.1093/bioinformatics/btu170>.
 58. Bray, N.L., Pimentel, H., Melsted, P., and Pachter, L. (2016). Near-optimal probabilistic RNA-seq quantification. *Nat. Biotechnol.* 34, 525–527. <https://doi.org/10.1038/nbt.3519>.
 59. Sonesson, C., Love, M.I., and Robinson, M.D. (2015). Differential analyses for RNA-seq: transcript-level estimates improve gene-level inferences. *F1000Res* 4, 1521. <https://doi.org/10.12688/f1000research.7563.2>.
 60. Love, M.I., Huber, W., and Anders, S. (2014). Moderated estimation of fold change and dispersion for RNA-seq data with DESeq2. *Genome Biol.* 15, 550. <https://doi.org/10.1186/s13059-014-0550-8>.
 61. Hilbert, M., Voll, L.M., Ding, Y., Hofmann, J., Sharma, M., and Zuccaro, A. (2012). Indole derivative production by the root endophyte *Piriformospora indica* is not required for growth promotion but for biotrophic colonization of barley roots. *New Phytol.* 196, 520–534. <https://doi.org/10.1111/j.1469-8137.2012.04275.x>.
 62. Livak, K.J., and Schmittgen, T.D. (2001). Analysis of Relative Gene Expression Data Using Real-Time Quantitative PCR and the 2– $\Delta\Delta CT$ Method. *Methods* 25, 402–408. <https://doi.org/10.1006/meth.2001.1262>.
 63. Werner, A.K., Sparkes, I.A., Romeis, T., and Witte, C.P. (2008). Identification, biochemical characterization, and subcellular localization of allantoate amidohydrolases from Arabidopsis and soybean. *Plant Physiol.* 146, 418–430. <https://doi.org/10.1104/pp.107.110809>.
 64. Myrach, T., Zhu, A., and Witte, C.P. (2017). The assembly of the plant urease activation complex and the essential role of the urease accessory protein G (UreG) in delivery of nickel to urease. *J. Biol. Chem.* 292, 14556–14565. <https://doi.org/10.1074/jbc.M117.780403>.
 65. Straube, H., Niehaus, M., Zwittian, S., Witte, C.P., and Herde, M. (2021). Enhanced nucleotide analysis enables the quantification of deoxynucleotides in plants and algae revealing connections between nucleoside and deoxynucleoside metabolism. *Plant Cell* 33, 270–289. <https://doi.org/10.1093/plcell/koa028>.
 66. Vijayaraghavareddy, P., Adhinarayanreddy, V., Vemanna, R.S., Sreeman, S., and Makarla, U. (2017). Quantification of Membrane Damage/Cell Death Using Evan's Blue Staining Technique. *Bio Protoc.* 7, e2519. <https://doi.org/10.21769/BioProtoc.2519>.
 67. Wanke, A., Rovenich, H., Schwanke, F., Velte, S., Becker, S., Hehemann, J.H., Wawra, S., and Zuccaro, A. (2020). Plant species-specific recognition of long and short beta-1,3-linked glucans is mediated by different receptor systems. *Plant J.* 102, 1142–1156. <https://doi.org/10.1111/tpj.14688>.
 68. Ochoa-Fernandez, R., Abel, N.B., Wieland, F.G., Schlegel, J., Koch, L.A., Miller, J.B., Engesser, R., Giuriani, G., Brandl, S.M., Timmer, J., et al. (2020). Optogenetic control of gene expression in plants in the presence of ambient white light. *Nat. Methods* 17, 717–725. <https://doi.org/10.1038/s41592-020-0868-y>.



STAR★METHODS

KEY RESOURCES TABLE

REAGENT or RESOURCE	SOURCE	IDENTIFIER
Antibodies		
Mouse Monoclonal Anti-HA	Sigma-Aldrich	RRID:AB_260092
Conjugated Monoclonal Anti-StreptII + HRP	Iba life sciences	RRID:AB_3095590
Bacterial and virus strains		
<i>Escherichia coli</i> Mach1	Lab strain	N/A
<i>Agrobacterium tumefaciens</i> GV3101 pmp90RK	Lab strain	N/A
<i>Serendipita indica</i>	German Collection of Microorganisms and Cell Cultures	DSM11827
Biological samples		
<i>Arabidopsis thaliana</i> Col-0	NASC	N60000
<i>Hordeum vulgare</i> “Golden Promise”	Lab stock	N/A
<i>Nicotiana benthamiana</i>	Lab stock	N/A
<i>Marchantia polymorpha</i> Tak1	Lab stock	N/A
<i>Marchantia polymorpha</i> Tak2	Lab stock	N/A
Chemicals, peptides, and recombinant proteins		
WGA-AF488 (Oregon Green)	Invitrogen /ThermoFisher	Catalogue No: W6748
DAPI	Invitrogen /ThermoFisher	Catalogue No: D1306
FGB1-FITC488	Wawra et al. ⁵⁴	N/A
SYTOX Orange	Invitrogen /ThermoFisher	Catalogue No: S11368
dAdo	Sigma-Aldrich	CAS No: 16373-93-6
Evans blue	Sigma-Aldrich	CAS No: 314-13-6
Adenosine	Sigma-Aldrich	CAS No: 58-61-7
SyproRuby	Invitrogen /ThermoFisher	Catalogue No: S12000
Coomassie Brilliant Blue	RAL Diagnostics	362740-0025
MVB072	Kolodziejek et al. ²⁷	N/A
Fig22	GenScript	Cat. No: RP19986
AMP	Sigma-Aldrich	CAS No: 4578-31-8
dAMP	Sigma-Aldrich	CAS No: 653-63-4
ADP	Sigma-Aldrich	CAS No: 20398-34-9
dADP	Sigma-Aldrich	CAS No: 72003-83-9
ATP	Sigma-Aldrich	CAS No: 34369-07-8
dATP	Sigma-Aldrich	CAS No: 74299-50-6
Coelenterazine	Roth	CAS No: 55779-48-1
Horseradish Peroxidase	Sigma-Aldrich	CAS No: 9003-99-0
Cellulase “Onozuka R-10”	SERVA Electrophoresis GmbH	CAS No: 9012-54-8
Macerozyme R10	SERVA Electrophoresis GmbH	CAS No: 9032-75-1
D-Luciferin	Biosynth	CAS No: 115144-35-9
FM4-64	Invitrogen /ThermoFisher	Catalogue No: F34653
Critical commercial assays		
First strand cDNA synthesis kit	ThermoFisher	Catalogue No: K1612
GoTaq® qPCR Master Mix, 2X	Promega	Catalogue No: A600A
NucleoSpin Plasmid prep	Macherey & Nagel	Catalogue No: 740588
NucleoSpin Gel & PCR Clean-Up	Macherey & Nagel	Catalogue No: 740609
Gateway BP clonase II Enzyme mix	Invitrogen/ThermoFisher	Catalogue No: 11789020
Gateway LR clonase II Enzyme mix	Invitrogen/ThermoFisher	Catalogue No: 11791020

(Continued on next page)

Continued		
REAGENT or RESOURCE	SOURCE	IDENTIFIER
Deposited data		
RNASeq data: Arabidopsis after dAdo treatment	this paper	GEO database: GSE209761 & GSM6394981
Experimental models: Organisms/strains		
<i>Arabidopsis</i> : UBQ10:H2B:mCherry	Marquès-Bueno et al. ⁵⁵	N/A
<i>Arabidopsis</i> : 35S::SiNucA	this paper	N/A
<i>Arabidopsis</i> : 35S::SiNucA:mCherry	this paper	N/A
<i>Arabidopsis</i> : 35S::SiNucA:mCherry(w/o SP)	this paper	N/A
<i>Arabidopsis</i> : Col-0 ^{AEQ}	Choi et al. ³³	N/A
<i>Arabidopsis</i> : Col-0 ^{AEQ} <i>dorm1</i>	Choi et al. ³³	N/A
<i>Arabidopsis</i> : <i>ent3</i>	NASC	SALK_204257C
<i>Arabidopsis</i> : <i>ent1</i>	NASC	SALK_025174C
<i>Arabidopsis</i> : <i>isi</i>	NASC	SALK_034517C
<i>Arabidopsis</i> : CRISPR <i>isi</i>	this paper	N/A
<i>Serendipita indica</i> : FGB1::SiNucA:HA:His	this paper	N/A
Oligonucleotides		
All oligonucleotides are listed in Table S8.	N/A	N/A
Recombinant DNA		
FGB1::SiNucA:HA:His for stable fungal transformation	this paper	N/A
35S::SiNucA for stable Arabidopsis transformation	this paper	N/A
35S::SiNucA:mCherry for stable Arabidopsis transformation	this paper	N/A
35S::SiNucA:mCherry (w/o SP) for stable Arabidopsis transformation	this paper	N/A
pDGE347_Cas9_4xsgRNA for stable Arabidopsis transformation targeting ISI for CRISPR-CAS9-induced KO	this paper	N/A
Software and algorithms		
Prism 8	Graphpad	https://www.graphpad.com/
Fiji software	Schindelin et al. ⁵⁶	https://imagej.net/software/fiji/
Trimmomatic v.0.36	Bolger et al. ⁵⁷	https://github.com/usadellab/Trimmomatic
Kallisto v.0.46.2	Bray et al. ⁵⁸	https://github.com/pachterlab/kallisto
R package: tximport	Soneson et al. ⁵⁹	https://github.com/thelovelab/tximport
R package: DESeq2	Love et al. ⁶⁰	https://github.com/thelovelab/DESeq2

EXPERIMENTAL MODEL AND STUDY PARTICIPANT DETAILS

Plant Material and Growth Conditions

Seeds of *A. thaliana* ecotype Columbia 0 (Col-0), Col-0^{AEQ}, and Col-0^{AEQ} *dorm1*,³³ the SALK lines SALK_034517C (*isi*), SALK_204257C (*ent3*) and SALK_025174C were used in the experiments. SALK lines and a matching Col-0 control were obtained from the Nottingham Arabidopsis Stock Centre (NASC, <http://arabidopsis.info>).

In addition, Col-0 expressing histone H2B fused to mCherry (H2B:2xmCherry) under the UBQ10 promoter in root cells⁵⁵ were used in this study. Col-0 transformation was performed using the floral dip method as described in Nizamet al.¹³ to generate the transgenic lines 35S::SiNucA, 35S::SiNucA:mCherry (with and without signal peptide) and the CRISPR*isi* line.

Arabidopsis seeds were surface sterilized (70 % ethanol for 10 minutes, 100 % ethanol for 7 minutes) and after 3 days of stratification, grown on ½ MS medium (Murashige-Skoog medium, with vitamins, pH 5.7) containing 1% (w/v) sucrose and 0.4% (w/v) Gelrite under short-day conditions (8 h light, 16 h dark) with 130 μmol m⁻² s⁻¹ light and 22 °C/18 °C. Two methods were used for fungal inoculation: 1) 7-day-old seedlings were transferred to ½ MS without sucrose or 1/10 PNM (Plant Nutrition Medium, pH 5.7) plates (15-20 seedlings per plate). 1 ml of water containing 5x10⁵ chlamydospores of *S. indica* was pipetted onto the root and surrounding area. Control plants were inoculated with sterile water. 2) Sterile *A. thaliana* seeds were incubated in 1 ml of water containing 5x10⁵ *S. indica* chlamydospores for one hour and then pipetted onto 1/10 PNM plates.

For experiments using barley, seeds of the cultivar “Golden Promise” were used. The seeds were surface sterilized with 6 % sodium hypochlorite for one hour under continuous shaking and subsequently washed with sterile water for four hours, including water

exchanges every 30 minutes. The sterilized seeds were transferred to petri dishes onto autoclaved filter papers wetted with 3 ml sterile water. After four days of germination in the dark at room temperature (20 °C, high temperatures inhibit germination), the germinated seedlings were transferred onto 1/10 PNM medium in sterile mason jars.

1/10 PNM medium contains: 0.005 % (w/v) KNO₃, 0.005 % (w/v) KH₂PO₄, 0.0025 % (w/v) K₂HPO₄, 0.049 % (w/v) MgSO₄, 0.00472 % (w/v) Ca(NO₃)₂, 0.0025 % (w/v) NaCl, 0.5 % (v/v) Fe-EDTA stock solution and 1.2 % (w/v) Gelrite. After the pH was adjusted to 5.6, the medium was autoclaved and 1 % (v/v) 1 M MES (pH 5.6) was added.

The Fe-EDTA stock solution contains: 2.78 % (w/v) FeSO₄ x 7 H₂O & 4.13 % (w/v) Na₂EDTA x 2 H₂O.

Barley plants were grown at a day/night cycle of 16/8 hours, 60 % humidity and a light intensity of 108 μmol/m²s.

For *Marchantia polymorpha*, the gemmae of the male Tak1 and female Tak2 gametophytes were cultured on half-strength B5 medium (1.5 g/l of 1/2 Gamborg B5 salt mixture, 0.5 g/l of MES, 10 g/l sucrose, 10 g/l plant agar – pH set to 5.2 with KOH) under continuous light.

Fungal strains and cultivation techniques

S. indica strain DSM11827 (German Collection of Microorganisms and Cell Cultures, Braunschweig, Germany) was cultured on complete medium (CM) as previously described in Hilbert et al.⁶¹

CM medium contains: 5 % (v/v) 20 x salt solution, 2 % (w/v) glucose, 0.2 % peptone (w/v), 0.1 % (w/v) yeast extract, 0.1 % (w/v) casamine acids, 0.1 % microelement solution (v/v) & 1.5 % (w/v) agar.

The 20x salt solution contains 12 % (w/v) NaNO₃, 1.04 % (w/v) KCl, 1.04 % (w/v) MgSO₄ x 7 H₂O & 3.04 % (w/v) KH₂PO₄. The microelement solution contains 0.6 % (w/v) MnCl₂ x 4 H₂O, 0.15 % (w/v) H₃BO₃, 0.265 % (w/v) ZnSO₄ x 7 H₂O, 0.075 % (w/v) KI, 0.00024 % (w/v) Na₂MoO₄ x 2 H₂O & 0.013 % (w/v) CuSO₄ x 5 H₂O.

Liquid (CM) cultures were incubated from spores at 28 °C and 120 rpm. Spores were collected from 4 weeks old plates.

METHOD DETAILS

Fungal inoculation

Two methods were used for fungal inoculation: 1) 7-day-old seedlings were transferred to ½ MS without sucrose or 1/10 PNM (Plant Nutrition Medium, pH 5.7) plates (15–20 seedlings per plate). 1 ml of water containing 5x10⁵ chlamydo spores of *S. indica* was pipetted onto the root and surrounding area. Control plants were inoculated with sterile water. 2) Sterile *A. thaliana* seeds were incubated in 1 ml of water containing 5x10⁵ *S. indica* chlamydo spores for one hour and then pipetted onto 1/10 PNM plates.

For harvesting, individual roots were thoroughly washed with water, a 4 cm root section was cut 0.5 cm below the shoot, and immediately frozen in liquid nitrogen. Two to three plates of 20 seedlings each were pooled per replicate.

Confocal microscopy

Colonized Arabidopsis roots were treated with 5 μg/ml Wheat Germ Agglutinin-Alexa Fluor 488 conjugate (WGA-AF 488, Life Technologies, Thermo Fisher Scientific, Schwerte, Germany) or 1 μM FGB1-FITC of⁵⁴ To visualize the fungal cell wall. 250 ng/ml 4',6-diamidino-2'-phenylindole dihydrochloride (DAPI) or 500 nM SYTOX Orange (Life Technologies, Thermo Fisher Scientific, Schwerte, Germany) were used as nucleic acid stain.

A TCS SP8 confocal microscope (Leica, Wetzlar, Germany) was used for confocal laser scanning microscopy on living cells. AF 488 and FITC were excited with an argon laser at 488 nm, and the emitted light was detected with a hybrid detector at 500–550 nm. mCherry and SYTOX orange were excited with a DPSS laser at 561 nm, and the signal was detected with a hybrid detector at 590–660 nm. DAPI was excited with a diode laser at 405 nm, and the emitted light was detected with a hybrid detector at 415–460 nm.

DNA and RNA extraction

DNA was extracted from frozen root or fungal material as described in Wawra et al.¹⁸ Briefly, approximately 500 mg of ground frozen material was dissolved in 1 ml of CTAB extraction buffer (100 mM TrisHCl pH 7.5, 50 mM EDTA pH 8, 1.5 M NaCl, 2% (w/v) cetyltrimethylammonium bromide, 0.05% (v/v) β-mercaptoethanol) and homogenized for 10 min. 500 μl chloroform:isoamyl alcohol mixture (24:1) was added and the tubes were mixed and centrifuged for 5 min. Ethanol and 1 volume of chloroform:isoamyl alcohol mixture (24:1) were added to the upper phase and centrifuged again. The DNA in the upper phase was precipitated with 1 volume of isopropanol at 4 °C for 1 h.

RNA was extracted with TRIzol (Invitrogen, Thermo Fisher Scientific, Schwerte, Germany) and DNA was digested with DNase I (Thermo Fisher Scientific, Schwerte, Germany) according to the manufacturer's instructions. cDNA was synthesized using the Fermentas First Strand cDNA Synthesis Kit (Thermo Fisher Scientific, Schwerte, Germany).

Quantitative RT-PCR analysis

For quantitative real-time PCR, the 2x GoTaq qPCR Master Mix (Promega, Mannheim, Germany) was used. 500 nM forward and reverse primers and 10–20 ng of cDNA or gDNA template were added to each. The reaction was performed in a CFX connect real time system (BioRad, Munich, Germany) with the following program: 95°C 3min, 95°C 15s, 59°C 20s, 72°C 30s, 40 cycles and melting curve analysis. Relative expression was calculated using the 2^{-ΔΔCT} method.⁶² All oligonucleotides used can be found in Table S8.

Serendipita indica transformation

S. indica protoplasts were transformed using the PEG-mediated transformation system as described in Wawra et al.⁵⁴: For the transformation of *S. indica*, a 250 ml culture in liquid CM was inoculated with 1 ml of a spore solution set to a concentration of 2.5×10^4 spores/ml and grown for 7 days at 28°C with 120 rpm of shaking. After 7 days the mycelium was collected by filtration through a Miracloth filter and washed with 50 ml 0.9 % NaCl solution before it was re-suspended in 20 ml fresh CM. The mycelial aggregates were disrupted using a Microtron® MB550 homogenizer (Kinematica, Lucerne, Switzerland) for 10 s and the homogenized culture was regenerated for 3 days at 28°C with 120 rpm of shaking in a total volume of 150 ml fresh CM. After regeneration the young mycelium was filtered again through a Miracloth filter and washed with 50 ml of 0.9 % NaCl solution to remove spores and residual medium. Protoplastation was carried out by re-suspending the filtrated mycelium in sterile filtrated 20 ml SMC buffer (1.33 M sorbitol, 50 mM $\text{CaCl}_2 \times 2\text{H}_2\text{O}$, 20 mM MES, pH 5.8) supplemented with 2 % (w/v) *Trichoderma harzianum* lysing enzymes (Sigma Aldrich, Taufkirchen, Germany). After incubation for 2 h at 32°C with 100 rpm of shaking the protoplastation was checked microscopically and the reaction was stopped by filtration through a Miracloth filter and addition of an equal volume of cold STC buffer (1 M sorbitol, 50 mM $\text{CaCl}_2 \times 2\text{H}_2\text{O}$, 10 mM Tris-HCl, pH 7.5). The protoplasts in the filtrate were pelleted at 3,000 xg in a swing out rotor for 10 min and washed three times with cold STC. The protoplasts were finally re-suspended in an appropriate volume of cold STC and stored on ice until transformation. 50 µg of the plasmid DNA were linearized by incubation with 20 units of the restriction enzyme *Bsa*I and precipitated for 10 min at room temperature by addition of 0.5 volumes of 7.5 M ammonium acetate and 2 volumes of 100 % isopropanol. The plasmid DNA was pelleted by centrifugation for 30 min at 17,000 x g, washed twice with 75 % ethanol, dried for 5 min at room temperature and finally re-suspended in 12 µl sterile ddH₂O. For a single transformation reaction 70 µl of protoplast solution was mixed with 10 µl linearized vector, 1 µl of a 15 mg/ml heparin solution and 10 units *Bsa*I on ice and incubated for 10 min. Subsequently, 0.5 ml of a freshly prepared ice cold, filter sterilized (0.45 µm filter) STC solution supplemented with 40 % (w/v) PEG 3350 (Sigma Aldrich, Taufkirchen, Germany) was added followed by a further incubation for 15 min on ice. Finally, the protoplast solution was mixed with 5 ml of the MYP top medium (0.7 % (w/v) malt extract, 0.1 % (w/v) peptone, 0.05 % (w/v) yeast extract, 0.6 % (w/v) agar, 0.3 M sucrose) which was kept at 45°C to prevent solidification and distributed on 20 ml solidified MYP bottom medium (0.7 % (w/v) malt extract, 0.1 % (w/v) peptone, 0.05 % (w/v) yeast extract, 1.2 % (w/v) agar, 0.3 M sucrose) containing 80 µg/ml hygromycin for selection of positive transformants. After solidification of the top medium the plates were incubated at 28°C. All clones that were further used were checked whether they were homokaryotic or dikaryotic.

Nuclease activity test

To assay the nuclease activity of the purified protein, 10 nM *Si*NucA was mixed with 100 ng linearized plasmid, 1 µg gDNA, or 1 µg RNA in buffer (5 mM Tris pH 8, 1 mM MgCl_2 , 1 mM CaCl_2 , 0.1 % microelement solution (from CM medium)). The mixture was incubated at RT for 1 to 30 min, then loading dye was added and samples were run on a 1-2 % agarose gel.

To test nuclease activity in the filtrate of an *S. indica* culture, a 5-day-old CM culture was minced and incubated for an additional 3 days. The culture was filtered through Miracloth (Millipore Merck, Darmstadt, Germany), and 50 µl of culture filtrate was added to linearized plasmid DNA, gDNA, or RNA.

SiNucA-HA-His purification

A 7-day-old liquid culture of *S. indica* grown in CM medium was filtered through Miracloth. The mycelium was washed with 0.9% NaCl and minced in fresh CM medium in a mixer (MicrotronR MB550 homogenizer (Kinematica, Lucerne, Switzerland)). The culture was regenerated for two days. Subsequently, the culture was filtered with Miracloth and through a 0.45 µm membrane filter. To this cell-free culture filtrate, 1 mM phenylmethanesulfonylfluoride (PMSF) was added and the pH was adjusted to pH 7 with 1 M Tris pH 8. Proteins were precipitated with 80% ammonium sulfate. The protein pellet was resuspended in 20 mM Tris pH 8. Proteins were separated by size exclusion chromatography (Sephadex G 200 column, Hiload 6/600) using a 20 mM Tris pH 8 / 150 mM NaCl buffer. Fractions containing *Si*NucA-HA-His were desalted by dialysis and checked by SDS-PAGE and anti-HA Western blot. The protein was stored in 20 mM Tris pH 8. The identity of the protein was verified by LC-MS/MS.

Measurement of enzyme kinetics of SiE5NT

*Si*E5NT fused to a C-terminal hemagglutinin (HA) and Strep tag (pXCScpmv-HAStrep, V69) was transiently expressed in *Nicotiana benthamiana* and purified by affinity chromatography as described by Werner et al.⁶³ and Myrach et al.⁶⁴ Enzyme concentrations were determined using bovine serum albumin standards after SDS-PAGE and Coomassie Blue staining with an Odyssey Fc Dual Mode Imaging System (Li-cor Biosciences, Germany).

To determine substrate specificity, different substrates were tested. Briefly, 10 µl of purified enzyme (1.9×10^{-4} mg protein) was added to 70 µl of reaction buffer (10 mM MES buffer, pH 6.0; 1 mM CaCl_2 and 1 mM MgCl_2) and pre-incubated for 5 minutes. Substrates were added (20 µl of a 5 mM stock solution) to give a final reaction volume of 100 µl. The reaction was quenched with 400 µl of MeOH at the indicated times and centrifuged for 10 min at 21,000g at 4°C. The supernatant was evaporated in a vacuum concentrator and the dry pellet resuspended in 100 µl of HPLC mobile phase A.

Samples were analyzed using an Agilent 1200 SL HPLC system equipped with a diode array detector. 10 µl of the sample was injected onto a Supelcosil LC-18-T column (Sigma-Aldrich) at a flow rate of 0.8 ml min⁻¹ and a column temperature of 25°C. The analytes were separated with the following gradient: 0 min, 100% A; 9 min, 100% A; 15 min, 75% A; 17.5 min, 10% A; 19 min, 0% A; 23 min, 0% A; 24 min, 100% A; 30 min, 100% A. Mobile phase A consisted of 100 mM KH_2PO_4 , pH 6.0, in deionized water and mobile

phase B consisted of 90% 100 mM KH_2PO_4 , pH 6.0, in deionized water and 10% MeOH. Appropriate standard solutions were used for quantification. Data were analyzed using Agilent Chemstation software.

Kinetic constants for deoxyadenosine monophosphate and adenosine monophosphate were determined using the EnzCheck (Thermo Fisher Scientific, Waltham, USA) phosphatase assay kit according to specifications, using only one-tenth of the recommended reaction volume.

Measurement of release of deoxynucleosides

10 μg of salmon sperm DNA was incubated with 4 μl of SiNucA, 10 μl of SiE5NT, or a combination of both in a final volume of 40 μl containing 10 mM HEPES, pH 7.2; 100 mM MgCl_2 ; and 1 mM DTT. The enzymes were incubated in the buffer mixture for 5 minutes prior to the addition of DNA. The reaction was incubated at 22 $^\circ\text{C}$ for 1 hour and inactivated at 95 $^\circ\text{C}$ for 5 minutes. Subsequently, centrifugation was performed at 40000 g and 4 $^\circ\text{C}$ for 20 minutes. 20 μl of the supernatant was analyzed on a 2% agarose gel. The remaining 20 μl of the supernatant was mixed with 50 μl of water and used for HPLC MS/MS analysis. Samples and standards were analyzed using an Agilent 1290 Infinity II HPLC system coupled to an Agilent 6470 triple quadrupole mass spectrometer. Analytes (10 μl samples) were separated on a 50 x 4.6 mm Polaris C18A column (Agilent) using the following gradient: 0 min, 96% A; 8 min, 35% A; 8.2 min, 0% A; 10 min, 0% A; 10.1 min, 96% A. Mobile phase A consisted of 10 mM ammonium acetate, pH 7.5, and mobile phase B was pure MeOH. The flow rate was 0.6 ml min^{-1} and the column temperature was 30 $^\circ\text{C}$. In-source parameters were set as previously described for deoxynucleoside analysis.⁶⁵ All analytes were measured in positive mode. Transitions (precursor and production), collision energies, and fragmentor energies are listed in Table S9.

PAM fluorometric measurements

PAM fluorometry measurements were performed by transferring 9-day-old *Arabidopsis* seedlings into 24 well plates containing 2 ml of 2.5 mM MES buffer (pH 5.6). 3 seedlings were pooled in one well. After 24 hours of regeneration, seedlings were treated with solutions of 5' deoxyadenosine (dAdo), adenosine (Ado), or methyl jasmonate (all Sigma-Aldrich, Taufkirchen, Germany), adjusting to a final concentration of 500 μM . Treated seedlings were incubated in complete darkness for 20 min to reach a dark-adapted condition. The photosynthetic activity of the plants was measured using the M-Series PAM fluorometer (Heinz Walz GmbH, Effeltrich, Germany). Data were analyzed using ImagingWin software (v.2.41a; Walz, Germany). When further analysis of photosynthetic area development was required, it was evaluated using Fiji (ImageJ).⁵⁶

Cell death staining with Evans blue

A modified protocol as described in Vijayaraghavareddy et al.⁶⁶ was used. To quantify cell death induced by *S. indica* in *Arabidopsis*, plants were used for cell death staining at three time points, 7, 10, and 14 days after fungal spore inoculation, using five plants per treatment. For cell death induced by dAdo (or chemically induced cell death), plants were microscopied after 4 days of cell death treatment. To remove external fungal growth or chemical treatment solutions, plants were washed three times in ddH₂O before cell death staining in a 2.5 mM Evans blue solution (Sigma-Aldrich, lot #MKCH7958) dissolved in 0.1 M CaCl_2 pH 5.6 for 15 minutes. After extensive washing for one hour with ddH₂O, images were captured using a Leica M165 FC microscope.

Activity-based protein profiling

After treatment with 500 μM dAdo, 500 μM Ado, or MES buffer, 9-day-old *Arabidopsis* seedlings were frozen in liquid nitrogen, ground, and dissolved in 50 mM Tris-HCl buffer (pH 7). After centrifugation, the supernatant was divided and treated with either the proteasome inhibitor MG132 (final concentration: 50 μM , company) or DMSO for 30 min. Samples were then incubated with 26S proteasome probe MVB072 (final concentration: 1 μM , company): 1 μM .²⁷ Samples were then denatured in SDS loading dye at 95 $^\circ\text{C}$ and separated on 12% SDS gels. The probe was visualized using the rhodamine settings (excitation: 532 nm, emission: 580 nm) on a ChemiDoc (BioRad, CA, USA). The protein content of the samples was visualized by staining the gel with SYPROTM Ruby (Invitrogen, Carlsbad, CA, USA) according to the manufacturer's instructions.

RNAseq

7-day-old seedlings were transferred from plates to individual wells of 24-well plates containing 0.5 ml of liquid $\frac{1}{2}$ MS medium containing 0.5% (w/v) sucrose. After 5 additional days in liquid culture, the medium was replaced with 1 ml of 500 μM dAdo in 2.5 mM MES buffer pH 5.6 or 2.5 mM MES buffer pH 5.6 alone as a negative control. Three replicates of four seedlings were harvested for each treatment at 0, 3, and 12 h after treatment (hpt), frozen in liquid nitrogen, and stored at -80 $^\circ\text{C}$ until processing for RNA extraction. Total RNA was extracted using TRIzol reagent as described above. RNA integrity was confirmed by gel electrophoresis, and quantity and purity were determined using a NanoDrop 2000. Stranded mRNA-seq libraries were prepared according to the manufacturer's instructions (Vazyme Biotech Co., Nanjing, China). Qualified libraries were sequenced on a HiSeq 3000 system instrument in the Genomics and Transcriptomics Laboratory at Heinrich Heine University to generate >100 million reads with a read length of 150 bp from three biological replicates. Trimmomatic v. 0.36,⁵⁷ was used for quality trimming and adapter clipping. Reads were then mapped to *Arabidopsis* TAIR10 CDS assembly and quantified using kallisto v. 0.46.2,⁵⁸ resulting in estimated counts and transcripts per million (TPM) values. The log₂ fold difference in gene expression between conditions was estimated using the R packages tximport⁵⁹ and DESeq2.⁶⁰ Genes with statistical significance were selected (FDR-adjusted p-value < 0.05). Data have been deposited at NCBI under GEO accession number GSE209761 and GSM6394981.

Collection of extracellular fluid

7-day-old Arabidopsis seedlings germinated on ½ MS agar containing 1% sucrose were transferred to 24 well plates. Each well contained 3 seedlings in 1.5 ml of 2.5 mM MES and the specific treatment. After transfer, the plants were returned to the growth chamber for three days. The seedlings were then removed and the liquid centrifuged at 4000 g for 15 minutes. The supernatant was freeze dried and sent for metabolite analysis.

Metabolite analysis

5 µl of the apoplastic liquid was injected into an Acquity UPLC (Waters Inc.) equipped with a Nucleoshell RP18 column (Macherey and Nagel, 150mm x 2 mm x 2.1 µm) using tributylammonium as the ion pairing agent. Solvent A: 10 mM tributylamine (aqueous) acidified with glacial acetic acid to pH 6.2; solvent B acetonitrile. Gradient: 0–2 min: 2% B, 2–18 min 2–36% B, 18–21 min 36–95% B, 21–22.5 min 95% B, 22.51–24 min 2% B. Column flow was 0.4 ml min^{−1} throughout. The column temperature was 40 °C. Scheduled metabolite detection based on multiple reaction monitoring (MRM) was performed in negative mode with electrospray ionization (ESI) on a QTrap 6500 (AB-Sciex GmbH, Darmstadt, Germany): Ion source gas 1: 60 psi, ion source gas 2: 70 psi, curtain gas: 35 psi, temperature: 450 °C, ion spray voltage floating: and −4500V. MRM transitions of 189 metabolites covering central carbon and energy metabolism were previously signal optimized and retention times determined (Table S10).

Ca²⁺ influx quantification

Calcium influx assays were performed as previously described in Wanke et al.⁶⁷ Briefly, individual 7-day-old Arabidopsis seedlings were placed in white 96-well plates filled with 200 µl reconstitution buffer (2.5 mM MES pH 5.7 [Sigma-Aldrich, Taufkirchen, Germany], 10 mM CaCl₂ [Roth, Karlsruhe, Germany]). Before incubation overnight in the dark, the solution was replaced with 133 µl reconstitution buffer containing 10 mM coelenterazine (Roth, Karlsruhe, Germany). The following day, chemiluminescence was measured using a TECAN SPARK 10M microplate reader. After baseline measurement, 67 µl of three-fold concentrated elicitor solutions (or Milli-Q water as a sham control) were added manually. Cytosolic calcium influx after addition of the trigger was measured continuously for 30 min. To determine the undischarged aequorin for treatment normalization, 100 µl 3 M CaCl₂ (in 30% EtOH) was injected into each well, followed by constant measurement for 1 minute. All steps were performed with an integration time of 450 msec.

Heterologous protein production in *Nicotiana benthamiana* and protein purification

For heterologous protein production in *Nicotiana benthamiana*, leaves of 4-week-old plants were infiltrated with *Agrobacterium tumefaciens* GV3101 strains. *A. tumefaciens* was grown in LB liquid medium with the appropriate antibiotics at 28°C and 180 rpm for 2 days until an OD₆₀₀ of 1 was achieved. Cultures were centrifuged at 3500 rpm for 15 min at RT, the supernatant was discarded and resuspended in 1 ml infiltration buffer (10 mM MES pH 5.5, 10 mM MgCl₂, 200 µM acetosyringone) and incubated for 1 h in the dark at 28°C, 180 rpm. All strains were diluted with the infiltration buffer to an OD₆₀₀ of 1. Each strain was mixed with P19-expressing strains at a 1:1 ratio. 2–3 leaves per plant were infiltrated with a needleless syringe. After 4 dpi, leaves were separated from the plant and crushed in liquid nitrogen. Protein purification was performed according to Werner et al.⁶³ with minor modifications performed: A 15-ml tube was filled to the 2-ml mark with ground leaf material, and 2 ml of cold extraction buffer (100 mM Tris pH 8.0, 100 mM NaCl, 5 mM EDTA, 0.5% Triton X100, 10 mM DTT, 100 µg/ml avidin) was added. The powder was resuspended by vortexing and then centrifuged at 12000 rpm and 4°C for 10 minutes. The supernatant was transferred to a new tube and 100 µl of Strep-Tactin® Macroprep (50% slurry) was added and incubated for 60 min at 4°C in a rotating wheel. The mixture was centrifuged at 700xg at RT for 30 s and the supernatant was completely removed from the beads. The beads were washed once with 4 ml and two additional times with 2 ml of wash buffer (50 mM Tris pH 8.0, 100 mM NaCl, 0.5 mM EDTA, 0.005% Triton X-100, 2 mM DTT) by centrifugation for 30 s at 700xg and the supernatant was discarded. During the final wash, beads were transferred to a 1.5 ml tube with a low binding level. The beads were either boiled directly for 5 min at 95°C with 6x SDS loading dye to run on an SDS-PAGE, or the proteins were eluted from the beads by adding 100 µl of elution buffer (wash buffer + 2.5 – 10 mM biotin) and incubating at 25°C, >800 rpm for 5 min. Samples were centrifuged at 700xg for 20 s and elution was repeated. Elution fractions were pooled, SDS loading dye was added, and samples were run on SDS-PAGE followed by Western blot.

Ion leakage measurements

The seedlings for measurement of ion leakage were prepared in the same manner as seedlings for PAM fluorometry measurements. Ion leakage was measured with a conductivity meter (LAQUATwin EC-11; Horiba, Newhampton, UK).

Seed germination test

Sterile Arabidopsis seedlings were transferred into 24-well plates containing 2 ml of 1/10 PNM medium. The medium contained either 500 µM dAdo or the same volume of 2.5 mM MES (pH 5.6). Ten seeds were placed in each well and grown under short-day conditions after 2 days of stratification. Seedling growth was monitored by PAM fluorometry.

Root length measurements

To evaluate root length, scans of the square plates containing seedlings were analyzed using Fiji (ImageJ) and the length of the primary root was measured.

Oxidative burst assay

Individual 7-day-old Arabidopsis seedlings were transferred to white 96-well plates containing 200 μ l reconstitution buffer (2.5 mM MES pH 5.7 (Sigma-Aldrich, Taufkirchen, Germany), 10 mM CaCl_2 (Roth, Karlsruhe, Germany) and incubated overnight in the growth chamber. The following day, the buffer was replaced with 133 μ l reconstitution solution containing 15 μgml^{-1} horseradish peroxidase (Sigma-Aldrich, Taufkirchen, Germany) and 15 μM L-O12 (Wako Chemicals, Neuss, Germany). After 10 min incubation, 67 μL of three-fold concentrated elicitor solutions (or Milli-Q water as a mock control) were added manually to the wells. Measurements were started immediately and chemiluminescence was measured continuously with a TECAN SPARK 10M microplate reader (Tecan, Männedorf, Switzerland) at an integration time of 450 ms.

Protoplast isolation and transformation

As described in Ochoa-Fernandez et al.,⁶⁸ protoplasts were isolated from 2-week-old *A. thaliana* seedlings (Col-0, *isi*, *ent3*) grown in 12 cm square plates containing SCA medium (0.32 % (wt/vol) Gamborg's B5 basal salt powder with vitamins (bioWORLD), 4 mM $\text{MgSO}_4 \cdot 7\text{H}_2\text{O}$, 43.8 mM sucrose and 0.8% (wt/vol) phytoagar in H_2O , pH 5.8, autoclaved, 0.1% (vol/vol) Gamborg's B5 Vitamin Mix (bioWORLD), with a 22 °C, 16-h light – 8-h dark cycle. The leaf material was sliced with a scalpel and incubated in darkness at 22 °C overnight in MMC solution (10 mM MES, 40 mM $\text{CaCl}_2 \cdot 2\text{H}_2\text{O}$, 467 mM mannitol, pH 5.8, sterile filtered) containing 0.5% cellulase Ono- zuka R10 and macerozyme R10 (SERVA Electrophoresis). After 18h, the lysate was thoroughly mixed, passed through a 70 mm pore size sieve and transferred to a MSC solution (10 mM MES, 0.4 M sucrose, 20 mM $\text{MgCl}_2 \cdot 6\text{H}_2\text{O}$, 467 mM mannitol, pH 5.8, sterile filtered) and carefully overlaid with MMM solution (15 mM MgCl_2 , 2.5 mM MES, 467 mM mannitol, pH 5.8, sterile filtered). After centrifugation the protoplasts were collected at the interphase and transferred to a W5 solution (2 mM MES, 154 mM NaCl, 125 mM $\text{CaCl}_2 \cdot 2\text{H}_2\text{O}$, 5 mM KCl, 5 mM glucose, pH 5.8, sterile filtered) and diluted to 10^6 protoplasts per 100 ml after counting in a Rosenthal chamber. The plasmids were transferred by PEG-mediated transformation. 10 μg of plasmid DNA (pSW209 – firefly luciferase reporter; pGEN016 – Stuffer; pGWB502 N-TIR; pGWB502N-trunc TIR) were used to transform 1,000,000 protoplasts in non-treated 6-well plates by drop-wise addition of a PEG solution (4 g PEG_{4000} , 2.5 ml of 800 mM mannitol, 1 ml of 1 M CaCl_2 and 3 ml H_2O). After 8-min incubation, 120 ml MMM and 1.8 ml PCA (0.32% (wt/vol) Gamborg's B5 basal salt powder with vitamins (bioWorld), 2 mM $\text{MgSO}_4 \cdot 7\text{H}_2\text{O}$, 3.4 mM $\text{CaCl}_2 \cdot 2\text{H}_2\text{O}$, 5 mM MES, 0.342 mM l-glutamine, 58.4 mM sucrose, 444 mM glucose, 8.4 mM calcium pantothenate, 2% (vol/vol) biotin from a biotin solution 0.02% (wt/vol) 0.1% (vol/vol) in H_2O , pH 5.8, sterile filtered, 0.1% (vol/vol) Gamborg's B5 Vitamin Mix, 64.52 mg ml^{-1} ampicillin), were added to a final volume of 2 ml protoplast suspension. 3 hours after transformation 0.9 ml of protoplast were transferred to non-treated 12 well plates and induced with dAdo (0 μM , 25 μM , 50 μM , 100 μM). The protoplasts were kept in darkness for 18 h at 22 °C.

Four technical replicates of 80 ml protoplast suspensions were pipetted into a 96-well white flat-bottom plates (Costar) for determination of activity luciferases as indicator for cell death. Addition of 20 ml of FLuc substrate (0.47 mM d-luciferin (Biosynth AG), 20 mM tricine, 2.67 mM $\text{MgSO}_4 \cdot 7\text{H}_2\text{O}$, 0.1 mM EDTA $2\text{H}_2\text{O}$, 33.3 mM dithiothreitol, 0.52 mM adenosine 5'-triphosphate, 0.27 mM acetyl-coenzyme A, 5 mM NaOH, 264 mM $\text{MgCO}_3 \cdot 5\text{H}_2\text{O}$, in H_2O , pH 8) was performed prior to luminescence determination in a plate reader (determination of 20-min kinetics, integration time 0.1 s).

QUANTIFICATION AND STATISTICAL ANALYSIS

To evaluate significant differences, ANOVA with post-hoc Tukey HSD test or Student's t-test were used in this study. Statistical analyses were performed using GraphPad Prism. Statistical details of the experiments can be found in the figure legends.

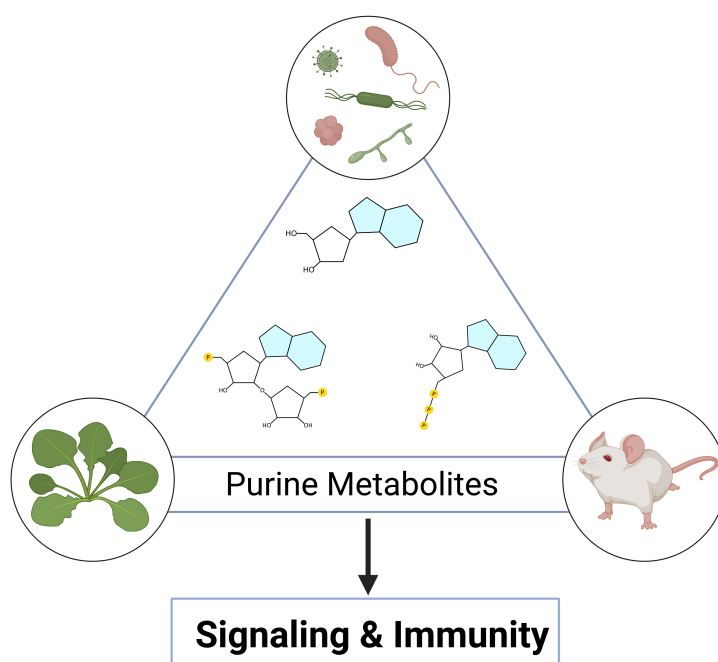
Chapter 5

Purine-Based Infochemicals and Immunometabolites: A Comparative Review of Emerging Signaling Pathways in Plants and Animals

Nick Dunken¹, Tim Thomsen¹, Alga Zuccaro^{1,2}

¹University of Cologne, Institute for Plant Sciences, Germany

²Cluster of Excellence on Plant Sciences (CEPLAS), Germany



Under review in FEMS MICROBIOLOGY REVIEWS upon invitation

Author Contributions

Nick Dunken and Tim Thomsen conceptualized and wrote the manuscript. Alga Zuccaro provided supervision, guidance, and critical revision of the text. **Nick Dunken** and Tim Thomsen designed all figures. All authors read and approved the final version of the manuscript.

One Sentence Summary

This review explores the emerging roles of purine metabolites in signaling and immunity across plants, animals, and bacteria, offering a new perspective on immunometabolism and infochemicals as key regulators of host-microbe interactions, shaping defense and symbiosis.

Abstract

Purine-based metabolites serve as essential mediators of signaling, immunity, and host-microbe interactions across biological kingdoms. This review explores their extracellular and intracellular functions, focusing on well-characterized molecules as well as emerging players, and examines the conserved and divergent mechanisms underlying purine-mediated responses in plants, animals, and bacteria. Key topics include the role of extracellular ATP in immune responses, the dual function of NAD^+ as both a metabolic co-factor and signaling molecule, and the emerging roles of deoxynucleosides and 2',3' cyclic adenosine monophosphate (cAMP) in stress and immunity regulation. Special emphasis is placed on TIR domain proteins, which generate novel purine-derived infochemicals — bioactive signaling metabolites that regulate immune responses and cell death while modulating host-microbe interactions. By integrating insights from plant, animal, and bacterial research, this review underscores the potential of purine-based signaling molecules and their natural and chemically modified functional derivatives as targets for therapeutic and agricultural innovation, bridging fundamental discoveries with practical applications. Finally, moving beyond purine-based metabolites, we offer a new perspective on immunometabolism and infochemicals as fundamental regulators of host-microbe interactions, shaping defense, symbiosis, and broader evolutionary dynamics.

Introduction

In organisms across all domains of life, purine-based metabolites such as ATP, ADP, adenosine monophosphate (AMP), nicotinamide adenine dinucleotide (NAD^+), and their derivatives play various roles as energy carriers, metabolic coenzymes, and signaling molecules. Beyond their well-documented intracellular functions, the release of these metabolites into the extracellular milieu, such as the plant apoplast, has revealed additional significance, particularly in intercellular communication and immune signaling through sensing or uptake. eATP has emerged as a key player in mediating cellular responses to environmental cues, stresses, and microbial colonization. Extracellular signaling of ATP is observed across kingdoms, emphasizing the conserved nature of purine signaling pathways.

Other nucleotides and nucleosides, including NAD^+ , oxidized nicotinamide adenine dinucleotide phosphate (NADP^+), and their derivatives exhibit redundant, as well as distinct roles in immune modulation. In plants, extracellular NAD^+ has been implicated in systemic acquired resistance (SAR), a critical defense mechanism against pathogens. Similarly, in animals, NAD^+ influences

immune cell function, apoptosis, and inflammatory processes, further underscoring the conserved nature of purine-based signaling across kingdoms.

An emerging area of interest is the role of deoxynucleosides, particularly dAdo and deoxyguanosine (dGuo), in immune responses and host-microbe interactions. These molecules, derived from extracellular DNA degradation, have been shown to trigger specific immune pathways in both plants and animals. In plants, dAdo has been linked to cell death induction via a TIR-NLR protein, whereas in animals, it plays a role in apoptosis and inflammation through caspase activation upon cell-type-specific uptake. The metabolic fate of these deoxynucleosides and their incorporation into the purine salvage pathway highlight the metabolic versatility and signaling potential of purine metabolites.

Another intriguing aspect of purine signaling is 2',3'cAMP, a positional isomer of the well-characterized second messenger 3',5'cAMP. In plants, 2',3'cAMP accumulates under stress conditions, where it has been implicated in the formation of stress granules and the regulation of stress responses. In animals, 2',3'cAMP has been associated with tissue-specific effects ranging from neurotoxicity to renoprotection, suggesting a complex and context-dependent role. The antagonistic relationship between 2',3'cAMP and adenosine add another layer of complexity to purine-mediated signaling.

Finally, the recent discovery of TIR domain enzymatic activity on both NAD⁺ and nucleic acids resulting in the production of purine-based infochemicals - bioactive metabolites that serve as chemical signals mediating interactions between organisms. These infochemicals include metabolites such as cADPR variants, pRib-AMP/ADP or 2',3'cAMP and their discovery has opened new avenues for exploring the intersection of purine metabolism and immune signaling. While NADase activity of TIR domain proteins has been identified in animals, bacteria, and plants; initial studies revealed kingdom-specific differences in the resulting purine products and their signaling roles. In animals and prokaryotes, NAD⁺ degradation leads to substrate depletion, which primarily drives signaling and induces cell death. In plants, TIR proteins generate a diverse repertoire of signaling molecules, where the products themselves predominantly regulate cell death and immunity through distinct, tightly regulated outputs.

This review provides a comprehensive overview of the diverse roles of extracellular purine metabolites in signaling, immunity, and host-microbe interactions. By combining recent findings with established insights from plant and animal systems, we aim to uncover commonalities and divergences in purine signaling mechanisms. We furthermore present recent studies that demonstrate how both microbes and hosts influence this signaling axis to initiate or inhibit interactions. In doing so, we hope to shed light on the potential of purine metabolites as therapeutic and agricultural innovations.

Extracellular ATP Signaling: Mechanisms and Functions in Plants and Animals

While intracellular ATP is well characterized in its role as an essential provider of energy in all living systems, eATP plays a pivotal role as a signaling molecule in both plants and animals, especially

in immunity-related processes. While the fundamental processes of eATP perception, release, hydrolysis and uptake are highly similar across kingdoms, the specific mechanisms and molecular key players are distinct.

In plants, ATP can be translocated into the extracellular space in several ways, including leakage from surrounding damaged cells (Song et al. 2006), exocytosis through vesicular pathways (Kim et al. 2006), and through active transporters such as PGP1 and PM-ANT1 (Thomas et al. 2000; Rieder and Neuhaus 2011). Similarly, in animals, eATP is released into the extracellular milieu through cell damage, vesicular secretion, pannexin and connexin channels or active transport via ABC transporters (Bodin and Burnstock 2001; Lazarowski et al. 2011; Lohman et al. 2012; Taruno 2018). The release mechanisms in both plants and animals are comparable, reflecting a conserved role of eATP in signaling stress and damage.

In the apoplast of plants, eATP is not directly imported into the cell. Instead, it undergoes hydrolysis by several enzymes such as ecto-apyrase (APY) (Clark and Roux 2011) as well as purple acid phosphatases (PAPs) (Bhadouria and Giri 2022), which degrade it to AMP. Further enzymatic conversions, including those mediated by 5′nucleotidase (5′NT) (Zrenner et al. 2006) and the Nucleoside Hydrolase 3 (NSH3) (Jung et al. 2011), lead to the generation of adenine and adenosine. These breakdown products are subsequently imported into the cell via nucleoside transporters like ENT3, ENT6, or purine permeases (PUPs), where the nucleosides contribute to metabolic pathways such as DNA and RNA synthesis through the purine salvage pathway (Gillissen et al. 2000; Li et al. 2003; Wormit et al. 2004; Ashihara et al. 2018). In animals, the hydrolysis of eATP is carried out by enzymes of the E-NTPDase family (which are known as apyrases in plants) and alkaline phosphatases (Yegutkin 2008; Zimmermann et al. 2012). Alternatively, ATP can directly be hydrolyzed to AMP by ecto-nucleotide pyrophosphatases (E-NPPs). Similar to the process in plant cells, in animals AMP can be converted to adenosine by ecto-5′-nucleotidases (E5′NTs), while adenosine can then further be imported and exported from the cell by equilibrative- and concentrative nucleoside transporters (ENTs, CNTs) (Gray et al. 2004; Matsuoka and Ohkubo 2004; King et al. 2006). Additionally, adenosine may undergo conversion or inactivation via adenosine deaminase (ADA) to inosine, which can further be metabolized to hypoxanthine by purine nucleoside phosphorylases (PNPs), leading to specialized metabolites inside or outside the cell (Shryock and Belardinelli 1997; Blackburn and Kellems 2005). Together with AMP, ADP, and ATP phosphorylation, this constitutes a major route of purine salvage in animal cells.

In the extracellular space, eATP functions as a DAMP recognized by specific purinergic receptors located at the plasma membrane. In plants, the primary purinoceptor, P2K1 (also known as DORN1), binds eATP, triggering signaling cascades involving Ca^{2+} influx, nitric oxide (NO) production, and accumulation of ROS via activation of plasma membrane-localized NADPH oxidases such as RBOHD (Song et al. 2006; Demidchik et al. 2009; Choi et al. 2014). These events activate MAPK pathways and induce transcriptional changes that enhance immunity and modulate phytohormone signaling like jasmonic acid (JA) pathways (Tanaka et al. 2014; Balagué et al. 2017; Jewell et al. 2024). A second receptor, P2K2, partially complements P2K1, underscoring the complexity of eATP signaling in plants (Pham et al., 2020). Studies using P2K1 knock-out and overexpression lines reveal its essential role in transcriptional responses, hormonal defense pathways and the regulation of defense-related transcription factors such as MYCs, acting downstream of the jasmonate receptor,

or calmodulin-binding transcription activators (CAMTAs) (Jewell et al. 2019). Recent findings also link eATP to the glucosinolate biosynthesis in leaves, further broadening our understanding of eATP in immunity (Jewell et al. 2022). Unlike in animals, no surface-localized receptors for adenosine or adenine have been identified in plants.

In animal systems, eATP is sensed by two distinct groups of plasma membrane-localized purinergic receptors: ionotropic/ligand-gated P2X and metabotropic P2Y receptors (Burnstock 2014). P2X receptors directly affect membrane channel activity, resulting in Ca^{2+} and Na^{+} influx and K^{+} efflux (Surprenant and North 2009). Prolonged activation of P2X receptors leads to ROS production by NADPH oxidases and the assembly of the NLRP3 inflammasome, driving the secretion of inflammatory cytokines (Hung et al. 2005; Ferrari et al. 2006; Di Virgilio 2007). Additionally, G-protein coupled P2Y receptors also bind eADP and activate the adenylate cyclase pathway, phospholipase C, NADPH oxidases and the production of ROS and cAMP (Lee and O'Grady 2003; Díaz-Vegas et al. 2015). While eATP primarily drives pro-inflammatory processes, extracellular adenosine mitigates inflammation by binding to P1 receptors, reducing ROS and inflammatory cytokine levels (Shryock and Belardinelli 1997; Ohta and Sitkovsky 2001; Faas et al. 2017). Adding to these mechanisms, microbes are also known to exploit eATP signaling to manipulate host immunity. In plant-microbe interactions, eATP and its derivatives play critical roles in mediating immune responses against pathogens, as well as in associations with mutualistic organisms. eATP perception mediates defense responses, as is evident in the model plant *Arabidopsis thaliana*, where *P2K1* knockout mutants show increased and overexpression lines reduced susceptibility to the bacterial pathogen *Pseudomonas syringae* (Balagué et al. 2017). Some microbes evade host immunity by producing enzymes that hydrolyze ATP into adenosine. For example, the beneficial root endophyte *Serendipita indica* secretes symbiosis-specific proteins, including an ecto-5'-nucleotidase, modulating apoplastic eATP concentrations and evading host immune responses (Thürich et al. 2018; Nizam et al. 2019). Similarly, the pathogenic ascomycete *Fusarium oxysporum*, upregulates a fungal ecto-5'-nucleotidase and adenosine transporters, suppressing immune responses by altering the apoplastic eATP/adenosine ratio and pH level (Kesten et al. 2019; Kesten et al. 2023). Supporting this, it has been shown that *A. thaliana ent3-nsh3* double mutants, which are affected in both purine uptake and extracellular salvage, accumulate adenosine extracellularly and have an increased susceptibility to the pathogen *Botrytis cinerea* (Daumann et al. 2015). The hijacking of the eATP signaling pathway by both mutualistic and pathogenic microbes thereby highlights its significance, not only in general plant immunity, but also in host-microbe compatibility.

In animals, eATP and its derivatives play a central role in both pro- and anti-inflammatory processes, influencing anti-microbial immunity (Vliet and Bove 2011; Cauwels et al. 2014). To counteract this, microbes like the opportunistic bacterial pathogen *Porphyromonas gingivalis* deplete eATP through the secretion of nucleoside diphosphate kinases (NDKs) and inhibition of ROS production initiated through P2X receptor triggered NADPH oxidase NOX2 activity, leading to a reduction of immune responses and apoptotic cell death in epithelial cells (Yilmaz et al. 2008; Choi et al. 2013; Roberts et al. 2017).

eATP therefore functions beyond its classical role in the cellular energy metabolism, acting as a key regulator of immune responses in both plants and animals. While plants and animals utilize distinct receptor families and signaling pathways, the role of eATP as a DAMP underscores a shared

evolutionary solution for immune activation. Microbial manipulation of eATP by organisms with diverse hosts and lifestyles highlights its central role as both a target and mediator of infection strategies and host defense, positioning it as an important regulator of immune responses across species.

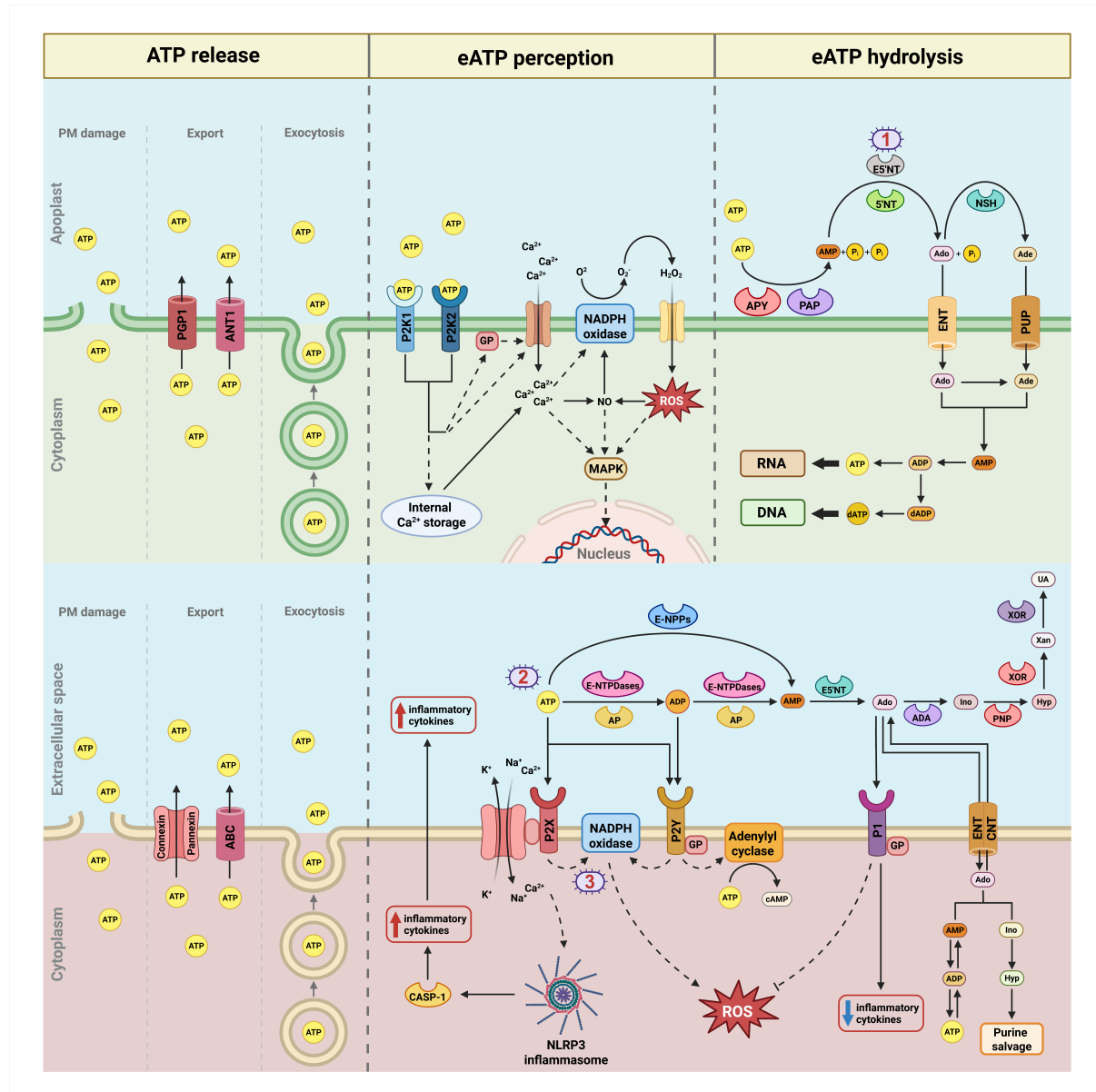


Figure 1: Overview of the release, perception and hydrolysis of extracellular ATP in plant and animal cells. Microbial interventions involving these processes are marked with a purple cell symbol and corresponding red numbers (1–3). In plant cells (upper panel), ATP gets released by plasma membrane damage, export through transporters (PGP1, ANT1) or exocytosis. eATP perception via P2K1 and P2K2 receptors triggers signal cascades supported by Gα (GP), resulting in the internal accumulation of calcium ions (Ca²⁺), nitric oxide (NO) and ROS through the activation of NADPH oxidases and transporters. These processes trigger a MAPK signaling cascade, leading to transcriptional changes. Extracellular dephosphorylation of ATP to AMP is catalyzed by enzymes such as ecto-apyrases (APY) and purple acid phosphatases (PAP), while dephosphorylation from AMP to adenosine (Ado) and adenine (Ade) is mediated by plant (5'NT) or microbe derived (ecto-)5'-nucleotidases (E5'NT) (1) as well as the nucleoside hydrolase 3 (NSH3).

(continued) Adenosine and adenine can be imported by transporters (ENTs, PUPs) and be used as internal resources. While in animal cells (lower panel) mechanisms of ATP release are mostly identical, they have pannexin and connexin channels and ABC transporters. Extracellular cleavage of ATP to ADP and AMP is mediated via E-NTPases, alkaline phosphatases (AP) or ecto-nucleotide pyrophosphatases (E-NPPs). AMP breakdown to adenosine can take place through E5'NTs, while further cleavage can generate inosine (Ino), hypoxanthine (Hyp), xanthine (Xan) and uric acid (UA) through ecto-deaminase (ADA), purine nucleoside phosphorylase (PNP) and xanthine oxidoreductase (XOR). eATP can bind to P2X and GP coupled P2Y receptors, which can be modulated by pathogenic microbes (2). P2X activation triggers potassium ion (K^+) outflux and the influx of calcium and sodium (Na^+) ions, leading to NLRP3 inflammasome oligomerization, caspase 1 (CASP-1) activation and the increase of inflammatory cytokines in- and outside the cell. ROS production increases through the activation of NADPH oxidases, which can be intercepted by intracellular pathogens (3). Some P2Y receptors can additionally bind eADP, also leading to ROS and cAMP production through NADPH oxidases and the adenylyl cyclase pathway. Extracellular adenosine can bind to GP coupled P1 receptors and trigger a counteracting response by lowering ROS- and inflammatory cytokine production, which are taken up via equilibrative- and concentrative nucleoside transporters (ENTs, CNTs) to be salvaged further.

Emerging Infochemicals: Deoxyadenosine and Other Purine-derived metabolites in Immunity and Cell Death

Deoxyadenosine

Purine-based molecules involved in extracellular and intracellular signaling in plant cells extend beyond ATP. In recent years, purine derivatives of deoxyribose have gained attention for their roles in immunity and host-microbe interactions in both animals and plants. Extracellular deoxynucleotides arise from the degradation of DNA released by damaged host cells or microbes. Additionally, plant- and animal cells deploy extracellular DNA traps, such as root extracellular traps (RETs) or neutrophil extracellular traps (NETs), to immobilize pathogens (Driouich et al. 2019). To evade these traps, certain adapted microbes secrete DNases. For instance, the animal pathogen *Staphylococcus aureus* and the plant pathogen *Fusarium oxysporum*, as well as the beneficial root endophyte *S. indica*, secrete enzymes such as DNases (Nuc, NucA) and 5'-nucleotidases (E5'NT, AdsA) to degrade DNA and generate deoxynucleosides (Thammavongsa et al. 2013; Tran et al. 2016; Winstel et al. 2018; Nizam et al. 2019). These deoxynucleosides, like nucleosides, are transported into cells via ENTs, such as hENT1 in human cells and AtENT3 in Arabidopsis roots (Winstel et al. 2018; Dunken et al. 2024). The subsequent intracellular salvage of deoxyribonucleosides appears to differ between plants and animals. In animals, dAdo and dGuo, for example, are phosphorylated by deoxycytidine kinases (dCKs) to deoxyribonucleoside-triphosphates (dATP, dGTP) after uptake via ENTs, inducing apoptosis through caspase activation (Winstel et al. 2019; Tantawy et al. 2022; Winstel et al. 2024). In plants, the mechanisms and metabolic cascades following deoxynucleoside uptake are not yet fully understood. Recent studies indicate a complex immunity and cell death response triggered by the application of dGuo and dAdo in leaf and root tissue (Lu et al. 2023; Dunken et al. 2024). For example, dGuo application in leaves upregulates immunity genes and enhances resistance to the pathogen *P. syringae* (Pst DC3000) (Lu et al. 2023). In contrast, in roots dAdo induces a specific

immune response involving TIR-NLR proteins, modulating cell death during beneficial interaction with *S. indica* (Dunken et al. 2024). Additionally, dAdo increases the abundance of the retrograde stress signaling metabolite 2-C-Methyl-d-erythritol-2,4-cyclopyrophosphate (MEcPP) in the apoplast of *A. thaliana*, suggesting that dAdo activates the non-mevalonate pathway in plastids (Xiao et al. 2012; Dunken et al. 2024).

In conclusion, the production of deoxyribonucleosides from extracellular DNA by pathogenic and beneficial microbes represents a conserved strategy across both animal and plant systems to hijack host immunity for their accommodation. However, once these molecules are imported into host cells, the mechanisms by which they elicit immune responses and cell death appear to differ significantly based on current understanding. In animals, phosphorylation of deoxyribonucleosides is associated with the initiation of caspase-mediated apoptosis, whereas in plants, stress signaling and cell death appear to be regulated through TIR-NLR proteins.

Additionally, purine-derived infochemicals serve as important signals during the recognition of cytoplasmic self- and non-self DNA. In animals, several mechanisms for cytoplasmic DNA recognition have been described. For example, cytoplasmic double-stranded DNA (dsDNA) is directly bound by cyclic GMP-AMP synthase (cGAS), inducing a conformational change in its active site that enables the synthesis of cyclic GMP-AMP (cGAMP) from ATP and guanosine triphosphate (GTP) (Gao et al. 2013; Wu et al. 2013). cGAMP then binds to the adaptor protein Stimulator of Interferon Genes (STING), a central component of multiple DNA sensing pathways, which facilitates the activation of interferon beta (IFN- β) signaling (Burdette and Vance 2013). This leads to downstream immune responses, including inflammation, apoptosis, and the inhibition of DNA viruses and bacterial pathogens. In plants, however, direct evidence for cytoplasmic DNA sensing is currently lacking, as clear orthologs of the corresponding animal proteins have not been identified. Nevertheless, the recent discovery of TIR-domain resistosomes that produce 2',3'cAMP and cyclic guanosine monophosphate (cGMP) from DNA substrates may represent an alternative mechanism of nucleic acid sensing in plants and will be discussed in a later chapter.

NAD⁺ / NADP⁺

As with ATP, NAD⁺ and its phosphorylated derivative NADP⁺ play critical roles beyond metabolism where they serve as electron carriers and signaling molecules in cellular processes. Both have been shown to induce upregulation of PR genes in plants, and the modulation of pro- as well as anti-inflammatory immune responses in animal cells (Zhang and Mou 2009; Pliyev et al. 2014).

Although active release of NAD⁺ and NADP⁺ from plant cells has not yet been demonstrated, cellular damage and lysis can contribute to their extracellular accumulation, similar to ATP release. In animal cells, eNAD⁺ is actively introduced into the extracellular space during tissue inflammation via connexin channels (Cx43), exocytotic vesicles or following cellular damage (Bruzzone et al. 2001; Billington et al. 2006).

No definitive evidence currently exists for the regulation of eNAD⁺ and eNADP⁺ levels outside of plant cells, but insights linking the extracellular accumulation of these molecules with heightened ROS levels (Li et al. 2023a) indicate unknown control mechanisms. In contrast to this, extracellular regulation of NAD⁺ levels in animals has been thoroughly described in the past. In animals, ecto-enzymes such as cluster of differentiation (CD) ecto-5'-nucleotidases, the nucleotide

pyrophosphatase / phosphodiesterase 1 (NPP1) or ecto-ADP ribosyltransferases (ARTs), catalyze the breakdown of eNAD⁺ into smaller signaling molecules, including nicotinamide mononucleotide (NMN), nicotinamide (NAM), nicotinamide riboside (NR), AMP, adenosine diphosphate ribose (ADPR) and cyclic adenosine diphosphate ribose (cADPR) (Billington et al. 2006; Hong et al. 2009; Gasparrini et al. 2021). As for NADP⁺, it can be further converted to oxidized nicotinic acid adenine dinucleotide phosphate (NAADP⁺) through CD enzymes in the extracellular space (Billington et al. 2006; Gasparrini et al. 2021). Some of the derivatives from NAD⁺ and NADP⁺, such as cADPR, NAADP⁺, NR and NAM, can be transported directly into the cell, though the exact channels and transporters are still mostly uncharacterized (Heidemann et al. 2005; Billington et al. 2006; Gasparrini et al. 2021).

In plants, extracellular NAD⁺ and NADP⁺ are perceived by the lectin receptor kinases LecRK-VI.2 and LecRK-1.8, initiating immune responses similar to eATP (Zhang and Mou 2009; Wang et al. 2017). These responses involve coreceptors such as BRASSINOSTEROID INSENSITIVE1-ASSOCIATED KINASE1 (BAK1) and BAK1-like 1 (BKK1), activate SAR and prime the immune system for pathogenic attacks through PR gene expression. In animal cells, eNAD⁺ and its derivatives are perceived by the P2Y and P2X receptor classes (Haag et al. 2007). The downstream responses to these interactions vary depending on the cell type, tissue and the mode of activation (direct/indirect), ranging from inducing to suppressing cell death (Seman et al. 2003; Pliyev et al. 2014). For instance, eNAD⁺ induces apoptosis in T-cells via the P2X7 receptor (Hong et al. 2009; Pliyev et al. 2014). However, it remains unclear whether this activation is direct or mediated by its degradation products (Seman et al. 2003; Gasparrini et al. 2021). Contrastingly, in human monocytes, eNAD⁺ delays apoptosis during inflammation via the P2Y11 receptor, exhibiting selective pro-survival effects (Moreschi et al. 2006; Pliyev et al. 2014). Similar to eNAD⁺, there is evidence that eNADP⁺ and its enzymatic product NAADP⁺ activate P2X receptors, while NAADP⁺ can also directly be taken up into the cell (Heidemann et al. 2005; Judkins et al. 2006).

While for plants, NAD⁺ and NADP⁺ modulation by microbes is still unclear, in animals intracellular concentrations can be influenced by pathogens such as *Mycobacterium tuberculosis* (Mtb) (Simeone et al. 2012). Mtb depletes cytosolic NAD⁺ and NADP⁺ pools of macrophages via glycohydrolase activity of the MtbCpnT proteins TNT domain, leading to necroptosis and therefore reduced immune response (Mittal et al. 2018; Tak et al. 2019; Pajuelo et al. 2021). TNT-like domains and NADase activity are shared features among other bacterial and also fungal-pathogens like *Aspergillus fumigatus*, suggesting NAD⁺-and NADP⁺ depletion as a conserved infection strategy (Strømmland et al. 2021; Ferrario et al. 2024).

Although parallels exist between plants and animals in the extracellular roles of NAD⁺ and NADP⁺, the underlying mechanisms differ considerably. In animals, extracellular metabolism of these nucleotides generates distinct signaling molecules that mediate pro- or anti-inflammatory responses in a cell-type-dependent manner. In contrast, plant signaling appears to rely more directly on NAD⁺ and NADP⁺ themselves, which may act as extracellular ligands triggering systemic immune responses such as SAR. Despite limited mechanistic detail in plants, emerging evidence points to their function in pathogen detection and immune priming during microbial colonization.

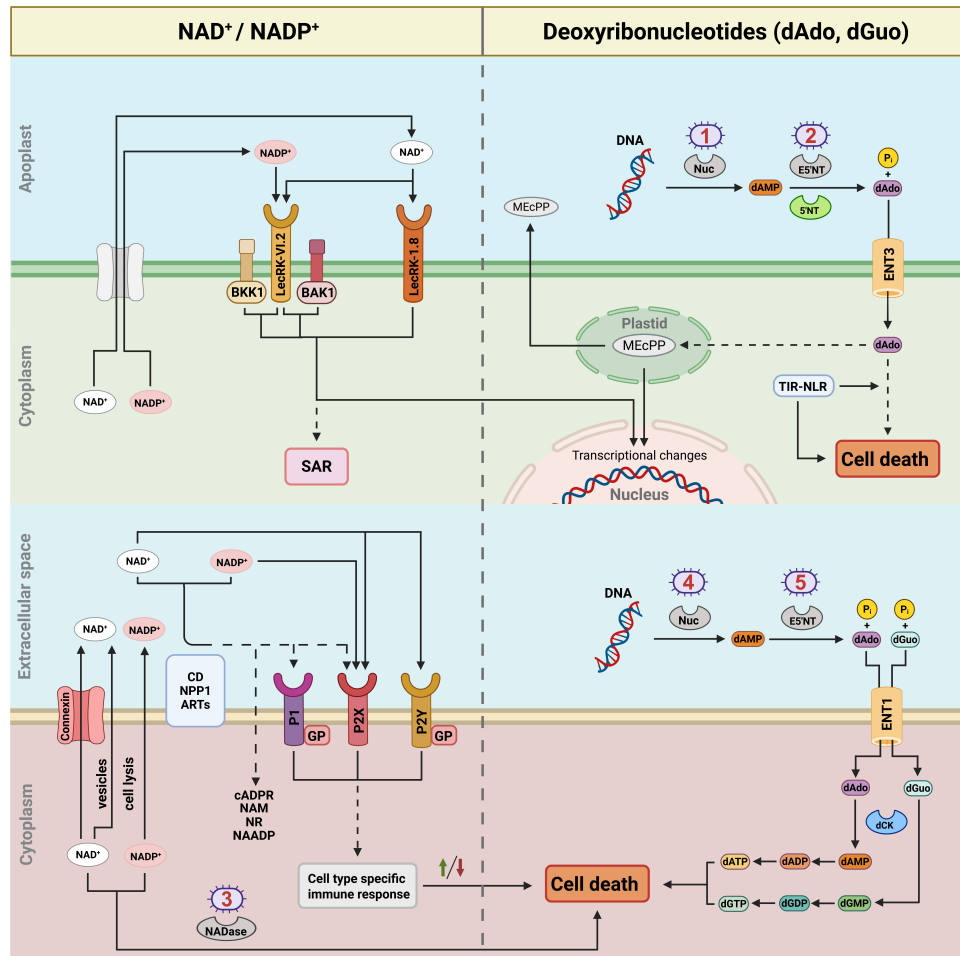


Figure 2: Model of the response to extracellular NAD^+ / NADP^+ and deoxynucleosides in plant and animal cells - Microbial interventions involving these processes are marked with a purple cell symbol and corresponding red numbers - (1–5). While the specific mechanisms of NAD^+ and NADP^+ release in plants (upper panel) remain unknown, the perception takes place via the receptors LecRK-1.8 and LecRK-VI.2. Interaction with the co-receptors BRASSINOSTEROID INSENSITIVE1-ASSOCIATED KINASE1 (BAK1) and BAK1-LIKE1 (BKK1) can induce systemic acquired resistance (SAR) and local transcriptional changes. Extracellular DNA outside of plant cells in the apoplast can be broken down to deoxynucleosides by microbe derived nucleases (Nuc) (1) and ecto-5'-nucleotidases (E5'NT) (2). Deoxynucleosides like deoxyadenosine (dAdo) are taken up into the cell via plasma-membrane located ENTs (ENT3). In the cell, dAdo induces cell death affected by TIR-NLRs, as well as the increase of the plastidial stress associated metabolite methylerythritol cyclodiphosphate (MEcPP) in the apoplast. NAD^+ release in animal cells (lower panel) is better characterized, with it entering the extracellular space through connexin channels during inflammation and, together with NADP^+ , during cell lysis. Both can additionally be depleted by intracellular microbial NADase activity (3) and therefore lead to cell death.

(continued) Extracellularly, NAD^+ is perceived by G-protein (GP) coupled P2Y or P2X receptors, with NADP^+ only binding the latter. Both NAD^+ and NADP^+ can be cleaved by membrane bound enzymes such as cluster of differentiation (CD) ecto-5'-nucleotidases, the nucleotide pyrophosphatase/phosphodiesterase 1 (NPP1) or ecto-ADP ribosyltransferases (ARTs). The resulting derivatives nicotinamide mononucleotide (NMN), nicotinamide (Nam), nicotinamide riboside (NR), NAADP^+ , AMP and (cyclic) ADP-ribose ((c)ADPR) can either bind to GP coupled P1 and P2X receptors, or be taken up by respective transporters, channels or diffusion. After receptor recognition, NAD^+ , NADP^+ and their derivatives induce cell type specific immune responses such as cell death. Like in the plant apoplast, deoxynucleosides like dAdo and deoxyguanosine (dGuo) can be generated from extracellular DNA by microbial nucleases (4) and ecto-5'-nucleotidases (E5'NT) (5). The import also takes place through ENTs (ENT1), after which both get phosphorylated by deoxycytidine kinases (dCKs) up to deoxyribonucleoside-triphosphates (dATP, dGTP) and induce cell death.

2',3'cAMP

While the cyclic nucleotide 3',5'cAMP has been studied as a second messenger for decades, the positional isomer 2',3'cAMP has only quite recently been identified in biological samples (Ren et al. 2009). It has been detected across all kingdoms and has been described as a byproduct of RNA degradation (Thompson et al. 1994). Since this discovery, 2',3'cAMP has been implicated in stress responses in both plants and animals. In plants, 2',3'cAMP was identified as both a component and inducer of stress granules (Kosmacz et al. 2018). It accumulates in response to wounding, darkness or heat stress and triggers a distinct stress response, which cannot be observed upon adenosine treatment (Chodasiewicz et al. 2022). Recently, it was shown that plant TIR domain proteins can also produce 2',3'cAMP and 2',3'cGMP from RNA, a topic explored further in subsequent chapters (Yu et al. 2022).

In animals, 2',3'cAMP is induced by brain trauma and is considered to be a neurotoxin (Verrier et al. 2012). Its accumulation can trigger flux of calcium from mitochondria, ultimately leading to apoptosis (Azarashvili et al. 2009). The removal of 2',3'cAMP by intracellular CNPases and RNases not only removes the neurotoxic metabolite but also produces adenosine, which has extensively been described as neuroprotective (Kochanek et al. 2013). Interestingly, this mechanism exhibits the opposite effect in renal tissue, suggesting a complex, tissue-specific role of 2',3'cAMP in animals similar to NAD^+ and NADP^+ (Jackson et al. 2016).

Overall, while research on 2',3'cAMP is still in its early stages, mounting evidence suggests that it plays a critical role in regulating stress responses across kingdoms. Moreover, it may act as an antagonistic signal to adenosine, which is often characterized as immune-suppressive or protective.

Purine-based metabolites produced by TIR activity

The TIR domain is a highly conserved molecular module found in both prokaryotes and eukaryotes. TIR domain proteins have primarily been known for their roles in the innate immunity of animals and plants. In animals, TIR modules are integral components of immunity-related receptors such as toll-like receptors (TLRs), interleukin-1 receptors (ILR1s), as well as their cytosolic adaptor proteins, where they are involved in the perception of both microbial and damage-associated

molecular patterns (reviewed in Kawai et al. 2024). In most dicotyledonous plants, TIR domains can be found as parts of intracellular nucleotide-binding leucine-rich repeat receptors (TNLs) or truncated versions like TIR-only, TIR-NB protein (TN) or TIR-NB-ARC-tetratricopeptide repeat proteins (TNPs). Monocotyledonous plants, such as cereals, lack TNL and TN and only possess a reduced set of TIR-only and TNPs (Meyers et al. 2002; Johannndrees et al. 2023). TNLs have been extensively characterized for their role in the perception of microbial effector molecules. In the field of plant immunity, effectors have classically been defined as small, secreted proteins that interfere with the host's immune system, facilitating colonization (Lo Presti et al. 2015). In resistant plant hosts, recognition of a microbial effector by a corresponding TNL can trigger a rapid programmed cell death induction called HR and confers immunity to the invading pathogen (Dodds et al. 2006). In bacteria, TIR domains are implicated in the defense against bacteriophages (Ofir et al. 2021) and are part of bacterial effector proteins essential for the successful infection of both animal and plant hosts (Sharma et al. 2016; Wan et al. 2019; Coronas-Serna et al. 2020; Eastman et al. 2022).

While the significance of TIR domain proteins in immunity has been acknowledged for many years, the TIR domain was long considered to have mainly a scaffolding function (Williams et al. 2014). This hypothesis was challenged by evidence demonstrating that the TIR domain of the intracellular adaptor protein SARM1 from humans, which plays a role in the execution of axonal cell death and neuronal degeneration, exhibits catalytic activity. The SARM1 TIR domain possesses intrinsic NADase activity, resulting in intracellular NAD⁺ depletion and the production of NAM and cyclic and non-cyclic ADP-ribose (Horsefield et al. 2019; Wan et al. 2019). This NAD⁺ depletion is essential for pathological axon loss, and other studies have shown that cADPR and ADPR influence intracellular calcium signaling in both animals and plants (Galione et al. 1991; Navazio et al. 2001). Similarly, several prokaryotic TIR domains linked to various other domains also exhibit NADase activity, depleting cellular NAD⁺ pools while generating ADPR, NAM and a non-canonical cADPR variant named 2'cADPR (Wan et al. 2019; Hogrel et al. 2022; Morehouse et al. 2022). During bacteriophage infection, bacterial TIR domains, like found in the weak NADase ThoerisB (ThsB), cleave NAD⁺ into another non-canonical cADPR variant called 3'cADPR. This process activates the non-TIR domain NADase ThoerisA (ThsA), leading to NAD⁺ depletion and subsequent cell death, thereby preventing viral replication (Ofir et al. 2021; Tamulaitiene et al. 2024).

TIR NADase activity can also be observed in plants, where it leads to the production of 2'- and 3'cADPR, without causing NAD⁺ depletion. Notably, 3'cADPR has been shown to suppress immunity and Enhanced Disease Susceptibility 1 (EDS1)-Senescence-Associated Gene 101 (SAG101)-dependent cell death induction (Eastman et al. 2022). Moreover, the TIR domain of plant TNLs can assemble into multimeric structures known as resistosomes upon effector-binding, forming active NADases (Ma et al. 2020; Martin et al. 2020; Huang et al. 2022; Jia et al. 2022). For example, binding of the effector ATR1 to the C-terminal LRR and post-LRR domain of the Arabidopsis TIR-NLR Recognition of *Peronospora parasitica* 1 (RPP1) induces tetramerization. This assembly leads to the formation of 2 NADase active sites, each formed by an asymmetric TIR domain homodimer. The resulting resistosomes can produce infochemicals like pRib-AMP/ADP, a small signaling metabolite that signals via the complex of the lipase-like proteins EDS1 and Phytoalexin Deficient 4 (PAD4). pRib-AMP/ADP allosterically binds the EDS1-PAD4 heterodimer, facilitating the binding of the helper NLR Activated Disease Resistance 1 (ADR1). This subsequently leads to the

assembly of another multimeric resistosome, amplifying the plant immune response by acting as calcium channels (Jacob et al. 2021; Yu et al. 2024). Conversely, TNL resistosomes also produce adenosine diphosphate ribose-ATP/diadenosine diphosphate ribose (ADPR-ATP/di-ADPR), which binds heterodimers consisting of EDS1 and SAG101, activating the helper NLR N Requirement Gene 1 (NRG1), leading to resistosome formation and induction of cell death. Interestingly, it has been shown that 2'cADPR can be hydrolyzed into the more transient pRib-AMP/ADP, suggesting its role as a more stable storage form (Yu et al. 2024). In addition to the assembly of TNLs into resistosomes, plant TIR-only proteins can not only form active NADases, but also filamentous structures and act as active nucleases, cleaving dsDNA and preferably dsRNA (Yu et al. 2022). This activity leads to the production of 2',3'cAMP, which promotes the formation of stress granules and induces a characteristic stress response (Kosmacz et al. 2018; Chodasiewicz et al. 2022).

Overall, the diverse roles of TIR-produced metabolites imply that their production must be strictly regulated by the host organism to ensure a balanced immune response. In contrast, the hijacking of TIR domain-related immune pathways presents an attractive target for pathogens seeking to modulate the host's immune system and facilitate a successful infection. For example, many bacteriophages utilize the Tad1 protein which has a sponge-like character, sequestering both 2'- and 3'cADPR produced by bacterial ThsA TIR domains to prevent the activation of ThsB and subsequent NAD⁺ depletion (Leavitt et al. 2022). Furthermore, bacterial pathogens of both animals and plants use TIR domain virulence factors such as TirS of *S. aureus* and HopAM1 of *P. syringae* to suppress immunity through NAD⁺ depletion or the production of 3'cADPR (Essuman et al. 2018; Essuman et al. 2022). In plants, recent evidence demonstrates a negative control of TIR-only activity by calcium sensors, which release TIR-only proteins after pathogen perception, thereby linking TIR function to PTI (Wang et al. 2024; Wu et al. 2024). The level of the stress signal 2',3'cAMP is regulated by the host plant itself via a family of Nudix phosphodiesterases like AtNUD7, which hydrolyze 2',3'cAMP and thereby negatively regulate EDS1 signaling (Bartsch et al. 2006; Ge et al. 2007). A similar mechanism is employed by various microbial Nudix effector enzymes, which also hydrolyze 2',3'cAMP and are essential for pathogen virulence (Kong et al. 2015; Adlung and Bonas 2017; Yu et al. 2022).

Although the enzymatic activity of TIR domains was only recently discovered, numerous studies have demonstrated that both NAD⁺ depletion and the production of recently identified nucleotides represent ancient mechanisms of innate immunity across the kingdoms of life. In animals and bacteria, the primary mode of action appears to be NAD⁺ depletion, leading to the suppression of immune signaling and cell death. In contrast, numerous enzymatically active TIR domains have been identified in plants, resulting in a broad spectrum of nucleotide products that can either enhance or dampen immune responses. Recent data suggests that not only full-length TNL, but also TIR-only proteins can assemble into NADases producing pRib-AMP/ADP (Jacob et al. 2023; Wu et al. 2024), supporting the idea that parallel pathways evolved and converged on the same signaling metabolites. Overall, the production and regulation of small nucleotide metabolites by TIR proteins adds another layer to our understanding of the complexity of immunity in all domains of life and offers a new target for both external improvement of immunity in host plants and human patients, as well as a target of inhibition of pathogenic microbes.

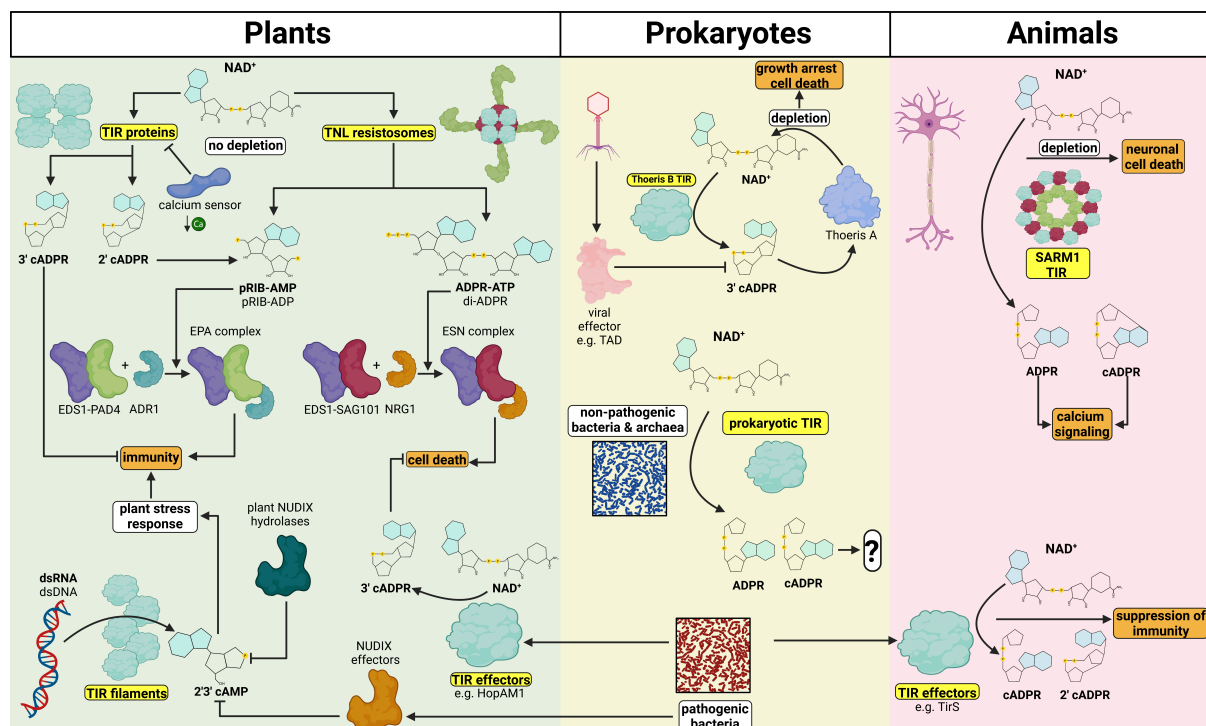


Figure 3: Infochemicals produced by TIR domains across different kingdoms– Plants (green) produce a variety of small, signaling metabolites from NAD^+ via the activity of both multimers of TIR-only and TIR-NLR multimers. Plant TIR-only proteins have also been described to form filaments that are active nucleases, producing the infochemicals 2',3'-cAMP. Prokaryotes (yellow) like bacteria have various anti-bacteriophage immune systems that consists of a TIR-domain coupled to another functional domain. NADase activity of these TIR domains can either deplete the intracellular NAD^+ pool, leading to cell death, or produce second messengers to activate downstream antiviral enzymes. TIR domain are also present in the effector proteins of pathogenic bacteria, contributing to virulence in both plant and animal hosts. In animals (red), only one active TIR domain has been characterized thus far. TIR domains of SARM1 octamers deplete intracellular NAD^+ pools, contributing to neuronal cell death.

Conclusion & Outlook on Purine Metabolites

Purine-based molecules are well-established as central components of energy metabolism and nucleic acid synthesis, yet their roles as extracellular signaling molecules, especially in immunity, have only recently emerged. These molecules exhibit conserved functions across biological kingdoms, yet their downstream signaling pathways differ significantly. For example, while eATP induces immunity in both plants and animals, its salvage product adenosine suppresses immunity in animals, with its role in plant immune suppression still under investigation (Kesten et al. 2023). Interestingly, the closely related deoxyadenosine utilizes the same transporters as adenosine but acts as a potent inducer of cell death in both plants and animals.

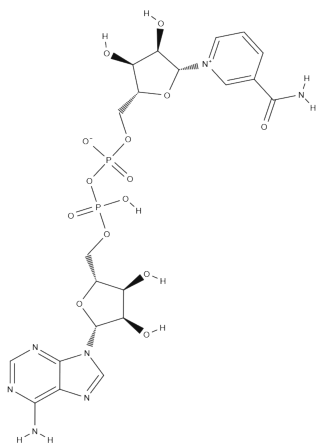
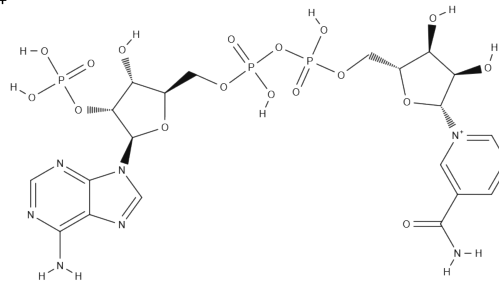
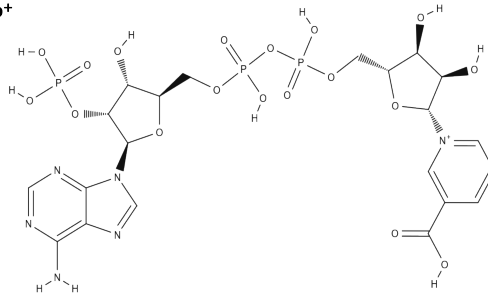
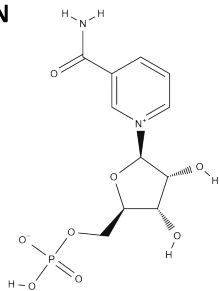
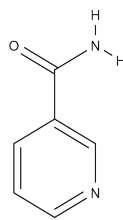
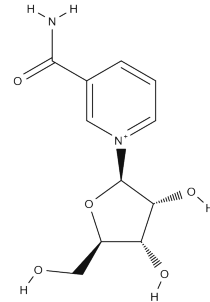
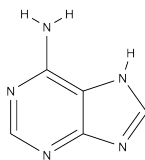
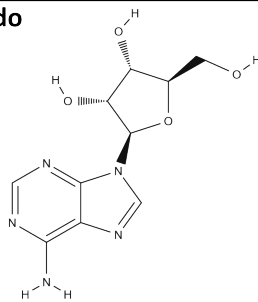
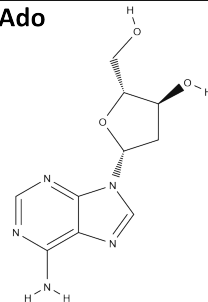
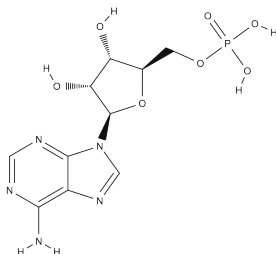
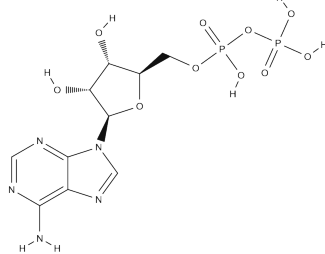
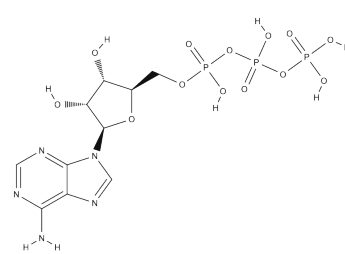
The recent discovery of purine-based infochemicals, produced by plants in response to microbial attack to bolster immune defenses against a wide range of pathogens, highlights the expanding complexity of nucleotide-based immune signaling. Specifically, TIR domain proteins in plants assemble into NADases, generating non-cyclic, polar ribosylated nucleotide second messengers such as pRib-AMP, pRib-ADP, ADPr-ATP, and di-ADPR. These small, often transitory molecules are not major players in central metabolism but serve as potent immune signals by binding to and activating EDS1 hetero-dimers and associated helper NLRs, thereby initiating robust immune responses. While only the SARM1 TIR domain has been described as enzymatically active in animals, plants possess a greater diversity of TIR domain proteins, including TIR-only proteins and multimeric TIR-NLR resistosomes. Notably, in animals, TIR activity is strongly associated with NAD⁺ depletion and subsequent cell death. In contrast, TIR activity in plants primarily leads to the production of diverse signaling molecules without necessarily depleting NAD⁺, adding another layer of complexity to plant innate immunity.

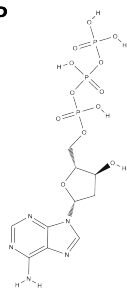
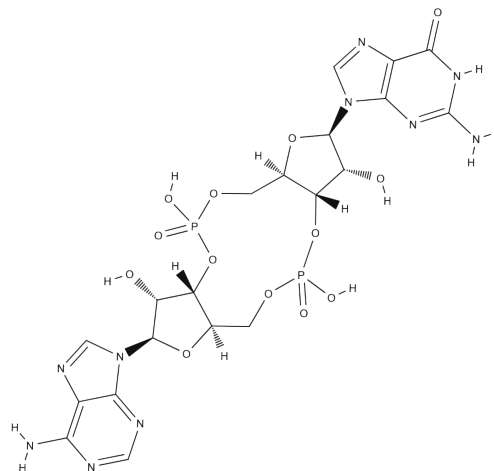
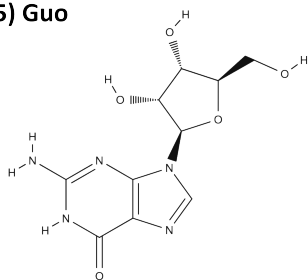
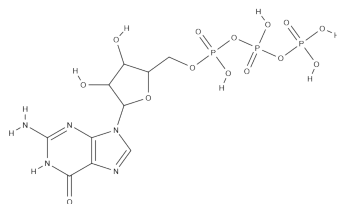
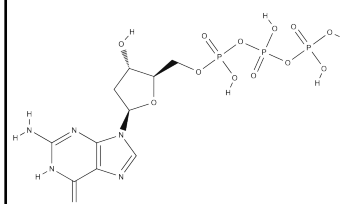
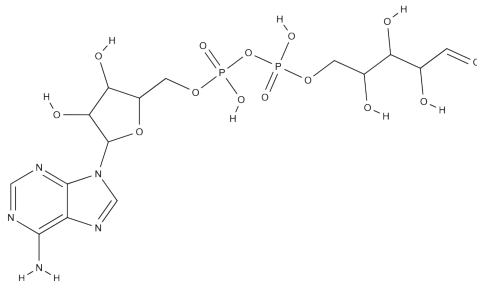
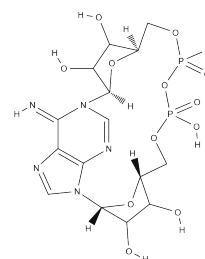
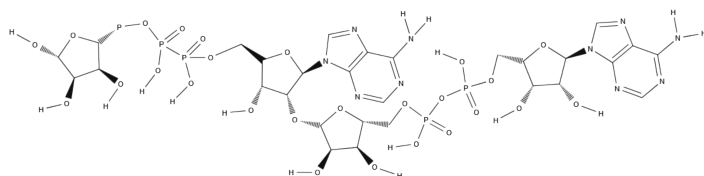
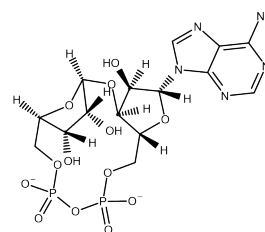
Due to the recent discovery of these TIR-produced purine-based metabolites, their precise roles and broader implications remain underexplored. However, both the ongoing development of efficient synthesis and modification techniques for purine-based infochemicals and the resulting possibility of exogenous application experiments, underscore the potential for chemical biology approaches to modify and harness these molecules (Huang et al. 2022; Dorrenhaus et al. 2023).

Although data on microbial strategies to regulate and manipulate purine signaling pathways in plants and animals remain limited, emerging insights into eATP scavenging, NAD⁺ depletion, and microbial TIR activity offer promising targets for interventions. These findings have implications for both medical and agricultural applications, offering new avenues to enhance immune defenses and mitigate microbial manipulation of host immunity.

Table 1: Overview of Purine-based Metabolites – Purine-based Metabolites discussed in this article. The numbers refer to the structures depicted in Figure 4. Column 3 shows the IUPAC-based names suggested by the Chemical Entities of Biological Interest (ChEBI) database (Hastings et al. 2016). If marked with an asterisk, no CHEBI entry exists and IUPAC-based names were generated by the authors.

#	Abbreviation	Trivial Name	IUPAC-based Name	Function in Immunity & Signaling
1	NAD ⁺	oxidized nicotinamide adenine dinucleotide	adenosine 5'-[3-[1-(3-carbamoylpyridinio)-1,4-anhydro-D-ribose-5-yl] dihydrogen diphosphate]	Plants & Animals: Extracellular DAMP, Induction of Immunity
2	NADP ⁺	oxidized nicotinamide adenine dinucleotide phosphate	2'-O-phosphonadenosine 5'-[3-[1-(3-carbamoylpyridinio)-1,4-anhydro-D-ribose-5-yl] dihydrogen diphosphate]	Plants & Animals: Extracellular DAMP, Induction of Immunity
3	NAADP ⁺	oxidized nicotinic acid adenine dinucleotide phosphate	2'-O-phosphonadenosine 5'-[3-[1-(3-carboxypyridinio)-1,4-anhydro-D-ribose-5-yl] dihydrogen diphosphate]	Animals: Induction of Immunity
4	NMN	Nicotinamide mononucleotide	3-carbamoyl-1-(5-O-phosphonato-β-D-ribofuranosyl)pyridinium	Plants & Animals: not immunogenic, NAD ⁺ salvage pathway
5	NAM	Nicotinamide	pyridine-3-carboxamide	Plants & Animals: not immunogenic, NAD ⁺ salvage pathway
6	NR	nicotinamide riboside	3-carbamoyl-1-β-D-ribofuranosylpyridinium	Plants & Animals: not immunogenic, NAD ⁺ salvage pathway
7	Ade	adenine	9H-purin-6-amine	Plants & Animals: not immunogenic, Adenosine salvage pathway
8	Ado	adenosine	adenosine	Plants & Animals: Suppression of immunity
9	dAdo	deoxyadenosine	2'-deoxyadenosine	Plants & Animals: Cell Death induction
10	AMP	adenosine monophosphate	5'-adenylic acid	Plants & Animals: not immunogenic, ATP salvage pathway
11	ADP	adenosine diphosphate	adenosine 5'-(trihydrogen diphosphate)	Plants & Animals: Induction of Immunity
12	ATP	adenosine triphosphate	adenosine 5'-(tetrahydrogen triphosphate)	Plants & Animals: Induction of Immunity Animals: Substrate for cGAMP production
13	dATP	deoxy adenosine triphosphate	2'-deoxyadenosine 5'-(tetrahydrogen triphosphate)	Plants: Induction of Immunity Animals: Intracellular Cell Death induction after dAdo uptake
14	cGAMP	2'3'cyclic GMP-AMP	2-amino-9-[(5R,7R,8R,12aR,14R,15R,15aS,16R)-14-(6-amino-9H-purin-9-yl)-2,10,15,16-tetrahydroxy-2,10-dioxidooctahydro-12H-5,8-methanofuro[3,2-l][1,3,6,9,11,2,10]pentaoxidaphosphacyclotetradecin-7-yl]-1,9-dihydro-6H-purin-6-one	only Animals: Induction of Immunity upon cytoplasmic DNA recognition
15	Guo	guanosine	guanosine	Animals: Anti-inflammatory and neuroprotective
16	dGuo	deoxyguanosine	2'-deoxyguanosine	Plants: Induction of Immunity Animals: Cell Death induction
17	GTP	guanosine triphosphate	guanosine 5'-(tetrahydrogen triphosphate)	Plants: little known Animals: Substrate for cGAMP production & immune GTPases
18	dGTP	deoxy guanosine triphosphate	2'-deoxyguanosine 5'-(tetrahydrogen triphosphate)	Plants: no direct role known yet Animals: Contextual evidence, possible role in apoptosis
19	ADPR	adenosine diphosphate ribose	adenosine 5'-[3-(D-ribofuranos-5-O-yl) dihydrogen diphosphate]	Plants: TIR NADase byproduct Animals: Role in Inflammation & Cell Death
20	cADPR	canonical cyclic ADPR	1-β-D-ribofuranosyl-1,2,3,4-tetrahydropyrrolo[2,3-d]pyrimidin-5-one 5'-monophosphate cyclic ester with adenosine 5'-monophosphate*	Plants: TIR product, direct function unknown Animals: Second Messenger in Immunity
21	di-ADPR	ADP-ribosylated ADPR	5'-O-[5''-(adenosine 5''-diphosphoribosyl)] adenosine diphosphoribose*	Plants: Activation of EDS1-SAG101 homodimer, cell death
22	3'cADPR	3'(v2)-cyclic adenosine diphosphate ribose	Adenosine 5'-monophosphate cyclic ester with 3'-hydroxyl of ribose of adenosine*	Plants: Suppression of Immunity Bacteria: Cell Death in phage defense
23	ADPR-ATP	ADP-ribosylated adenosine triphosphate	Adenosine 5'-(tetrahydrogen triphosphate), P''~γ~ester with [(2R,3S,4R,5R)-5-(6-amino-9H-purin-9-yl)-3,4-dihydroxytetrahydrofuran-2-yl]methyl [(2R,3S,4R,5R)-3,4,5-trihydroxytetrahydrofuran-2-yl] methyl hydrogen diphosphate*	Plants: Activation of EDS1-SAG101 homodimer, cell death
24	2'cADPR	2' (v)-cyclic adenosine diphosphate ribose	Adenosine 5'-monophosphate cyclic ester with 2'-hydroxyl of ribose of adenosine*	Plants: Conversion into pRib-AMP, possible storage form
25	pRib-AMP	phosphoribosyl-AMP	5'-O-phosphonadenosine N1-(5-phospho-β-D-ribofuranosyl)*	Plants: Activation of EDS1-PAD4 homodimer, immunity
26	2',3'cAMP	2',3'-cyclic adenosine monophosphate	adenosine 2',3'-(hydrogen phosphate)	Plants: Intracellular Stress Signal, Animals: Neurotoxin & Cell Death Induction
27	pRib-ADP	phosphoribosyl-ADP	5'-O-[[[(phospho-β-D-ribofuranosyl)oxy] phosphoryl]adenosine 5'-diphosphate*	Plants: Activation of EDS1-PAD4 homodimer, immunity
28	3',5'cAMP	3',5'-cyclic adenosine monophosphate	adenosine 3',5'-(hydrogen phosphate)	Plants: little known Animals: Major second messenger in G-Protein receptor induced immunity

1) NAD⁺**2) NADP⁺****3) NAADP⁺****4) NMN****5) NAM****6) NR****7) Ade****8) Ado****9) dAdo****10) AMP****11) ADP****12) ATP**

13) dATP**14) cGAMP****15) Guo****17) GTP****18) dGTP****19) ADPR****20) cADPR****21) di-ADPR****22) 3'cADPR**

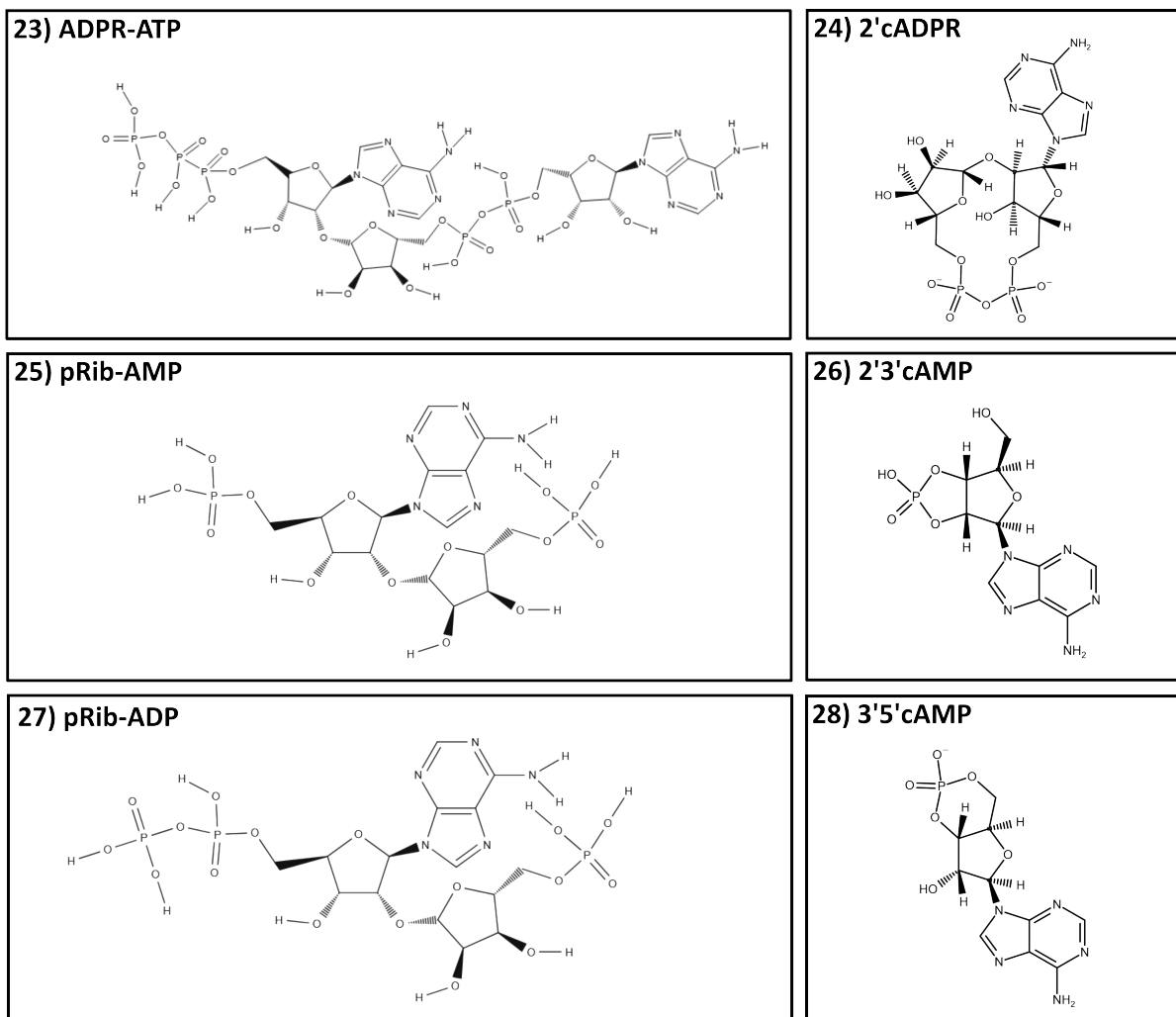


Figure 4: Structures of Purine-based Metabolites - Structural formulas of metabolites discussed in this article. The structural formulas were created with MolView or the Chemical Sketch Tool of the RCBS Protein Data Bank (Berman et al. 2000) and based on the InChI identifier.

Perspective: Rethinking Immunometabolism and Infochemical Signaling Across Biological Kingdoms

Traditional views on host-microbe interactions have primarily focused on immune signaling while often overlooking the fundamental role of metabolic regulation. Historically, metabolism and immunity were studied as separate disciplines, with metabolism regarded mainly as a cellular maintenance process rather than an active regulator of immune responses. However, increasing evidence reveals that metabolic processes dynamically shape immune function and host-microbe interactions. This perspective is grounded in the hypothesis that immunometabolism is a fundamental property of immune systems across biological kingdoms, driving the evolution of both universal and kingdom-specific infochemicals. In pathogenic interactions, infochemicals act as metabolic signals linking host metabolism to immune functions, triggering defense mechanisms. In beneficial interactions, they facilitate metabolic integration between hosts and microbiota, regulating immune and metabolic homeostasis, promoting accommodation, and contributing to host

health.

This shift is underpinned by two paradigm changes. First, microbes are no longer viewed solely as aggressors that dictate host functions and determine interaction outcomes; instead, they are recognized as integral players in host biology. Most microbes associated with plants and animals are not pathogens but rather essential contributors to host homeostasis, nutrient exchange, and immune modulation. This realization necessitates a new framework to explain how hosts establish stable interactions with beneficial microbes while maintaining defenses against pathogens. Equally important is understanding the conditions that drive microbes to transition between symbiotic and pathogenic lifestyles, causing disease in some hosts while remaining harmless or beneficial in others. A key aspect of this paradigm change is recognizing that microbes, whether individually or within a community, actively shape host immunity by modulating defense mechanisms. This ability is fundamental to their successful colonization, whether as pathogens or symbionts (Mahdi et al. 2021; Snelders et al. 2022). Comparative analysis across kingdoms helps identify shared immune strategies while also highlighting unique evolutionary adaptations developed in response to distinct ecological pressures.

Second, immune signaling alone does not fully account for host-microbe interactions—metabolic regulation is equally crucial. Host-microbial metabolic interdependence, host metabolic imbalances, and small bioactive molecules derived from central metabolism, immune receptor activities, or microbial sources act as key mediators in these processes, influencing immune activation, microbial colonization, and host physiology. This emerging perspective underscores the need to integrate metabolic and immune regulation into a unified framework of immunometabolism to fully understand host-microbe dynamics across biological kingdoms. While immunometabolism has been extensively studied in animal systems, its role in plants remains underexplored. However, the recent discovery of small bioactive metabolites that regulate plant immunity and microbial accommodation has driven a surge of research in plant sciences. A critical question arises: Are infochemicals inherently more significant in plant immunity and immunometabolism more central in animals, or is this distinction a result of historical research focus? Despite the recent advances, the integration of immunometabolic insights and infochemical signaling across plants and animals remains incomplete, highlighting a key direction for future research. A unified framework incorporating both perspectives is essential to fully understand the role of metabolism and infochemicals in immune regulation across biological kingdoms.

Purine-based metabolites, particularly ATP, NAD⁺, and deoxynucleosides, exemplify this shift (Nizam et al. 2019; Huang et al. 2022; Jia et al. 2022; Dunken et al. 2024). Once regarded solely as intracellular energy carriers or precursors for nucleic acid synthesis, these molecules have now been identified as extracellular immune regulators in both plants and animals. Their role extends beyond immunity, shaping microbial strategies for immune evasion or accommodation. The discovery that TIR domain proteins generate purine-based second messengers in plant immunity adds another layer to this complexity. Similarly, in animal systems, metabolic intermediates such as itaconate, succinate, and fumarate regulate macrophage activity, while nucleotide imbalances contribute to immune modulation via mitochondrial DNA release and subsequent activation of cytosolic DNA-sensing pathways (Sprenger et al. 2021; Williams et al. 2022). These findings suggest that immune-metabolic crosstalk involves conserved mechanisms that have been adapted to diverse

biological contexts across kingdoms.

Advances in synthetic chemistry, structural biology, and microbiome research, including the development of synthetic microbial communities (SynComs) and gnotobiotic host systems, are accelerating our understanding of these metabolic-immune interactions (Hiruma et al. 2016; Castrillo et al. 2017; Harbort et al. 2020; Dorrenhaus et al. 2023; Lawson et al. 2025). Theoretical and computational research has also provided valuable insights into the regulatory networks governing microbiome and host metabolism, contributing to the development of predictive models for protein-ligand interactions and metabolic flux analysis. Machine-learning approaches and genome-scale metabolic models are set to advance our understanding of how nucleotide metabolism and infochemicals influence microbiome composition and immune function. These models will help identify conserved metabolic pathways linking nucleotide turnover to immune regulation across plant and animal hosts (Vos et al. 2017; Töpfer et al. 2020; Ansmann and Bollenbach 2021; Camborda et al. 2022; Sprent et al. 2024). Looking ahead, integrating immunometabolism into plant and animal research will provide a holistic view of how biological systems regulate defense and symbiosis. By exploring the evolutionary and functional conservation of metabolic signaling pathways, we can develop innovative strategies to enhance immune resilience, optimize host-microbiota health, and improve disease resistance in both medical and agricultural contexts.

Acknowledgments

AZ gratefully acknowledges support from the Cluster of Excellence on Plant Sciences (CEPLAS) funded by the German Research Foundation (DFG) under the Excellence Strategy - EXC 2048/1 - Project ID: 390686111. AZ and ND additionally acknowledge support from iHEAD (NRW Profilbildung ID: PB22-025A) and CRC 1403 Project ID: 1403-414786233. TT was supported by the International Max Planck Research School (IMPRS) and the TRR 341 Project ID: 341/1-456082119.

Chapter 6

Discussion

6.1 Cell death in beneficial host-microbe interactions

Regulated cell death is a fundamental component of the immune response during several host–microbe interactions, particularly in the defense against biotrophic and intracellular pathogens. The deliberate elimination of infected cells removes a replicative niche for the pathogen and exposes both intracellular microbes and immunogenic DAMPs to immune surveillance (Lamkanfi and Dixit 2010).

In animals, RCD manifests in distinct forms such as apoptosis, pyroptosis, necroptosis, and ferroptosis, each defined by unique mechanisms and immunogenic outcomes. In plants, RCD in response to microbial attack is traditionally equated with the hypersensitive response, triggered by recognition of pathogen effectors by NLR proteins of the host. This HR-mediated response is typically seen as a defense mechanism against biotrophic pathogens.

In contrast, cell death induced by necrotrophic pathogens was long thought to be a passive, unspecific process, driven primarily by pathogen-derived toxins and independent of the host's immune system. However, this view has shifted significantly in recent years. It is now recognized that many necrotrophs, particularly those of the dothideomycetes class, produce host-specific toxins—termed necrotrophic effectors—that actively exploit the host cell death machinery (Faris and Friesen 2020; Leng et al. 2025; Stergiopoulos et al. 2013). A striking example is the *Arabidopsis* pathogen *Cochliobolus victoriae*, which produces the necrotrophic effector victorin. Victorin induces HR-like cell death specifically in accessions carrying the CC-NLR gene Locus Orchestrating Victorin effects 1 (LOV1) (Navarre and Wolpert 1999). Remarkably, LOV1 also confers resistance to the biotrophic rust pathogen *Puccinia coronata*, illustrating how necrotrophic pathogens can hijack NLR-mediated cell death mechanisms evolved for biotroph resistance (Lorang et al. 2007; Lorang et al. 2007). This suggests a more complex coevolutionary landscape, in which NLRs may be simultaneously shaped by both biotrophic and necrotrophic pathogens. Comparable strategies are observed in animal–microbe systems, such as during infection with the human pathogen *Salmonella* sp., which deploy toxins to induce host pyroptosis via caspase-1 activation in motile immune cells, thereby evading detection and clearance (Fink et al. 2008).

Beyond pathogenic interactions, RCD also plays crucial roles in beneficial plant–microbe associations. For instance, root nodule formation in the legume *Sesbania rostrata* involves the formation of an infection pocket mediated by ROS production and subsequent cell death (D'Haeze et al. 2003). Similarly, a comparative study of *Pinus sylvestris* root colonization by pathogenic, saprotrophic, and mutualistic fungi showed that all lifestyles, including that of the mutualistic ectomycorrhizal fungus *Hebeloma crustuliniforme*, involve the induction of cell death in host tissues, although to varying degrees (Mucha et al. 2014).

The mutualistic root endophyte *Serendipita indica* also relies heavily on host cell death induction

for successful colonization. It has long been known that RCD is required for establishing mutualistic interactions with both barley and Arabidopsis (Deshmukh et al. 2006; Qiang et al. 2012), yet the underlying molecular mechanisms remained poorly understood. In our recent work (Dunken et al. 2024) (Chapter 4), we identified fungal dAdo production as a central mechanism for inducing cell death during Arabidopsis root colonization by *S. indica*. Disruption of dAdo uptake in the host via mutation of the nucleoside transporter ENT3 abolished fungus-induced cell death in the root's developmental zones and reduced fungal colonization (Dunken et al. 2024; Zecua-Ramirez et al. 2023) (Chapter 4; Figure 5 & S9). Notably, root growth promotion still occurred in colonized *ent3* seedlings, suggesting that even reduced colonization levels under cell death-compromised conditions are sufficient to trigger beneficial mutualistic effects.

In addition to the active dAdo-mediated induction of cell death, *S. indica* also benefits from increased host cell death caused by other mechanisms. For instance, in the *ANAC033/SOMBRERO* mutant *smb3*, defective root cap cell clearance leads to enhanced fungal colonization, including of the root cap itself, which is normally not colonized by *S. indica*. This suggests that developmentally regulated RCD in the root cap may restrict microbial entry into sensitive, meristematic root zones. Furthermore, *S. indica* colonization leads to a suppressed expression of *BFN1* in differentiated epidermal cells. Bifunctional Nuclease 1 (BFN1) is a senescence-associated nuclease involved in dead cell clearance, pointing to a strategy in which *S. indica* exploits impaired host clearance mechanisms to access additional nutritional niches (Charura et al. 2024).

Although this thesis significantly advances our understanding of cell death induction during root colonization by *S. indica*, many questions remain unanswered. A frequently observed trend is the negative correlation between the intensity of root cell death and nutrient availability—supporting previous suggestions that nutrient depletion serves as a major trigger for the transition from the early biotrophic to the later cell death-associated phase of colonization (Lahrmann et al. 2013). However, it remains unclear how the induction and extent of cell death are influenced by nutrient limitation, both from the perspective of the host plant and the fungal endophyte. Further investigation is needed to determine whether this effect is driven by general nutrient scarcity or is specific to the limitation of particular elements, such as nitrogen or phosphorus. Another hypothesis suggests that the shift in colonization phase is critical for the formation of chlamydospores, which are frequently observed in dead host cells (Deshmukh et al. 2006).

Overall, the characterization of cell death in beneficial plant–microbe interactions is still in its early stages. Yet, *S. indica* emerges as a valuable model, demonstrating that both the induction and manipulation of host RCD pathways are integral to establishing and maintaining long-term mutualism. Building on these insights, it becomes clear that cell death should not be viewed solely as a defense mechanism against microbial invasion. Rather, it also plays a pivotal role in niche differentiation, shaping the outcome of both necrotrophic and beneficial interactions.

6.2 Redefining the role of TIR domain proteins in immunity

The involvement of host cell death in both pathogenic and mutualistic interactions highlights the importance of understanding the underlying immune regulators. Among these, TIR domain proteins have recently emerged as key mediators of immune signaling and cell death, not only in classical

defense but potentially in symbiotic contexts as well. TIR domains are conserved across kingdoms and occur in various protein architectures. They typically range from 150 to 250 amino acids in length and adopt a flavodoxin-like α/β -fold, characterized by a pentameric β -sheet which is surrounded by five α -helices. TIR domain-containing proteins are highly versatile, and TIR domains are often fused to a nucleotide-binding (NB)- and either a repeat or sensor domain. Predominantly, they play key roles in immunity and cell death (Ve et al. 2015).

The first characterized TIR protein was the *Drosophila melanogaster* Toll receptor. Initially identified as a key regulator of the development of the dorsoventral axis, it was quickly recognized for its role in innate immunity against fungal pathogens (Anderson et al. 1985; Lemaitre et al. 1996). The discovery of the mammalian Toll-like receptors, involved in adaptive immunity, along with the identification of the first TIR-NLR gene of tobacco, which confers immunity to the tobacco mosaic virus, reinforced the role of TIR domain proteins as central players in immunity across kingdoms (Medzhitov et al. 1997; Whitham et al. 1996).

Unlike vertebrates, plants lack an adaptive immune system but possess expansive NLR repertoires. In *Arabidopsis thaliana* alone, TIR-containing proteins exhibit 53 distinct architectures, including TIR-only proteins and TIR-NB proteins with either a leucine-rich repeat domain (TIR-NLRs) or a tetratricopeptide repeat domain (TNPs) (Weyer et al. 2019). For a long time, research focused primarily on TIR-NLRs, which detect microbial effectors or modified host proteins and can trigger HR-induction. While their role in ETI was established decades ago, the downstream signaling mechanisms remained unclear for long. A key breakthrough came with the characterization of the lipase-like proteins EDS1, PAD4, and SAG101, which form exclusive heterodimers that determine TIR signaling outcomes (Wagner et al. 2013; Wirthmueller et al. 2007). The EDS1-PAD4 heterodimer amplifies immune signaling, whereas the EDS1-SAG101 heterodimer promotes host cell death. Further downstream, EDS1 heterodimer formation requires the presence of RPW8-CC helper NLRs, such as NRG1 and ADR1, to establish a robust ETI response (Qi et al. 2018).

The functional mechanism linking TIR—NLR signaling to EDS1 and helper NLR activation has only recently been elucidated. Upon activation, plant TIR-NLRs oligomerize into tetrameric resistosomes, in which the TIR domains function as active NADases (Wan et al. 2019; Horsefield et al. 2019). Although NADase activity was first described in animals (Essuman et al. 2017), plant TIR-NLRs resistosomes are also enzymatically active but primarily generate a variety of small infochemicals rather than depleting cellular NAD^+ . Their enzymatic activity produces purine-based metabolites, including pRib-AMP/ADP and ADPR-ATP/di-ADPR, which specifically bind to EDS1-PAD4 or EDS1-SAG101 heterodimers, inducing conformational changes that facilitate helper NLR binding (Jia et al. 2022; Huang et al. 2022). This interaction leads to the formation of membrane-localized helper NLR resistosomes, which function as calcium-permeable channels (Jacob et al. 2021). Recent findings suggest a convergence between TIR- and CC-NLR signaling, both culminating in CC-resistosome formation and calcium influx, a crucial step in immune activation.

In addition to the new consideration of TIR-NLR as resistosome-forming, active enzymes that produce a variety of small infochemicals that modulate downstream signaling, the role of TIR-only proteins in plant immunity has undergone significant redefinition in the recent years. Previously, these proteins were considered truncated TIR-NLRs without a clear function in immunity,

overlooking the fact that monocots lack full-length TIR-NLRs and that the Col-0 reference accession contains over 50 TIR-only and TIR-NB proteins, most of which are expressed (Meyers et al. 2002). The discovery of the TIR-only protein Response to the bacterial type III effector protein HopBA1 (RBA1) in *Arabidopsis*, which induces EDS1-dependent cell death upon recognition of the bacterial effector HopBA1, demonstrated that TIR-only proteins are active components of the ETI response (Nishimura et al. 2017). Since then, studies have shown that TIR-only proteins can assemble into tetrameric resistosomes, exhibiting enzymatic activity and production of purine-based infochemicals comparable to TIR-NLRs (Jia et al. 2022; Huang et al. 2022; Wang et al. 2019a). Furthermore, certain TIR-only proteins can form filamentous superstructures that function as nucleases, generating the stress signaling molecule 2',3'-cAMP by digesting both dsRNA and dsDNA (Yu et al. 2022). Recent research has also confirmed that TIR-only proteins in monocots are catalytically active and regulate immune responses by producing pRib-AMP/ADP or the proposed storage form 2'-cADPR (Zhang et al. 2025; Wu et al. 2024). Moreover, two recent studies have revealed that TIR-only proteins are negatively regulated by calcium-sensing proteins such as resistance of rice to diseases1 (ROD1) and Inhibitor of Stomatal Immunity C2-domain protein 1 (ISIC1) and are released upon pathogen infections (Wang et al. 2024; Wu et al. 2024). These findings further blur the traditional boundaries between PTI and ETI. Historically, TIR-NLRs and related proteins were considered exclusive components of the ETI response, activated by the recognition of microbial effectors or effector targets. While the role of TIR-only proteins in effector recognition and downstream signaling has been established (Nishimura et al. 2017), their regulation by inhibitory calcium sensors suggests a direct link between PRR-mediated calcium influx and TIR-only enzymatic activity, ultimately activating the EDS1-PAD4-ADR1 signaling node. These discoveries, along with evidence that ETI both requires PTI signaling and amplifies the PTI response, contribute to a new perspective on plant immunity (Ngou et al. 2021; Yuan et al. 2021). While the two-tiered zig-zag model of plant immunity (Jones and Dangl 2006) has been instrumental in describing immune signaling, the expanding roles of TIR proteins and their enzymatic products suggest the need for a more interconnected framework.

6.2.1 Regulation of TIR protein activity in immunity and cell death

Given their central role in initiating immune responses and triggering cell death, TIR domain proteins must be tightly regulated to prevent detrimental effects on the host. Therefore, the intensity of TIR domain protein-induced immune responses is controlled at multiple levels.

At the transcriptional level, NLR genes are typically expressed at low abundance but can be induced by pathogen invasion or the accumulation of phytohormones such as salicylic acid (Mohr et al. 2010). Additionally, defense responses can trigger alternative splicing of TIR-NLR transcripts, yielding isoforms with distinct immune functions (Zhang and Gassmann 2007). Beyond pathogen responses, TIR domain protein gene expression is also influenced by beneficial microbial interactions. For example, the root endophyte *S. indica* induces multiple TIR domain protein genes, potentially contributing to fungal restriction within a balanced mutualistic symbiosis (Dunken et al. 2024) (Chapter 4, Figure 7 & S13). Moreover, legumes like *Medicago truncatula* produce trans-acting small interfering RNAs (siRNAs) that target immunity genes, including TIR-NLRs, to facilitate mutualistic relationships with mycorrhizal fungi and rhizobial root nodulation (Zhai et al.

2011).

Beyond transcriptional regulation, subcellular localization critically affects TIR protein function. The flax TIR-NLR L6 localizes to the Golgi membrane, and loss of this attachment impairs its ability to induce cell death (Bernoux et al. 2023). In *Arabidopsis*, the TIR-NLR Resistant to *P. syringae* 4 (RPS4) and the downstream signaling hub EDS1 exist in both cytoplasmic and nuclear pools, each contributing differently to immune signaling and cell death (Heidrich et al. 2011). While recent data implies that tightly controlled TIR domain protein localization could impact the formation of catalytically active resistosomes (Bernoux et al. 2023), whether specific intra- or intercellular transport mechanisms exist to distribute, store, or sequester the products of TIR activity remains an open question, with potential implications for agricultural interventions.

TIR domain protein activity is also regulated at the enzymatic level. In plants, calcium-sensing proteins such as ROD1 and ISIC1 act as direct inhibitors of TIR-only proteins (Wang et al. 2024; Wu et al. 2024). Calcium influx both activates TIR domain proteins and results from their activity through the allosteric activation of EDS1 heterodimers and helper NLR resistosomes (Jacob et al. 2021). Furthermore, helper NLRs modulate downstream TIR signaling. Truncated versions of the RPW8-CC-NLR NRG1 bind activated EDS1-SAG101 heterodimers but fail to form functional resistosomes, thereby blocking further signaling (Xiao et al. 2025; Huang et al. 2025).

TIR activity has also been implicated in microbial immunity, particularly in antiviral defense. In bacteria, TIR domains contribute to defense mechanisms that are directly counteracted by viral proteins. For example, the Tad family of phage proteins sequesters TIR-generated signaling molecules, such as cADPR variants, thereby inhibiting downstream NADase activation and neutralizing bacterial defense (Leavitt et al. 2022). Interestingly, similar interference strategies are employed by plant-associated pathogens. Several plant pathogens secrete Nudix hydrolase effectors that degrade TIR-generated molecules like 2'3'-cAMP, disrupting host immune signaling (Kong et al. 2015; Adlung and Bonas 2017). Beyond interfering with immune responses, these Nudix effectors also manipulate host phosphate signaling, decoupling phosphate starvation responses from nutrient availability to suppress defense (McCombe et al. 2025). At the same time, plants themselves encode Nudix hydrolases that regulate the abundance of 2'3'-cAMP, suggesting a conserved role for these enzymes in immune modulation (Yu et al. 2022; Bartsch et al. 2006; Ge et al. 2007). Notably, while plant TIR domain proteins predominantly generate 2'cADPR, bacterial TIR domains can produce 3'cADPR — a structurally related molecule that effectively inhibits plant immunity. These observations raise important questions about evolutionary convergence and cross-kingdom signaling interference. Future research should aim to clarify how these signaling pathways intersect or diverge, and how microbial pathogens and mutualists manipulate immunometabolic networks to establish symbioses.

6.2.2 ISI - a TIR-NLR with function in immunometabolic cell death and root colonization

The complexity of TIR domain protein regulation is exemplified by ISI, a previously uncharacterized TIR-NLR whose mutation impacts both cell death and microbial colonization. Our work sheds light on how this single protein integrates immune and metabolic signals during root-microbe interactions (Dunken et al. 2024) (Chapter 4, Figure 6 & 7). A mutation in the AT5G45240 locus, encoding ISI, is

sufficient to reduce dAdo-mediated cell death. Since dAdo treatment does not induce the canonical responses associated with PTI and the resulting cell death is not EDS1-dependent, integrating both dAdo and ISI into the current model of TIR-mediated immunity remains challenging. *ISI* expression is upregulated during the cell death-associated phase of *Serendipita indica* colonization, and *isi* mutant plants exhibit increased susceptibility to both *S. indica* and the pathogenic fungus *Bipolaris sorokiniana*, suggesting a role for ISI in microbial root colonization. Intriguingly, *isi* seedlings also show enhanced root cell death in the absence of microbes, pointing to the possibility of an autoimmune phenotype. Whether the increased susceptibility to colonization in *isi* mutants results from a lack of ISI-mediated immune signaling or from elevated root cell death providing additional nutrients for colonizing microbes remains to be determined. This raises the intriguing possibility that beneficial microbes like *S. indica* may compensate for deficiencies in host immune architecture, such as the loss of *ISI*, by providing functional substitutes through metabolic signaling. Such microbial buffering could act as a stabilizing force in genetically diverse host populations, potentially promoting symbiosis even in the presence of compromised immune components.

While previous studies have shown that *S. indica* can exploit dysregulated root cell death (Charura et al. 2024), a recent screen additionally supports the hypothesis that ISI plays a role in root immunity. Differences in Arabidopsis accession susceptibility to *B. sorokiniana* colonization could partially be explained by the presence or absence of TIR domain genes, including *ISI* (Zuccaro et al., unpublished). While TIR domain proteins have been extensively studied in foliar host-pathogen interactions, their roles in root immunity and beneficial microbial interactions remain largely unexplored. Our data suggest that a TIR-NLR contributes to both beneficial and pathogenic interactions with root-colonizing microbes. Similarly, the Arabidopsis TIR-NLR VARIATION IN COMPOUND TRIGGERED ROOT GROWTH RESPONSE (VICTR) has been implicated in regulating both abiotic salt stress and ETI-mediated root growth arrest (Kim et al. 2012; Ariga et al. 2017). Similar to *ISI*, *VICTR* expression is induced upon *S. indica* colonization and that knockout mutants exhibit higher levels of colonization, reinforcing the significance of TIR-NLRs in root immunity (Zuccaro et al., unpublished). Additionally, recent findings demonstrate that the Arabidopsis TIR-NLR Mediator of Microbiome Feedback 1 (MMF1) influences bacterial root microbiota recruitment and is essential for the microbial community feedback loop that promotes plant growth (Rensburg et al. 2025).

Collectively, these studies suggest that TIR-NLRs play important roles in root immunity, distinct from their functions in leaves. Although TIR-NLR-mediated HR has not been reported in roots, emerging evidence highlights their importance in shaping interactions with both beneficial and pathogenic microbes, either in bipartite interactions or within complex microbial communities. Whether these findings extend to other TIR domain proteins, such as TIR-only proteins, and whether their signaling pathways also rely on the formation of active resistosomes and the production of small signaling metabolites remains to be determined. Currently, we are investigating the biochemical properties of the ISI TIR domain, focusing on its potential for oligomerization, catalytic activity, and downstream signaling. While dAdo has not yet been identified as a substrate or product of TIR domains, we aim to elucidate its precise role in plant cell death by utilizing synthetic derivatives and identifying interaction partners. Whether dAdo functions as a purine-based infochemical directly linked to TIR activity or signals through an EDS1-independent pathway remains an open question.

6.3 dAdo – a purine-based infochemical inducing immunometabolic cell death

Our discovery of ISI as a modulator of dAdo-induced cell death suggests a functional link between TIR signaling and purine-based metabolic cues. To understand this connection, it is essential to investigate dAdo itself—not just as a metabolite, but as an immunometabolic signal that triggers cell death across kingdoms. In the context of this thesis Dunken et al. 2024 (Chapter 4), we demonstrate that the synergistic production of the purine nucleoside dAdo by the apoplastic fungal hydrolases SiNucA and SiE5NT is the initial trigger for cell death during root colonization by *S. indica*. Chemically, dAdo closely resembles adenosine, differing only by the absence of a hydroxyl group at the 2' position of the sugar moiety. While dAdo has only recently gained attention beyond its classical role in purine and nucleic acid metabolism, extracellular adenosine is well-established in animal systems as an anti-inflammatory mediator. It acts through P1 surface-localized receptors to suppress ROS production and inflammatory cytokine release (Shryock and Belardinelli 1997; Ohta and Sitkovsky 2001; Faas et al. 2017). In plants, extracellular adenosine has only recently been characterized. Similar to its role in animals, elevated extracellular adenosine levels relative to extracellular ATP (the so-called eAdo/eATP ratio) are known to inhibit immune signaling. As such, adenosine secretion is a virulence strategy employed by pathogenic microbes like *Fusarium oxysporum* (Kesten et al. 2023).

In contrast, dAdo was first implicated in host-microbe interactions as a byproduct of extracellular DNA (eDNA) degradation. Both animal immune cells such as neutrophils and plant root cells release DNA containing antimicrobial proteins and metabolites to immobilize or kill invading microbes. The degradation of these inhibitory eDNA structures by secreted nucleases is a well-documented strategy among both animal- and plant-associated microbes (Seper et al. 2013; Tran et al. 2016; Thammavongsa et al. 2013). Notably, both the human pathogen *Staphylococcus aureus* and the beneficial endophyte *S. indica* secrete a combination of nucleases and nucleotidases. The synergistic activity of these enzymes leads not only to eDNA degradation but also to the generation of purine nucleosides such as dAdo, which induces cell death in mammalian macrophages and plant cells alike (Dunken et al. 2024; Thammavongsa et al. 2013). Although this mechanism is likely dependent on the presence of extracellular DNA, its presence across biological kingdoms and microbial lifestyles suggests that enzymatic dAdo production may represent a conserved strategy in host-microbe interactions characterized by cell death.

Unlike adenosine, dAdo does not signal through cell surface receptors in either animal or plant systems. Instead, it is imported into host cells via ENTs, which are integral to the purine salvage pathway (Young et al. 2013; Wormit et al. 2004; Traub et al. 2007). Once inside the cell, the signaling mechanisms triggered by dAdo differ substantially between animals and plants. In animal systems, dAdo is phosphorylated to deoxyadenosine triphosphate (dATP) by cytoplasmic nucleoside kinases, triggering apoptotic cell death via caspase-3 activation (Winstel et al. 2019). Plants, however, lack caspases. In our own experiments, *Arabidopsis* knockout mutants lacking the metacaspases MC1 and MC2, all four VPEs, or the sole annotated deoxyadenosine kinase (AT1G72040) (Clausen et al. 2012) showed no altered sensitivity to dAdo (Zuccaro, unpublished). This suggests that the mechanisms of dAdo-induced cell death diverge significantly between plant

and animal systems. In both kingdoms, however, rapidly dividing cells exhibit higher susceptibility to dAdo-induced cell death (Dunken et al. 2024; Carson et al. 1979)(Chapter 4, Figure 4). In animals, this cell type specificity is partially explained by the expression of ADA, which detoxifies dAdo. Supporting this, the ADA-resistant dAdo analogue 2-chloro-2'-deoxyadenosine (CldAdo) induces more potent cell death at lower concentrations (Carrera et al. 1990). Interestingly, plants lack ADA homologs and detectable ADA-like activity (Brady and Hegarty 1966; Ashihara et al. 2018), yet also show greater sensitivity to CldAdo. This points to alternative, possibly parallel, enzymatic detoxification mechanisms in plants (Zuccaro, unpublished).

Another key difference lies in the response to other purine nucleosides, such as dGuo. In animal systems, dGuo induces cell death to a similar extent as dAdo, and co-treatment leads to additive effects, likely due to purine salvage pathway overload (Winstel et al. 2024; Winstel et al. 2019; Tantawy et al. 2022). In plants, while dGuo can trigger immune responses (Lu et al. 2023) during fungal colonization, it does not induce cell death (preliminary data). Moreover, we observed that co-treatment with dAdo and dGuo does not enhance cell death, but rather reduces it, likely due to competitive inhibition at the transporter level—an effect also seen with adenosine co-treatment (Dunken et al. 2024)(Chapter 4, Figure 5). Interestingly, this host-specific susceptibility is mirrored in the enzymatic profiles of associated microbes. The nucleotidase Adsa from *S. aureus* produces both dAdo and dGuo in comparable amounts (Tantawy et al. 2022), whereas the *S. indica* nucleotidase SiE5NT shows a strong substrate preference for dAdo production (Dunken et al. 2024)(Chapter 4, Figure 3). The observed specificity of SiE5NT for dAdo, in contrast to the broader activity spectrum of *S. aureus* Adsa, may reflect selective pressure to align fungal enzymatic output with the substrate preference of host nucleoside transporters such as ENT3 or other factors influencing host susceptibility. This co-evolutionary adaptation could explain interspecies differences in infochemical production and host susceptibility, and suggests that microbial enzyme specificity is closely adapted to the specific host.

Another notable difference between dAdo-mediated cell death in plants and animals is the involvement of a TIR-NLR protein on the plant side. Our initial screen of nearly 7,000 Arabidopsis mutant lines identified a knockout of the previously uncharacterized TIR-NLR gene *ISI* as one of only 13 lines exhibiting resistance to dAdo-induced cell death (Dunken et al. 2024) (Chapter 4, Figure 6 & S10). TIR-NLRs are a broad class of intracellular immune receptors that have undergone massive expansion in dicotyledonous plants such as Arabidopsis, but are completely absent in animals (Toshchakov and Neuwald 2020). Although we characterized independent *ISI* mutants that were resistant to dAdo, *ISI* itself is not conserved among all Arabidopsis accessions (Weyer et al. 2019), and we found no clear correlation between its presence and dAdo susceptibility. This suggests that other TIR-NLR proteins might also be involved in intracellular dAdo sensing in Arabidopsis. While the precise mechanism remains to be determined, this could explain our consistent observation that monocots like barley and maize—which lack TIR-NLR proteins—exhibit higher resistance to dAdo compared to dicots like Arabidopsis or tobacco.

The direct connection between dAdo and *ISI* remains elusive. However, recent discoveries have shown that plant TIR domain proteins can oligomerize into enzymatically active complexes with NADase or nuclease activity, producing small signaling molecules that activate downstream immune and cell death pathways (Yu et al. 2022; Huang et al. 2022; Jia et al. 2022; Wan et

al. 2019). It is conceivable that dAdo itself could act as a substrate, product, or co-factor in a similar enzymatic process. While most studies have focused on the NADase activity of plant TIR domains, it has also been shown that filamentous TIR oligomers can digest DNA, suggesting that interactions with deoxynucleotides are possible (Yu et al. 2022). Additionally, studies on CC-NLR proteins like HopZ-Activated Resistance 1 (ZAR1) have demonstrated that not only ATP but also dATP can substitute ADP in the NB-ARC domain binding site, leading to receptor activation and oligomerization (Wang et al. 2019a). Remarkably, the deoxynucleotide dATP binds with even higher affinity than its ribose counterpart, highlighting a potentially overlooked role of deoxypurines in plant immunity and signaling. Alas, further studies are needed to elucidate the potential connections between dAdo, ISI, and TIR-domain proteins in general. Interestingly, although animals lack TIR-NLRs, recent findings have shown that the deamination of dAdo into deoxyinosine by the lysosomal enzyme ADA2 actively regulates immune responses via the Toll-like receptor TLR9. TLR9 recognizes foreign DNA and is frequently implicated in autoimmune responses (Greiner-Tollersrud et al. 2024; Hemmi et al. 2000; Greiner-Tollersrud et al. 2024). This further supports a link between deoxynucleosides and TIR-domain-containing proteins, reinforcing our hypothesis of a previously uncharacterized immunometabolic axis connecting purine metabolism with immune signaling.

While individual components of the dAdo-mediated cell death have now been identified in both plants and animals, the determinants of species- and cell type-specific sensitivity remain poorly understood. Given that dAdo is a core metabolite in all living organisms, its capacity to induce stress and trigger cell death must be tightly regulated. Notably, both the beneficial fungal endophyte *S. indica* and the pathogenic bacterium *S. aureus* utilize homologous pathways to produce dAdo and induce host cell death. This raises the possibility that the manipulation of the immunometabolic axis via purine metabolites represents a conserved strategy in diverse host–microbe interactions. Further elucidation of these processes will deepen our understanding of metabolic–immune crosstalk during symbiosis and pathogenesis, and may reveal novel intervention points relevant to both agriculture and medicine.

6.4 Open Questions and Outlook

The findings discussed in the previous chapters place dAdo at the intersection of metabolism and immunity, revealing new layers of complexity in plant–microbe interactions. However, they also raise several key questions that point the way for future research. The initial aim of this thesis and the underlying doctoral research was to deepen our understanding of fungal-mediated cell death, with a particular focus on the previously understudied phenomenon of root cell death induced by beneficial fungi such as the endophyte *S. indica*. By adapting novel methods for quantifying cell death (Chapter 3) in combination with multi-omics approaches, we advanced our understanding of several processes spanning multiple domains of plant–microbe interactions.

Our discovery that SiNucA and SiE5NT synergistically produce dAdo underscores how microbial effectors can generate emergent immune-modulatory functions. Such combinatorial activity highlights the importance of studying effector networks rather than isolated gene functions. We further identified dAdo as an infochemical that induces cell death across kingdoms and established it as the main molecular driver of *S. indica*-induced cell death in *Arabidopsis*. In addition, we

characterized both the *S. indica*- and dAdo-mediated cell death responses at transcriptional and metabolic levels, thereby providing deeper insights into the underlying cellular processes. Finally, we linked dAdo-mediated cell death in the Arabidopsis ecotype Col-0 to the TIR-NLR ISI (Chapter 4), reinforcing the emerging importance of immunometabolism, a topic we further explored in a review article (Chapters 5).

Although the findings presented in this thesis have advanced our understanding of cell death in plant–microbe interactions and current publications have highlighted the role of small molecules as infochemicals in plant immunity, several previously unanswered questions remain, and new ones have emerged. This chapter summarizes eight open key questions (Figure 6.1) that frame future directions for research on the complex regulation of cell death and the intimate interaction between plants and microbes.

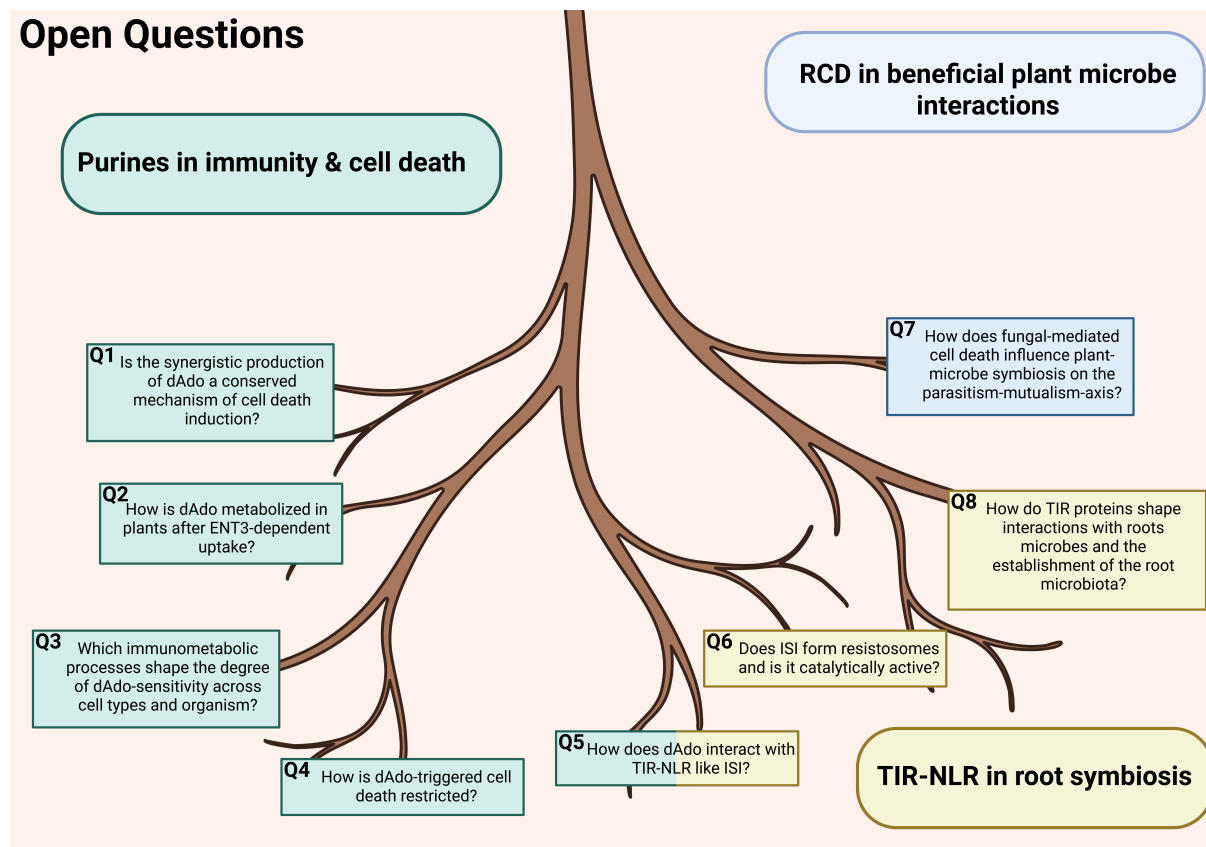


Figure 6.1: Open Questions on the integrations of root cell death, TIR-NLRs and purine metabolism in plant-microbe interactions - Eight main questions arising from the context of this thesis. The questions are divided between the three fields of **Purines in immunity & cell death** (green), **TIR-NLR in root symbiosis** (yellow) and **RCD in beneficial plant-microbe interactions** (blue). The Q (Question) number refers to the order of mention in the text and does not represent a hierarchy.

In the expanding field of purine metabolites in immunity and cell death (Chapter 5), it remains open which mechanisms are conserved and divergent across plants and animals. Notably, the synergistic production of dAdo from DNA by nucleases and nucleotidases has been described in both the bacterial pathogen *S. aureus* and the beneficial root endophytic fungus *S. indica*. This raises the question whether dAdo production is a conserved mechanism across kingdoms and microbial lifestyles (**Q1**) (Thammavongsa et al. 2013) (Chapter 4, Figure 3). Although direct evidence for dAdo production remains limited, a recent study demonstrated that the necrotrophic plant pathogen *Fusarium oxysporum* secretes an active nucleotidase that reduces apoplastic adenosine levels, thereby dampening immune signaling by lowering the eATP/extracellular adenosine ratio (Kesten et al. 2023). However, this study did not measure dAdo production, so it remains unclear whether the *F. oxysporum* nucleotidase also acts on dATP, as observed for SiE5NT (Chapter 4, Figure 3). A major challenge in detecting dAdo production during plant-microbe interactions is the reliable measurement of apoplastic dAdo accumulation using metabolomic approaches. Alternatively, a combined genetic and transcriptomic strategy, focused on identifying secreted microbial nucleotidases expressed *in planta*, followed by biochemical validation, could offer a promising path toward uncovering dAdo production in diverse microbes. Future studies could assess whether microbial communities coordinate immunometabolic outputs through division of labor or synergistic effector deployment, similar to what we observe in *S. indica*. This would extend the principles described here to more complex root-associated consortia.

We demonstrated that, in contrast to eATP, apoplastic dAdo does not trigger canonical DAMP responses such as ROS production or Ca^{2+} influx. Instead, dAdo must be transported into the plant cell via ENT3 to induce cell death (Chapter 4, Figures 5 and S7). In animal systems, it has been shown that phosphorylation of dAdo by nucleoside kinases is essential for its cell death-inducing activity, whereas deamination by enzymes such as ADA counteracts this effect (Winstel et al. 2019; Carrera et al. 1990). In plants, however, the downstream processes that contribute to dAdo-induced cell death remain unclear (**Q2**). Since plants lack ADA activity (Brady and Hegarty 1966; Ashihara et al. 2018) and mutants deficient in the deoxyribonucleoside kinase (AT1G72040) do not exhibit reduced sensitivity to dAdo (Zuccaro, unpublished), it is likely that the intracellular mechanisms of dAdo-mediated cell death differ significantly between plants and animals.

To identify the key components of this pathway in plants, and to uncover the factors driving differential dAdo sensitivity across cell types and species (**Q3**), single-cell transcriptomic analyses focusing on the expression of *ENTs* and other purine salvage genes could be highly informative. In parallel, thermal proteome profiling (TPP) and development of modified dAdo probes for affinity-based pull-down assays can be used to identify dAdo-interacting proteins. Addressing these knowledge gaps will improve our understanding of intracellular dAdo metabolism and its role in the broader context of purine immunometabolism and RCD in plants.

Another major open question is how dAdo-mediated cell death is spatially restricted during root colonization by *S. indica* (**Q4**). Despite its ability to induce cell death, *S. indica* colonization does not cause widespread root necrosis, but cell death is confined to heavily colonized cells in the epidermis and outer cortex layers of the differentiation zone. This suggests the existence of regulatory mechanisms that limit the spread of cell death. Such regulation is particularly crucial because cell death leads to the release of additional DNA and dATP into the apoplast, which could otherwise

amplify the death signal in a feed-forward loop. Interestingly, the plastid-derived retrograde stress metabolite MECPP accumulates in the apoplast following both dAdo treatment and *S. indica* colonization (Chapter 4, Figures 4 and 5). Since MECPP does not induce cell death on its own (Chapter 4, Figure S6), it may act either as a factor in the dAdo signaling pathway or as an inhibitor that primes neighboring cells to resist cell death. Preliminary experiments further indicate that lower concentrations of dAdo induce the expression of immunity marker genes downstream of EDS1 (Zuccaro, unpublished), commonly associated with ETI and HR (Sun et al. 2015; Wang et al. 2011). Given that HR is also a highly localized form of cell death, characterized by distinct transcriptional signatures in dying versus neighboring cells (Lukan et al. 2020; Salguero-Linares et al. 2022), it is plausible that dAdo may function in a concentration-dependent manner, promoting either cell death or immune priming depending on its local concentration. Taken together, these findings suggest that immunometabolic signals such as dAdo do not merely modulate host defense, but may also play a role in spatially organizing immune responses. The localized nature of dAdo-induced cell death, coupled with its concentration-dependent effects, indicates that immunometabolic signals such as dAdo could act as positional cues. This supports a broader model in which immunometabolism operates as a spatial logic layer, encoding information about where and how immune responses should be deployed along the root axis. Although dAdo serves as a central model in this thesis, other microbially derived metabolites such as 2',3'-cAMP, NAD⁺ derivatives, and plastid-derived signals like MECPP are likely to contribute to spatial immune regulation and merit future investigation.

While the involvement of the TIR-NLR ISI in dAdo-mediated cell death is intriguing, our understanding of the molecular link between this infochemical and immune receptors remains at an early stage. Recent advances have redefined plant TIR domain proteins as enzymatically active components that generate a diverse array of immunoactive small molecules (Huang et al. 2022; Jia et al. 2022; Yu et al. 2022; Wan et al. 2019). This raises the hypothesis that dAdo may act as a substrate, product, or cofactor of TIR-NLRs, including ISI (Q5), although dAdo is currently not classified among known TIR substrates (such as NAD⁺ or nucleic acids) or products (e.g. cADPR isoforms, pRib-AMP/ADP, or ADPR-ATP/di-ADPR). Continued characterization of TIR proteins, and ISI in particular, may yet reveal a functional connection. Interestingly, we did not observe dAdo resistance in other TIR-NLR or *eds1* mutants, suggesting that ISI and dAdo may signal through a non-canonical, EDS1-independent pathway—similar to that proposed for the Arabidopsis TIR-NLR SADR1 or certain maize TNPs (Johannndrees et al. 2023; Jacob et al. 2023). In contrast, preliminary transcriptomic analyses revealed a concentration-dependent induction of genes downstream of EDS1 at early time points following dAdo treatment (Zuccaro, unpublished), hinting at a more complex signaling interplay. To further elucidate the relationship between dAdo and TIR proteins, we aim to identify dAdo-binding proteins, focussing on known components of plant immune signaling to construct a more integrated view of plant immunometabolism.

Given its involvement in dAdo-mediated cell death and the striking root cell death phenotype observed in the *isi* knockout mutant (Chapter 4, Figure 6-7), an important question arises: does ISI form resistosomes and exhibit catalytic activity, as demonstrated for other TIR-NLRs (Q6)? Sequence predictions of *ISI* indicate the presence of a conserved glutamate residue, previously shown to be essential for TIR enzymatic activity (Wan et al. 2019; Essuman et al. 2017; Yu et al. 2022). Interestingly, a recent study examining the Arabidopsis Col-0 TIRome failed to detect 2'-cADPR

production or cell death induction upon heterologous expression of the ISI TIR domain in *Nicotiana benthamiana* (Bayless et al. 2025). However, we did observe cell death induction following *ISI* TIR expression in Arabidopsis protoplasts (Chapter 4, Figure 6E). These findings suggest a possible species-specific response and point toward a mechanism of action distinct from NAD⁺-dependent 2'cADPR synthesis. Hence, ISI may operate via an alternative catalytic mode, such as a nuclease generating 2',3'cAMP, as described in Yu et al. 2022 for other TIR domain proteins. To further explore this, we are aiming to employ cryo-electron microscopy (Cryo-EM) to resolve the structure of ISI oligomers, with the expectation of identifying either tetrameric or filamentous assemblies, as previously reported for other TIR-containing resistosomes.

In this thesis, we identified synergistic dAdo production and its subsequent uptake via ENT3 as key steps in *S. indica*-induced cell death in Arabidopsis (Chapter 4). While *ent3* mutant seedlings did not exhibit root cell death during fungal colonization (Chapter 4, Figure 5), the symbiosis still promoted root growth, and fungal colonization was only transiently reduced (Chapter 4, Figures S9, S12). This raises the important question, what role fungal-induced cell death plays in shaping the *S. indica*–Arabidopsis interaction and what we can extrapolate from this onto other plant-fungal interaction (Q7). Although previous studies have highlighted the importance of host cell death during *S. indica* colonization (Qiang et al. 2012; Deshmukh et al. 2006), our studies could only partially support this. To fully assess the contribution of dAdo-mediated cell death, long-term studies are needed that evaluate additional fitness parameters—such as Arabidopsis seed yield and *S. indica* chlamydospore production—under both standard and stress conditions. Comparing these outcomes in wild-type (Col-0) and *ent3* backgrounds could provide deeper insight into the ecological role of dAdo-mediated cell death in mutualistic interactions. Notably, earlier work suggests that host-mediated restriction of cell death is critical for sustaining beneficial interactions. For instance, mutants defective in immune-related pathways such as glucosinolate biosynthesis or autophagy often show increased cell death and higher colonization rates (Zecua-Ramirez et al. 2023; Lahrmann et al. 2015). However, these effects do not always correlate with a loss of mutualistic benefits like growth promotion, highlighting the complexity of this relationship. A direct link between the extent of cell death, colonization intensity, and net plant benefit remains to be clearly established.

While dAdo is a key driver of *S. indica*-induced cell death in Arabidopsis, evidence suggests that the fungus also engages other RCD pathways. For example, in the *smb3* developmental regulated cell death (dRCD) mutant, which accumulates dying root cap cells due to defective clearance, *S. indica* shows enhanced colonization. *S. indica* appears to exploit the dysregulated dRCD by scavenging dead cells and expanding into typically uncolonized zones such as the root tip. Moreover, *S. indica* actively downregulates host genes involved in developmental cell death, such as the nuclease BFN1, suggesting a capacity to suppress host RCD when advantageous (Charura et al. 2024). Together, these observations support a model in which *S. indica* exploits and modulates host RCD—inducing it via dAdo to create entry points and niches, while simultaneously being restrained by the host plant to prevent overcolonization or fungal penetration of meristematic zones. This dual strategy underscores the nuanced role of cell death in beneficial plant–microbe interactions, a field that remains relatively unexplored. Because non-developmental cell death itself is generally disadvantageous for the host, it would be informative to investigate *S. indica* mutants deficient in cell death induction. Such strains may either confer enhanced benefits to the host or suffer from the loss

of a colonization niche, thus compromising long-term association. Either outcome would provide valuable insight into the evolutionary trade-offs underpinning this symbiosis. Overall, these findings highlight that cell death, traditionally associated with defense or disease, also plays complex and context-dependent roles in mutualistic interactions. The concept of beneficial microbe-induced host cell death challenges conventional classifications and emphasizes the importance of considering all processes within the dynamic context of plant–microbe interactions, rather than as isolated events determining interaction outcomes.

The identification of the TIR-NLR ISI as a factor involved in both dAdo-mediated cell death and endophyte colonization was highly unexpected. To date, most studies on TIR domain proteins in plants have focused on their role in recognizing pathogenic effectors via TIR-NLR receptors, which subsequently activate the immune signaling hub EDS1, leading to ETI and often culminating in HR. While the molecular interplay between TIR-NLRs, EDS1, and other components of the plant immune system has been extensively studied, these insights are derived almost exclusively from leaf tissue models. In contrast, our understanding of TIR-NLR function in root tissues remains limited. One of the few characterized examples is the *Arabidopsis* TIR-NLR VICTR, which mediates EDS1-dependent root growth arrest and has been implicated in osmotic stress tolerance and bacterial resistance (Ariga et al. 2017; Kim et al. 2012). Although this provides initial evidence for a role of TIR-NLRs in roots, the underlying mechanisms remain elusive, raising fundamental questions about the role of TIR-domain proteins in root-microbe interactions and in the assembly and maintenance of the root microbiota (Q8).

Interestingly, the lack of documented HR-like cell death in roots suggests that TIR-NLR proteins may exert functions distinct from those in leaves. The recent discovery of TIR domain enzymatic activity, producing small infochemicals, introduces a compelling alternative to the classical cell death-centric view of TIR-NLR function. Molecules such as pRib-AMP/ADP, a product of TIR activity, have been proposed to prime immune responses without inducing cell death, offering a more nuanced role for TIR-NLRs in root immunity. Supporting this notion, our study demonstrated that *S. indica* colonization induces the transcription of multiple NLR genes, including both TIR-NLRs and CC-NLRs (Chapter 4, Figures 7 & S13). This transcriptional response underscores a potential role for NLRs, including TIR-NLRs, in modulating root immune responses during beneficial microbe interactions. Further corroborating this idea, a recent study identified the *Arabidopsis* TIR-NLR MMF1 as a key regulator of root microbiota composition and an essential component of the feedback loop between the plant and its microbial partners (Rensburg et al. 2025). In addition, a large-scale screen of diverse European *Arabidopsis* accessions revealed two closely related lines with striking differences in pathogen susceptibility. Genetic analyses uncovered the absence of approximately 40 genes in the susceptible accession, notably including 10 genes encoding TIR-domain proteins, among them ISI (Zuccaro *et al.*, unpublished). This finding further emphasizes the importance of TIR domain proteins in shaping plant-microbe interactions beyond classical pathogen recognition.

Taken together, these observations suggest that TIR-NLRs and other TIR-domain proteins play crucial roles in roots, influencing interactions with beneficial microbes, pathogens, and the complex root microbiota. To further elucidate these functions, it will be necessary to move beyond the well-characterized effector-NLR paradigms of leaf immunity and to investigate the roles of TIR-only proteins in root-associated immune responses. Unlike NLRs, TIR-only proteins are not known to

bind effectors but have recently been shown to be regulated by calcium influx and coupled to PTI signaling (Wang et al. 2024; Wu et al. 2024). This positions them as attractive candidates for orchestrating immune responses during root interactions with diverse soil-borne microbes.

Collectively, the experiments and insights presented in this thesis redefine dAdo as an overlooked infochemical that induces cell death across kingdoms, positioning it at the intersection of two previously separate fields: immunometabolism and regulated cell death. By linking these interconnected processes, this work broadens our understanding of host-microbe interactions. Notably, the identification of dAdo production by two distinct fungal effector enzymes highlights a new level of synergism and emergence, where novel properties arise from complex biological interactions. This finding illustrates how pathogenic and mutualistic microbes alike can exploit host cell death pathways, challenging the prevailing view of host RCD as a response solely triggered by pathogens. While based on evidence mainly from *Arabidopsis* and *S. indica*, this thesis supports the concept that induction of host RCD by mutualistic microbes is a common strategy to establish and maintain long-term symbioses. This perspective adds a new layer to our understanding of mutualism, suggesting that controlled modulation of host cell death can be central to shaping beneficial plant-microbe interactions. Given its pivotal role, the manipulation of host cell death emerges as a promising target for future interventions, not only in enhancing pathogen resistance but also in facilitating the accommodation of mutualists and engineering plant-associated microbiomes. Such strategies hold great potential for securing crop productivity and promoting sustainable agriculture. Nevertheless, several key questions remain unanswered. Elucidating the precise molecular mechanisms of dAdo-induced cell death, functionally characterizing ISI, and unraveling the roles of TIR domain proteins in root immunity represent crucial challenges ahead. Addressing these questions will require cutting-edge approaches, including single-cell omics, structural biology, and advances in chemical biology. Ultimately, I hope the molecular insights gained through this work will contribute to a more comprehensive understanding of plant-microbe interactions from an evolutionary perspective, bridging molecular immunology, cell death research, and ecological dynamics.

Bibliography

- Achatz, Beate et al. (2010). "Piriformospora indica mycorrhization increases grain yield by accelerating early development of barley plants". In: *Plant Signaling Behavior* 5.12, pp. 1685–1687. ISSN: 1559-2324. DOI: 10.4161/psb.5.12.14112. URL: <https://doi.org/10.4161/psb.5.12.14112>.
- Adesemoye, Anthony O. and Joseph W. Kloepper (2009). "Plant–microbes interactions in enhanced fertilizer-use efficiency". In: *Applied Microbiology and Biotechnology* 85.1, pp. 1–12. ISSN: 1432-0614. DOI: 10.1007/s00253-009-2196-0. URL: <https://doi.org/10.1007/s00253-009-2196-0>.
- Adlung, N. and U. Bonas (2017). "Dissecting virulence function from recognition: cell death suppression in *Nicotiana benthamiana* by XopQ/HopQ1-family effectors relies on EDS1-dependent immunity". In: *Plant J* 91.3, pp. 430–442. ISSN: 1365-313X (Electronic), 0960-7412 (Linking). DOI: 10.1111/tpj.13578. URL: <https://www.ncbi.nlm.nih.gov/pubmed/28423458>.
- Aist, James R. and William R. Bushnell (1991). "Invasion of Plants by Powdery Mildew Fungi, and Cellular Mechanisms of Resistance". In: *The Fungal Spore and Disease Initiation in Plants and Animals*. Ed. by Garry T. Cole and Harvey C. Hoch. Boston, MA: Springer US, pp. 321–345. ISBN: 978-1-4899-2635-7. DOI: 10.1007/978-1-4899-2635-7_15. URL: https://doi.org/10.1007/978-1-4899-2635-7_15.
- Akum, Fidele N. et al. (2015). "The *Piriformospora indica* effector PIIN_08944 promotes the mutualistic Sebacinalean symbiosis". In: *Frontiers in Plant Science* 6. ISSN: 1664-462X. URL: <https://www.frontiersin.org/journals/plant-science/articles/10.3389/fpls.2015.00906>.
- Albert, Isabell et al. (2020). "Surface Sensor Systems in Plant Immunity". In: *Plant Physiology* 182.4, pp. 1582–1596. ISSN: 0032-0889. DOI: 10.1104/pp.19.01299. URL: <https://doi.org/10.1104/pp.19.01299>.
- Ali, Rashid et al. (2007). "Death Don't Have No Mercy and Neither Does Calcium: Arabidopsis CYCLIC NUCLEOTIDE GATED CHANNEL2 and Innate Immunity". In: *The Plant Cell* 19.3, pp. 1081–1095. ISSN: 1040-4651. DOI: 10.1105/tpc.106.045096. URL: <https://doi.org/10.1105/tpc.106.045096>.
- Amaral, Eduardo P. et al. (2019). "A major role for ferroptosis in *Mycobacterium tuberculosis*-induced cell death and tissue necrosis". In: *Journal of Experimental Medicine* 216.3, pp. 556–570. ISSN: 0022-1007. DOI: 10.1084/jem.20181776. URL: <https://doi.org/10.1084/jem.20181776>.
- Anderson, K. V. et al. (1985). "Establishment of dorsal-ventral polarity in the *Drosophila* embryo: the induction of polarity by the Toll gene product". In: *Cell* 42.3. Anderson, K V Bokla, L Nusslein-Volhard, C eng Comparative Study Research Support, Non-U.S. Gov't 1985/10/01 Cell. 1985 Oct;42(3):791-8. doi: 10.1016/0092-8674(85)90275-2., pp. 791–8. ISSN: 0092-8674

- (Print) 0092-8674 (Linking). DOI: 10.1016/0092-8674(85)90275-2. URL: <https://www.ncbi.nlm.nih.gov/pubmed/3931919>.
- Ansmann, Gerrit and Tobias Bollenbach (2021). “Building clone-consistent ecosystem models”. In: *PLOS Computational Biology* 17.2, e1008635. DOI: 10.1371/journal.pcbi.1008635. URL: <https://doi.org/10.1371/journal.pcbi.1008635>.
- Ariga, Hirotaka et al. (2017). “NLR locus-mediated trade-off between abiotic and biotic stress adaptation in Arabidopsis”. In: *Nature Plants* 3.6, p. 17072. ISSN: 2055-0278. DOI: 10.1038/nplants.2017.72. URL: <https://doi.org/10.1038/nplants.2017.72>.
- Ashihara, Hiroshi et al. (2018). “Purine salvage in plants”. In: *Phytochemistry* 147. Journal Article Review, 89–124. DOI: 10.1016/j.phytochem.2017.12.008.
- Azarashvili, Tamara et al. (2009). “Ca²⁺-dependent permeability transition regulation in rat brain mitochondria by 2',3'-cyclic nucleotides and 2',3'-cyclic nucleotide 3'-phosphodiesterase”. In: *American Journal of Physiology - Cell Physiology* 296.6, pp. C1428–C1439. ISSN: 0363-6143. DOI: 10.1152/ajpcell.00006.2009. URL: <https://doi.org/10.1152/ajpcell.00006.2009>.
- Bai, Yang et al. (2015). “Functional overlap of the Arabidopsis leaf and root microbiota”. In: *Nature* 528.7582, pp. 364–369. ISSN: 0028-0836. DOI: 10.1038/nature16192. URL: <https://doi.org/10.1038/nature16192>.
- Balagué, Claudine et al. (2017). “The Arabidopsis thaliana lectin receptor kinase LecRK-I.9 is required for full resistance to Pseudomonas syringae and affects jasmonate signalling”. In: *Molecular plant pathology* 18.7. Journal Article, 937–948. DOI: 10.1111/mpp.12457.
- Balint-Kurti, P. (2019). “The plant hypersensitive response: concepts, control and consequences”. In: *Mol Plant Pathol* 20.8, pp. 1163–1178. ISSN: 1364-3703 (Electronic), 1464-6722 (Print), 1364-3703 (Linking). DOI: 10.1111/mpp.12821. URL: <https://www.ncbi.nlm.nih.gov/pubmed/31305008>.
- Banhara, Aline et al. (2015). “Colonization of root cells and plant growth promotion by Piriformospora indica occurs independently of plant common symbiosis genes”. In: *Frontiers in Plant Science* 6. ISSN: 1664-462X. DOI: 10.3389/fpls.2015.00667.
- Bartsch, M. et al. (2006). “Salicylic acid-independent ENHANCED DISEASE SUSCEPTIBILITY1 signaling in Arabidopsis immunity and cell death is regulated by the monooxygenase FMO1 and the Nudix hydrolase NUDT7”. In: *Plant Cell* 18.4, pp. 1038–51. ISSN: 1040-4651 (Print), 1532-298X (Electronic), 1040-4651 (Linking). DOI: 10.1105/tpc.105.039982. URL: <https://www.ncbi.nlm.nih.gov/pubmed/16531493>.
- Bayless, Adam M. et al. (2025). “The Arabidopsis TIRome informs the design of artificial TIR (Toll/interleukin-1 receptor) domain proteins”. In: *bioRxiv*, p. 2025.03.15.643477. DOI: 10.1101/2025.03.15.643477. URL: <https://www.biorxiv.org/content/biorxiv/early/2025/03/17/2025.03.15.643477.full.pdf>.
- Berman, H. M. et al. (2000). “The Protein Data Bank”. In: *Nucleic Acids Res* 28.1. Berman, H M Westbrook, J Feng, Z Gilliland, G Bhat, T N Weissig, H Shindyalov, I N Bourne, P E eng Research Support, U.S. Gov't, Non-P.H.S. Research Support, U.S. Gov't, P.H.S. England 1999/12/11 Nucleic Acids Res. 2000 Jan 1;28(1):235-42. doi: 10.1093/nar/28.1.235., pp. 235–42. ISSN: 0305-1048

- (Print) 1362-4962 (Electronic) 0305-1048 (Linking). DOI: 10.1093/nar/28.1.235. URL: <https://www.ncbi.nlm.nih.gov/pubmed/10592235>.
- Bernoux, Maud et al. (2023). "Subcellular localization requirements and specificities for plant immune receptor Toll-interleukin-1 receptor signaling". In: *The Plant Journal* 114.6, pp. 1319–1337. ISSN: 0960-7412. DOI: <https://doi.org/10.1111/tpj.16195>. URL: <https://onlinelibrary.wiley.com/doi/abs/10.1111/tpj.16195>.
- Bestwick, C. S. et al. (1995). "Hrp Mutant of *Pseudomonas syringae* pv *phaseolicola* Induces Cell Wall Alterations but Not Membrane Damage Leading to the Hypersensitive Reaction in Lettuce". In: *Plant Physiology* 108.2, pp. 503–516. ISSN: 0032-0889. DOI: 10.1104/pp.108.2.503. URL: <https://doi.org/10.1104/pp.108.2.503>.
- Beyari, Eman A. (2025). "Alternatives to chemical pesticides: the role of microbial biocontrol agents in phytopathogen management: a comprehensive review". In: *Journal of Plant Pathology* 107.1, pp. 291–314. ISSN: 2239-7264. DOI: 10.1007/s42161-024-01808-8. URL: <https://doi.org/10.1007/s42161-024-01808-8>.
- Bhadouria, Jyoti and Jitender Giri (2022). "Purple acid phosphatases: roles in phosphate utilization and new emerging functions". In: *Plant cell reports* 41.1. Journal Article Review, 33–51. DOI: 10.1007/s00299-021-02773-7.
- Bi, G. et al. (2021). "The ZAR1 resistosome is a calcium-permeable channel triggering plant immune signaling". In: *Cell* 184.13, 3528–3541 e12. ISSN: 1097-4172 (Electronic), 0092-8674 (Linking). DOI: 10.1016/j.cell.2021.05.003. URL: <https://www.ncbi.nlm.nih.gov/pubmed/33984278>.
- Bidzinski, Przemyslaw et al. (2016). "Transcriptional Basis of Drought-Induced Susceptibility to the Rice Blast Fungus *Magnaporthe oryzae*". In: *Frontiers in Plant Science* 7. ISSN: 1664-462X. DOI: 10.3389/fpls.2016.01558. URL: <https://www.frontiersin.org/journals/plant-science/articles/10.3389/fpls.2016.01558>.
- Billington, Richard A. et al. (2006). "Emerging functions of extracellular pyridine nucleotides". In: *Molecular medicine (Cambridge, Mass.)* 12.11-12. Journal Article, 324–327. ISSN: 1076-1551. DOI: 10.2119/2006-00075.Billington.
- Blackburn, Michael R. and Rodney E. Kellems (2005). "Adenosine Deaminase Deficiency: Metabolic Basis of Immune Deficiency and Pulmonary Inflammation". In: *Advances in Immunology*. Elsevier, 1–41. ISBN: 9780120044863. DOI: 10.1016/s0065-2776(04)86001-2.
- Blechert, O. et al. (1999). "First Remarks on the Symbiotic Interaction Between *Piriformospora indica* and Terrestrial Orchids". In: *Mycorrhiza: Structure, Function, Molecular Biology and Biotechnology*. Ed. by Ajit Varma and Bertold Hock. Berlin, Heidelberg: Springer Berlin Heidelberg, pp. 683–688. ISBN: 978-3-662-03779-9. DOI: 10.1007/978-3-662-03779-9_28. URL: https://doi.org/10.1007/978-3-662-03779-9_28.
- Bodin, P. and G. Burnstock (2001). "Purinergic signalling: ATP release". In: *Neurochemical research* 26.8-9. Journal Article Research Support, Non-U.S. Gov't Review Journal Article Research Support, Non-U.S. Gov't Review, 959–969. ISSN: 0364-3190. DOI: 10.1023/a:1012388618693.

- Brady, Thomas G. and Vincent J. Hegarty (1966). “An Investigation of Plant Seeds for Adenosine Deaminase”. In: *Nature* 209.5027, pp. 1027–1028. ISSN: 1476-4687. DOI: 10 . 1038 / 2091027a0. URL: <https://doi.org/10.1038/2091027a0>.
- Brinkmann, V. et al. (2004). “Neutrophil extracellular traps kill bacteria”. In: *Science* 303.5663. Brinkmann, Volker Reichard, Ulrike Goosmann, Christian Fauler, Beatrix Uhlemann, Yvonne Weiss, David S Weinrauch, Yvette Zychlinsky, Arturo eng AI037720/AI/NIAID NIH HHS/ Research Support, U.S. Gov’t, P.H.S. 2004/03/06 05:00 Science. 2004 Mar 5;303(5663):1532-5. doi: 10.1126/science.1092385., pp. 1532–5. ISSN: 1095-9203 (Electronic) 0036-8075 (Linking). DOI: 10 . 1126 / science . 1092385. URL: <https://www.ncbi.nlm.nih.gov/pubmed/15001782>.
- Bruzzone, S. et al. (2001). “Connexin 43 hemi channels mediate Ca²⁺-regulated transmembrane NAD⁺ fluxes in intact cells”. In: *FASEB J* 15.1, pp. 10–12. ISSN: 0892-6638 (Print), 0892-6638 (Linking). DOI: 10 . 1096 / fj . 00 - 0566fje. URL: <https://www.ncbi.nlm.nih.gov/pubmed/11099492>.
- Burdette, Dara L. and Russell E. Vance (2013). “STING and the innate immune response to nucleic acids in the cytosol”. In: *Nature Immunology* 14.1, pp. 19–26. ISSN: 1529-2916. DOI: 10.1038/ni.2491. URL: <https://doi.org/10.1038/ni.2491>.
- Burnstock, Geoffrey (2014). “Purinergic signalling: from discovery to current developments”. In: *Experimental physiology* 99.1. Journal Article Review Journal Article Review, 16–34. DOI: 10 . 1113 / expphysiol . 2013 . 071951.
- Camborda, Stefano et al. (2022). “CobraMod: a pathway-centric curation tool for constraint-based metabolic models”. In: *Bioinformatics* 38.9, pp. 2654–2656. ISSN: 1367-4803. DOI: 10.1093/bioinformatics/btac119. URL: <https://doi.org/10.1093/bioinformatics/btac119>.
- Camini, Fernanda Caetano et al. (2017). “Implications of oxidative stress on viral pathogenesis”. In: *Archives of Virology* 162.4, pp. 907–917. ISSN: 1432-8798. DOI: 10.1007/s00705-016-3187-y. URL: <https://doi.org/10.1007/s00705-016-3187-y>.
- Carrera, C. J. et al. (1990). “Potent toxicity of 2-chlorodeoxyadenosine toward human monocytes in vitro and in vivo: A novel approach to immunosuppressive therapy”. In: *J Clin Invest* 86.5, pp. 1480–1488. ISSN: 0021-9738. DOI: 10.1172/JCI114865. URL: <http://www.ncbi.nlm.nih.gov/pubmed/1700795>.
- Carson, D A et al. (1979). “Biochemical basis for the enhanced toxicity of deoxyribonucleosides toward malignant human T cell lines”. In: *Proceedings of the National Academy of Sciences* 76.5, pp. 2430–2433. DOI: doi:10.1073/pnas.76.5.2430. URL: <https://www.pnas.org/doi/abs/10.1073/pnas.76.5.2430>.
- Castrillo, Gabriel et al. (2017). “Root microbiota drive direct integration of phosphate stress and immunity”. In: *Nature* 543.7646, pp. 513–518. ISSN: 1476-4687. DOI: 10.1038/nature21417. URL: <https://doi.org/10.1038/nature21417>.
- Cauwels, A. et al. (2014). “Extracellular ATP drives systemic inflammation, tissue damage and mortality”. In: *Cell death disease* 5.3. Journal Article Research Support, Non-U.S. Gov’t Journal Article Research Support, Non-U.S. Gov’t, e1102. DOI: 10.1038/cddis.2014.70.

- Charura, Nyasha et al. (2024). “Root cap cell corpse clearance limits microbial colonization in *Arabidopsis thaliana*”. In: *eLife* 13, RP96266. ISSN: 2050-084X. DOI: 10.7554/eLife.96266. URL: <https://doi.org/10.7554/eLife.96266>.
- Chia, K. S. and P. Carella (2023). “Taking the lead: NLR immune receptor N-terminal domains execute plant immune responses”. In: *New Phytol* 240.2, pp. 496–501. DOI: 10.1111/nph.19170. URL: <https://www.ncbi.nlm.nih.gov/pubmed/37525357>.
- Chodasiewicz, M. et al. (2022). “2',3'-cAMP treatment mimics the stress molecular response in *Arabidopsis thaliana*”. In: *Plant Physiol* 188.4. Chodasiewicz, Monika Kerber, Olga Gorka, Michal Moreno, Juan C Maruri-Lopez, Israel Minen, Romina I Sampathkumar, Arun Nelson, Andrew D L Skirycz, Aleksandra eng Research Support, Non-U.S. Gov't 2022/01/20 Plant Physiol. 2022 Mar 28;188(4):1966-1978. doi: 10.1093/plphys/kiac013., pp. 1966–1978. ISSN: 1532-2548 (Electronic) 0032-0889 (Print) 0032-0889 (Linking). DOI: 10.1093/plphys/kiac013. URL: <https://www.ncbi.nlm.nih.gov/pubmed/35043968>.
- Choi, Chul Hee et al. (2013). “*Porphyromonas gingivalis*-nucleoside-diphosphate-kinase inhibits ATP-induced reactive-oxygen-species via P2X7 receptor/NADPH-oxidase signalling and contributes to persistence”. In: *Cellular microbiology* 15.6. Journal Article Research Support, N.I.H., Extramural Journal Article Research Support, N.I.H., Extramural, 961–976. DOI: 10.1111/cmi.12089.
- Choi, Jeongmin et al. (2014). “Identification of a plant receptor for extracellular ATP”. In: *Science (New York, N.Y.)* 343.6168. Journal Article Research Support, Non-U.S. Gov't Research Support, U.S. Gov't, Non-P.H.S., 290–294. ISSN: 1095-9203. DOI: 10.1126/science.343.6168.290. URL: <https://pubmed.ncbi.nlm.nih.gov/24436418/>.
- Clark, Greg and Stanley J. Roux (2011). “Apyrases, extracellular ATP and the regulation of growth”. In: *Current opinion in plant biology* 14.6. Journal Article Research Support, U.S. Gov't, Non-P.H.S. Review, 700–706. DOI: 10.1016/j.pbi.2011.07.013.
- Clausen, Anders R. et al. (2012). “Two thymidine kinases and one multisubstrate deoxyribonucleoside kinase salvage DNA precursors in *rabidopsis thaliana*”. In: *The FEBS Journal* 279.20, pp. 3889–3897. ISSN: 1742-464X. DOI: <https://doi.org/10.1111/j.1742-4658.2012.08747.x>. URL: <https://febs.onlinelibrary.wiley.com/doi/abs/10.1111/j.1742-4658.2012.08747.x>.
- Cohen, Stephen P and Jan E. Leach (2020). “High temperature-induced plant disease susceptibility: more than the sum of its parts”. In: *Current Opinion in Plant Biology* 56, pp. 235–241. ISSN: 1369-5266. DOI: <https://doi.org/10.1016/j.pbi.2020.02.008>. URL: <https://www.sciencedirect.com/science/article/pii/S1369526620300285>.
- Collemare, J. et al. (2019). “Nonproteinaceous effectors: the terra incognita of plant-fungal interactions”. In: *New Phytol* 223.2, pp. 590–596. ISSN: 1469-8137 (Electronic), 0028-646X (Linking). DOI: 10.1111/nph.15785. URL: <https://www.ncbi.nlm.nih.gov/pubmed/30851201>.
- Cook, Nicola M. et al. (2025). “Autoactive CNGC15 enhances root endosymbiosis in legume and wheat”. In: *Nature* 638.8051, pp. 752–759. ISSN: 1476-4687. DOI: 10.1038/s41586-024-08424-7. URL: <https://doi.org/10.1038/s41586-024-08424-7>.

- Coronas-Serna, J. M. et al. (2020). “The TIR-domain containing effectors BtpA and BtpB from *Brucella abortus* impact NAD metabolism”. In: *PLoS Pathog* 16.4. Coronas-Serna, Julia Maria Louche, Arthur Rodriguez-Escudero, Maria Roussin, Morgane Imbert, Paul R C Rodriguez-Escudero, Isabel Terradot, Laurent Molina, Maria Gorvel, Jean-Pierre Cid, Victor J Salcedo, Suzana P eng Research Support, Non-U.S. Gov’t 2020/04/17 PLoS Pathog. 2020 Apr 16;16(4):e1007979. doi: 10.1371/journal.ppat.1007979. eCollection 2020 Apr., e1007979. ISSN: 1553-7374 (Electronic) 1553-7366 (Print) 1553-7366 (Linking). DOI: 10 . 1371 / journal.ppat.1007979. URL: <https://www.ncbi.nlm.nih.gov/pubmed/32298382>.
- Curtis, T. P et al. (2002). “Estimating prokaryotic diversity and its limits”. In: *Proc Natl Acad Sci U S A* 99.16, pp. 10494–9. ISSN: 0027-8424 (Print), 1091-6490 (Electronic), 0027-8424 (Linking). DOI: 10 . 1073 / pnas . 142680199. URL: <https://www.ncbi.nlm.nih.gov/pubmed/12097644>.
- Dangol, Sarmina et al. (2019). “Iron- and Reactive Oxygen Species-Dependent Ferroptotic Cell Death in Rice-Magnaporthe oryzae Interactions”. In: *The Plant Cell* 31.1, pp. 189–209. ISSN: 1040-4651. DOI: 10 . 1105 / tpc . 18 . 00535. URL: <https://doi.org/10.1105/tpc.18.00535>.
- Daumann, Manuel et al. (2015). “Apoplastic Nucleoside Accumulation in Arabidopsis Leads to Reduced Photosynthetic Performance and Increased Susceptibility Against Botrytis cinerea”. In: *Frontiers in plant science* 6. Journal Article, p. 1158. ISSN: 1664-462X. DOI: 10 . 3389 / fppls . 2015 . 01158.
- Delgado-Baquerizo, Manuel et al. (2020). “The proportion of soil-borne pathogens increases with warming at the global scale”. In: *Nature Climate Change* 10.6, pp. 550–554. ISSN: 1758-6798. DOI: 10 . 1038 / s41558 - 020 - 0759 - 3. URL: <https://doi.org/10.1038/s41558-020-0759-3>.
- Delledonne, Massimo et al. (2001). “Signal interactions between nitric oxide and reactive oxygen intermediates in the plant hypersensitive disease resistance response”. In: *Proceedings of the National Academy of Sciences* 98.23, pp. 13454–13459. DOI: doi:10.1073/pnas.231178298. URL: <https://www.pnas.org/doi/abs/10.1073/pnas.231178298>.
- Demidchik, Vadim et al. (2009). “Plant extracellular ATP signalling by plasma membrane NADPH oxidase and Ca²⁺ channels”. In: *The Plant journal : for cell and molecular biology* 58.6. Journal Article Research Support, Non-U.S. Gov’t, 903–913. ISSN: 0960-7412. DOI: 10 . 1111 / j . 1365 - 313X . 2009 . 03830 . x.
- Deshmukh, Sachin et al. (2006). “The root endophytic fungus Piriformospora indica requires host cell death for proliferation during mutualistic symbiosis with barley”. In: *Proceedings of the National Academy of Sciences of the United States of America* 103.49, pp. 18450–18457. ISSN: 0027-8424. DOI: 10 . 1073 / pnas . 0605697103. URL: <https://doi.org/10.1073/pnas.0605697103>.
- D’Haeze, Wim et al. (2003). “Reactive oxygen species and ethylene play a positive role in lateral root base nodulation of a semiaquatic legume”. In: *Proceedings of the National Academy of Sciences* 100.20, pp. 11789–11794. DOI: 10 . 1073 / pnas . 1333899100. URL: <https://www.pnas.org/content/pnas/100/20/11789.full.pdf>.

- Di Virgilio, Francesco (2007). “Liaisons dangereuses: P2X(7) and the inflammasome”. In: *Trends in Pharmacological Sciences* 28.9. Journal Article Research Support, Non-U.S. Gov’t Review, 465–472. ISSN: 0165-6147. DOI: 10.1016/j.tips.2007.07.002.
- Distéfano, Ayelén Mariana et al. (2017). “Heat stress induces ferroptosis-like cell death in plants”. In: *Journal of Cell Biology* 216.2, pp. 463–476. ISSN: 0021-9525. DOI: 10.1083/jcb.201605110. URL: <https://doi.org/10.1083/jcb.201605110>.
- Dixon, Scott J et al. (2012). “Ferroptosis: An Iron-Dependent Form of Nonapoptotic Cell Death”. In: *Cell* 149.5. doi: 10.1016/j.cell.2012.03.042, pp. 1060–1072. ISSN: 0092-8674. DOI: 10.1016/j.cell.2012.03.042. URL: <https://doi.org/10.1016/j.cell.2012.03.042>.
- Dodds, P. N. et al. (2006). “Direct protein interaction underlies gene-for-gene specificity and coevolution of the flax resistance genes and flax rust avirulence genes”. In: *Proc Natl Acad Sci U S A* 103.23, pp. 8888–8893. ISSN: 0027-8424, 1091-6490. DOI: 10.1073/pnas.0602577103. URL: <https://www.ncbi.nlm.nih.gov/pubmed/16731621>.
- Dorrenhaus, R. et al. (2023). “Two are not enough: synthetic strategies and applications of unnatural base pairs”. In: *Biol Chem* 404.10. Dorrenhaus, Robert Wagner, Philip K Kath-Schorr, Stephanie eng Research Support, Non-U.S. Gov’t Review Germany 2023/06/24 21:03 Biol Chem. 2023 Jun 26;404(10):883-896. doi: 10.1515/hsz-2023-0169. Print 2023 Sep 26., pp. 883–896. ISSN: 1437-4315 (Electronic) 1431-6730 (Linking). DOI: 10.1515/hsz-2023-0169. URL: <https://www.ncbi.nlm.nih.gov/pubmed/37354104>.
- Drew, G. C. et al. (2021). “Microbial evolution and transitions along the parasite-mutualist continuum”. In: *Nat Rev Microbiol* 19.10, pp. 623–638. ISSN: 1740-1534 (Electronic), 1740-1526 (Print), 1740-1526 (Linking). DOI: 10.1038/s41579-021-00550-7. URL: <https://www.ncbi.nlm.nih.gov/pubmed/33875863>.
- Driouich, Azeddine et al. (2019). “Root extracellular traps versus neutrophil extracellular traps in host defence, a case of functional convergence?” In: *Biological reviews of the Cambridge Philosophical Society* 94.5. Journal Article Research Support, Non-U.S. Gov’t Review, 1685–1700. DOI: 10.1111/brv.12522.
- Dunken, N. et al. (2022). “Monitoring Cell Death Via Ion Leakage and PAM Fluorometry”. In: *Methods Mol Biol* 2447. Dunken, Nick Mahdi, Lisa Hausler, Rainer E Zuccaro, Alga eng Research Support, Non-U.S. Gov’t 2022/05/19 Methods Mol Biol. 2022;2447:175-183. doi: 10.1007/978-1-0716-2079-3_14., pp. 175–183. ISSN: 1940-6029 (Electronic) 1064-3745 (Linking). DOI: 10.1007/978-1-0716-2079-3_14. URL: <https://www.ncbi.nlm.nih.gov/pubmed/35583781>.
- Dunken, Nick et al. (2024). “A nucleoside signal generated by a fungal endophyte regulates host cell death and promotes root colonization”. In: *Cell Host & Microbe* 32.12, 2161–2177.e7. ISSN: 1931-3128. DOI: 10.1016/j.chom.2024.10.020. URL: <https://doi.org/10.1016/j.chom.2024.10.020>.
- Díaz-Vegas, Alexis et al. (2015). “ROS Production via P2Y1-PKC-NOX2 Is Triggered by Extracellular ATP after Electrical Stimulation of Skeletal Muscle Cells”. In: *PloS one* 10.6. Journal Article Research Support, Non-U.S. Gov’t Competing Interests: The authors have declared that no competing interests exist. Journal Article Research Support, Non-U.S. Gov’t Competing Interests:

- The authors have declared that no competing interests exist., e0129882. DOI: 10.1371/journal.pone.0129882.
- Eastman, S. et al. (2022). “A phyto bacterial TIR domain effector manipulates NAD(+) to promote virulence”. In: *New Phytol* 233.2, pp. 890–904. ISSN: 1469-8137 (Electronic), 0028-646X (Print), 0028-646X (Linking). DOI: 10.1111/nph.17805. URL: <https://www.ncbi.nlm.nih.gov/pubmed/34657283>.
- Eichfeld, R. et al. (2024). “Transcriptomics reveal a mechanism of niche defense: two beneficial root endophytes deploy an antimicrobial GH18-CBM5 chitinase to protect their hosts”. In: *New Phytol* 244.3, pp. 980–996. ISSN: 1469-8137 (Electronic), 0028-646X (Linking). DOI: 10.1111/nph.20080. URL: <https://www.ncbi.nlm.nih.gov/pubmed/39224928>.
- Essuman, K. et al. (2017). “The SARM1 Toll/Interleukin-1 Receptor Domain Possesses Intrinsic NAD(+) Cleavage Activity that Promotes Pathological Axonal Degeneration”. In: *Neuron* 93.6. Essuman, Kow Summers, Daniel W Sasaki, Yo Mao, Xianrong DiAntonio, Aaron Milbrandt, Jeffrey eng R01 NS087632/NS/NINDS NIH HHS/ P41 GM103422/GM/NIGMS NIH HHS/ R01 AG013730/AG/NIA NIH HHS/ UL1 TR000448/TR/NCATS NIH HHS/ P30 CA091842/CA/NCI NIH HHS/ R01 NS065053/NS/NINDS NIH HHS/ 2017/03/24 *Neuron*. 2017 Mar 22;93(6):1334-1343.e5. doi: 10.1016/j.neuron.2017.02.022., 1334–1343 e5. ISSN: 1097-4199 (Electronic) 0896-6273 (Print) 0896-6273 (Linking). DOI: 10.1016/j.neuron.2017.02.022. URL: <https://www.ncbi.nlm.nih.gov/pubmed/28334607>.
- Essuman, K. et al. (2018). “TIR Domain Proteins Are an Ancient Family of NAD(+)-Consuming Enzymes”. In: *Curr Biol* 28.3, 421–430 e4. ISSN: 1879-0445 (Electronic), 0960-9822 (Print), 0960-9822 (Linking). DOI: 10.1016/j.cub.2017.12.024. URL: <https://www.ncbi.nlm.nih.gov/pubmed/29395922>.
- Essuman, K. et al. (2022). “Shared TIR enzymatic functions regulate cell death and immunity across the tree of life”. In: *Science* 377.6605, eabo0001. ISSN: 0036-8075, 1095-9203. DOI: 10.1126/science.abo0001. URL: <https://www.ncbi.nlm.nih.gov/pubmed/35857622>.
- Faas, M. M. et al. (2017). “Extracellular ATP and adenosine: The Yin and Yang in immune responses?” In: *Molecular aspects of medicine* 55. Journal Article Review Research Support, Non-U.S. Gov't, 9–19. DOI: 10.1016/j.mam.2017.01.002.
- Fakhro, Ahmad et al. (2010). “Impact of Piriformospora indica on tomato growth and on interaction with fungal and viral pathogens”. In: *Mycorrhiza* 20.3, pp. 191–200. ISSN: 1432-1890. DOI: 10.1007/s00572-009-0279-5. URL: <https://doi.org/10.1007/s00572-009-0279-5>.
- Faris, Justin D. and Timothy L. Friesen (2020). “Plant genes hijacked by necrotrophic fungal pathogens”. In: *Current Opinion in Plant Biology* 56, pp. 74–80. ISSN: 1369-5266. DOI: <https://doi.org/10.1016/j.pbi.2020.04.003>. URL: <https://www.sciencedirect.com/science/article/pii/S1369526620300431>.
- Felix, Georg et al. (1999). “Plants have a sensitive perception system for the most conserved domain of bacterial flagellin”. In: *The Plant Journal* 18.3, pp. 265–276. ISSN: 0960-7412. DOI: <https://doi.org/10.1046/j.1365-313X.1999.00265.x>. URL: <https://onlinelibrary.wiley.com/doi/abs/10.1046/j.1365-313X.1999.00265.x>.
- Ferrari, D. et al. (2006). “The P2X7 receptor: a key player in IL-1 processing and release”. In: *J Immunol* 176.7. Ferrari, Davide Pizzirani, Cinzia Adinolfi, Elena Lemoli, Roberto

- M Curti, Antonio Idzko, Marco Panther, Elisabeth Di Virgilio, Francesco eng Research Support, Non-U.S. Gov't Review 2006/03/21 J Immunol. 2006 Apr 1;176(7):3877-83. doi: 10.4049/jimmunol.176.7.3877., pp. 3877–83. ISSN: 0022-1767 (Print) 0022-1767 (Linking). DOI: 10.4049/jimmunol.176.7.3877. URL: <https://www.ncbi.nlm.nih.gov/pubmed/16547218>.
- Ferrario, Eugenio et al. (2024). “Evolution of fungal tuberculosis necrotizing toxin (TNT) domain-containing enzymes reveals divergent adaptations to enhance NAD cleavage”. In: *Protein Science* 33.7, e5071. ISSN: 0961-8368. DOI: <https://doi.org/10.1002/pro.5071>. URL: <https://onlinelibrary.wiley.com/doi/abs/10.1002/pro.5071>.
- Fink, Susan L. et al. (2008). “Anthrax lethal toxin and *Salmonella* elicit the common cell death pathway of caspase-1-dependent pyroptosis via distinct mechanisms”. In: *Proceedings of the National Academy of Sciences* 105.11, pp. 4312–4317. DOI: 10.1073/pnas.0707370105. URL: <https://www.pnas.org/doi/abs/10.1073/pnas.0707370105>.
- Flor, H H (1971). “Current Status of the Gene-For-Gene Concept”. In: *Annual Review of Phytopathology* 9. Volume 9, 1971, pp. 275–296. ISSN: 1545-2107. DOI: <https://doi.org/10.1146/annurev.py.09.090171.001423>. URL: <https://www.annualreviews.org/content/journals/10.1146/annurev.py.09.090171.001423>.
- Forderer, A. et al. (2022). “A wheat resistosome defines common principles of immune receptor channels”. In: *Nature* 610.7932, pp. 532–539. ISSN: 1476-4687 (Electronic), 0028-0836 (Print), 0028-0836 (Linking). DOI: 10.1038/s41586-022-05231-w. URL: <https://www.ncbi.nlm.nih.gov/pubmed/36163289>.
- Franchi, Luigi et al. (2009). “The inflammasome: a caspase-1-activation platform that regulates immune responses and disease pathogenesis”. In: *Nature Immunology* 10.3, pp. 241–247. ISSN: 1529-2916. DOI: 10.1038/ni.1703. URL: <https://doi.org/10.1038/ni.1703>.
- Franken, Philipp et al. (2000). “Molecular analysis of the Arbuscular mycorrhiza symbiosis”. In: *Archives of Agronomy and Soil Science* 45.4. doi: 10.1080/03650340009366129, pp. 271–286. ISSN: 0365-0340. DOI: 10.1080/03650340009366129. URL: <https://doi.org/10.1080/03650340009366129>.
- Friedmann Angeli, Jose Pedro et al. (2014). “Inactivation of the ferroptosis regulator Gpx4 triggers acute renal failure in mice”. In: *Nature Cell Biology* 16.12, pp. 1180–1191. ISSN: 1476-4679. DOI: 10.1038/ncb3064. URL: <https://doi.org/10.1038/ncb3064>.
- Galione, Antony et al. (1991). “Ca²⁺-Induced Ca²⁺ Release in Sea Urchin Egg Homogenates: Modulation by Cyclic ADP-Ribose”. In: *Science* 253.5024, pp. 1143–1146. DOI: doi:10.1126/science.1909457. URL: <https://www.science.org/doi/abs/10.1126/science.1909457>.
- Gans, J. et al. (2005). “Computational improvements reveal great bacterial diversity and high metal toxicity in soil”. In: *Science* 309.5739. Gans, Jason Wolinsky, Murray Dunbar, John eng Research Support, Non-U.S. Gov't 2005/08/27 Science. 2005 Aug 26;309(5739):1387-90. doi: 10.1126/science.1112665., pp. 1387–90. ISSN: 1095-9203 (Electronic) 0036-8075 (Linking). DOI: 10.1126/science.1112665. URL: <https://www.ncbi.nlm.nih.gov/pubmed/16123304>.

- Gao, Pu et al. (2013). "Cyclic [G(2,5)pA(3,5)p] Is the Metazoan Second Messenger Produced by DNA-Activated Cyclic GMP-AMP Synthase". In: *Cell* 153.5, pp. 1094–1107. ISSN: 0092-8674. DOI: <https://doi.org/10.1016/j.cell.2013.04.046>. URL: <https://www.sciencedirect.com/science/article/pii/S0092867413005229>.
- Gasparrini, Massimiliano et al. (2021). "Enzymology of extracellular NAD metabolism". In: *Cellular and Molecular Life Sciences: CMLS* 78.7. Journal Article Review Journal Article Review The authors declare that they have no conflict of interest., 3317–3331. ISSN: 1420-682X. DOI: 10.1007/s00018-020-03742-1.
- Gaumann, E (1950). *Principles of plant infection*. Crosby Lockwood amp; Son Ltd., London, pp. xvi + 543.
- Ge, X. et al. (2007). "AtNUDT7, a negative regulator of basal immunity in Arabidopsis, modulates two distinct defense response pathways and is involved in maintaining redox homeostasis". In: *Plant Physiol* 145.1, pp. 204–15. ISSN: 0032-0889 (Print), 1532-2548 (Electronic), 0032-0889 (Linking). DOI: 10.1104/pp.107.103374. URL: <https://www.ncbi.nlm.nih.gov/pubmed/17660350>.
- Gillissen, B. et al. (2000). "A new family of high-affinity transporters for adenine, cytosine, and purine derivatives in Arabidopsis". In: *The Plant cell* 12.2. Journal Article Research Support, Non-U.S. Gov't Journal Article Research Support, Non-U.S. Gov't, 291–300. ISSN: 1040-4651. DOI: 10.1105/tpc.12.2.291.
- Gomez-Perez, D. et al. (2023). "Proteins released into the plant apoplast by the obligate parasitic protist *Albugo* selectively repress phyllosphere-associated bacteria". In: *New Phytol* 239.6, pp. 2320–2334. ISSN: 1469-8137 (Electronic), 0028-646X (Linking). DOI: 10.1111/nph.18995. URL: <https://www.ncbi.nlm.nih.gov/pubmed/37222268>.
- Gray, J. H. et al. (2004). "The concentrative nucleoside transporter family, SLC28". In: *Pflugers Arch* 447.5, pp. 728–34. ISSN: 0031-6768 (Print), 0031-6768 (Linking). DOI: 10.1007/s00424-003-1107-y. URL: <https://www.ncbi.nlm.nih.gov/pubmed/12856181>.
- Greiner-Tollersrud, Ole Kristian et al. (2024). "ADA2 is a lysosomal deoxyadenosine deaminase acting on DNA involved in regulating TLR9-mediated immune sensing of DNA". In: *Cell Reports* 43.11. doi: 10.1016/j.celrep.2024.114899. ISSN: 2211-1247. DOI: 10.1016/j.celrep.2024.114899. URL: <https://doi.org/10.1016/j.celrep.2024.114899>.
- Haag, Friedrich et al. (2007). "Extracellular NAD and ATP: Partners in immune cell modulation". In: *Purinergic signalling* 3.1-2. Journal Article, 71–81. ISSN: 1573-9538. DOI: 10.1007/s11302-006-9038-7.
- Harbort, Christopher J. et al. (2020). "Root-Secreted Coumarins and the Microbiota Interact to Improve Iron Nutrition in Arabidopsis". In: *Cell Host & Microbe* 28.6, 825–837.e6. ISSN: 1931-3128. DOI: 10.1016/j.chom.2020.09.006. URL: <https://doi.org/10.1016/j.chom.2020.09.006>.
- Hastings, J. et al. (2016). "ChEBI in 2016: Improved services and an expanding collection of metabolites". In: *Nucleic Acids Res* 44.D1, pp. D1214–D1219. ISSN: 0305-1048, 1362-4962. DOI: 10.1093/nar/gkv1031. URL: <https://www.ncbi.nlm.nih.gov/pubmed/26467479>.

- Hatsugai, Noriyuki et al. (2004). "A Plant Vacuolar Protease, VPE, Mediates Virus-Induced Hypersensitive Cell Death". In: *Science* 305.5685, pp. 855–858. DOI: doi:10.1126/science.1099859. URL: <https://www.science.org/doi/abs/10.1126/science.1099859>.
- Heidemann, Antje C. et al. (2005). "Extracellular application of nicotinic acid adenine dinucleotide phosphate induces Ca²⁺ signaling in astrocytes in situ". In: *The Journal of biological chemistry* 280.42. Journal Article Research Support, Non-U.S. Gov't Journal Article Research Support, Non-U.S. Gov't, 35630–35640. ISSN: 0021-9258. DOI: 10.1074/jbc.M507338200.
- Heidrich, Katharina et al. (2011). "Arabidopsis EDS1 Connects Pathogen Effector Recognition to Cell Compartment Specific Immune Responses". In: *Science* 334.6061, pp. 1401–1404. DOI: doi:10.1126/science.1211641. URL: <https://www.science.org/doi/abs/10.1126/science.1211641>.
- Hemmi, Hiroaki et al. (2000). "A Toll-like receptor recognizes bacterial DNA". In: *Nature* 408.6813, pp. 740–745. ISSN: 1476-4687. DOI: 10.1038/35047123. URL: <https://doi.org/10.1038/35047123>.
- Hiruma, K. et al. (2016). "Root Endophyte *Colletotrichum tofieldiae* Confers Plant Fitness Benefits that Are Phosphate Status Dependent". In: *Cell* 165.2, pp. 464–474. ISSN: 0092-8674. DOI: 10.1016/j.cell.2016.02.028. URL: <https://doi.org/10.1016/j.cell.2016.02.028>.
- Hogrel, G. et al. (2022). "Cyclic nucleotide-induced helical structure activates a TIR immune effector". In: *Nature* 608.7924, pp. 808–812. ISSN: 0028-0836, 1476-4687. DOI: 10.1038/s41586-022-05070-9. URL: <https://www.ncbi.nlm.nih.gov/pubmed/35948638>.
- Hong, Shiyuan et al. (2009). "Differential regulation of P2X7 receptor activation by extracellular nicotinamide adenine dinucleotide and ecto-ADP-ribosyltransferases in murine macrophages and T cells". In: *Journal of immunology (Baltimore, Md. : 1950)* 183.1. Journal Article Comparative Study Journal Article, 578–592. ISSN: 0022-1767. DOI: 10.4049/jimmunol.0900120.
- Hoorn, R. A. van der and J. D. Jones (2004). "The plant proteolytic machinery and its role in defence". In: *Curr Opin Plant Biol* 7.4. van der Hoorn, Renier A L Jones, Jonathan D G eng Research Support, Non-U.S. Gov't Review England 2004/07/03 Curr Opin Plant Biol. 2004 Aug;7(4):400-7. doi: 10.1016/j.pbi.2004.04.003., pp. 400–7. ISSN: 1369-5266 (Print) 1369-5266 (Linking). DOI: 10.1016/j.pbi.2004.04.003. URL: <https://www.ncbi.nlm.nih.gov/pubmed/15231262>.
- Horsefield, S. et al. (2019). "NAD(+) cleavage activity by animal and plant TIR domains in cell death pathways". In: *Science* 365.6455. Horsefield, Shane Burdett, Hayden Zhang, Xiaoxiao Manik, Mohammad K Shi, Yun Chen, Jian Qi, Tiancong Gilley, Jonathan Lai, Jhih-Siang Rank, Maxwell X Casey, Lachlan W Gu, Weixi Ericsson, Daniel J Foley, Gabriel Hughes, Robert O Bosanac, Todd von Itzstein, Mark Rathjen, John P Nanson, Jeffrey D Boden, Mikael Dry, Ian B Williams, Simon J Staskawicz, Brian J Coleman, Michael P Ve, Thomas Dodds, Peter N Kobe, Bostjan eng Australian Research Council/International Research Support, Non-U.S. Gov't 2019/08/24 06:00 Science. 2019 Aug 23;365(6455):793-799. doi: 10.1126/science.aax1911., pp. 793–799. ISSN: 1095-9203 (Electronic) 0036-8075 (Linking). DOI: 10.1126/science.aax1911. URL: <https://www.ncbi.nlm.nih.gov/pubmed/31439792>.
- Huang, S. et al. (2022). "Identification and receptor mechanism of TIR-catalyzed small molecules in plant immunity". In: *Science* 377.6605, eabq3297. ISSN: 1095-9203 (Electronic), 0036-8075

- (Linking). DOI: 10.1126/science.abq3297. URL: <http://www.ncbi.nlm.nih.gov/pubmed/35857645>.
- Huang, Shijia et al. (2025). “Balanced plant helper NLR activation by a modified host protein complex”. In: *Nature* 639.8054, pp. 447–455. ISSN: 1476-4687. DOI: 10.1038/s41586-024-08521-7. URL: <https://doi.org/10.1038/s41586-024-08521-7>.
- Hubert, David A. et al. (2009). “Specific Arabidopsis HSP90.2 alleles recapitulate RAR1 cochaperone function in plant NB-LRR disease resistance protein regulation”. In: *Proceedings of the National Academy of Sciences* 106.24, pp. 9556–9563. DOI: doi:10.1073/pnas.0904877106. URL: <https://www.pnas.org/doi/abs/10.1073/pnas.0904877106>.
- Hung, C. Y. et al. (2005). “A metalloproteinase of *Coccidioides posadasii* contributes to evasion of host detection”. In: *Infect Immun* 73.10, pp. 6689–6703. ISSN: 0019-9567. DOI: 10.1128/IAI.73.10.6689-6703.2005. URL: <http://www.ncbi.nlm.nih.gov/pubmed/16177346>.
- Hückelhoven, R. (2004). “BAX Inhibitor-1, an ancient cell death suppressor in animals and plants with prokaryotic relatives”. In: *Apoptosis* 9.3, pp. 299–307. ISSN: 1573-675X. DOI: 10.1023/B:APPT.0000025806.71000.1c. URL: <https://doi.org/10.1023/B:APPT.0000025806.71000.1c>.
- Jackson, E. K. et al. (2016). “Renal 2',3'-Cyclic Nucleotide 3'-Phosphodiesterase Is an Important Determinant of AKI Severity after Ischemia-Reperfusion”. In: *J Am Soc Nephrol* 27.7, pp. 2069–2081. ISSN: 1046-6673, 1533-3450. DOI: 10.1681/ASN.2015040397. URL: <http://www.ncbi.nlm.nih.gov/pubmed/26574047>.
- Jacob, P et al. (2021). “Plant “helper” immune receptors are Ca(2+)-permeable nonselective cation channels”. In: *Science* 373.6553, pp. 420–425. ISSN: 1095-9203 (Electronic), 0036-8075 (Print), 0036-8075 (Linking). DOI: 10.1126/science.abg7917. URL: <https://www.ncbi.nlm.nih.gov/pubmed/34140391>.
- Jacob, P et al. (2023). “Broader functions of TIR domains in Arabidopsis immunity”. In: *Proc Natl Acad Sci U S A* 120.11, e2220921120. ISSN: 0027-8424 (Print), 0027-8424. DOI: 10.1073/pnas.2220921120.
- Jacobs, Sophie et al. (2011). “Broad-spectrum suppression of innate immunity is required for colonization of Arabidopsis roots by the fungus *Piriformospora indica*”. In: *Plant Physiology* 156.2, pp. 726–740. ISSN: 0032-0889. DOI: 10.1104/pp.111.176446. URL: <https://doi.org/10.1104/pp.111.176446>.
- Jewell, Jeremy B. et al. (2019). “Extracellular ATP Shapes a Defense-Related Transcriptome Both Independently and along with Other Defense Signaling Pathways”. In: *Plant physiology* 179.3. Journal Article Research Support, U.S. Gov't, Non-PH.S., 1144–1158. DOI: 10.1104/pp.18.01301.
- Jewell, Jeremy B. et al. (2022). “Activation of indolic glucosinolate pathway by extracellular ATP in Arabidopsis”. In: *Plant physiology* 190.3. Journal Article Research Support, U.S. Gov't, Non-PH.S., 1574–1578. DOI: 10.1093/plphys/kiac393.
- Jewell, Jeremy B. et al. (2024). “Jasmonate Primes Plant Responses to Extracellular ATP through Purinoceptor P2K1”. In: *bioRxiv*, p. 2024.11.07.622526. DOI: 10.1101/2024.11.07.622526. URL: <https://www.biorxiv.org/content/biorxiv/early/2024/11/08/2024.11.07.622526.full.pdf>.

- Jia, A. et al. (2022). "TIR-catalyzed ADP-ribosylation reactions produce signaling molecules for plant immunity". In: *Science* 377.6605, eabq8180. ISSN: 1095-9203 (Electronic), 0036-8075 (Linking). DOI: 10.1126/science.abq8180. URL: <http://www.ncbi.nlm.nih.gov/pubmed/35857644>.
- Johannndrees, O. et al. (2023). "Variation in plant Toll/Interleukin-1 receptor domain protein dependence on ENHANCED DISEASE SUSCEPTIBILITY 1". In: *Plant Physiol* 191.1, pp. 626–642. ISSN: 0032-0889, 1532-2548. DOI: 10.1093/plphys/kiac480. URL: <https://www.ncbi.nlm.nih.gov/pubmed/36227084>.
- Jones, J. D. and J. L. Dangl (2006). "The plant immune system". In: *Nature* 444.7117. Jones, Jonathan D G Dangl, Jeffery L eng Research Support, N.I.H., Extramural Research Support, Non-U.S. Gov't Research Support, U.S. Gov't, Non-P.H.S. Review England 2006/11/17 09:00 Nature. 2006 Nov 16;444(7117):323-9., pp. 323–9. ISSN: 1476-4687 (Electronic) 0028-0836 (Linking). DOI: 10.1038/nature05286. URL: <http://www.ncbi.nlm.nih.gov/pubmed/17108957>.
- Judkins, Courtney P et al. (2006). "NADPH-induced contractions of mouse aorta do not involve NADPH oxidase: a role for P2X receptors". In: *The Journal of pharmacology and experimental therapeutics* 317.2. Journal Article Research Support, Non-U.S. Gov't Journal Article Research Support, Non-U.S. Gov't, 644–650. ISSN: 0022-3565. DOI: 10.1124/jpet.105.096610.
- Jung, Benjamin et al. (2011). "Arabidopsis nucleoside hydrolases involved in intracellular and extracellular degradation of purines". In: *The Plant journal : for cell and molecular biology* 65.5. Journal Article Research Support, Non-U.S. Gov't Journal Article Research Support, Non-U.S. Gov't, 703–711. ISSN: 0960-7412. DOI: 10.1111/j.1365-313X.2010.04455.x.
- Kawai, Taro et al. (2024). "Decoding Toll-like receptors: Recent insights and perspectives in innate immunity". In: *Immunity* 57.4. doi: 10.1016/j.immuni.2024.03.004, pp. 649–673. ISSN: 1074-7613. DOI: 10.1016/j.immuni.2024.03.004. URL: <https://doi.org/10.1016/j.immuni.2024.03.004>.
- Kesten, Christopher et al. (2019). "Pathogen-induced pH changes regulate the growth-defense balance in plants". In: *The EMBO journal* 38.24. Journal Article Research Support, Non-U.S. Gov't The authors declare that they have no conflict of interest., e101822. DOI: 10.15252/embj.2019101822.
- Kesten, Christopher et al. (2023). "Soil-borne fungi alter the apoplastic purinergic signaling in plants by deregulating the homeostasis of extracellular ATP and its metabolite adenosine". In: *eLife* 12. Journal Article CK, VL, SD, JS, JD, CZ, CD, CS No competing interests declared. DOI: 10.7554/eLife.92913.
- Kilian, Joachim et al. (2007). "The AtGenExpress global stress expression data set: protocols, evaluation and model data analysis of UV-B light, drought and cold stress responses". In: *The Plant Journal* 50.2, pp. 347–363. ISSN: 0960-7412. DOI: <https://doi.org/10.1111/j.1365-313X.2007.03052.x>. URL: <https://onlinelibrary.wiley.com/doi/abs/10.1111/j.1365-313X.2007.03052.x><https://onlinelibrary.wiley.com/doi/10.1111/j.1365-313X.2007.03052.x>.

- Kim, Sung-Yong et al. (2006). “Extracellular ATP in plants. Visualization, localization, and analysis of physiological significance in growth and signaling”. In: *Plant physiology* 142.3. Journal Article Research Support, U.S. Gov’t, Non-PH.S., 984–992. DOI: 10.1104/pp.106.085670.
- Kim, T. H. et al. (2012). “Natural variation in small molecule-induced TIR-NB-LRR signaling induces root growth arrest via EDS1- and PAD4-complexed R protein VICTR in Arabidopsis”. In: *Plant Cell* 24.12, pp. 5177–92. ISSN: 1532-298X (Electronic), 1040-4651 (Print), 1040-4651 (Linking). DOI: 10.1105/tpc.112.107235. URL: <https://www.ncbi.nlm.nih.gov/pubmed/23275581>.
- King, Anne E. et al. (2006). “Nucleoside transporters: from scavengers to novel therapeutic targets”. In: *Trends in Pharmacological Sciences* 27.8. Journal Article Research Support, Non-U.S. Gov’t Review, 416–425. ISSN: 0165-6147. DOI: 10.1016/j.tips.2006.06.004. URL: [https://www.cell.com/ajhg/fulltext/S0165-6147\(06\)00152-0](https://www.cell.com/ajhg/fulltext/S0165-6147(06)00152-0).
- Kochanek, Patrick M. et al. (2013). “The Many Roles of Adenosine in Traumatic Brain Injury”. In: *Adenosine: A Key Link between Metabolism and Brain Activity*. Ed. by Susan Masino and Detlev Boison. New York, NY: Springer New York, pp. 307–322. ISBN: 978-1-4614-3903-5. DOI: 10.1007/978-1-4614-3903-5_15. URL: https://doi.org/10.1007/978-1-4614-3903-5_15.
- Kong, G. et al. (2015). “The Activation of Phytophthora Effector Avr3b by Plant Cyclophilin is Required for the Nudix Hydrolase Activity of Avr3b”. In: *PLoS Pathog* 11.8. Kong, Guanghui Zhao, Yao Jing, Maofeng Huang, Jie Yang, Jin Xia, Ye qiang Kong, Liang Ye, Wenwu Xiong, Qin Qiao, Yongli Dong, Suomeng Ma, Wenbo Wang, Yuanchao eng Research Support, Non-U.S. Gov’t 2015/09/01 PLoS Pathog. 2015 Aug 28;11(8):e1005139. doi: 10.1371/journal.ppat.1005139. eCollection 2015 Aug., e1005139. ISSN: 1553-7374 (Electronic) 1553-7366 (Print) 1553-7366 (Linking). DOI: 10.1371/journal.ppat.1005139. URL: <https://www.ncbi.nlm.nih.gov/pubmed/26317500>.
- Kosmacz, M. et al. (2018). “Interaction of 2’,3’-cAMP with Rbp47b Plays a Role in Stress Granule Formation”. In: *Plant Physiol* 177.1, pp. 411–421. ISSN: 1532-2548 (Electronic), 0032-0889 (Print), 0032-0889 (Linking). DOI: 10.1104/pp.18.00285. URL: <https://www.ncbi.nlm.nih.gov/pubmed/29618637>.
- Kourelis, Giorgos and Renier A.L. van der Hoorn (2018). “Defended to the Nines: 25 Years of Resistance Gene Cloning Identifies Nine Mechanisms for R Protein Function”. In: *The Plant Cell* 30.2, pp. 285–299. ISSN: 1040-4651. DOI: 10.1105/tpc.17.00579. URL: <https://doi.org/10.1105/tpc.17.00579>.
- Lahrman, Urs et al. (2013). “Host-related metabolic cues affect colonization strategies of a root endophyte”. In: *Proceedings of the National Academy of Sciences of the United States of America* 110.34, pp. 13965–13970. ISSN: 0027-8424. DOI: 10.1073/pnas.1301653110. URL: <http://www.ncbi.nlm.nih.gov/pmc/articles/PMC3752250/pdf/pnas.201301653.pdf>.
- Lahrman, Urs et al. (2015). “Mutualistic root endophytism is not associated with the reduction of saprotrophic traits and requires a noncompromised plant innate immunity”. In: *New Phytologist* 207.3, pp. 841–857. ISSN: 0028-646X;1469-8137. DOI: 10.1111/nph.13411. URL: <http://onlinelibrary.wiley.com/store/10.1111/nph.13411/asset/nph13411.pdf?v=1&t=ijx5dp5a&s=75b1e4bb8c99877a3e11fbcd9063962a0540ab3e>.

- Lamkanfi, Mohamed and Vishva M. Dixit (2010). "Manipulation of Host Cell Death Pathways during Microbial Infections". In: *Cell Host Microbe* 8.1. doi: 10.1016/j.chom.2010.06.007, pp. 44–54. ISSN: 1931-3128. DOI: 10.1016/j.chom.2010.06.007. URL: <https://doi.org/10.1016/j.chom.2010.06.007>.
- Lamo, Francisco J. de and Frank L. W. Takken (2020). "Biocontrol by *Fusarium oxysporum* Using Endophyte-Mediated Resistance". In: *Frontiers in Plant Science* 11. ISSN: 1664-462X. DOI: 10.3389/fpls.2020.00037. URL: <https://www.frontiersin.org/journals/plant-science/articles/10.3389/fpls.2020.00037>.
- Lawson, A. W. et al. (2025). "The barley MLA13-AVR(A13) heterodimer reveals principles for immunoreceptor recognition of RNase-like powdery mildew effectors". In: *EMBO J.* Lawson, Aaron W Flores-Ibarra, Andrea Cao, Yu An, Chunpeng Neumann, Ulla Gunkel, Monika Saur, Isabel M L Chai, Jijie Behrmann, Elmar Schulze-Lefert, Paul eng SFB-1403 - 414786233 B08/Deutsche Forschungsgemeinschaft (DFG)/ INST 216/949-1 FUGG/Deutsche Forschungsgemeinschaft (DFG)/ INST 216/512/1 FUGG/Deutsche Forschungsgemeinschaft (DFG)/ EXC-2048/1/Germany's Excellence Strategy CEPLAS/ iHEAD/Ministry of Culture and Science of the State of Rhine-Westphalia North/ SA 4093/1-1/DFG Emmy Noeter Programme/ England 2025/02/14 EMBO J. 2025 Feb 13. doi: 10.1038/s44318-025-00373-9. ISSN: 1460-2075 (Electronic) 0261-4189 (Linking). DOI: 10.1038/s44318-025-00373-9. URL: <https://www.ncbi.nlm.nih.gov/pubmed/39948409>.
- Lazarowski, Eduardo R. et al. (2011). "Molecular mechanisms of purine and pyrimidine nucleotide release". In: *Advances in pharmacology (San Diego, Calif.)* 61. Journal Article Research Support, N.I.H., Extramural Review, 221–261. DOI: 10.1016/b978-0-12-385526-8.00008-4.
- Leavitt, A. et al. (2022). "Viruses inhibit TIR gcADPR signalling to overcome bacterial defence". In: *Nature* 611.7935, pp. 326–331. ISSN: 0028-0836, 1476-4687. DOI: 10.1038/s41586-022-05375-9. URL: <https://www.ncbi.nlm.nih.gov/pubmed/36174646>.
- Lee, So Yeong and Scott M. O'Grady (2003). "Modulation of ion channel function by P2Y receptors". In: *Cell biochemistry and biophysics* 39.1. Journal Article Review Journal Article Review, 75–88. ISSN: 1085-9195. DOI: 10.1385/cbb:39:1:75.
- Lemaitre, Bruno et al. (1996). "The Dorsoventral Regulatory Gene Cassette *spätzle/Toll/cactus* Controls the Potent Antifungal Response in *Drosophila* Adults". In: *Cell* 86.6, pp. 973–983. ISSN: 0092-8674. DOI: 10.1016/S0092-8674(00)80172-5. URL: [https://doi.org/10.1016/S0092-8674\(00\)80172-5](https://doi.org/10.1016/S0092-8674(00)80172-5).
- Leng, Yueqiang et al. (2025). "A barley MLA immune receptor is activated by a fungal nonribosomal peptide effector for disease susceptibility". In: *New Phytologist* 245.3, pp. 1197–1215. ISSN: 0028-646X. DOI: <https://doi.org/10.1111/nph.20289>. URL: <https://nph.onlinelibrary.wiley.com/doi/abs/10.1111/nph.20289>.
- Li, G. et al. (2003). "Equilibrative nucleoside transporters of *Arabidopsis thaliana*. cDNA cloning, expression pattern, and analysis of transport activities". In: *J Biol Chem* 278.37, pp. 35732–42. ISSN: 0021-9258 (Print), 0021-9258. DOI: 10.1074/jbc.M304768200.
- Li, Qi et al. (2023a). "N-hydroxypipicolinic acid triggers systemic acquired resistance through extracellular NAD(P)". In: *Nature Communications* 14.1, p. 6848. ISSN: 2041-1723. DOI: 10.1038/s41467-023-42629-0. URL: <https://doi.org/10.1038/s41467-023-42629-0>.

- Li, Yini et al. (2017). “Mechanistic insights into caspase-9 activation by the structure of the apoptosome holoenzyme”. In: *Proceedings of the National Academy of Sciences* 114.7, pp. 1542–1547. DOI: doi:10.1073/pnas.1620626114. URL: <https://www.pnas.org/doi/abs/10.1073/pnas.1620626114>.
- Li, Yuejiao et al. (2023b). “Comparative metabolomic profiling reveals molecular mechanisms underlying growth promotion and disease resistance in wheat conferred by *Piriformospora indica* in the field”. In: *Plant Signaling Behavior* 18.1. doi: 10.1080/15592324.2023.2213934, p. 2213934. ISSN: null. DOI: 10.1080/15592324.2023.2213934. URL: <https://doi.org/10.1080/15592324.2023.2213934>.
- Livak, K. J. and T. D. Schmittgen (2001). “Analysis of relative gene expression data using real-time quantitative PCR and the $2^{-\Delta\Delta C_T}$ method”. In: *Methods* 25.4, pp. 402–408. ISSN: 1046-2023. DOI: 10.1006/meth.2001.1262. URL: <https://doi.org/10.1006/meth.2001.1262>.
- Lo Presti, Libera et al. (2015). “Fungal Effectors and Plant Susceptibility”. In: *Annual Review of Plant Biology*, Vol 66. Vol. 66, pp. 513–545. ISBN: 1543-5008;978-0-8243-0666-3. DOI: 10.1146/annurev-arplant-043014-114623. URL: <http://www.annualreviews.org/doi/pdf/10.1146/annurev-arplant-043014-114623>.
- Lockshin, Richard A. and Carroll M. Williams (1964). “Programmed cell death—II. Endocrine potentiation of the breakdown of the intersegmental muscles of silkmooths”. In: *Journal of Insect Physiology* 10.4, pp. 643–649. ISSN: 0022-1910. DOI: [https://doi.org/10.1016/0022-1910\(64\)90034-4](https://doi.org/10.1016/0022-1910(64)90034-4). URL: <https://www.sciencedirect.com/science/article/pii/0022191064900344>.
- Lohman, Alexander W. et al. (2012). “Mechanisms of ATP release and signalling in the blood vessel wall”. In: *Cardiovascular research* 95.3. Journal Article Research Support, N.I.H., Extramural Research Support, Non-U.S. Gov’t Review Journal Article Research Support, N.I.H., Extramural Research Support, Non-U.S. Gov’t Review, 269–280. DOI: 10.1093/cvr/cvs187.
- Lolle, S. et al. (2020). “Plant NLR-triggered immunity: from receptor activation to downstream signaling”. In: *Curr Opin Immunol* 62, pp. 99–105. ISSN: 0952-7915, 1879-0372. DOI: 10.1016/j.coi.2019.12.007. URL: <https://www.ncbi.nlm.nih.gov/pubmed/31958770>.
- Loon, L. C. van et al. (2006). “Significance of inducible defense-related proteins in infected plants”. In: *Annu Rev Phytopathol* 44. van Loon, L C Rep, M Pieterse, C M J eng Review 2006/04/11 Annu Rev Phytopathol. 2006;44:135-62. doi: 10.1146/annurev.phyto.44.070505.143425., pp. 135–62. ISSN: 0066-4286 (Print) 0066-4286 (Linking). DOI: 10.1146/annurev.phyto.44.070505.143425. URL: <https://www.ncbi.nlm.nih.gov/pubmed/16602946>.
- Lorang, J. M. et al. (2007). “Plant disease susceptibility conferred by a "resistance" gene”. In: *Proc Natl Acad Sci U S A* 104.37, pp. 14861–6. ISSN: 0027-8424 (Print), 1091-6490 (Electronic), 0027-8424 (Linking). DOI: 10.1073/pnas.0702572104. URL: <https://www.ncbi.nlm.nih.gov/pubmed/17804803>.
- Lu, Chongchong et al. (2023). “Discovery of a novel nucleoside immune signaling molecule 2'-deoxyguanosine in microbes and plants”. In: *Journal of advanced research* 46. Journal Article Research Support, Non-U.S. Gov’t Declaration of Competing Interest The authors declare that they have no known competing financial interests or personal relationships that could have

- appeared to influence the work reported in this paper., 1–15. DOI: 10.1016/j.jare.2022.06.014.
- Ludwig, N. et al. (2021). “A cell surface-exposed protein complex with an essential virulence function in *Ustilago maydis*”. In: *Nat Microbiol* 6.6, pp. 722–730. ISSN: 2058-5276 (Electronic), 2058-5276 (Linking). DOI: 10.1038/s41564-021-00896-x. URL: <https://www.ncbi.nlm.nih.gov/pubmed/33941900>.
- Lukan, Tjaša et al. (2020). “Precision transcriptomics of viral foci reveals the spatial regulation of immune-signaling genes and identifies RBOHD as an important player in the incompatible interaction between potato virus Y and potato”. In: *The Plant Journal* 104.3, pp. 645–661. ISSN: 0960-7412. DOI: <https://doi.org/10.1111/tpj.14953>. URL: <https://onlinelibrary.wiley.com/doi/abs/10.1111/tpj.14953>.
- López, Miguel et al. (2008). “Trehalose and trehalase in root nodules of *Medicago truncatula* and *Phaseolus vulgaris* in response to salt stress”. In: *Physiologia Plantarum* 134.4, pp. 575–582. ISSN: 0031-9317. DOI: <https://doi.org/10.1111/j.1399-3054.2008.01162.x>. URL: <https://onlinelibrary.wiley.com/doi/abs/10.1111/j.1399-3054.2008.01162.x>.
- Ma, S. et al. (2020). “Direct pathogen-induced assembly of an NLR immune receptor complex to form a holoenzyme”. In: *Science* 370.6521. Ma, Shoucai Lapin, Dmitry Liu, Li Sun, Yue Song, Wen Zhang, Xiaoxiao Logemann, Elke Yu, Dongli Wang, Jia Jirschitzka, Jan Han, Zhifu Schulze-Lefert, Paul Parker, Jane E Chai, Jijie eng Research Support, Non-U.S. Gov’t 2020/12/05 Science. 2020 Dec 4;370(6521):eabe3069. doi: 10.1126/science.abe3069. ISSN: 1095-9203 (Electronic) 0036-8075 (Linking). DOI: 10.1126/science.abe3069. URL: <https://www.ncbi.nlm.nih.gov/pubmed/33273071>.
- Macharia, Mercy et al. (2020). “iTRAQ-based quantitative proteomics reveals a ferroptosis-like programmed cell death in plants infected by a highly virulent tobacco mosaic virus mutant 24A+UPD”. In: *Phytopathology Research* 2.1, p. 1. ISSN: 2524-4167. DOI: 10.1186/s42483-019-0043-5. URL: <https://doi.org/10.1186/s42483-019-0043-5>.
- Macho, A. P and C. Zipfel (2015). “Targeting of plant pattern recognition receptor-triggered immunity by bacterial type-III secretion system effectors”. In: *Curr Opin Microbiol* 23, pp. 14–22. ISSN: 1879-0364 (Electronic), 1369-5274 (Linking). DOI: 10.1016/j.mib.2014.10.009. URL: <https://www.ncbi.nlm.nih.gov/pubmed/25461568>.
- Maekawa, Takaki et al. (2023). “Dying in self-defence: a comparative overview of immunogenic cell death signalling in animals and plants”. In: *Cell Death Differentiation* 30.2, pp. 258–268. ISSN: 1476-5403. DOI: 10.1038/s41418-022-01060-6. URL: <https://doi.org/10.1038/s41418-022-01060-6>.
- Mahdi, L. K. et al. (2020). “Discovery of a Family of Mixed Lineage Kinase Domain-like Proteins in Plants and Their Role in Innate Immune Signaling”. In: *Cell Host Microbe* 28.6, 813–824 e6. ISSN: 1934-6069 (Electronic), 1931-3128 (Linking). DOI: 10.1016/j.chom.2020.08.012. URL: <https://www.ncbi.nlm.nih.gov/pubmed/33053377>.
- Mahdi, Lisa K. et al. (2021). “The fungal root endophyte *Serendipita vermifera* displays inter-kingdom synergistic beneficial effects with the microbiota in *Arabidopsis thaliana* and barley”. In: *The ISME Journal*. ISSN: 1751-7370. DOI: 10.1038/s41396-021-01138-y. URL: <https://doi.org/10.1038/s41396-021-01138-y>.

- Martin, R. et al. (2020). "Structure of the activated ROQ1 resistosome directly recognizing the pathogen effector XopQ". In: *Science* 370.6521. ISSN: 0036-8075, 1095-9203. DOI: 10.1126/science.abd9993. URL: <https://www.ncbi.nlm.nih.gov/pubmed/33273074>.
- Matsuoka, I. and S. Ohkubo (2004). "ATP- and adenosine-mediated signaling in the central nervous system: Adenosine receptor activation by ATP through rapid and localized generation of adenosine by ecto-nucleotidases". In: *Journal of Pharmacological Sciences* 94.2, pp. 95–99. ISSN: 1347-8613. DOI: 10.1254/jphs.94.95. URL: <https://doi.org/10.1254/jphs.94.95>.
- McCombe, Carl L. et al. (2025). "Plant pathogenic fungi hijack phosphate signaling with conserved enzymatic effectors". In: *Science* 387.6737, pp. 955–962. DOI: doi: 10.1126/science.ad15764. URL: <https://www.science.org/doi/abs/10.1126/science.ad15764>.
- Medzhitov, Ruslan et al. (1997). "A human homologue of the Drosophila Toll protein signals activation of adaptive immunity". In: *Nature* 388.6640, pp. 394–397. ISSN: 1476-4687. DOI: 10.1038/41131. URL: <https://doi.org/10.1038/41131>.
- Meyers, B. C. et al. (2002). "TIR-X and TIR-NBS proteins: two new families related to disease resistance TIR-NBS-LRR proteins encoded in Arabidopsis and other plant genomes". In: *Plant J* 32.1. Meyers, Blake C Morgante, Michele Michelmore, Richard W eng Research Support, U.S. Gov't, Non-PH.S. England 2002/10/09 Plant J. 2002 Oct;32(1):77-92. doi: 10.1046/j.1365-313x.2002.01404.x., pp. 77–92. ISSN: 0960-7412 (Print) 0960-7412 (Linking). DOI: 10.1046/j.1365-313x.2002.01404.x. URL: <https://www.ncbi.nlm.nih.gov/pubmed/12366802>.
- Mishra, Abhay P et al. (2018). "Programmed Cell Death, from a Cancer Perspective: An Overview". In: *Molecular Diagnosis Therapy* 22.3, pp. 281–295. ISSN: 1179-2000. DOI: 10.1007/s40291-018-0329-9. URL: <https://doi.org/10.1007/s40291-018-0329-9>.
- Mitsuhara, Ichiro et al. (1999). "Animal cell-death suppressors Bcl-x_L and Ced-9 inhibit cell death in tobacco plants". In: *Current Biology* 9.14. doi: 10.1016/S0960-9822(99)80341-8, S1. ISSN: 0960-9822. DOI: 10.1016/S0960-9822(99)80341-8. URL: [https://doi.org/10.1016/S0960-9822\(99\)80341-8](https://doi.org/10.1016/S0960-9822(99)80341-8).
- Mittal, Ekansh et al. (2018). "Mycobacterium tuberculosis Type VII Secretion System Effectors Differentially Impact the ESCRT Endomembrane Damage Response". In: *mBio* 9.6, 10.1128/mbio.01765-18. DOI: doi: 10.1128/mbio.01765-18. URL: <https://journals.asm.org/doi/abs/10.1128/mbio.01765-18>.
- Mohr, Toni J. et al. (2010). "The Arabidopsis Downy Mildew Resistance Gene RPP8 Is Induced by Pathogens and Salicylic Acid and Is Regulated by W Box cis Elements". In: *Molecular Plant-Microbe Interactions*® 23.10, pp. 1303–1315. DOI: 10.1094/mpmi-01-10-0022. URL: <https://apsjournals.apsnet.org/doi/abs/10.1094/MPMI-01-10-0022>.
- Morehouse, B. R. et al. (2022). "Cryo-EM structure of an active bacterial TIR-STING filament complex". In: *Nature* 608.7924, pp. 803–807. ISSN: 1476-4687 (Electronic), 0028-0836 (Print), 0028-0836 (Linking). DOI: 10.1038/s41586-022-04999-1. URL: <https://www.ncbi.nlm.nih.gov/pubmed/35859168>.
- Morel, J. B. and J. L. Dangel (1997). "The hypersensitive response and the induction of cell death in plants". In: *Cell Death Differ* 4.8. Morel, J B Dangel, J L eng England 2006/02/09 Cell Death Differ. 1997 Dec;4(8):671-83. doi: 10.1038/sj.cdd.4400309., pp. 671–83. ISSN: 1350-9047 (Print)

- 1350-9047 (Linking). DOI: 10.1038/sj.cdd.4400309. URL: <https://www.ncbi.nlm.nih.gov/pubmed/16465279>.
- Moreschi, Iliana et al. (2006). “Extracellular NAD⁺ Is an Agonist of the Human P2Y₁₁ Purinergic Receptor in Human Granulocytes”. In: *J Biol Chem* 281.42, pp. 31419–31429. ISSN: 0021-9258. DOI: 10.1016/s0021-9258(19)84054-1.
- Mucha, J. et al. (2014). “Strategies utilized by trophically diverse fungal species for *Pinus sylvestris* root colonization”. In: *Tree Physiol* 34.1, pp. 73–86. ISSN: 0829-318X. DOI: 10.1093/treephys/tpt111. URL: <https://www.ncbi.nlm.nih.gov/pubmed/24319062>.
- Myrach, T. et al. (2017). “The assembly of the plant urease activation complex and the essential role of the urease accessory protein G (UreG) in delivery of nickel to urease”. In: *J Biol Chem* 292.35, pp. 14556–14565. ISSN: 1083-351X (Electronic), 0021-9258 (Linking). DOI: 10.1074/jbc.M117.780403. URL: <https://www.ncbi.nlm.nih.gov/pubmed/28710280>.
- Navarre, D. A. and T. J. Wolpert (1999). “Victorin induction of an apoptotic/senescence-like response in oats”. In: *The Plant Cell* 11.2, pp. 237–249. ISSN: 1040-4651. DOI: 10.1105/tpc.11.2.237. URL: <https://doi.org/10.1105/tpc.11.2.237>.
- Navazio, Lorella et al. (2001). “Mobilization of Ca²⁺ by Cyclic ADP-Ribose from the Endoplasmic Reticulum of Cauliflower Florets¹”. In: *Plant Physiology* 125.4, pp. 2129–2138. ISSN: 0032-0889. DOI: 10.1104/pp.125.4.2129. URL: <https://doi.org/10.1104/pp.125.4.2129>.
- Ngou, B. P. M. et al. (2021). “Mutual potentiation of plant immunity by cell-surface and intracellular receptors”. In: *Nature* 592.7852, pp. 110–115. ISSN: 0028-0836, 1476-4687. DOI: 10.1038/s41586-021-03315-7. URL: <https://www.ncbi.nlm.nih.gov/pubmed/33692545>.
- Nishimura, Marc T. et al. (2017). “TIR-only protein RBA1 recognizes a pathogen effector to regulate cell death in Arabidopsis”. In: *Proceedings of the National Academy of Sciences* 114.10, E2053–E2062. DOI: doi:10.1073/pnas.1620973114. URL: <https://www.pnas.org/doi/abs/10.1073/pnas.1620973114>.
- Nizam, Shadab et al. (2019). “Serendipita indica E5^{NT} modulates extracellular nucleotide levels in the plant apoplast and affects fungal colonization”. In: *EMBO reports* 20.2. Journal Article Research Support, Non-U.S. Gov't. DOI: 10.15252/embr.201847430.
- Nostadt, R. et al. (2020). “A secreted fungal histidine- and alanine-rich protein regulates metal ion homeostasis and oxidative stress”. In: *New Phytol*. Nostadt, Robin Hilbert, Magdalena Nizam, Shadab Rovenich, Hanna Wawra, Stephan Martin, Jorg Kupper, Hendrik Mijovilovich, Ana Ursinus, Astrid Langen, Gregor Hartmann, Marcus D Lupas, Andrei N Zuccaro, Alga eng England 2020/04/15 06:00 New Phytol. 2020 Apr 13. doi: 10.1111/nph.16606. ISSN: 1469-8137 (Electronic) 0028-646X (Linking). DOI: 10.1111/nph.16606. URL: <https://www.ncbi.nlm.nih.gov/pubmed/32285459>.
- Ofir, G. et al. (2021). “Antiviral activity of bacterial TIR domains via immune signalling molecules”. In: *Nature* 600.7887, pp. 116–120. ISSN: 0028-0836, 1476-4687. DOI: 10.1038/s41586-021-04098-7. URL: <https://www.ncbi.nlm.nih.gov/pubmed/34853457>.
- Ogasawara, Y. et al. (2008). “Synergistic activation of the Arabidopsis NADPH oxidase AtrbohD by Ca²⁺ and phosphorylation”. In: *J Biol Chem* 283.14, pp. 8885–92. ISSN: 0021-9258 (Print), 0021-9258 (Linking). DOI: 10.1074/jbc.M708106200. URL: <https://www.ncbi.nlm.nih.gov/pubmed/18218618>.

- Ohta, A. and M. Sitkovsky (2001). "Role of G-protein-coupled adenosine receptors in downregulation of inflammation and protection from tissue damage". In: *Nature* 414.6866, pp. 916–920. ISSN: 0028-0836. DOI: 10.1038/414916a. URL: <https://www.ncbi.nlm.nih.gov/pubmed/11780065>.
- Olvera-Carrillo, Y. et al. (2015). "A Conserved Core of Programmed Cell Death Indicator Genes Discriminates Developmentally and Environmentally Induced Programmed Cell Death in Plants". In: *Plant Physiol* 169.4, pp. 2684–99. ISSN: 1532-2548 (Electronic), 0032-0889 (Linking). DOI: 10.1104/pp.15.00769. URL: <https://www.ncbi.nlm.nih.gov/pubmed/26438786>.
- Ordon, Jana et al. (2023). "Targeted gene deletion with SpCas9 and multiple guide RNAs in *Arabidopsis thaliana*: four are better than two". In: *Plant Methods* 19.1, p. 30. ISSN: 1746-4811. DOI: 10.1186/s13007-023-01010-4. URL: <https://doi.org/10.1186/s13007-023-01010-4>.
- Pajuelo, David et al. (2021). "Toxin secretion and trafficking by *Mycobacterium tuberculosis*". In: *Nature Communications* 12.1, p. 6592. ISSN: 2041-1723. DOI: 10.1038/s41467-021-26925-1. URL: <https://doi.org/10.1038/s41467-021-26925-1>.
- Peškan-Berghöfer, Tatjana et al. (2004). "Association of *Piriformospora indica* with *Arabidopsis thaliana* roots represents a novel system to study beneficial plant-microbe interactions and involves early plant protein modifications in the endoplasmic reticulum and at the plasma membrane". In: *Physiol Plant* 122.4, pp. 465–477. ISSN: 0031-9317. DOI: 10.1111/j.1399-3054.2004.00424.x. URL: <https://onlinelibrary.wiley.com/doi/abs/10.1111/j.1399-3054.2004.00424.x>.
- Plett, J. M. et al. (2014). "Effector MiSSP7 of the mutualistic fungus *Laccaria bicolor* stabilizes the *Populus* JAZ6 protein and represses jasmonic acid (JA) responsive genes". In: *Proc Natl Acad Sci U S A* 111.22, pp. 8299–304. ISSN: 1091-6490 (Electronic), 0027-8424 (Linking). DOI: 10.1073/pnas.1322671111. URL: <http://www.ncbi.nlm.nih.gov/pubmed/24847068>.
- Plijev, Boris K. et al. (2014). "Extracellular NAD(+) inhibits human neutrophil apoptosis". In: *Apoptosis : an international journal on programmed cell death* 19.4. Journal Article Research Support, Non-U.S. Gov't, 581–593. DOI: 10.1007/s10495-013-0948-x.
- Qi, Tiancong et al. (2018). "NRG1 functions downstream of EDS1 to regulate TIR-NLR-mediated plant immunity in *Nicotiana benthamiana*". In: *Proceedings of the National Academy of Sciences* 115.46, E10979–E10987. DOI: doi:10.1073/pnas.1814856115. URL: <https://www.pnas.org/doi/abs/10.1073/pnas.1814856115>.
- Qiang, X. et al. (2012). "The mutualistic fungus *Piriformospora indica* colonizes *Arabidopsis* roots by inducing an endoplasmic reticulum stress-triggered caspase-dependent cell death". In: *Plant Cell* 24.2, pp. 794–809. ISSN: 1532-298X (Electronic), 1040-4651 (Linking). DOI: 10.1105/tpc.111.093260. URL: <http://www.ncbi.nlm.nih.gov/pubmed/22337916>.
- Rafiqi, M. et al. (2013). "Effector candidates in the secretome of *Piriformospora indica*, a ubiquitous plant-associated fungus". In: *Front Plant Sci* 4. Rafiqi, Maryam Jelonek, Lukas Akum, Ndifor F Zhang, Feng Kogel, Karl-Heinz eng Switzerland 2013/07/23 06:00 Front Plant Sci. 2013 Jul 11;4:228. doi: 10.3389/fpls.2013.00228. eCollection 2013., p. 228. ISSN: 1664-462X (Electronic) 1664-462X (Linking). DOI: 10.3389/fpls.2013.00228. URL: <http://www.ncbi.nlm.nih.gov/pubmed/23874344>.

- Ragnelli, A. M. et al. (2014). “The cell death phenomenon during Tuber ectomycorrhiza morphogenesis”. In: *Plant Biosystems - An International Journal Dealing with all Aspects of Plant Biology* 148.3, pp. 473–482. ISSN: 1126-3504. DOI: 10.1080/11263504.2013.788575. URL: <https://doi.org/10.1080/11263504.2013.788575>.
- Ray, J. G. and N. Valsalakumar (2010). “ARBUSCULAR MYCORRHIZAL FUNGI AND PIRIFORMOSPORA INDICA INDIVIDUALLY AND IN COMBINATION WITH RHIZOBIUM ON GREEN GRAM”. In: *Journal of Plant Nutrition* 33.2. doi: 10.1080/01904160903435409, pp. 285–298. ISSN: 0190-4167. DOI: 10.1080/01904160903435409. URL: <https://doi.org/10.1080/01904160903435409>.
- Ren, J. et al. (2009). “Identification and quantification of 2',3'-cAMP release by the kidney”. In: *J Pharmacol Exp Ther* 328.3, pp. 855–865. ISSN: 0022-3565, 1521-0103. DOI: 10.1124/jpet.108.146712. URL: <https://www.ncbi.nlm.nih.gov/pubmed/19033554>.
- Rensburg, Henry Janse van et al. (2025). “A TNL receptor mediates microbiome feedbacks in Arabidopsis”. In: *bioRxiv*, p. 2025.02.25.640125. DOI: 10.1101/2025.02.25.640125. URL: <https://www.biorxiv.org/content/biorxiv/early/2025/02/25/2025.02.25.640125.full.pdf>.
- Rieder, Benjamin and H. Ekkehard Neuhaus (2011). “Identification of an Arabidopsis plasma membrane-located ATP transporter important for anther development”. In: *The Plant cell* 23.5. Journal Article Research Support, Non-U.S. Gov't Journal Article Research Support, Non-U.S. Gov't, 1932–1944. ISSN: 1040-4651. DOI: 10.1105/tpc.111.084574.
- Roberts, J. S. et al. (2017). “Opportunistic pathogen *Porphyromonas gingivalis* modulates danger signal ATP-mediated antibacterial NOX2 pathways in primary epithelial cells”. In: *Front Cell Infect Microbiol* 7, p. 291. ISSN: 2235-2988. DOI: 10.3389/fcimb.2017.00291. URL: <https://www.ncbi.nlm.nih.gov/pubmed/28725637>.
- Salguero-Linares, Jose et al. (2022). “Robust transcriptional indicators of immune cell death revealed by spatiotemporal transcriptome analyses”. In: *Mol Plant* 15.6, pp. 1059–1075. ISSN: 1674-2052. DOI: 10.1016/j.molp.2022.04.010. URL: <https://doi.org/10.1016/j.molp.2022.04.010>.
- Saur, I. M. L. et al. (2021). “NOD-like receptor-mediated plant immunity: from structure to cell death”. In: *Nat Rev Immunol* 21.5, pp. 305–318. ISSN: 1474-1741 (Electronic), 1474-1733 (Linking). DOI: 10.1038/s41577-020-00473-z. URL: <https://www.ncbi.nlm.nih.gov/pubmed/33293618>.
- Savary, Serge et al. (2019). “The global burden of pathogens and pests on major food crops”. In: *Nature Ecology Evolution* 3.3, pp. 430–439. ISSN: 2397-334X. DOI: 10.1038/s41559-018-0793-y. URL: <https://doi.org/10.1038/s41559-018-0793-y>.
- Schäfer, Patrick et al. (2009). “Manipulation of plant innate immunity and gibberellin as factor of compatibility in the mutualistic association of barley roots with Piriformospora indica”. In: *The Plant Journal* 59.3, pp. 461–474. ISSN: 0960-7412. DOI: 10.1111/j.1365-313X.2009.03887.x. URL: <https://doi.org/10.1111/j.1365-313X.2009.03887.x>.
- Selvaraj, Muniyandi et al. (2024). “Activation of plant immunity through conversion of a helper NLR homodimer into a resistosome”. In: *PLOS Biology* 22.10, e3002868. DOI: 10.1371/journal.pbio.3002868. URL: <https://doi.org/10.1371/journal.pbio.3002868>.

- Seman, Michel et al. (2003). "NAD-induced T cell death: ADP-ribosylation of cell surface proteins by ART2 activates the cytolytic P2X7 purinoceptor". In: *Immunity* 19.4. Journal Article Research Support, Non-U.S. Gov't, 571–582. ISSN: 1074-7613. DOI: 10.1016/s1074-7613(03)00266-8.
- Seo, Jinho et al. (2021). "Necroptosis molecular mechanisms: Recent findings regarding novel necroptosis regulators". In: *Experimental Molecular Medicine* 53.6, pp. 1007–1017. ISSN: 2092-6413. DOI: 10.1038/s12276-021-00634-7. URL: <https://doi.org/10.1038/s12276-021-00634-7>.
- Seper, Andrea et al. (2013). "Vibrio cholerae Evades Neutrophil Extracellular Traps by the Activity of Two Extracellular Nucleases". In: *PLOS Pathogens* 9.9, e1003614. DOI: 10.1371/journal.ppat.1003614. URL: <https://doi.org/10.1371/journal.ppat.1003614>.
- Shahollari, Bationa et al. (2005). "Expression of a receptor kinase in Arabidopsis roots is stimulated by the basidiomycete Piriformospora indica and the protein accumulates in Triton X-100 insoluble plasma membrane microdomains". In: *Journal of Plant Physiology* 162.8, pp. 945–958. ISSN: 0176-1617. URL: <https://pubmed.ncbi.nlm.nih.gov/16146321/>.
- Sharma, O. et al. (2016). "NAD⁺-Glycohydrolase Promotes Intracellular Survival of Group A Streptococcus". In: *PLoS Pathog* 12.3. Sharma, Onkar O'Seaghdha, Magnus Velarde, Jorge J Wessels, Michael R eng K12 HD000850/HD/NICHD NIH HHS/ AI29952/AI/NIAID NIH HHS/ R01 AI070926/AI/NIAID NIH HHS/ R56 AI070926/AI/NIAID NIH HHS/ AI070926/AI/NIAID NIH HHS/ R01 AI029952/AI/NIAID NIH HHS/ Research Support, N.I.H., Extramural 2016/03/05 PLoS Pathog. 2016 Mar 3;12(3):e1005468. doi: 10.1371/journal.ppat.1005468. eCollection 2016 Mar., e1005468. ISSN: 1553-7374 (Electronic) 1553-7366 (Print) 1553-7366 (Linking). DOI: 10.1371/journal.ppat.1005468. URL: <https://www.ncbi.nlm.nih.gov/pubmed/26938870>.
- Shen, Q. et al. (2024). "Cytoplasmic calcium influx mediated by plant MLKLs confers TNL-triggered immunity". In: *Cell Host Microbe* 32.4, 453–465 e6. ISSN: 1934-6069 (Electronic), 1931-3128 (Linking). DOI: 10.1016/j.chom.2024.02.016. URL: <https://www.ncbi.nlm.nih.gov/pubmed/38513655>.
- Sherameti, Irena et al. (2008). "The Root-Colonizing Endophyte Pirifomospora indica Confers Drought Tolerance in Arabidopsis by Stimulating the Expression of Drought Stress-Related Genes in Leaves". In: *Molecular Plant-Microbe Interactions®* 21.6, pp. 799–807. DOI: 10.1094/mpmi-21-6-0799. URL: <https://apsjournals.apsnet.org/doi/abs/10.1094/MPMI-21-6-0799>.
- Shryock, J. C. and L. Belardinelli (1997). "Adenosine and adenosine receptors in the cardiovascular system: biochemistry, physiology, and pharmacology". In: *The American journal of cardiology* 79.12A. Journal Article Review, 2–10. ISSN: 0002-9149. DOI: 10.1016/s0002-9149(97)00256-7.
- Simeone, Roxane et al. (2012). "Phagosomal Rupture by Mycobacterium tuberculosis Results in Toxicity and Host Cell Death". In: *PLOS Pathogens* 8.2, e1002507. DOI: 10.1371/journal.ppat.1002507. URL: <https://doi.org/10.1371/journal.ppat.1002507>.

- Singh, Brajesh K. et al. (2023). "Climate change impacts on plant pathogens, food security and paths forward". In: *Nature Reviews Microbiology* 21.10, pp. 640–656. ISSN: 1740-1534. DOI: 10.1038/s41579-023-00900-7. URL: <https://doi.org/10.1038/s41579-023-00900-7>.
- Snelders, N. C. et al. (2020). "Microbiome manipulation by a soil-borne fungal plant pathogen using effector proteins". In: *Nat Plants* 6.11, pp. 1365–1374. ISSN: 2055-0278 (Electronic), 2055-0278 (Linking). DOI: 10.1038/s41477-020-00799-5. URL: <https://www.ncbi.nlm.nih.gov/pubmed/33139860>.
- Snelders, N. C. et al. (2022). "Microbiota manipulation through the secretion of effector proteins is fundamental to the wealth of lifestyles in the fungal kingdom". In: *FEMS Microbiol Rev* 46.5. Snelders, Nick C Rovenich, Hanna Thomma, Bart P H J eng Research Support, Non-U.S. Gov't Review England 2022/05/24 FEMS Microbiol Rev. 2022 Sep 2;46(5):fuac022. doi: 10.1093/femsre/fuac022. ISSN: 1574-6976 (Electronic) 0168-6445 (Print) 0168-6445 (Linking). DOI: 10.1093/femsre/fuac022. URL: <https://www.ncbi.nlm.nih.gov/pubmed/35604874>.
- Song, Charlotte J. et al. (2006). "Extracellular ATP induces the accumulation of superoxide via NADPH oxidases in Arabidopsis". In: *Plant physiology* 140.4. Journal Article Research Support, U.S. Gov't, Non-P.H.S. Journal Article Research Support, U.S. Gov't, Non-P.H.S., 1222–1232. DOI: 10.1104/pp.105.073072.
- Sprenger, Hans-Georg et al. (2021). "Cellular pyrimidine imbalance triggers mitochondrial DNA-dependent innate immunity". In: *Nat Metab* 3.5, pp. 636–650. ISSN: 2522-5812. DOI: 10.1038/s42255-021-00385-9. URL: <https://doi.org/10.1038/s42255-021-00385-9>.
- Sprenst, Noah et al. (2024). "Metabolic modeling reveals distinct roles of sugars and carboxylic acids in stomatal opening as well as unexpected carbon fluxes". In: *The Plant Cell* 37.1. ISSN: 1040-4651. DOI: 10.1093/plcell/koae252. URL: <https://doi.org/10.1093/plcell/koae252>.
- Stakman, EC (1915). "VOL. IV". In: *Journal of Agricultural Research* 4, p. 193.
- Stein, E. et al. (2008). "Systemic resistance in Arabidopsis conferred by the mycorrhizal fungus Piriformospora indica requires jasmonic acid signaling and the cytoplasmic function of NPR1". In: *Plant Cell Physiol* 49.11, pp. 1747–51. ISSN: 1471-9053 (Electronic), 0032-0781 (Linking). DOI: 10.1093/pcp/pcn147. URL: http://www.ncbi.nlm.nih.gov/entrez/query.fcgi?cmd=Retrieve&db=PubMed&dopt=Citation&list_uids=18842596.
- Stergiopoulos, Ioannis et al. (2013). "Phytotoxic secondary metabolites and peptides produced by plant pathogenic Dothideomycete fungi". In: *FEMS Microbiology Reviews* 37.1, pp. 67–93. ISSN: 0168-6445. DOI: 10.1111/j.1574-6976.2012.00349.x. URL: <https://doi.org/10.1111/j.1574-6976.2012.00349.x>.
- Stotz, H. U. et al. (2014). "Effector-triggered defence against apoplastic fungal pathogens". In: *Trends Plant Sci* 19.8, pp. 491–500. ISSN: 1360-1385, 1878-4372. DOI: 10.1016/j.tplants.2014.04.009. URL: <https://www.ncbi.nlm.nih.gov/pubmed/24856287>.
- Straube, H. et al. (2021). "Enhanced nucleotide analysis enables the quantification of deoxynucleotides in plants and algae revealing connections between nucleoside and deoxynucleoside metabolism". In: *Plant Cell* 33.2. Straube, Henryk Niehaus, Markus Zwitter, Sarah Witte, Claus-Peter Herde, Marco eng Research Support, Non-U.S. Gov't England

- 2021/04/02 06:00 Plant Cell. 2021 Apr 17;33(2):270-289. doi: 10.1093/plcell/koaa028., pp. 270–289. ISSN: 1532-298X (Electronic) 1040-4651 (Linking). DOI: 10.1093/plcell/koaa028. URL: <https://www.ncbi.nlm.nih.gov/pubmed/33793855>.
- Strømmand, Øyvind et al. (2021). “Discovery of fungal surface NADases predominantly present in pathogenic species”. In: *Nature Communications* 12.1, p. 1631. ISSN: 2041-1723. DOI: 10.1038/s41467-021-21307-z. URL: <https://doi.org/10.1038/s41467-021-21307-z>.
- Stuttman, Johannes et al. (2021). “Highly efficient multiplex editing: one-shot generation of 8× *Nicotiana benthamiana* and 12× *Arabidopsis* mutants”. In: *The Plant Journal* 106.1, pp. 8–22. ISSN: 0960-7412. DOI: <https://doi.org/10.1111/tpj.15197>. URL: <https://onlinelibrary.wiley.com/doi/abs/10.1111/tpj.15197>.
- Sun, Chao et al. (2014). “The beneficial fungus *Piriformospora indica* protects *Arabidopsis* from *Verticillium dahliae* infection by downregulation plant defense responses”. In: *BMC Plant Biology* 14.1, p. 268. ISSN: 1471-2229. DOI: 10.1186/s12870-014-0268-5. URL: <https://doi.org/10.1186/s12870-014-0268-5>.
- Sun, Liming et al. (2012). “Mixed Lineage Kinase Domain-like Protein Mediates Necrosis Signaling Downstream of RIP3 Kinase”. In: *Cell* 148.1. doi: 10.1016/j.cell.2011.11.031, pp. 213–227. ISSN: 0092-8674. DOI: 10.1016/j.cell.2011.11.031. URL: <https://doi.org/10.1016/j.cell.2011.11.031>.
- Sun, Tongjun et al. (2015). “ChIP-seq reveals broad roles of SARD1 and CBP60g in regulating plant immunity”. In: *Nature Communications* 6.1, p. 10159. ISSN: 2041-1723. DOI: 10.1038/ncomms10159. URL: <https://doi.org/10.1038/ncomms10159>.
- Surprenant, Annmarie and R. Alan North (2009). “Signaling at purinergic P2X receptors”. In: *Annual review of physiology* 71. Journal Article Research Support, Non-U.S. Gov’t Review Journal Article Research Support, Non-U.S. Gov’t Review, 333–359. DOI: 10.1146/annurev.physiol.70.113006.100630.
- Tak, Uday et al. (2019). “The tuberculosis necrotizing toxin is an NAD⁺ and NADP⁺ glycohydrolase with distinct enzymatic properties”. In: *J Biol Chem* 294.9, pp. 3024–3036. ISSN: 0021-9258. DOI: 10.1074/jbc.RA118.005832. URL: <https://doi.org/10.1074/jbc.RA118.005832>.
- Tamulaitiene, G. et al. (2024). “Activation of Thoris antiviral system via SIR2 effector filament assembly”. In: *Nature* 627.8003, pp. 431–436. ISSN: 1476-4687 (Electronic), 0028-0836 (Linking). DOI: 10.1038/s41586-024-07092-x. URL: <https://www.ncbi.nlm.nih.gov/pubmed/38383786>.
- Tan, Xiaoping et al. (2007). “Global expression analysis of nucleotide binding site-leucine rich repeat-encoding and related genes in *Arabidopsis*”. In: *BMC Plant Biology* 7.1, p. 56. ISSN: 1471-2229. DOI: 10.1186/1471-2229-7-56. URL: <https://doi.org/10.1186/1471-2229-7-56>.
- Tanaka, Kiwamu et al. (2014). “Extracellular ATP acts as a damage-associated molecular pattern (DAMP) signal in plants”. In: *Frontiers in plant science* 5. Journal Article Review, p. 446. ISSN: 1664-462X. DOI: 10.3389/fpls.2014.00446.
- Tantawy, Eshraq et al. (2022). “*Staphylococcus aureus* Multiplexes Death-Effector Deoxyribonucleosides to Neutralize Phagocytes”. In: *Frontiers in immunology* 13. Journal Article Research Support, Non-U.S. Gov’t The authors declare that the research was conducted

- in the absence of any commercial or financial relationships that could be construed as a potential conflict of interest. Journal Article Research Support, Non-U.S. Gov't The authors declare that the research was conducted in the absence of any commercial or financial relationships that could be construed as a potential conflict of interest., p. 847171. DOI: 10.3389/fimmu.2022.847171.
- Taruno, Akiyuki (2018). "ATP Release Channels". In: *International journal of molecular sciences* 19.3. Journal Article Review The author declares no conflict of interest. Journal Article Review The author declares no conflict of interest. DOI: 10.3390/ijms19030808.
- Thammavongsa, V. et al. (2009). "Staphylococcus aureus synthesizes adenosine to escape host immune responses". In: *J Exp Med* 206.11, pp. 2417–2427. ISSN: 0022-1007, 1540-9538. DOI: 10.1084/jem.20090097. URL: <https://www.ncbi.nlm.nih.gov/pubmed/19808256>.
- Thammavongsa, Vilasack et al. (2013). "Staphylococcus aureus degrades neutrophil extracellular traps to promote immune cell death". In: *Science (New York, N.Y.)* 342.6160. Journal Article Research Support, N.I.H., Extramural Research Support, Non-U.S. Gov't, 863–866. ISSN: 1095-9203. DOI: 10.1126/science.1242255.
- Thomas, C. et al. (2000). "A role for ectophosphatase in xenobiotic resistance". In: *The Plant cell* 12.4. Journal Article Research Support, Non-U.S. Gov't Research Support, U.S. Gov't, Non-P.H.S., 519–533. ISSN: 1040-4651. DOI: 10.1105/tpc.12.4.519.
- Thompson, J. E. et al. (1994). "Energetics of catalysis by ribonucleases: fate of the 2',3'-cyclic phosphodiester intermediate". In: *Biochemistry* 33.23. Thompson, J E Venegas, F D Raines, R T eng GM07215/GM/NIGMS NIH HHS/ GM44783/GM/NIGMS NIH HHS/ RR02301/RR/NCRR NIH HHS/ Research Support, Non-U.S. Gov't Research Support, U.S. Gov't, P.H.S. 1994/06/14 Biochemistry. 1994 Jun 14;33(23):7408-14. doi: 10.1021/bi00189a047., pp. 7408–14. ISSN: 0006-2960 (Print) 0006-2960 (Linking). DOI: 10.1021/bi00189a047. URL: <https://www.ncbi.nlm.nih.gov/pubmed/8003506>.
- Thürich, Johannes et al. (2018). "Arabidopsis thaliana responds to colonisation of Piriformospora indica by secretion of symbiosis-specific proteins". In: *PLOS ONE* 13.12, e0209658. DOI: 10.1371/journal.pone.0209658. URL: <https://doi.org/10.1371/journal.pone.0209658>.
- Torres, M. A. et al. (2002). "Arabidopsis gp91^{phox} homologues AtrbohD and AtrbohF are required for accumulation of reactive oxygen intermediates in the plant defense response". In: *Proc Natl Acad Sci U S A* 99.1, pp. 517–522. ISSN: 0027-8424, 1091-6490. DOI: 10.1073/pnas.012452499. URL: <https://www.ncbi.nlm.nih.gov/pubmed/11756663>.
- Toshchakov, Vladimir Y. and Andrew F. Neuwald (2020). "A survey of TIR domain sequence and structure divergence". In: *Immunogenetics* 72.3, pp. 181–203. ISSN: 1432-1211. DOI: 10.1007/s00251-020-01157-7. URL: <https://doi.org/10.1007/s00251-020-01157-7>.
- Tran, Tuan Minh et al. (2016). "Escaping Underground Nets: Extracellular DNases Degrade Plant Extracellular Traps and Contribute to Virulence of the Plant Pathogenic Bacterium Ralstonia solanacearum". In: *PLoS pathogens* 12.6. Journal Article Research Support, U.S. Gov't, Non-P.H.S. Research Support, Non-U.S. Gov't The authors have declared that no competing interests exist., e1005686. DOI: 10.1371/journal.ppat.1005686.

- Traub, Michaela et al. (2007). “The fluorouridine insensitive 1 (*fur1*) mutant is defective in equilibrative nucleoside transporter 3 (*ENT3*), and thus represents an important pyrimidine nucleoside uptake system in *Arabidopsis thaliana*”. In: *The Plant journal : for cell and molecular biology* 49.5. Journal Article Research Support, Non-U.S. Gov’t Journal Article Research Support, Non-U.S. Gov’t, 855–864. ISSN: 0960-7412. DOI: 10.1111/j.1365-313X.2006.02998.x.
- Töpfer, Nadine et al. (2020). “Alternative Crassulacean Acid Metabolism Modes Provide Environment-Specific Water-Saving Benefits in a Leaf Metabolic Model”. In: *The Plant Cell* 32.12, pp. 3689–3705. ISSN: 1040-4651. DOI: 10.1105/tpc.20.00132. URL: <https://doi.org/10.1105/tpc.20.00132>.
- Varma, A. et al. (1999). “*Piriformospora indica*, a cultivable plant-growth-promoting root endophyte”. In: *Appl Environ Microbiol* 65.6, pp. 2741–2744. ISSN: 0099-2240, 1098-5336. URL: <http://www.ncbi.nlm.nih.gov/pubmed/10347070>.
- Ve, Thomas et al. (2015). “Structure and function of Toll/interleukin-1 receptor/resistance protein (TIR) domains”. In: *Apoptosis* 20.2, pp. 250–261. ISSN: 1573-675X. DOI: 10.1007/s10495-014-1064-2. URL: <https://doi.org/10.1007/s10495-014-1064-2>.
- Verma, S. et al. (1998). “*Piriformospora indica*, gen. et sp. nov., a new root-colonizing fungus”. In: *Mycologia* 90.5, pp. 896–903. ISSN: 0027-5514. URL: <https://www.jstor.org/stable/3761211>.
- Verrier, J. D. et al. (2012). “The brain in vivo expresses the 2',3'-cAMP-adenosine pathway”. In: *J Neurochem* 122.1, pp. 115–125. ISSN: 0022-3042, 1471-4159. DOI: 10.1111/j.1471-4159.2012.07705.x. URL: <https://www.ncbi.nlm.nih.gov/pubmed/22360621>.
- Vliet, Albert van der and Peter F. Bove (2011). “Purinergic Signaling in Wound Healing and Airway Remodeling”. In: *Purinergic Regulation of Respiratory Diseases*. Ed. by Maryse Picher and Richard C. Boucher. Dordrecht: Springer Netherlands, pp. 139–157. ISBN: 978-94-007-1217-1. DOI: 10.1007/978-94-007-1217-1_6. URL: https://doi.org/10.1007/978-94-007-1217-1_6.
- Vos, Marjon G. J. de et al. (2017). “Interaction networks, ecological stability, and collective antibiotic tolerance in polymicrobial infections”. In: *Proceedings of the National Academy of Sciences* 114.40, pp. 10666–10671. DOI: doi:10.1073/pnas.1713372114. URL: <https://www.pnas.org/doi/abs/10.1073/pnas.1713372114>.
- Wagner, Stephan et al. (2013). “Structural basis for signaling by exclusive EDS1 heteromeric complexes with SAG101 or PAD4 in plant innate immunity”. In: *Cell Host & Microbe* 14.6, pp. 619–630. ISSN: 1931-3128. DOI: 10.1016/j.chom.2013.11.006. URL: <https://doi.org/10.1016/j.chom.2013.11.006>.
- Waller, Frank et al. (2005). “The endophytic fungus *Piriformospora indica* reprograms barley to salt-stress tolerance, disease resistance, and higher yield”. In: *Proceedings of the National Academy of Sciences* 102.38, pp. 13386–13391. DOI: doi:10.1073/pnas.0504423102. URL: <https://www.pnas.org/doi/abs/10.1073/pnas.0504423102>.
- Wan, L. et al. (2019). “TIR domains of plant immune receptors are NAD⁺-cleaving enzymes that promote cell death”. In: *Science* 365.6455, pp. 799–803. ISSN: 0036-8075, 1095-9203. DOI: 10.1126/science.aax1771. URL: <https://www.ncbi.nlm.nih.gov/pubmed/31439793>.

- Wang, Chenggang et al. (2017). “A lectin receptor kinase as a potential sensor for extracellular nicotinamide adenine dinucleotide in *Arabidopsis thaliana*”. In: *eLife* 6. Journal Article The authors declare that no competing interests exist. Journal Article The authors declare that no competing interests exist. DOI: 10.7554/eLife.25474.
- Wang, G. F. et al. (2015). “Molecular and functional analyses of a maize autoactive NB-LRR protein identify precise structural requirements for activity”. In: *PLoS Pathog* 11.2. Wang, Guan-Feng Ji, Jiabing El-Kasmi, Farid Dangl, Jeffery L Johal, Guri Balint-Kurti, Peter J eng Howard Hughes Medical Institute/ Research Support, Non-U.S. Gov’t Research Support, U.S. Gov’t, Non-PH.S. 2015/02/27 PLoS Pathog. 2015 Feb 26;11(2):e1004674. doi: 10.1371/journal.ppat.1004674. eCollection 2015 Feb., e1004674. ISSN: 1553-7374 (Electronic) 1553-7366 (Print) 1553-7366 (Linking). DOI: 10.1371/journal.ppat.1004674. URL: <https://www.ncbi.nlm.nih.gov/pubmed/25719542>.
- Wang, H. et al. (2023). “Uptake of oomycete RXLR effectors into host cells by clathrin-mediated endocytosis”. In: *Plant Cell* 35.7, pp. 2504–2526. ISSN: 1040-4651, 1532-298X. DOI: 10.1093/plcell/koad069. URL: <https://www.ncbi.nlm.nih.gov/pubmed/36911990>.
- Wang, Hanling et al. (2024). “Switch of TIR signaling by a Ca²⁺ sensor activates ADR1 recognition of pRib-AMP-EDS1-PAD4 for stomatal immunity”. In: *bioRxiv*, p. 2024.10.29.620780. DOI: 10.1101/2024.10.29.620780. URL: <https://www.biorxiv.org/content/biorxiv/early/2024/11/02/2024.10.29.620780.full.pdf>.
- Wang, J. et al. (2019a). “Reconstitution and structure of a plant NLR resistosome conferring immunity”. In: *Science* 364.6435. Wang, Jizong Hu, Meijuan Wang, Jia Qi, Jinfeng Han, Zhifu Wang, Guoxun Qi, Yijun Wang, Hong-Wei Zhou, Jian-Min Chai, Jijie eng Research Support, Non-U.S. Gov’t 2019/04/06 06:00 Science. 2019 Apr 5;364(6435). pii: 364/6435/eaav5870. doi: 10.1126/science.aav5870. ISSN: 1095-9203 (Electronic) 0036-8075 (Linking). DOI: 10.1126/science.aav5870. URL: <https://www.ncbi.nlm.nih.gov/pubmed/30948527>.
- Wang, Jizong et al. (2019b). “Ligand-triggered allosteric ADP release primes a plant NLR complex”. In: *Science* 364.6435, eaav5868. DOI: doi:10.1126/science.aav5868. URL: <https://www.science.org/doi/abs/10.1126/science.aav5868>.
- Wang, Lin et al. (2011). “CBP60g and SARD1 play partially redundant critical roles in salicylic acid signaling”. In: *The Plant Journal* 67.6, pp. 1029–1041. ISSN: 0960-7412. DOI: <https://doi.org/10.1111/j.1365-313X.2011.04655.x>. URL: <https://onlinelibrary.wiley.com/doi/abs/10.1111/j.1365-313X.2011.04655.x>.
- Wang, Yanpeng et al. (2014). “Simultaneous editing of three homoeoalleles in hexaploid bread wheat confers heritable resistance to powdery mildew”. In: *Nature Biotechnology* 32.9, pp. 947–951. ISSN: 1546-1696. DOI: 10.1038/nbt.2969. URL: <https://doi.org/10.1038/nbt.2969>.
- Wawra, S. et al. (2016). “The fungal-specific beta-glucan-binding lectin FGB1 alters cell-wall composition and suppresses glucan-triggered immunity in plants”. In: *Nat Commun* 7. Wawra, Stephan Fesel, Philipp Widmer, Heidi Timm, Malte Seibel, Jurgen Leson, Lisa Kessler, Leona Nostadt, Robin Hilbert, Magdalena Langen, Gregor Zuccaro, Alga eng England 2016/10/28 06:00 Nat Commun. 2016 Oct 27;7:13188. doi: 10.1038/ncomms13188., p. 13188. ISSN:

- 2041-1723 (Electronic) 2041-1723 (Linking). DOI: 10.1038/ncomms13188. URL: <https://www.ncbi.nlm.nih.gov/pubmed/27786272>.
- Wawra, S. et al. (2019). "FGB1 and WSC3 are in planta-induced beta-glucan-binding fungal lectins with different functions". In: *New Phytol.* Wawra, Stephan Fesel, Philipp Widmer, Heidi Neumann, Ulla Lahrmann, Urs Becker, Stefan Hehemann, Jan-Hendrik Langen, Gregor Zuccaro, Alga eng CEPLAS, EXC 1028/Deutsche Forschungsgemeinschaft ZU 263/2-1/Deutsche Forschungsgemeinschaft ZU 263/3-1/Deutsche Forschungsgemeinschaft 7217/1-1/Deutsche Forschungsgemeinschaft England 2019/01/29 06:00 New Phytol. 2019 Jan 28. doi: 10.1111/nph.15711. ISSN: 1469-8137 (Electronic) 0028-646X (Linking). DOI: 10.1111/nph.15711. URL: <https://www.ncbi.nlm.nih.gov/pubmed/30688363>.
- Wei, H. L. et al. (2018). "Modular study of the type III effector repertoire in *Pseudomonas syringae* pv. tomato DC3000 reveals a matrix of effector interplay in pathogenesis". In: *Cell Rep* 23.6, pp. 1630–1638. ISSN: 2211-1247. DOI: 10.1016/j.celrep.2018.04.037. URL: <https://www.ncbi.nlm.nih.gov/pubmed/29742421>.
- Weiss, M. et al. (2011). "Sebacinales everywhere: previously overlooked ubiquitous fungal endophytes". In: *PLoS One* 6.2, e16793. ISSN: 1932-6203. DOI: 10.1371/journal.pone.0016793. URL: <http://www.ncbi.nlm.nih.gov/pubmed/21347229>.
- Weiss, Michael et al. (2016). "Sebacinales — one thousand and one interactions with land plants". In: *New Phytologist* 211.1, pp. 20–40. ISSN: 0028-646X. DOI: 10.1111/nph.13977. URL: <https://doi.org/10.1111/nph.13977>.
- Weyer, Anna-Lena Van de et al. (2019). "A Species-Wide Inventory of NLR Genes and Alleles in *Arabidopsis thaliana*". In: *Cell* 178.5, 1260–1272.e14. ISSN: 0092-8674. DOI: 10.1016/j.cell.2019.07.038. URL: <https://doi.org/10.1016/j.cell.2019.07.038>.
- Whitham, S. et al. (1996). "The N gene of tobacco confers resistance to tobacco mosaic virus in transgenic tomato". In: *Proc Natl Acad Sci U S A* 93.16. Whitham, S McCormick, S Baker, B eng Research Support, U.S. Gov't, Non-PH.S. 1996/08/06 Proc Natl Acad Sci U S A. 1996 Aug 6;93(16):8776-81. doi: 10.1073/pnas.93.16.8776., pp. 8776–81. ISSN: 0027-8424 (Print) 1091-6490 (Electronic) 0027-8424 (Linking). DOI: 10.1073/pnas.93.16.8776. URL: <https://www.ncbi.nlm.nih.gov/pubmed/8710948>.
- Williams, Niamh C. et al. (2022). "Signaling metabolite L-2-hydroxyglutarate activates the transcription factor HIF-1 in lipopolysaccharide-activated macrophages". In: *J Biol Chem* 298.2, p. 101501. ISSN: 0021-9258. DOI: 10.1016/j.jbc.2021.101501. URL: <https://www.sciencedirect.com/science/article/pii/S0021925821013119>.
- Williams, S. J. et al. (2014). "Structural basis for assembly and function of a heterodimeric plant immune receptor". In: *Science* 344.6181, pp. 299–303. ISSN: 0036-8075. DOI: 10.1126/science.1247357. URL: <https://www.ncbi.nlm.nih.gov/pubmed/24744375>.
- Winstel, Volker et al. (2018). "Staphylococcus aureus targets the purine salvage pathway to kill phagocytes". In: *Proceedings of the National Academy of Sciences of the United States of America* 115.26. Journal Article Research Support, N.I.H., Extramural Research Support, Non-U.S. Gov't The authors declare no conflict of interest., 6846–6851. DOI: 10.1073/pnas.1805622115.
- Winstel, Volker et al. (2019). "Staphylococcus aureus Exploits the Host Apoptotic Pathway To Persist during Infection". In: *mBio* 10.6. Journal Article Research Support, N.I.H., Extramural Research

Support, Non-U.S. Gov't Journal Article Research Support, N.I.H., Extramural Research Support, Non-U.S. Gov't. DOI: 10.1128/mBio.02270-19.

- Winstel, Volker et al. (2024). "Targeting host deoxycytidine kinase mitigates Staphylococcus aureus abscess formation". In: *eLife* 12. Journal Article VW, EA Inventor in a patent application covering the use of dCK inhibitors as a treatment for bacterial infectious diseases (patent pending, No. 63/450,304 USPTO), TL No competing interests declared, CR Co-inventor of the dCK inhibitor used in this study. This intellectual property has been patented by the University of California and optioned to Trethera Corporation, a company that CGR owns equity in (US 9,598,404; US 9,688,673). Inventor in a patent application covering the use of dCK inhibitors as a treatment for bacterial infectious diseases (patent pending, No. 63/450,304 USPTO). DOI: 10.7554/eLife.91157.
- Wirthmueller, Lennart et al. (2007). "Nuclear Accumulation of the Arabidopsis Immune Receptor RPS4 Is Necessary for Triggering EDS1-Dependent Defense". In: *Current Biology* 17.23. doi: 10.1016/j.cub.2007.10.042, pp. 2023–2029. ISSN: 0960-9822. DOI: 10.1016/j.cub.2007.10.042. URL: <https://doi.org/10.1016/j.cub.2007.10.042>.
- Wormit, Alexandra et al. (2004). "Characterization of three novel members of the Arabidopsis thaliana equilibrative nucleoside transporter (ENT) family". In: *The Biochemical journal* 383.Pt 1. Journal Article Research Support, Non-U.S. Gov't Journal Article Research Support, Non-U.S. Gov't, 19–26. DOI: 10.1042/bj20040389.
- Wu, Jiayi et al. (2013). "Cyclic GMP-AMP Is an Endogenous Second Messenger in Innate Immune Signaling by Cytosolic DNA". In: *Science* 339.6121, pp. 826–830. DOI: doi:10.1126/science.1229963. URL: <https://www.science.org/doi/abs/10.1126/science.1229963>.
- Wu, Y. et al. (2024). "A canonical protein complex controls immune homeostasis and multipathogen resistance". In: *Science*. Wu, Yue Xu, Weiying Zhao, Guoyan Lei, Ziyao Li, Kui Liu, Jiyun Huang, Shijia Wang, Junli Zhong, Xiangbin Yin, Xin Wang, Yuandong Zhang, Haochen He, Yang Ye, Zian Meng, Yonggang Chang, Xiaoyu Lin, Hui Wang, Xin Gao, Yuanyuan Chai, Jijie Parker, Jane E Deng, Yiwen Zhang, Yu Gao, Mingjun He, Zuhua eng 2024/11/13 Science. 2024 Nov 7:eadr2138. doi: 10.1126/science.adr2138., eadr2138. ISSN: 1095-9203 (Electronic) 0036-8075 (Linking). DOI: 10.1126/science.adr2138. URL: <https://www.ncbi.nlm.nih.gov/pubmed/39509474>.
- Wu, Z. et al. (2019). "Differential regulation of TNL-mediated immune signaling by redundant helper CNLs". In: *New Phytol* 222.2, pp. 938–953. ISSN: 1469-8137 (Electronic), 0028-646X (Linking). DOI: 10.1111/nph.15665. URL: <https://www.ncbi.nlm.nih.gov/pubmed/30585636>.
- Xiao, Y. et al. (2012). "Retrograde signaling by the plastidial metabolite MEcPP regulates expression of nuclear stress-response genes". In: *Cell* 149.7. Xiao, Yanmei Savchenko, Tatyana Baidoo, Edward E K Chehab, Wassim E Hayden, Daniel M Tolstikov, Vladimir Corwin, Jason A Kliebenstein, Daniel J Keasling, Jay D Dehesh, Katayoon eng Research Support, U.S. Gov't, Non-P.H.S. 2012/06/26 06:00 Cell. 2012 Jun 22;149(7):1525-35. doi: 10.1016/j.cell.2012.04.038., pp. 1525–35. ISSN: 1097-4172 (Electronic) 0092-8674 (Linking). DOI: 10.1016/j.cell.2012.04.038. URL: <https://www.ncbi.nlm.nih.gov/pubmed/22726439>.

- Xiao, Yinyan et al. (2025). "Activation and inhibition mechanisms of a plant helper NLR". In: *Nature* 639.8054, pp. 438–446. ISSN: 1476-4687. DOI: 10.1038/s41586-024-08517-3. URL: <https://doi.org/10.1038/s41586-024-08517-3>.
- Xu, G. et al. (2022). "A tale of many families: calcium channels in plant immunity". In: *Plant Cell* 34.5, pp. 1551–1567. ISSN: 1040-4651, 1532-298X. DOI: 10.1093/plcell/koac033. URL: <https://www.ncbi.nlm.nih.gov/pubmed/35134212>.
- Xu, Haixin and Michèle C. Heath (1998). "Role of Calcium in Signal Transduction during the Hypersensitive Response Caused by Basidiospore-Derived Infection of the Cowpea Rust Fungus". In: *The Plant Cell* 10.4, pp. 585–597. ISSN: 1040-4651. DOI: 10.1105/tpc.10.4.585. URL: <https://doi.org/10.1105/tpc.10.4.585>.
- Yang, Y. et al. (2023). "Convergent evolution of plant pattern recognition receptors sensing cysteine-rich patterns from three microbial kingdoms". In: *Nat Commun* 14.1, p. 3621. ISSN: 2041-1723. DOI: 10.1038/s41467-023-39208-8. URL: <https://www.ncbi.nlm.nih.gov/pubmed/37336953>.
- Yegutkin, Gennady G. (2008). "Nucleotide- and nucleoside-converting ectoenzymes: Important modulators of purinergic signalling cascade". In: *Biochimica et biophysica acta* 1783.5. Journal Article Research Support, Non-U.S. Gov't Review Journal Article Research Support, Non-U.S. Gov't Review, 673–694. ISSN: 0006-3002. DOI: 10.1016/j.bbamcr.2008.01.024.
- Yilmaz, Ozlem et al. (2008). "ATP scavenging by the intracellular pathogen *Porphyromonas gingivalis* inhibits P2X7-mediated host-cell apoptosis". In: *Cellular microbiology* 10.4. Journal Article Research Support, N.I.H., Extramural Journal Article Research Support, N.I.H., Extramural, 863–875. DOI: 10.1111/j.1462-5822.2007.01089.x.
- Young, James D. et al. (2013). "The human concentrative and equilibrative nucleoside transporter families, SLC28 and SLC29". In: *Molecular Aspects of Medicine* 34.2, pp. 529–547. ISSN: 0098-2997. DOI: <https://doi.org/10.1016/j.mam.2012.05.007>. URL: <https://www.sciencedirect.com/science/article/pii/S0098299712000532>.
- Yu, Dongli et al. (2022). "TIR domains of plant immune receptors are 2',3' cAMP/cGMP synthetases mediating cell death". In: *Cell* 185.13. doi: 10.1016/j.cell.2022.04.032, 2370–2386.e18. ISSN: 0092-8674. DOI: 10.1016/j.cell.2022.04.032. URL: <https://doi.org/10.1016/j.cell.2022.04.032>.
- Yu, G. et al. (2020). "A bacterial effector protein prevents MAPK-mediated phosphorylation of SGT1 to suppress plant immunity". In: *PLoS Pathog* 16.9. Yu, Gang Xian, Liu Xue, Hao Yu, Wenjia Rufian, Jose S Sang, Yuying Morcillo, Rafael J L Wang, Yaru Macho, Alberto P eng Research Support, Non-U.S. Gov't 2020/09/26 PLoS Pathog. 2020 Sep 25;16(9):e1008933. doi: 10.1371/journal.ppat.1008933. eCollection 2020 Sep., e1008933. ISSN: 1553-7374 (Electronic) 1553-7366 (Print) 1553-7366 (Linking). DOI: 10.1371/journal.ppat.1008933. URL: <https://www.ncbi.nlm.nih.gov/pubmed/32976518>.
- Yu, H. et al. (2024). "Activation of a helper NLR by plant and bacterial TIR immune signaling". In: *Science*. Yu, Hua Xu, Weiying Chen, Sisi Wu, Xiaoxian Rao, Weiwei Liu, Xiaoxiao Xu, Xiaoyan Chen, Jingqi Nishimura, Marc T Zhang, Yu Wan, Li eng 2024/11/13 Science. 2024 Nov 7:eadr3150. doi: 10.1126/science.adr3150., eadr3150. ISSN: 1095-9203 (Electronic)

- 0036-8075 (Linking). DOI: 10.1126/science.adr3150. URL: <https://www.ncbi.nlm.nih.gov/pubmed/39509471>.
- Yuan, M. et al. (2021). “Pattern-recognition receptors are required for NLR-mediated plant immunity”. In: *Nature* 592.7852, pp. 105–109. ISSN: 1476-4687. DOI: 10.1038/s41586-021-03316-6. URL: <https://www.ncbi.nlm.nih.gov/pubmed/33692546>.
- Yuan, P. et al. (2017). “Calcium signatures and signaling events orchestrate plant-microbe interactions”. In: *Curr Opin Plant Biol* 38, pp. 173–183. ISSN: 1369-5266, 1879-0356. DOI: 10.1016/j.pbi.2017.06.003. URL: <https://www.ncbi.nlm.nih.gov/pubmed/28692858>.
- Zarea, M. J. et al. (2012). “Effect of Piriformospora indica and Azospirillum strains from saline or non-saline soil on mitigation of the effects of NaCl”. In: *Soil Biology and Biochemistry* 45, pp. 139–146. ISSN: 0038-0717. DOI: <https://doi.org/10.1016/j.soilbio.2011.11.006>. URL: <https://www.sciencedirect.com/science/article/pii/S0038071711003919>.
- Zecua-Ramirez, Patricia et al. (2023). *Autophagy restricts fungal accommodation in the roots of Arabidopsis thaliana*. DOI: 10.1101/2023.07.21.550010.
- Zeng, T. et al. (2020). “A lysin motif effector subverts chitin-triggered immunity to facilitate arbuscular mycorrhizal symbiosis”. In: *New Phytologist* 225.1, pp. 448–460. ISSN: 0028-646X. DOI: 10.1111/nph.16245. URL: <https://www.ncbi.nlm.nih.gov/pubmed/31596956>.
- Zhai, J. et al. (2011). “MicroRNAs as master regulators of the plant NB-LRR defense gene family via the production of phased, trans-acting siRNAs”. In: *Genes Dev* 25.23. Zhai, Jixian Jeong, Dong-Hoon De Paoli, Emanuele Park, Sunhee Rosen, Benjamin D Li, Yupeng Gonzalez, Alvaro J Yan, Zhe Kitto, Sherry L Grusak, Michael A Jackson, Scott A Stacey, Gary Cook, Douglas R Green, Pamela J Sherrier, D Janine Meyers, Blake C eng Research Support, U.S. Gov’t, Non-PH.S. 2011/12/14 *Genes Dev.* 2011 Dec 1;25(23):2540-53. doi: 10.1101/gad.177527.111., pp. 2540–53. ISSN: 1549-5477 (Electronic) 0890-9369 (Print) 0890-9369 (Linking). DOI: 10.1101/gad.177527.111. URL: <https://www.ncbi.nlm.nih.gov/pubmed/22156213>.
- Zhang, M. et al. (2010). “Structural basis for assembly of Hsp90-Sgt1-CHORD protein complexes: implications for chaperoning of NLR innate immunity receptors”. In: *Molecular Cell* 39.2, pp. 269–281. ISSN: 1097-2765. DOI: 10.1016/j.molcel.2010.05.010. URL: <https://www.ncbi.nlm.nih.gov/pubmed/20670895>.
- Zhang, Qiang et al. (2025). “Toll/interleukin-1 receptor-only genes contribute to immune responses in maize”. In: *Plant Physiology* 197.2. ISSN: 0032-0889. DOI: 10.1093/plphys/kiaf030. URL: <https://doi.org/10.1093/plphys/kiaf030>.
- Zhang, Xudong and Zhonglin Mou (2009). “Extracellular pyridine nucleotides induce PR gene expression and disease resistance in Arabidopsis”. In: *The Plant journal : for cell and molecular biology* 57.2. Journal Article Research Support, Non-U.S. Gov’t Journal Article Research Support, Non-U.S. Gov’t, 302–312. ISSN: 0960-7412. DOI: 10.1111/j.1365-313X.2008.03687.x.
- Zhang, Xue-Cheng and Walter Gassmann (2007). “Alternative Splicing and mRNA Levels of the Disease Resistance Gene RPS4 Are Induced during Defense Responses”. In: *Plant Physiology* 145.4, pp. 1577–1587. ISSN: 0032-0889. DOI: 10.1104/pp.107.108720. URL: <https://doi.org/10.1104/pp.107.108720>.

- Zhao, Yan-Bo et al. (2022). "Pathogen effector AvrSr35 triggers Sr35 resistosome assembly via a direct recognition mechanism". In: *Science Advances* 8.36, eabq5108. DOI: doi : 10 . 1126 / sciadv . abq5108. URL: <https://www.science.org/doi/abs/10.1126/sciadv.abq5108>.
- Zimmermann, Heinrich et al. (2012). "Cellular function and molecular structure of ecto-nucleotidases". In: *Purinergic Signalling* 8.3, pp. 437–502. ISSN: 1573-9538. DOI: 10.1007/s11302-012-9309-4. URL: <https://doi.org/10.1007/s11302-012-9309-4>.
- Zipfel, C. (2014). "Plant pattern-recognition receptors". In: *Trends in Immunology* 35.7, pp. 345–351. ISSN: 1471-4906. DOI: 10.1016/j.it.2014.05.004. URL: <https://www.ncbi.nlm.nih.gov/pubmed/24946686>.
- Zipfel, Cyril and Giles E. D. Oldroyd (2017). "Plant signalling in symbiosis and immunity". In: *Nature* 543.7645, pp. 328–336. ISSN: 0028-0836. DOI: 10.1038/nature22009. URL: <https://doi.org/10.1038/nature22009>.
- Zrenner, Rita et al. (2006). "Pyrimidine and purine biosynthesis and degradation in plants". In: *Annual Review of Plant Biology* 57. Volume 57, 2006. Journal Article Research Support, Non-U.S. Gov't Review, 805–836. ISSN: 1545-2123. DOI: 10.1146/annurev.arplant.57.032905.105421.
- Zuccaro, Alga et al. (2009). "Karyotype analysis, genome organization, and stable genetic transformation of the root colonizing fungus *Piriformospora indica*". In: *Fungal Genetics and Biology* 46.8, pp. 543–550. ISSN: 1087-1845. DOI: 10.1016/j.fgb.2009.03.009. URL: <https://doi.org/10.1016/j.fgb.2009.03.009>.
- Zuccaro, Alga et al. (2011). "Endophytic Life Strategies Decoded by Genome and Transcriptome Analyses of the Mutualistic Root Symbiont *Piriformospora indica*". In: *PLoS Pathogens* 7.10. ISSN: 1553-7374. DOI: 10.1371/journal.ppat.1002290. URL: <https://doi.org/10.1371/journal.ppat.1002290>.

Cell Host & Microbe, Volume 32

Supplemental information

**A nucleoside signal generated by a fungal endophyte
regulates host cell death and promotes root
colonization**

Nick Dunken, Heidi Widmer, Gerd U. Balcke, Henryk Straube, Gregor Langen, Nyasha M. Charura, Pia Saake, Concetta De Quattro, Jonas Schön, Hanna Rövenich, Stephan Wawra, Mamoon Khan, Armin Djamei, Matias D. Zurbriggen, Alain Tissier, Claus-Peter Witte, and Alga Zuccaro

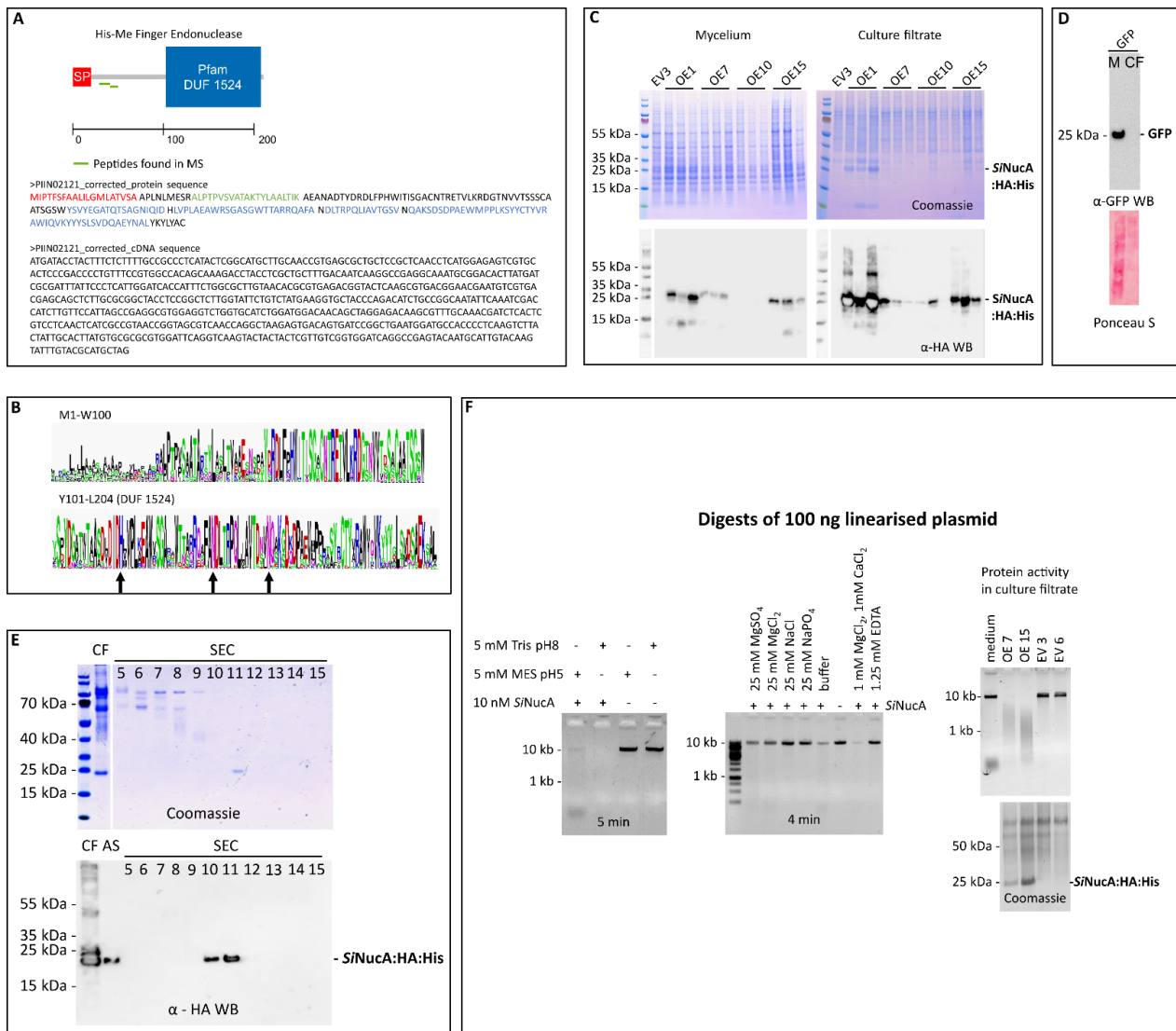


Fig. S1: SiNucA – Prediction, purification and function, related to Figure 2.

(A) SiNucA (PIIN_02121) is 211 amino acids long, has a predicted signal peptide SP (first 20 amino acids) and the Pfam domain DUF 1524 belonging to the His-Me finger endonuclease superfamily. Two unique peptides (in green) were found in the apoplastic fluid (APF) of inoculated barley roots at 5 dpi by LC-MS/MS (Nizam et al.¹³). cDNA sequence was verified by rapid amplification of cDNA-ends with polymerase chain reaction (RACE-PCR), which revealed a 30 bp earlier start and a SNP at bp 33.

(B) Protein logo of multiple alignment of SiNucA and ten best protein BLAST hits for bacteria, Basidiomycetes and Ascomycetes each. Amino acids M1-W100 and Y101-L204 (DUF 1524 domain) shown. With the exception of the SP, the protein sequence is highly conserved. Arrows show the conserved HNN motif.

(C) *S. indica* SiNucA:HA:His (OE 1, 7, 10, 15) and the empty vector strain 3 (EV 3) were grown for 5 days in CM medium followed by 2 days in MYP medium. Protein expression and secretion was analyzed with mycelium (M) and culture filtrate (CF) on Coomassie-stained SDS-PAGEs and anti-HA Western blots (C).

(D) Control for intracellular protein contamination from M into CF with *S. indica* strain expressing cytosolic GFP processed in parallel. (C) Anti-HA Western blots of *S. indica* SiNucA:HA:His strains from (A).

(E) SiNucA:HA:His protein enrichment from culture filtrate (CF) precipitated with 80% ammonium sulfate (AS) and separated by size exclusion chromatography (SEC, fractions 5- 15 shown). Fractions 10 and 11 were confirmed to contain SiNucA:HA:His by an anti-HA Western blot.

(F) Left: 100 ng linearized plasmid added to 10 nM purified SiNucA in 5 mM Tris pH 8 or 5 mM MES pH 5 with 1mM MgCl₂, 1mM CaCl₂ and microelements incubated at RT for 5 min and loaded on an agarose gel. Middle: 100 ng linearized plasmid added to 10 nM purified SiNucA in buffer 5 mM Tris pH 8 supplemented with microelements. The influence of the addition of different salts and EDTA on protein activity was tested. The linearized plasmid in the different solutions with SiNucA was incubated for 4 min at RT and loaded on an agarose gel. Right: Culture filtrate (CF) of *S. indica* SiNucA:HA:His overexpression strains OE 7 and OE 15 and empty vector strains EV 3 and EV 6 incubated with 100 ng linearized plasmid for 30 min and loaded on an agarose gel. 20 ml CF precipitated with trichloroacetic acid and loaded on SDS-PAGE as control for total protein amount in CF.

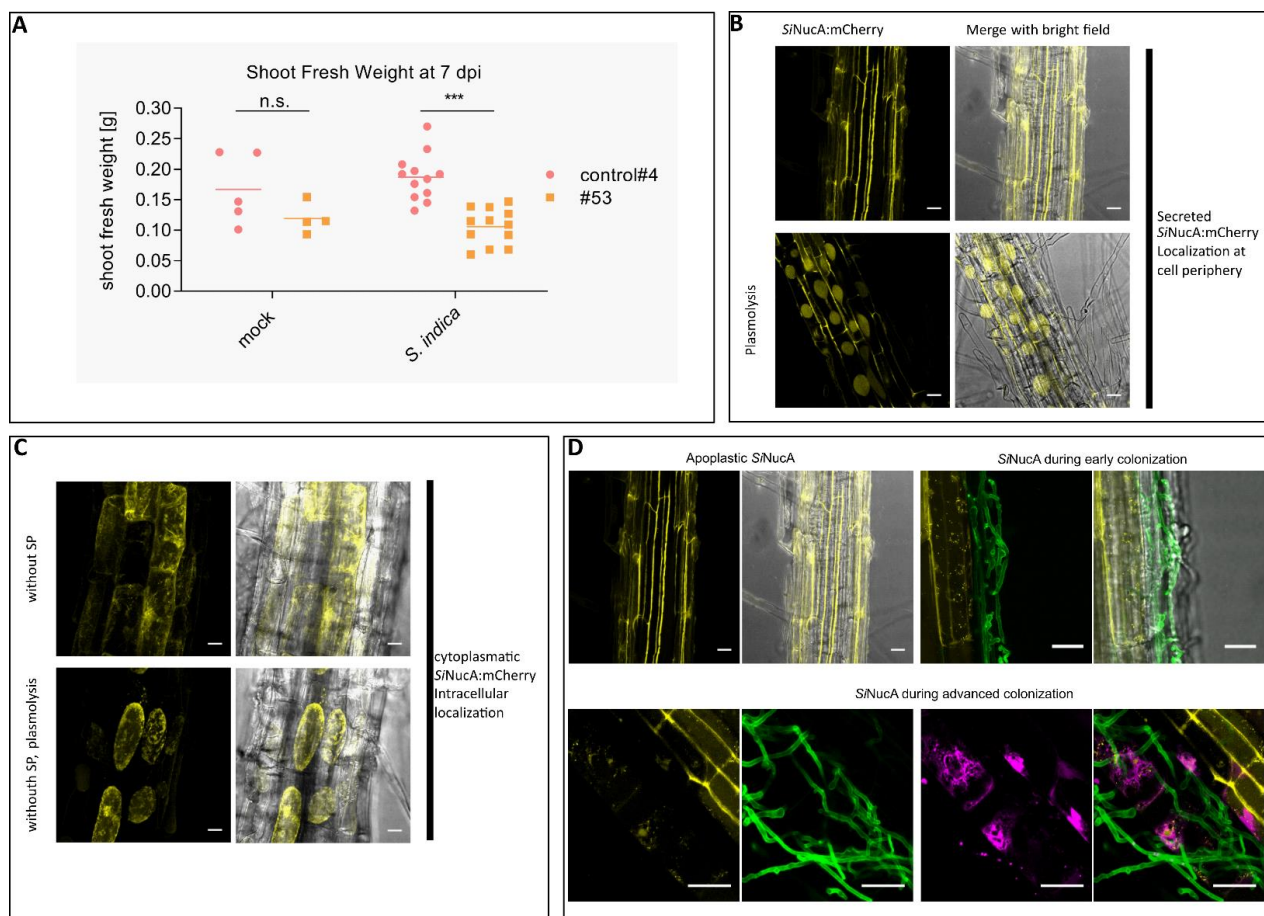


Fig. S2: Heterologous *SiNucA* expression affects fungal colonization, related to Figure 2.

A) Shoot fresh weight of *A. thaliana* seedlings overexpressing *SiNucA* (#53) and the corresponding control line (control#4). The data show the shoot fresh weight of *S. indica* and mock-inoculated seedlings at 7 dpi. Data points depict independent biological replicates. Asterisks represent significant difference between different genotypes analyzed by Student's t-test - $p < 0.005$ (***).

(B) CLSM live cell imaging of Arabidopsis roots heterologously expressing *SiNucA*:mCherry with or without plasmolysis. (C) Arabidopsis root expressing *SiNucA* (w/o SP):mCherry with and without plasmolysis. Maximum projection of z-stacks. Plasmolysis was achieved using 1 M sorbitol or NaCl. Bars = 20 μ m. CLSM microscopy was repeated with 3 independent samples.

(D) Effect of fungal colonization on the localization of *SiNucA* in Arabidopsis heterologously expressing *SiNucA*:mCherry. CLSM live cell images of Arabidopsis root expressing *SiNucA*:mCherry (yellow) inoculated with *S. indica*. Fungal cell wall of hyphae stained with WGA-AF 488 (green) and nuclei with DAPI (magenta). Top left: *SiNucA*:mCherry accumulates in the apoplast in non-inoculated roots. Top right: *SiNucA*:mCherry accumulates around penetrating hyphae (intracellular hyphae in living cells not stainable with WGA-AF 488 in the biotrophic interaction phase). Bottom: In a later phase, *SiNucA*:mCherry is mainly present in nuclei of colonized cells. Bars = 20 μ m.

Identification of products upon *Si*E5NT incubation

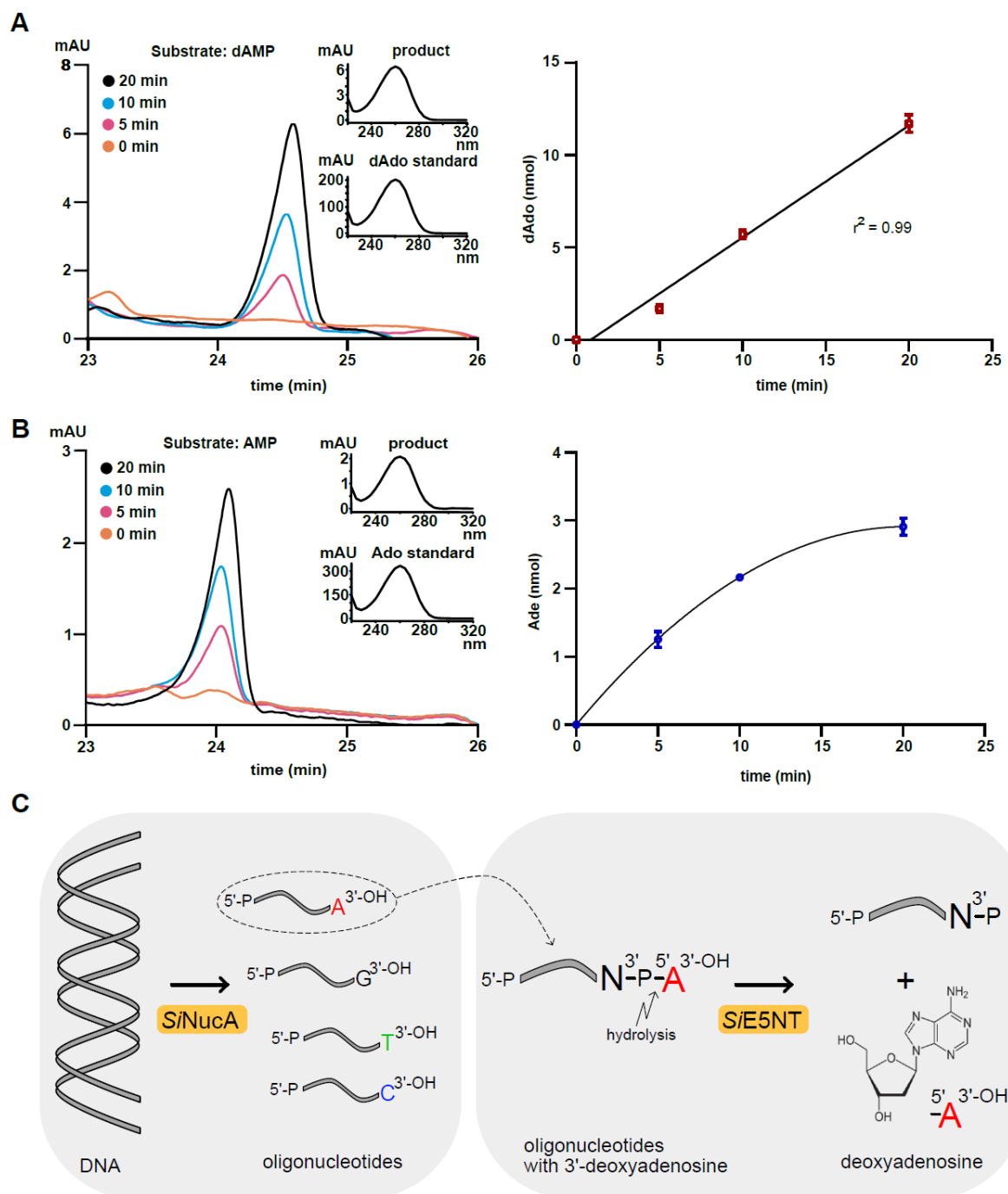


Figure S3: Analysis of metabolites derived from incubation of *Si*E5NT with deoxyadenosine monophosphate (dAMP) or adenosine monophosphate (AMP) and model of the reaction mechanism, related to Figure 3.

(A) Left panel, HPLC trace from spectrometric detection at 254 nm for deoxyadenosine (dAdo) derived from dAMP converted by *Si*E5NT after the indicated incubation times. 1 mM dAMP was incubated with 1.9×10 mg protein in 100 μ l. The insert compares the spectra of standard and reaction product. Right panel, dAdo generated after 0, 5, 10 and 20 min of incubation ($n = 3$). The data was fitted by linear regression.

(B) Same as in (A) but using AMP as a substrate ($n = 3$).

(C) Model of the reaction mechanism of *Si*NucA and *Si*E5NT with DNA as substrate, showing preference for dAdo production.

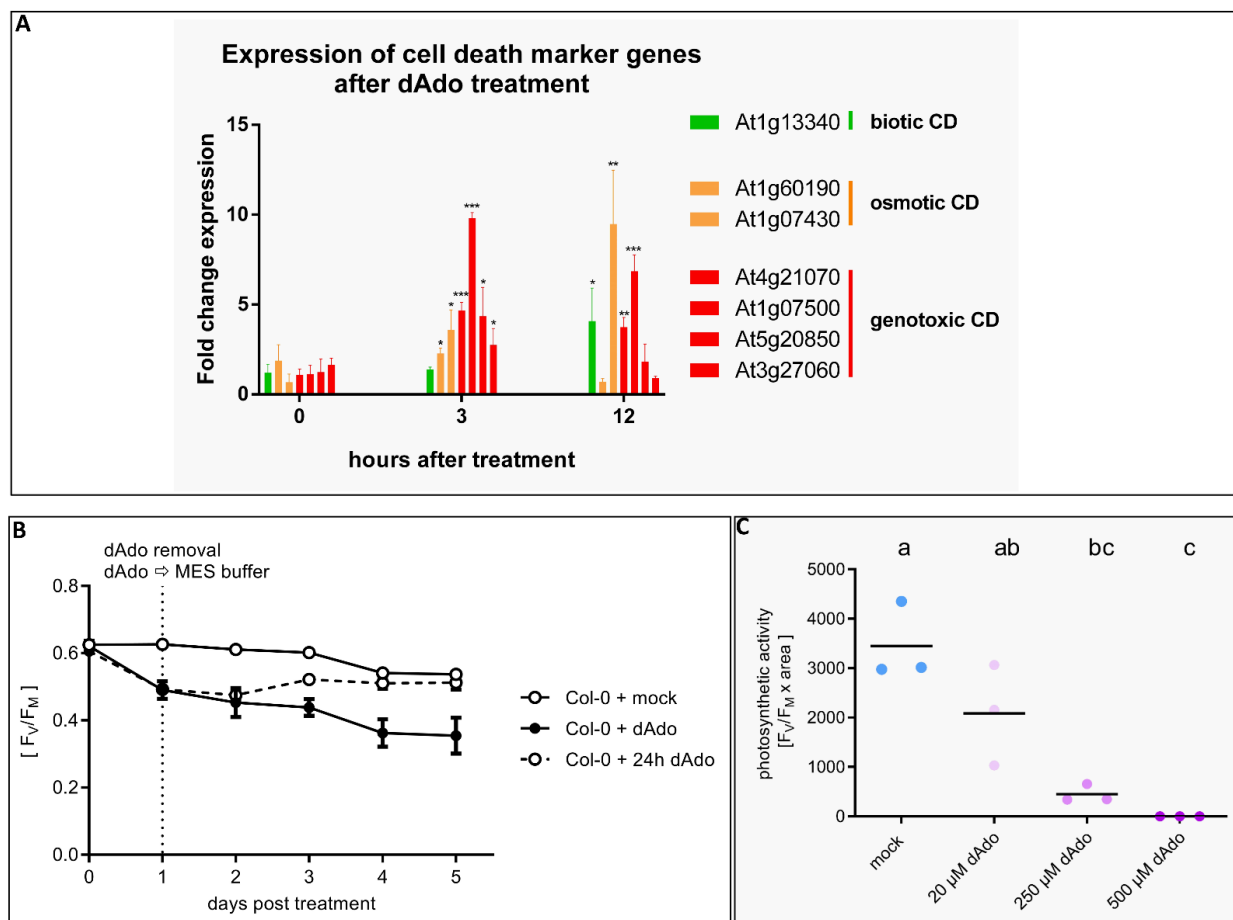


Fig. S4: The nucleoside dAdo induces cell death, related to Figure 4.

(A) Relative expression of cell death marker genes in Arabidopsis seedlings after 500 μM dAdo treatment measured by qRT-PCR.

Expression values relative to mock-treated seedlings were calculated using the $\Delta\Delta\text{Ct}$ -method. Bars represent the average of three independent biological replicates while error bars represent the standard deviation. Asterisks represent significant difference to the mock-treated sample analyzed by Student's t-test. $p < 0.05$ (*), $p < 0.01$ (**), $p < 0.005$ (***)). Marker genes were selected based on Olvera-Carrillo et al.²⁷.

(B) Photosynthetic activity (F_v/F_m) multiplied with corresponding photosynthetically active area) of 9-day-old Col-0 seedlings incubated with different concentrations of dAdo at 7 dpt. Dots represent 3 biologically independent replicates. Different letters indicate significant different groups determined with a one-way ANOVA with post-hoc Tukey HSD test ($p < 0.05$).

(C) Photosynthetic activity (F_v/F_m) of 7-day-old Col-0 seedlings incubated with 500 μM dAdo or 2.5 mM MES buffer (pH = 5.6). After 24 hours, the dAdo containing solution was replaced with MES buffer (Col-0 + 24 h dAdo). Dots represent 12 biological replicates, while error bars represent the SEM. Asterisks represent significant differences to the buffer-treated sample analyzed by Student's t-test. $p < 0.005$ (***)).

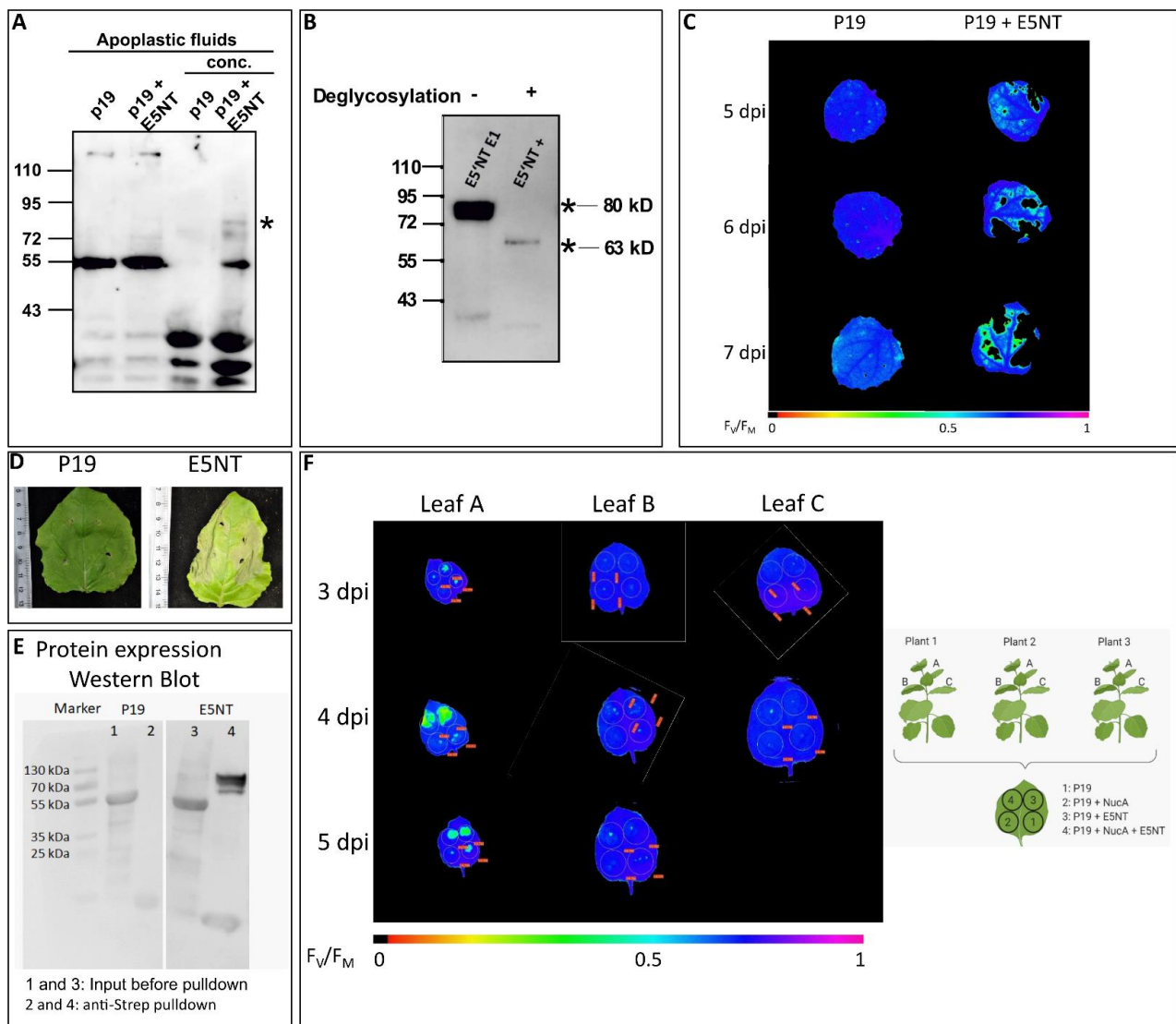


Fig. S5: Heterologous SiE5NT expression in *Nicotiana benthamiana*, related to Figure 4.

(A) SiE5NT is detected in the apoplastic fluids of *Nicotiana benthamiana* leaves after transient overexpression using *Agrobacterium*. The leaves of *N. benthamiana* were infiltrated with *Agrobacterium* carrying either p19 or E5NT expression construct. To validate secretion of SiE5NT, the apoplastic fluids were collected from the leaves at 4 dpi. The proteins in the apoplastic fluids were concentrated with 100% acetone and were separated via SDS-PAGE. The StrepII-tagged-SiE5NT in the apoplastic fluids were detected via Western Blot using the StrepMAB antibody.

(B) Deglycosylation of SiE5NT overexpressed in the leaves of *N. benthamiana* leaves from (A). The purified SiE5NT was treated with protein deglycosylation mix and incubated 37 °C for 16 hours. The deglycosylated SiE5NT was separated using SDS-PAGE and blotted onto nitrocellulose membrane. The StrepII-tagged SiE5NT in the apoplastic fluids were detected using the StrepMAB antibody.

(C) Visualization of F_v/F_m measured via PAM fluorometry. Blue indicates a high value while green decreased and yellow strongly decreased photosynthetic activity. Depicted are leaves of *N. benthamiana* heterologously expressing p19 or a combination of p19 and E5NT after *Agrobacterium* infiltration.

(D) Image of leaves of *N. benthamiana* heterologously expressing p19 or a combination of p19 and E5NT after *Agrobacterium* infiltration.

(E) Protein expression in *N. benthamiana* leaves. Proteins were extracted from infiltrated *N. benthamiana* leaves using Anti-Strep-beads for pulldown and analyzed by Western Blot using an anti-Strep antibody. Lane 1 and 3 represent raw extract prior to pulldown, whereas lane 2 and 4 represent pulled-down proteins. E5NT = 80 kDa.

(F) Heterologous expression of E5NT in *N. benthamiana* leaves induces cell death in younger leaves.

Visualization of F_v/F_m measured via PAM fluorometry. Blue indicates a high, while green indicates decreased and yellow strongly decreased photosynthetic activity. Depicted are leaves of *N. benthamiana* infiltrated with different mixtures of *Agrobacterium tumefaciens* strains expressing: 1 = p19, 2 = p19 + NucA, 3 = p19 + E5NT, 4 = p19 + NucA + E5NT. Photosynthetic activity was measured in three leaves of different ages (A to C = younger to older) originating from three different plants at each time point.

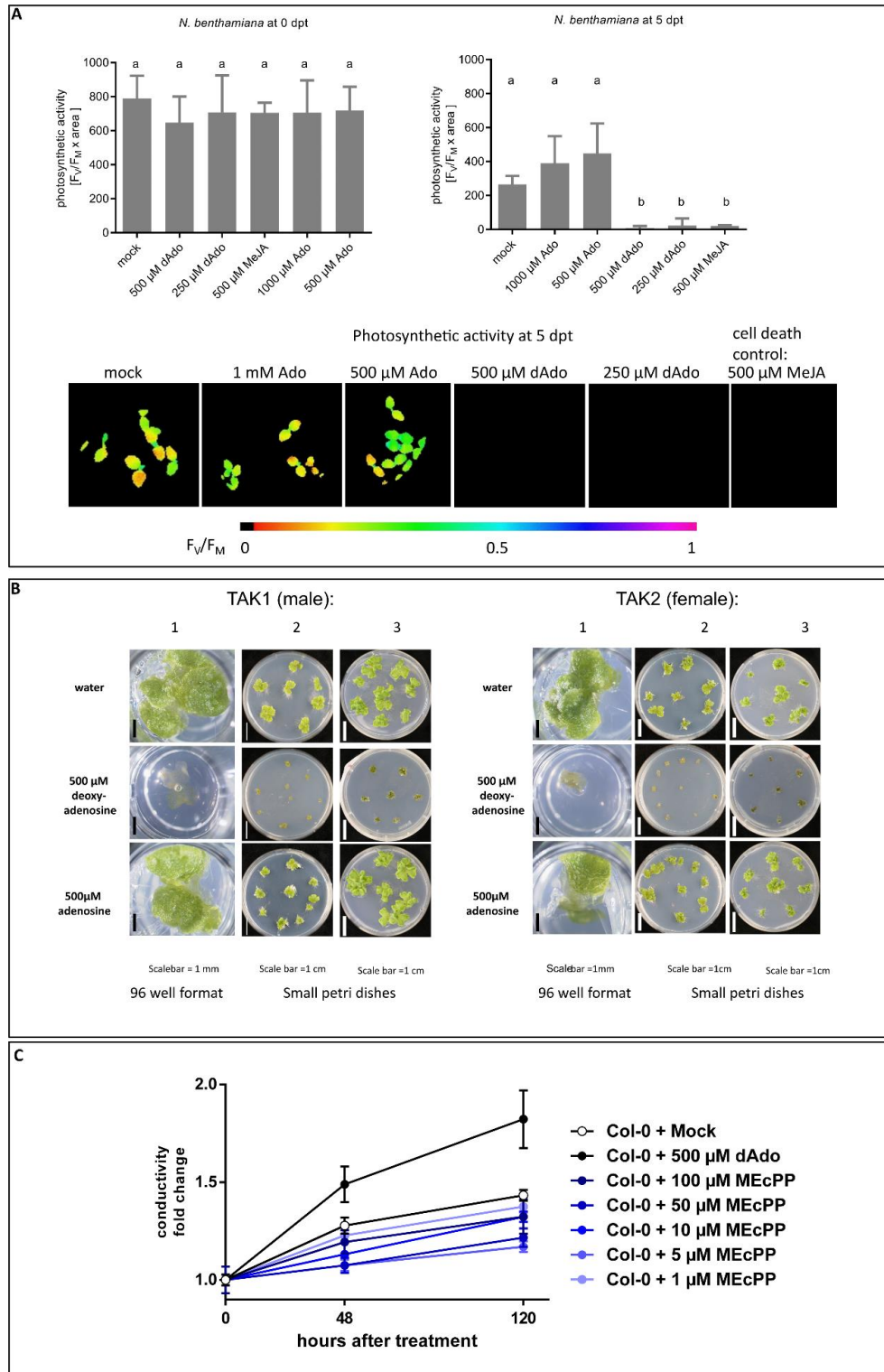


Fig. S6: The nucleoside dAdo induces cell death in a variety of plant species – MEcPP does not, related to Figure 4.

(A) dAdo induces cell death in *N. benthamiana*. Photosynthetic activity ($F_v/F_m \times$ photosynthetic area) of 7-day-old *N. benthamiana* seedlings incubated with dAdo, Ado, MeJA (cell death control) or mock (2.5 mM MES, pH = 5.6) at 0 and 5 dpt. Bars represent the average of four independent biological replicates, while error bars represent the SEM. Letters indicate significant different groups determined with a one-way ANOVA with post-hoc Tukey HSD test ($p < 0.05$).

(B) : dAdo induces cell death in *Marchantia polymorpha*. Gemmae of *Marchantia polymorpha* Tak-1 and Tak-2 were cultured on half-strength B5 medium* under continuous light at 22°C for 5 days. (*1/2 Gamborg B5 salt mixture 1.5g/l, MES 0.5g/l, sucrose 10g/l, plant agar 10g/l, pH5.2 set with KOH; containing 500 μ M dAdo, 500 μ M Ado or water). The phenotype was monitored at 5 days post transfer (column 1 and 2) and at 8 days post transfer (column 3).

(C) MEcPP does not induce cell death. Conductivity of MES buffer containing Col-0 seedlings (9-day-old) after mock-, dAdo or MEcPP treatment. Data points depicts the mean, while error bars depict the standard error of the mean (SEM) obtained from 3 biological independent replicates.

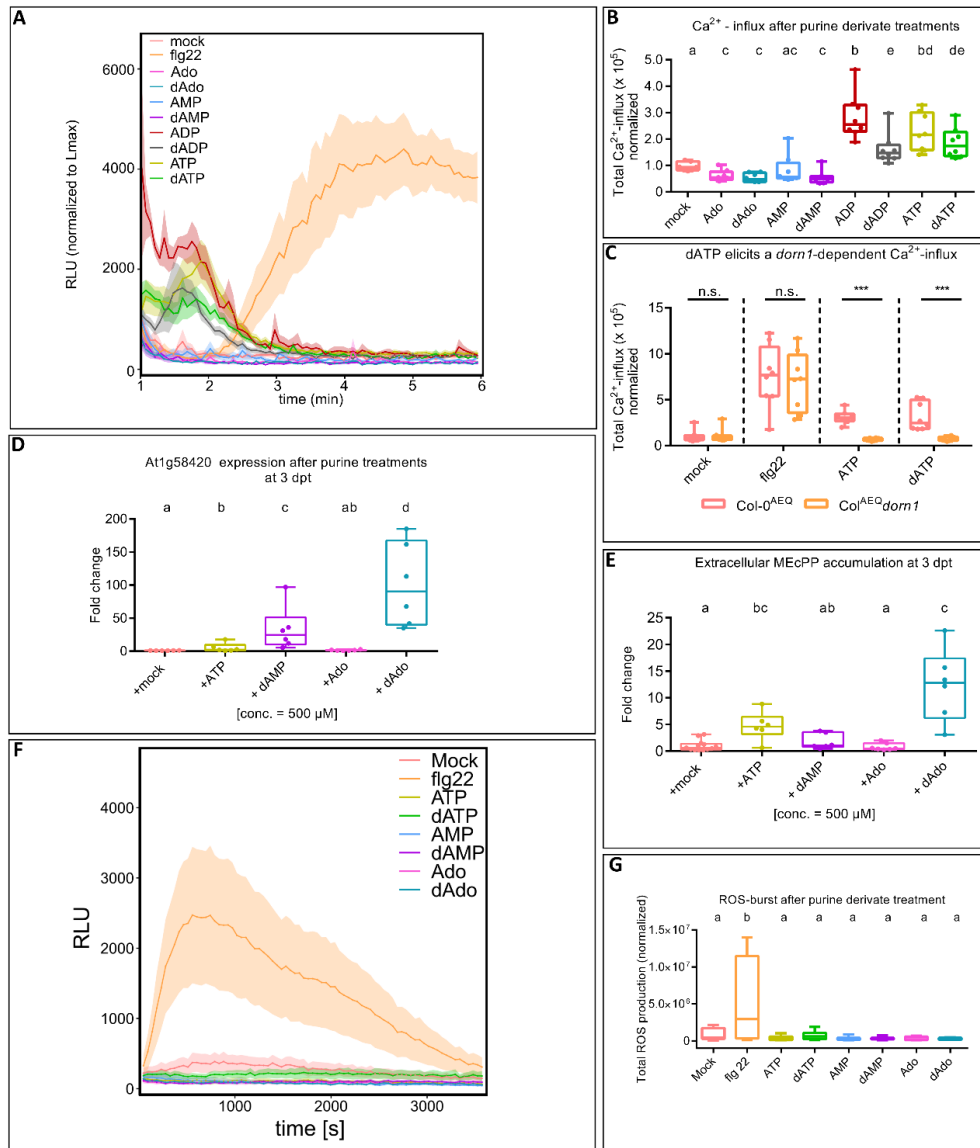


Fig. S7: dAdo-triggered signaling and cell death are not mediated by canonical pattern-triggered immune responses, related to Figure 4.

(A) Ca^{2+} influx after treatment of 7-day-old Arabidopsis Col-0^{AEQ} seedlings with 500 μM purine derivatives dissolved in 2.5 mM MES buffer (pH 5.7). Buffer and 33 μM flg22 were used as positive and negative controls, respectively. Ca^{2+} influx was monitored using a coelenterazine-based chemiluminescence assay and measured as relative light units (RLU). After discharge of the remaining aequorin by addition of CaCl_2 , the discharge kinetics were integrated and normalized to the maximum Ca^{2+} level. The discharge integral was then used to normalize the kinetics of Ca^{2+} in response to elicitor treatment. The curves represent eight biological replicates, and the experiments were additionally repeated three times independently with similar results.

(B) Boxplots show the total Ca^{2+} influx over the measured time period. Calculations were performed as described in (A). Values are means \pm SEM of eight biological replicates, each consisting of one seedling. Different letters indicate significant differences as determined by a Kruskal-Wallis test and Dunn's post-hoc test ($p < 0.05$). The experiment was repeated three times with similar results.

(C) Comparison of total Ca^{2+} influx in 7-day-old Arabidopsis Col-0^{AEQ} and Arabidopsis Col-0^{AEQ} *dorn1* seedlings after treatment with 500 μM ATP, dATP, 33 μM flg22, or 2.5 mM MES pH 5.7 (mock). Data represent values from eight biological replicates. Calculations were performed as described in (A). Asterisks indicate significant differences between the two genotypes analyzed by Student's t-test ($p < 0.005$ ***). The experiment was repeated three times with similar results.

(D) Expression of the marker gene AT1G58420, which responds to wounding and *S. indica* colonization, in treated 7-day-old Col-0 seedlings. Fold change expression was calculated in comparison to the housekeeping gene *AtUbi* and mock treatment using method $2^{-\Delta\Delta\text{CT}}$. Data represent 6 independent biological replicates. Different letters indicate significant differences between groups as determined by Kruskal-Wallis test and post-hoc Wilcoxon BH adjustment ($p < 0.05$).

(E) Metabolic analysis of supernatant from 7-day-old purine-treated Col-0 seedlings at 3 dpt. Points represent data from at least 6 biologically independent replicates normalized to the average of the corresponding mock samples. Different letters indicate significantly different groups as determined by a Kruskal-Wallis test and post-hoc Wilcoxon BH adjustment ($p < 0.05$).

(F) Apoplastic ROS production after treatment of seven-day-old *A. thaliana* Col-0^{AEQ} seedlings with 500 μM purine derivatives solved in 2.5 mM MES buffer (pH 5.7 buffer). Buffer and 33 μM flg22 were used as controls. ROS production was monitored via a luminol-based chemiluminescence assay. The curve represents eight biological replicates. The experiment was repeated three times with similar results.

(G) Boxplots represent total ROS production over the measured time period. Values represent eight biological replicates, each containing one seedling. Different letters indicate significant different groups determined with a one-way ANOVA with post-hoc Tukey HSD test ($p < 0.05$).

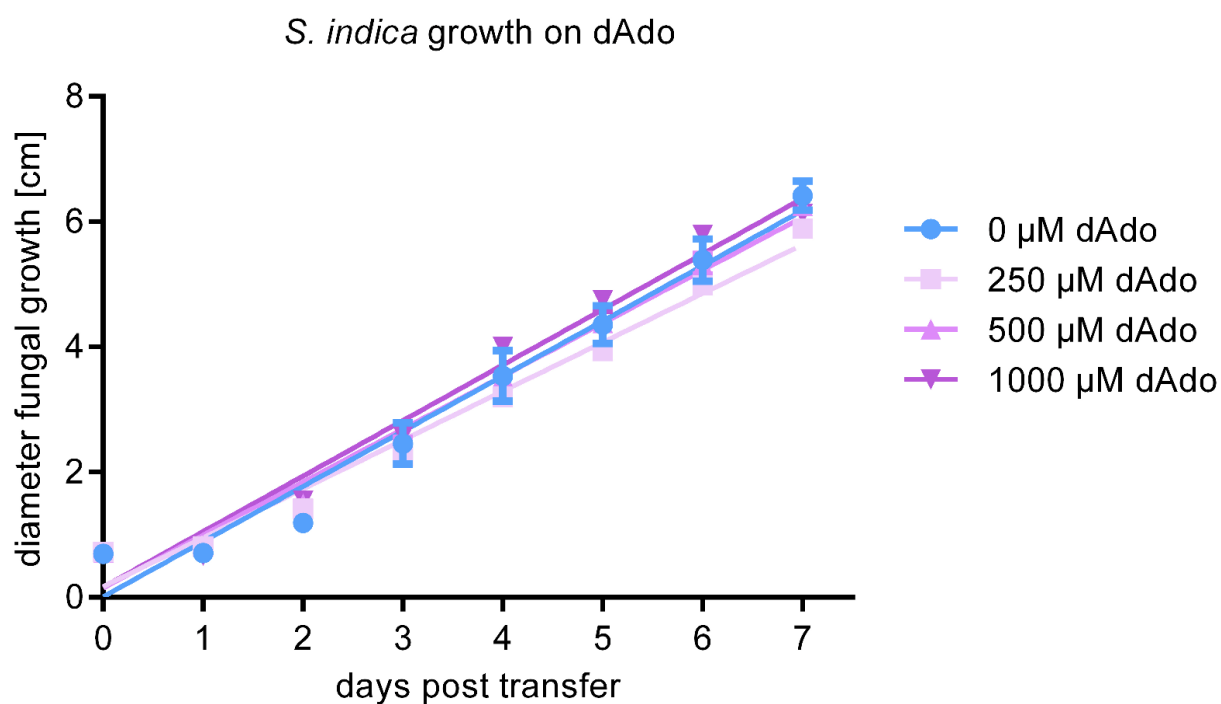


Fig. S8: Growth of *S. indica* on CM medium containing different concentrations of dAdo, related to Figure 4.

Dots represent the average diameter of 3 technical replicates while error bars represent the SD. Lines represent the linear regression describing the fungal growth calculated from the raw data. The experiment was repeated thrice showing comparable results (Data not shown). Growth was measured extending from the agar plug (diameter 0.7 cm).

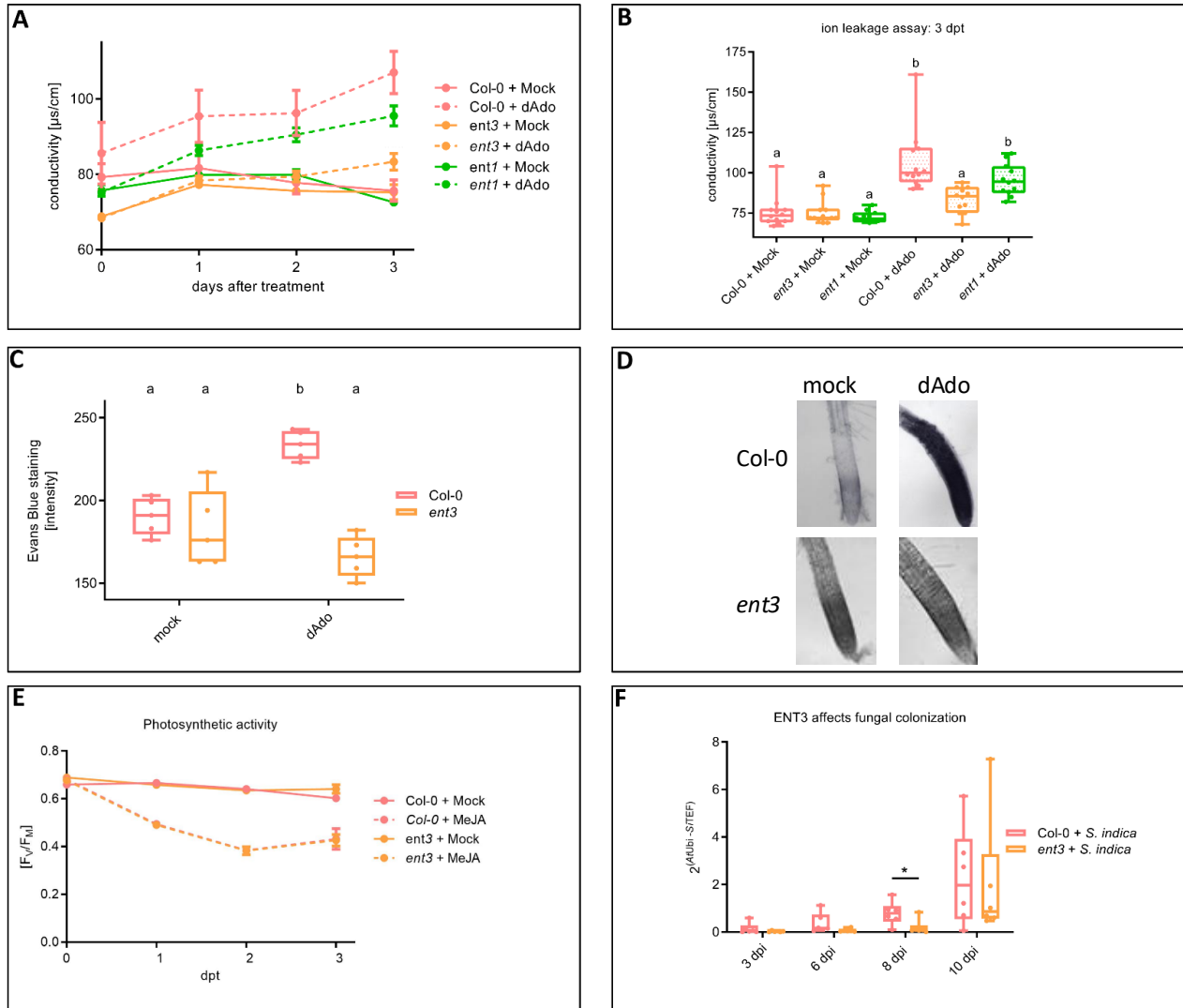


Fig. S9: ENT3 – a purine transporter affects cell death and fungal colonization in the plant root, related to Figure 5.

(A) Conductivity of 2.5 mM MES buffer containing Arabidopsis seedlings (9-day-old) after mock- or dAdo-treatment. Data points depicts the mean, while error bars depict the standard error of the mean (SEM) obtained from 12 biological replicates. Asterisks represent significant difference between dAdo-treated Col-0 and *ent3* analyzed by Student's t-test. The experiment was repeated three times with similar results.

(B) Conductivity of samples from A at 3 dpt. Different letters indicate significant different groups determined with a one-way ANOVA with post-hoc Tukey HSD test ($p < 0.05$).

(C) Quantification of root cell death in Arabidopsis roots at 4 days after dAdo-treatment. Cell death quantity was evaluated via Evans blue staining and normalized to the mock-treated roots. Boxplots represent the data obtained from 5 biological replicates. Different letters indicate significant different groups determined with a one-way ANOVA with post-hoc Tukey HSD test ($p < 0.05$).

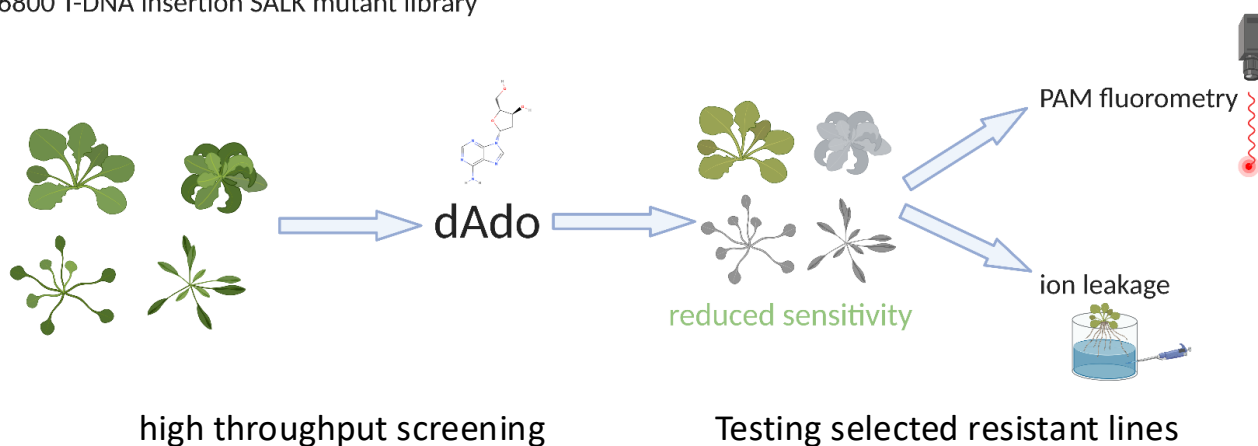
(D) Evans blue stained roots tips from (C). The experiment was repeated three times with similar results.

(E) Photosynthetic activity (F_v/F_m) of 9-day-old mock- and MeJA-treated (500 μM) Col-0 and *ent3* seedlings. Measurements were taken 3 days after treatment (dpt) every 24 hours. Data show the mean and error bars show the standard error of the mean (SEM) obtained from 12 technical replicates with 3 seedlings each. The experiment was repeated more than three times independently with similar results.

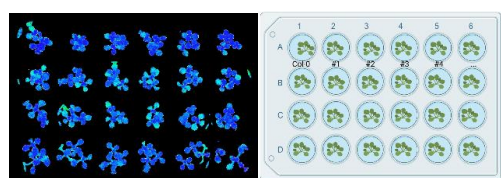
(F) : *S. indica* abundance in 7-day-old Arabidopsis seedlings. The ratio of fungus (*S/TEF*) to plant (*AtUbi*) was calculated using cDNA as template and the $2^{-\Delta\text{CT}}$ method. Boxplots represent 6 independent biological replicates. Asterisks indicate significant difference from Col-0 samples (Student's t-test, $p < 0.05$ *).

A

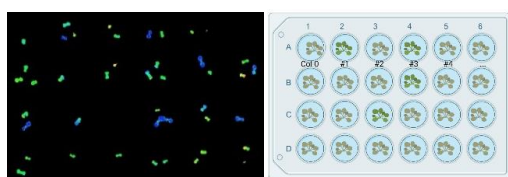
6800 T-DNA insertion SALK mutant library



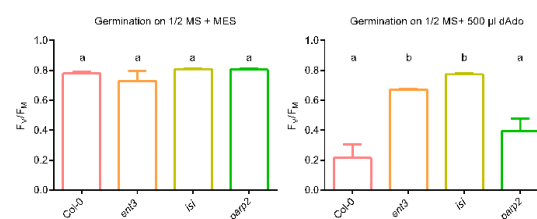
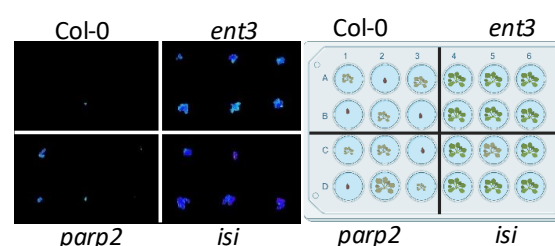
mock



dAdo



dAdo



B

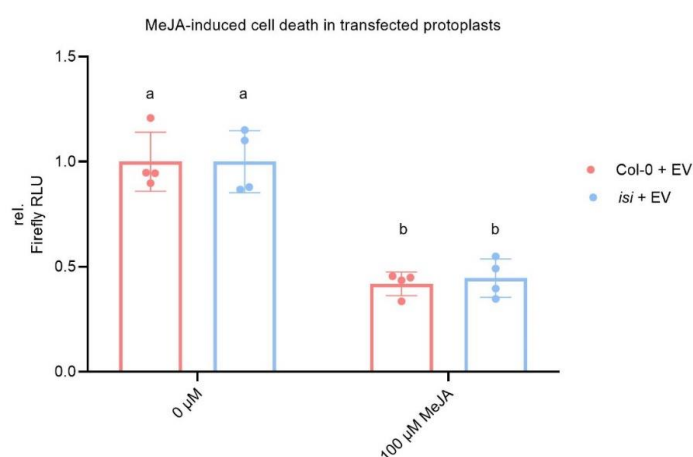


Fig. S10: Screening of an *A. thaliana* library of T-DNA insertion mutants lines for affected dAdo-sensitivity, related to Figure 6.

(A) The model shows our screening process to identify mutants affected in dAdo-sensitivity. We screened over 6800 T-DNA insertion SALK lines for an altered response to dAdo. For high-throughput screening the mutant lines were analyzed via PAM fluorometry on 24 well plates, including Col-0 WT as control in each plate. Arabidopsis mutant lines with a resistant phenotype to dAdo were subsequently analyzed in ion leakage assays. The screening was repeated 3 times. Mutants that showed reproducible resistant phenotypes in the high-throughput screening were analyzed by germination assays on solid plant media with and without dAdo additionally tested as described in STAR Methods.

(B) : Relative Luciferase activity of *A. thaliana* protoplasts transfected with a luciferase. Values were normalized to mock treatment (0 μ M). Different letters indicate significantly different groups per treatment, as determined by a two-way ANOVA with post-hoc Tukey HSD test ($p < 0.05$).

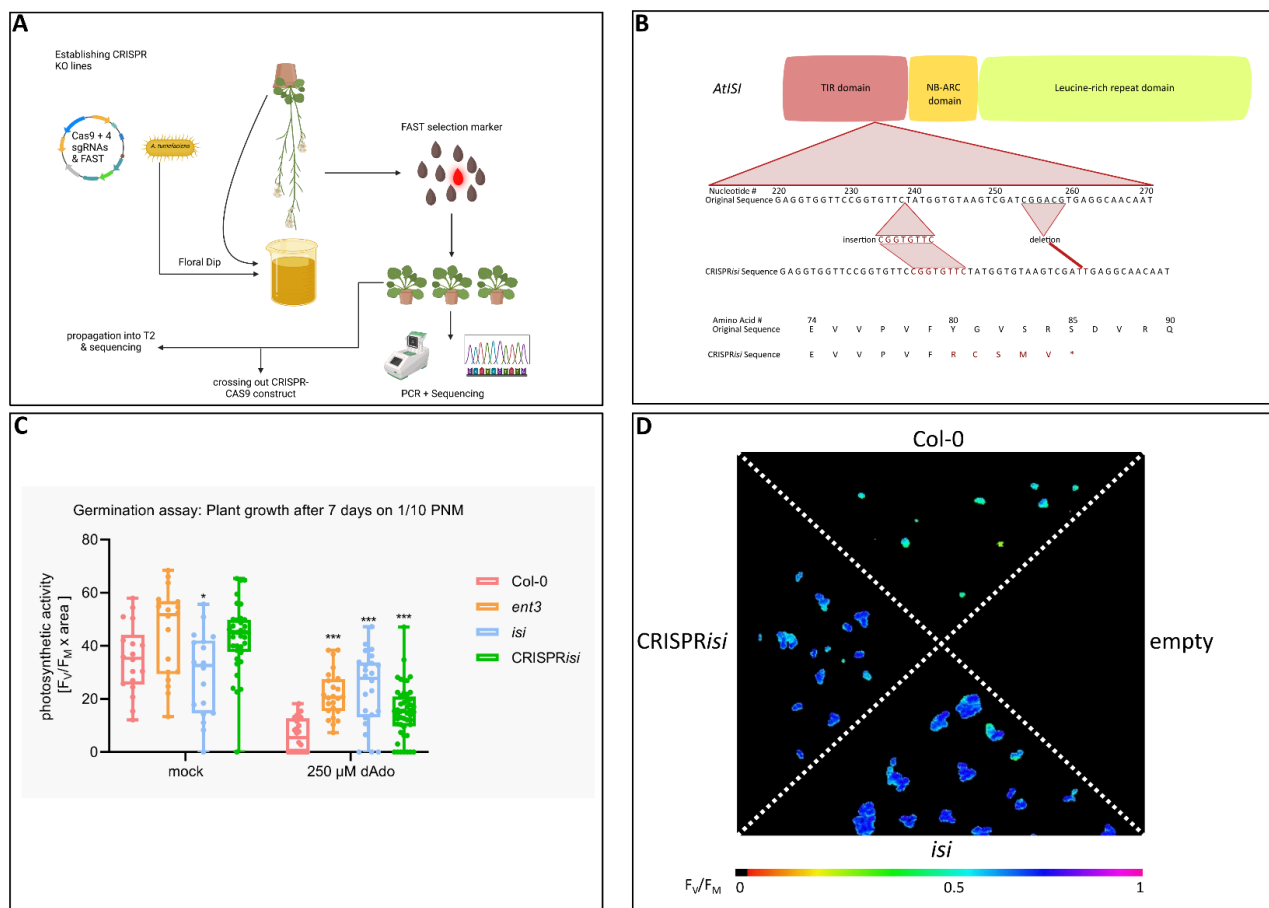


Fig. S11: Establishing and testing an independent CRISPR line, related to Figure 6.

(A) Description of the transformation protocol. The vector, carrying four sgRNA constructs targeting the TIR domain of *AtIS1* was based on the plasmid pDGE347 as described in Stuttmann et al.³⁸ and was assembled via Golden Gate cloning. *Agrobacterium tumefaciens* strain GV3101 was transformed with it. The resulting strain was used to transform Col-0 *A. thaliana* plants via floral dip. Seeds of the resulting T₀ generation were screened for fluorescence, and positive seeds were transferred to pots for propagation. In the T₁ generation, seeds were screened for mutations in the *AtIS1* gene via PCR and sequencing and seeds that were not fluorescent were selected to breed out the CRISPR-CAS9 construct. After homozygosity was confirmed by further sequencing, seeds of the T₂ generation were used for subsequent experiments. (B) : Relative expression of TNL genes of the NLR locus in Arabidopsis seedlings at 8 days after germination in *S. indica* presence on 1/10 PNM medium. Expression values relative to Col-0 seedlings were calculated using the $\Delta\Delta C_t$ -method. Dots represent three independent biological replicates while bars represent the average. Asterisks represent significant difference to the mock-treated sample analyzed by Student's t-test. $p < 0.05$ (*).

(B) : Mutations of the *AtIS1* gene found in the CRISPR*isi* line. Corresponding to the predicted binding sites of the sgRNAs of the knockout construct (A), CRISPR*isi* carries an 8 bp insertion mutation after bp 237 of the *AtIS1* coding region and a 6 bp deletion ranging from bp 254-259. These mutations translate to mutated amino acids from AA 80-84 and a subsequent premature stop codon.

(C) Germination of seedlings on 1/10 PNM medium containing 250 μ M dAdo or MES. The graph depicts the quantification of the photosynthetic activity ($F_v/F_m \times \text{area}$) measured by PAM fluorometry at 7 days after sowing. Boxplots show measurements of single seedlings in a single well. The experiment was repeated twice independently with similar results. Asterisks represent significant difference to the Col-0 data of the same treatment analyzed by Student's t-test. $p < 0.05$ (*), $p < 0.005$ (***).

(D) Visualization of F_v/F_m measured via PAM fluorometry. The pictures depict seeds grown on a square plate with 1/10 PNM medium containing 250 μ M dAdo. The measurement was performed at 7 days after sowing the seeds.

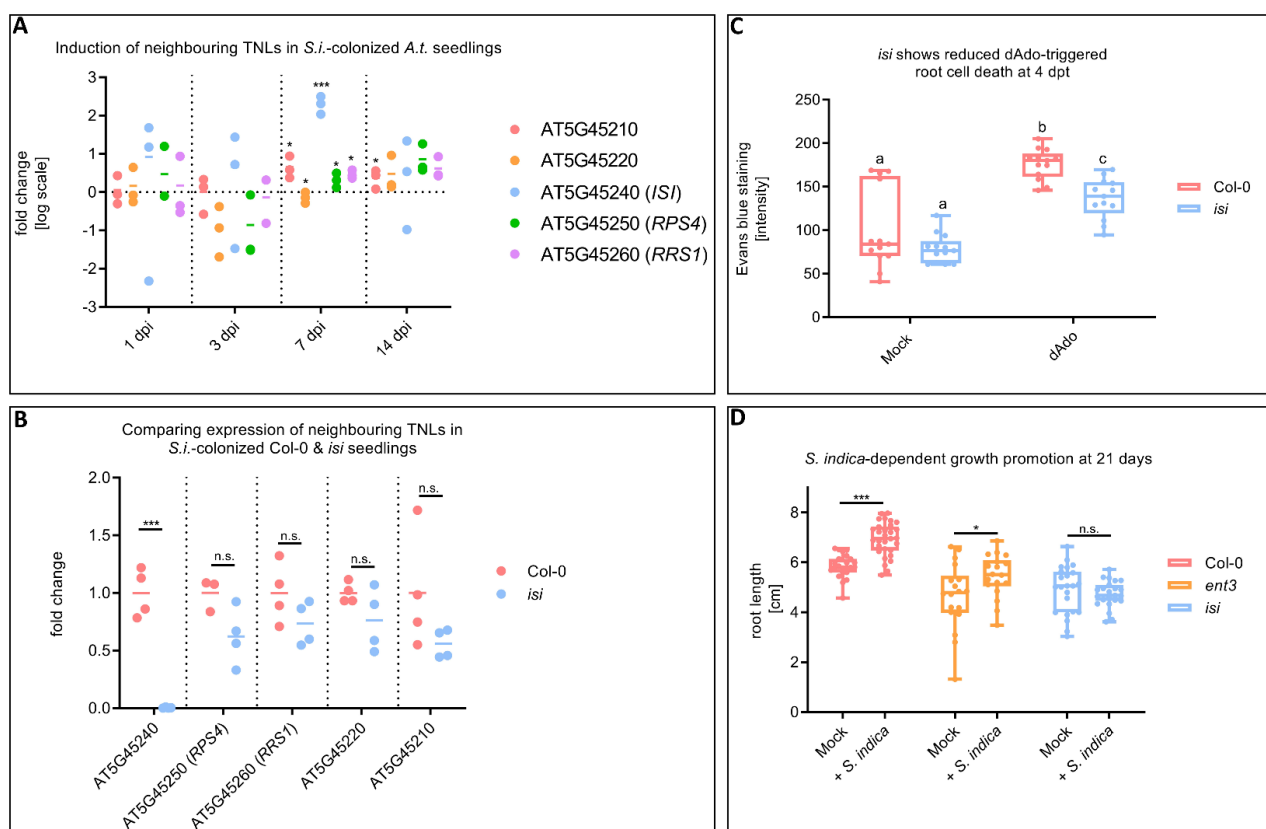


Fig. S12: Characterization of the AT5G45240 locus and corresponding mutants, related to Figure 6 & 7.

(A) Gene locus of NLR gene and expression during *S. indica* colonization - Relative expression of TNL genes of the *ISI* locus in Arabidopsis seedlings at different time points of *S. indica* colonization. Expression values relative to mock-treated seedlings at 1 dpi were calculated using the $\Delta\Delta C_t$ -method. Dots represent three independent biological replicates while bars represent the average. The data is presented on a log2 scale. Asterisks represent significant difference to the mock-treated sample analyzed by Student's t-test. $p < 0.05$ (*).

(B) : Relative expression of TNL genes of the NLR locus in Arabidopsis seedlings at 8 days after germination in *S. indica* presence on 1/10 PNM medium. Expression values relative to Col-0 seedlings were calculated using the $\Delta\Delta C_t$ -method. Dots represent three independent biological replicates while bars represent the average. Asterisks represent significant difference to the mock-treated sample analyzed by Student's t-test. $p < 0.05$ (*).

(C) : Evans blue staining of dAdo-treated *A. thaliana isi* KO line. Quantification of root cell death in Col-0 and *isi* root tips at 4 days after dAdo-treatment. Cell death was evaluated using Evans blue staining. Boxplots represent the data obtained from 13 biological replicates. Different letters indicate significant differences determined with a two-way ANOVA with post-hoc Tukey HSD test ($p < 0.05$). The experiment was repeated independently 2 times with similar results.

(D) Root growth promotion in Arabidopsis seedlings. Quantification of root length in Col-0, *ent3* and *isi* knockout lines at 21 days after germination. Seeds were treated with *S. indica* spores or a mock control. Root length was evaluated from scans of the plates with Fiji (ImageJ). Boxplots represent the data obtained from 18-23 biological replicates. Asterisks represent significant difference to the mock-treated sample analyzed by Student's t-test. $p < 0.05$ (*).

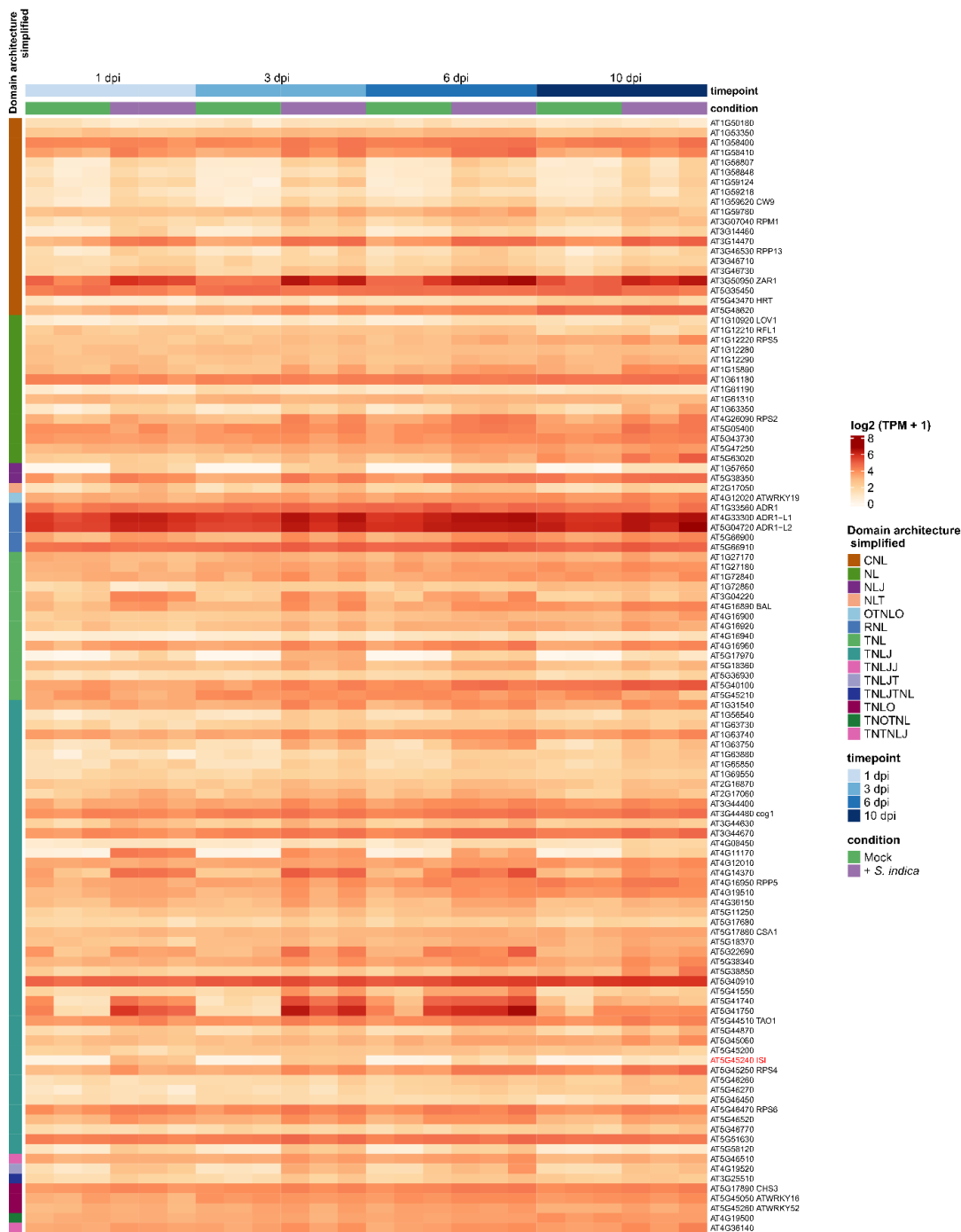


Fig. S13: Expression of different domain NLR proteins during *S. indica* colonization, related to Figure 7.

(A) Gene locus of NLR gene and expression during *S. indica* colonization. The heatmap shows the expression values of *A. thaliana* NLR genes with at least NB-ARC and LRR (NL) domains in *A. thaliana* root samples. Specifically, *A. thaliana* plants were inoculated with mock or *S. indica*. Roots samples were collected at 1 dpi, 3dpi, 6 dpi and 10 dpi. For each sample, stranded RNAseq libraries were generated and quantified by qPCR. RNA-seq libraries production and the sequencing were performed at the U.S. Department of Energy Joint Genome Institute under a project proposal (Proposal ID: 505829) (Zuccaro and Langen, 2020). The raw reads were filtered and trimmed using the JGI QC pipeline. Filtered reads from each library were aligned to the Arabidopsis TAIR10 reference genome using HISAT2 version 2.2.0. The gene counts were generated using featureCounts. NLR genes were identified in Arabidopsis TAIR10 proteins sequences using the software NLRtracker (Kourelis et al.) which also provides the domain architecture of NLR proteins. Based on NLRtracker annotation, NLR genes with at least NB-ARC (N) and LRR (L) domains were selected. Next, genes with at least NL domains with an average TPM value > 1 TPM across all samples were selected. The \log_2 transformed TPM values of selected Arabidopsis NLR genes are shown in the heatmap generated using ComplexHeatmap package. In addition, the annotation of the protein domains annotation of selected NLR genes provided by NLRtracker are shown: TIR domain (T), NB-ARC domain (N), coiled-coil domain (CC), LRR domain (L), Other domain (O), C-JID domain (J), RPW8-type CC domain (R).

Project: Zuccaro, A., & Langen, G. (2020). Host-specific regulation of effector gene expression in mutualistic root endophytic fungi (Proposal ID: 505829). JGI Award DOI: 10.46936/10.25585/60001292. More details about the experimental conditions underlying this data set can be found in Eichfeld et al.⁵³.

S. indica colonization of *A. thaliana* root tip

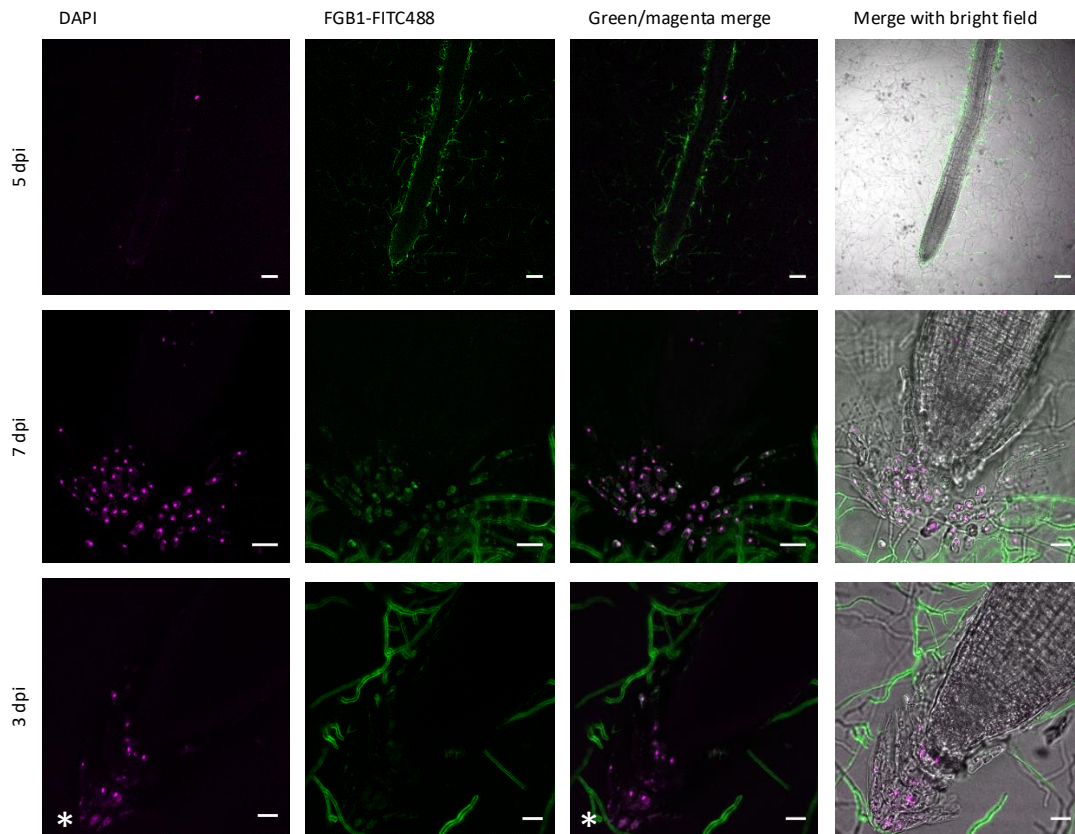


Fig. S14: *S. indica* growth at the root tip of *A. thaliana*, related to Figure 2 and discussion.

CLSM live cell imaging of *S. indica*-colonized *A. thaliana* roots. Nuclei stained with DAPI (magenta) and fungal cell wall and matrix with FGB1-FITC488 (green). Roots were directly stained and imaged on plate to avoid removing the border-like cells (BLC) and RET. Nuclei of BLC are visible in magenta. *S. indica* is growing around the root tip and among the BLC/RET of the root cap. Nuclei of the outer BLC layer are often blurred when in contact with *S. indica* (asterisk). Bars = 100 μ m (Row 1), Bars = 20 μ m (Row 2-3)